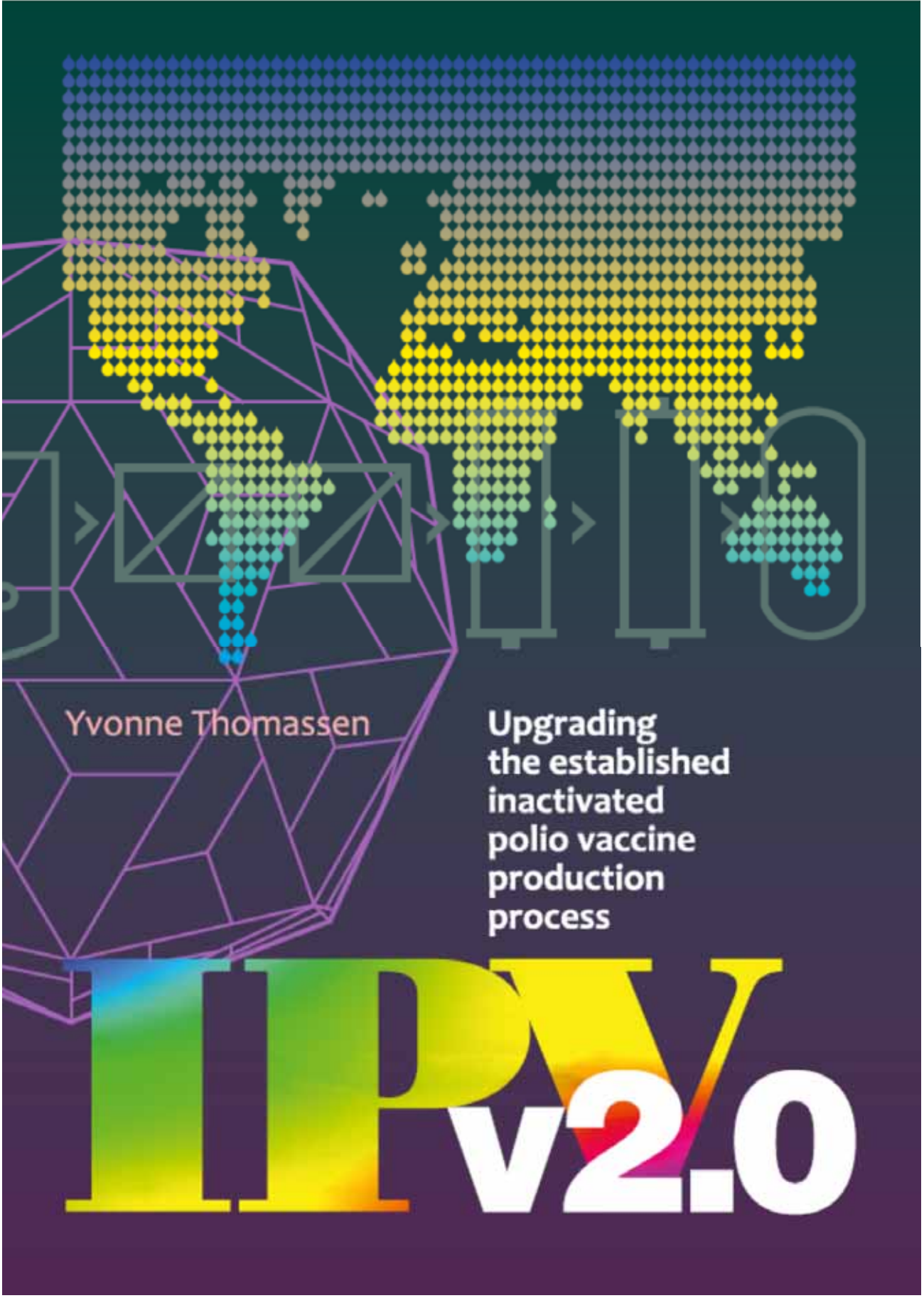
Yvonne Thomassen
Upgrading the established inactivated polio vaccine production process
IPV2.0

IPV v2.0

Upgrading the established

inactivated polio vaccine production process

Yvonne Elisabeth Thomassen

Thesis committee

Promotor
Prof. Dr R.H. Wijffels
Professor of Bioprocess Engineering
Wageningen University

Co-promoters
Dr W.A.M. Bakker
Senior scientist, Institute for Translational Vaccinology, Bilthoven
Dr L.A. van der Pol
Senior scientist, Institute for Translational Vaccinology, Bilthoven

Other members
Prof. Dr M.M. van Oers, Wageningen University
Prof. Dr J.J. Heijnen, Delft University of Technology
Prof. Dr -Ing. U. Reichl, Max Planck Institute for Dynamics of Complex Technical Systems, Magdeburg, Germany
Dr G.M. Zijlstra, DSM Biologics, Groningen

This research was conducted under the auspices of the Graduate School of VLAG (Advanced studies in Food Technology, Agrobiotechnology, Nutrition and Health Sciences).

IPV v2.0

Upgrading the established

inactivated polio vaccine production process

Yvonne Elisabeth Thomassen

Thesis

submitted in fulfillment of the requirements for the degree of doctor
at Wageningen University
by the authority of the Rector Magnificus
Prof. Dr M.J. Kropff,
in the presence of the
Thesis committee appointed by the Academic Board
to be defended in public
on Tuesday 15 April 2014
at 4 p.m. in the Aula.

Yvonne E. Thomassen
IPV v2.0 - Upgrading the established inactivated polio vaccine production process,
232 pages.

PhD thesis, Wageningen University, Wageningen, NL, (2014)
With references, with summaries in Dutch and English

ISBN 978-94-6173-856-1

"You have to *believe*. Otherwise, it will never happen."

— Neil Gaiman (Stardust)

Contents

Chapter 1

Introduction

Polio

Polio (or poliomyelitis) is a highly infectious viral disease that can cause paralysis. The typical signature of the disease is crippled legs. Paralysis of breathing muscles may also occur and is potentially fatal. Infections, generally localized to the small intestine, are often asymptomatic or lead to mild symptoms such as sore throat, fever or malaise, enteritis and diarrhea. They are caused by ingestion of fecal contamination from an infected human. Upon infection, an immune response is elicited which results in good protection against reinfection. On rare occasions, one in 200 cases, poliovirus enters the blood stream and invades the central nervous system. There it infects and destroys motor neurons, which results in the typical irreversible paralysis (Racaniello 2007). Polio cannot be cured. However, there are highly effective vaccines available.

Poliovirus

The causative agent of polio, the poliovirus, belongs to the *Enterovirus* genus of the *Picornaviridae* family. It is a small (30 nm in diameter) non-enveloped, positive strand RNA virion with icosahedral symmetry (Figure 1A). Virus capsid includes 60 protomers, each consisting of one copy of capsid protein VP1, VP2, VP3 and VP4 (Figure 1A). VP1, VP2 and VP3 are located on the outside of the capsid while VP4 resides on the inner site of the capsid (Hogle et al. 1985). The capsid encloses the mRNA genome, ~7500 bp in length (Figure 1B). Its 5´ non-coding region (~740 nt) is required for replication initiation and ribosome entry, which is essential for cap-independent initiation of translation (Wimmer et al. 1993). The 3´ non-coding region is vital for negative strand RNA synthesis. The protein coding region, in between the 5´ and 3´ non-coding regions, encodes a single polyprotein. This protein can be proteolytically cleaved into precursor proteins, which give the final four capsid proteins and seven non-structural proteins. These are required for virus replication and assembly and include proteases (2A, 3C and 3CD), the RNA polymerase (3D), a helicase (2C) other replication essential proteins (2B, 2BC, 3A, and 3B) and a 5´ capping protein (3B or VPg) (Wimmer et al. 1993).

Polioviruses are classified into three serotypes (type 1, 2 and 3) based on the cross-neutralization of poliovirus isolates by polyclonal sera raised against the different poliovirus strains (Bodian 1951). Four major epitopes, or antigenic sites, have been recognized. These are located on the surface-exposed loops in of the capsid proteins VP1-3 (Minor 1990). VP1, VP2 and VP3 also form the location for the poliovirus receptor (CD155) which is located on cell membranes.

Two distinct antigenic forms of poliovirus exist, D- and C-antigen, sometimes referred to as N- and H antigen (Mayer et al. 1957). The D-antigenic form represents the native infectious virus whereas C-antigen represents non-infectious empty particles. Recovery against

disease and an effective immune response is associated with the development of antibodies against D-antigen. Vaccine potency has therefore always been expressed in arbitrarily defined D-antigen units (Beale and Ungar 1962).

Polio vaccines

The first polio vaccine, IPV, was developed by Jonas Salk in the 1950s (Salk 1953; Salk et al. 1954). It was licensed in the US in 1955. IPV consists of formalin inactivated polioviruses of all three existing serotypes (type 1 (Mahoney or Brunhilde), 2 (MEF-1) and 3 (Saukett)). IPV is given by intramuscular injection and antibodies are generated in the blood that will protect against poliomyelitis by preventing the spread of poliovirus to the nervous system.

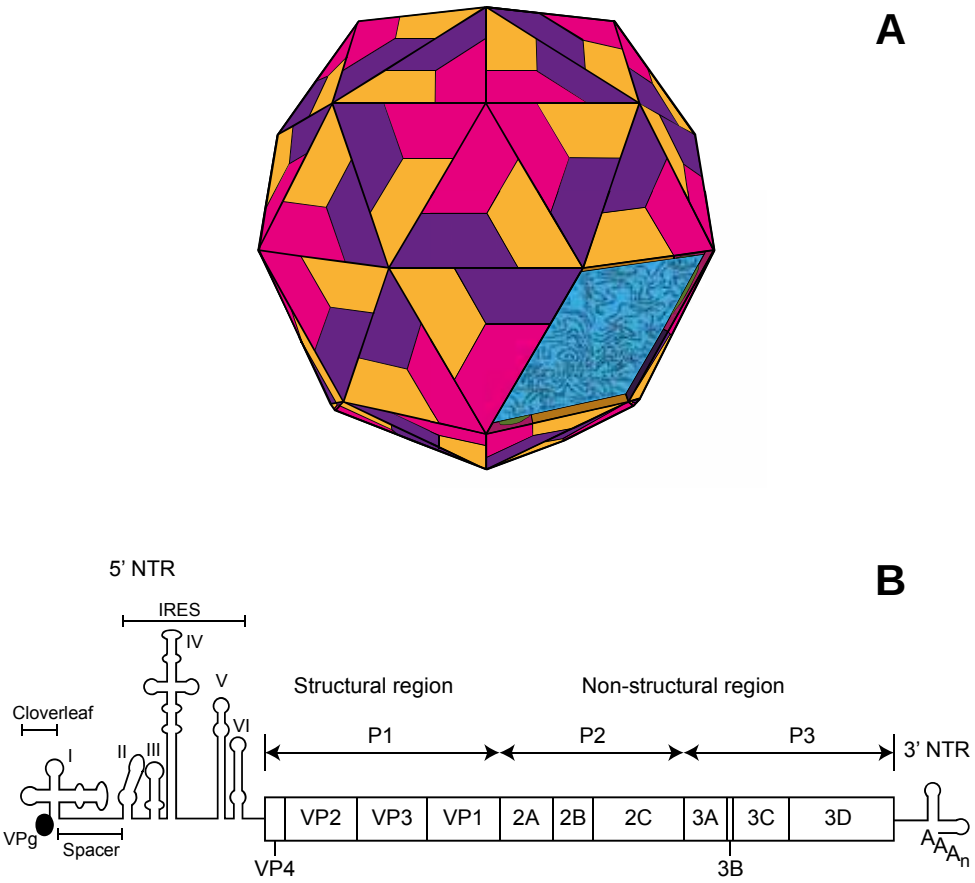

Figure 1. Schematic overview of A: the polio virion structure based on (Hogle et al. 1985). VP1 is in the center of a five-fold axis of symmetry; VP2 and VP3 from a threefold axis of symmetry; VP4 is on the inside of the capsid. B: its RNA genome adapted from (De Jesus 2007).

In 1978, a method of producing a more potent IPV was developed by van Wezel in the Netherlands (van Wezel et al. 1980). This vaccine has been referred to as enhanced-potency IPV (eIPV) and currently is referred to as conventional IPV (cIPV) or Salk-IPV.

The other vaccine, oral polio vaccine (OPV), was developed in the 1960s by Albert Sabin (Sabin and Boulger 1973) and was licensed in the US in 1961-1962. It is a trivalent vaccine, against all serotypes, based on attenuated poliovirus strains, the so-called Sabin strains. Attenuation was obtained by repeatedly passaging virulent strains of type 1 (Mahoney) and type 3 (Leon), in monkeys under conditions that triggered high selection pressure. Sabin type 2 originated from a naturally low neurovirulent poliovirus type 2 isolate (Sabin and Boulger 1973). OPV is administered orally and antibodies are generated both in the blood and, like in natural infection, a local immune response in the intestinal and nasal mucosa, the primary sites for poliovirus entry and multiplication, is obtained (Ogra et al. 2011). This intestinal immune response can rapidly stop person-to-person transmission of wild poliovirus (Okayasu et al. 2011).

Both vaccines are considered extremely safe, however, in rare occasions (1 in every 2.7×10^6 first doses) the live attenuated vaccine, OPV, can cause paralysis (Nkowane et al. 1987). This disease is referred to as vaccine-associated paralytic poliomyelitis (VAPP). A second disadvantage of the use of OPV is the possibility that the attenuated polioviruses revert and start to circulate in a population. These viruses are known as circulating vaccine derived polioviruses (cVDPV) and possess the same neurovirulence and transmission properties as wild-type polioviruses (Kew et al. 2005).

OPV was adopted by most of the countries, except the Netherlands, Sweden and Finland, mainly due to the ease of administration and the low costs (Sabin 1985). It has also been the main tool for use in the polio eradication program. In the last decade, an increasing number of (polio-free) countries have switched to IPV for routine immunization because of its better safety profile.

Polio eradication program

In 1988, the World Health Assembly adopted a resolution to eliminate wild polioviruses globally and the Global Polio Eradication Initiative (GPEI) was established. It was estimated that, at that time, over 350,000 children developed polio annually and polio was endemic in 125 countries (Hadler et al. 2008). By the year 2012, the annual incidence of polio had decreased >99.9% (to 223 cases) compared with 1988 and the number of countries where polio is endemic had reduced to 3 (Afghanistan, Nigeria and Pakistan) (WHO 2013b) (Figure 2). Eradication of polio has shown to be more difficult than initially anticipated and the targets for eradication have not been met, the initial target for eradication was the year

2000. Eradication of wild type poliovirus type 2 has been achieved; the last wild type was reported in India in 1999.

From 2005 to 2009 monovalent OPV (mOPV) against poliovirus type 1 and from late 2009 onwards bivalent OPV (bOPV) were used to specifically target poliovirus type 1 and 3. Both mOPV and bOPV induced better immune responses compared to trivalent OPV indicating interference of poliovirus type 2 in the trivalent vaccine (Sutter et al. 2010). The introduction of mOPV and bOPV campaigns resulted in a polio-free India in 2012, which had long been one of the remaining endemic countries, and a rapid decrease in wild-type polio cases (Figure 2 insert). In 2012, the World Health Assembly declared the completion of the polio eradication a programmatic emergency (WHO 2012b). The main reasons are the persistence of endemic wild poliovirus transmission and the recurring outbreaks in polio-free countries.

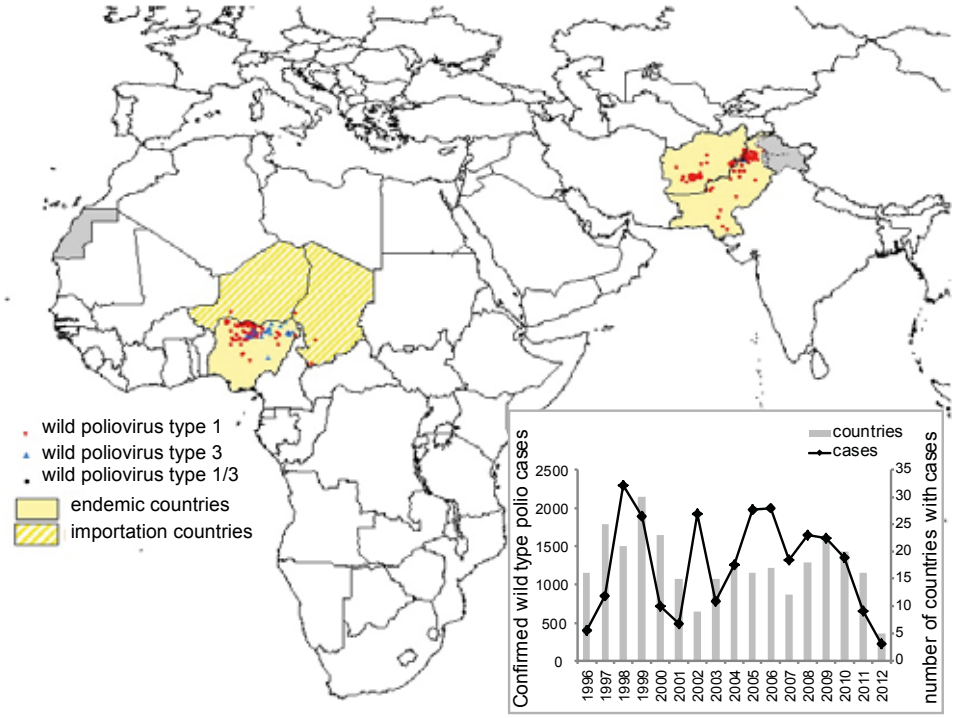

Figure 2. Geographical distribution of children with polio associated with wild-type poliovirus in 2012 and (insert) the total number of polio cases reported and the number of countries with polio cases in the years 1996-2012. Map and data are from WHO (www.polioeradication.org).

In 2013, a new strategy plan was drafted for the endgame in polio eradication. Key objectives are i) to stop all WPV transmission by the end of 2014 and any new outbreaks due to a cVDPV within 120 days of confirmation of the index case; ii) cVDPV elimination by termination of OPV use (starting with type 2) and introduction of (new) inactivated vaccines; iii) certification of polio-free regions (3 years without cases) and safe containment of all polioviruses; iv) transfer of the knowledge and experience from the polio eradication program towards other health and development benefits (WHO, 2013c). Preceding this plan the Strategic Advisory Group of Experts (SAGE) recommended that at least one dose of IPV is introduced into all routine immunization programs to safeguard against the withdrawal of the type 2 serotype prior to the switch from tOPV to bOPV (excluding poliovirus type 2) (WHO 2013a). The expected global increase in IPV demands pushes manufacturers to accommodate. The current four IPV manufacturers (GSK, Sanofi, Staten Serum Institute, Bilthoven Biologicals (formerly Netherlands Vaccine Institute; acquired in 2011 by Serum Institute India)) may increase production capacity and additional IPV producers will arise, and will likely be situated in the new economies. In addition, the large difference in cost prices for IPV (at $3/dose) and OPV (at $0.15-0.20/dose) (Venczel et al. 2009) and the ability from the new markets to carry those additional costs requires an endeavor for IPV cost price reduction. Moreover, in view of biosafety aspects after achievement of polio eradication, the use of wild type viruses in areas with potential low vaccine coverage should not be established. Development of an IPV production process using attenuated Sabin strains may open the possibility for new industries to meet the biosafety criteria.

Thesis outline

With polio eradication on our doorstep, the World Health Organization is pursuing a new IPV based on non-wild-type strains to increase the biosafety of vaccine manufacturing (Aylward et al. 2006; Heymann et al. 2005). In addition, and due to the pending OPV cessation, the demand for affordable IPV is increasing (Venczel et al. 2009). To accommodate these questions two research programs were started at the Netherlands Vaccine Institute. One concerned optimization of the current Salk-IPV production process, the other the manufacturing of an affordable Sabin-IPV with the aim of technology transfer to developing countries manufacturers.

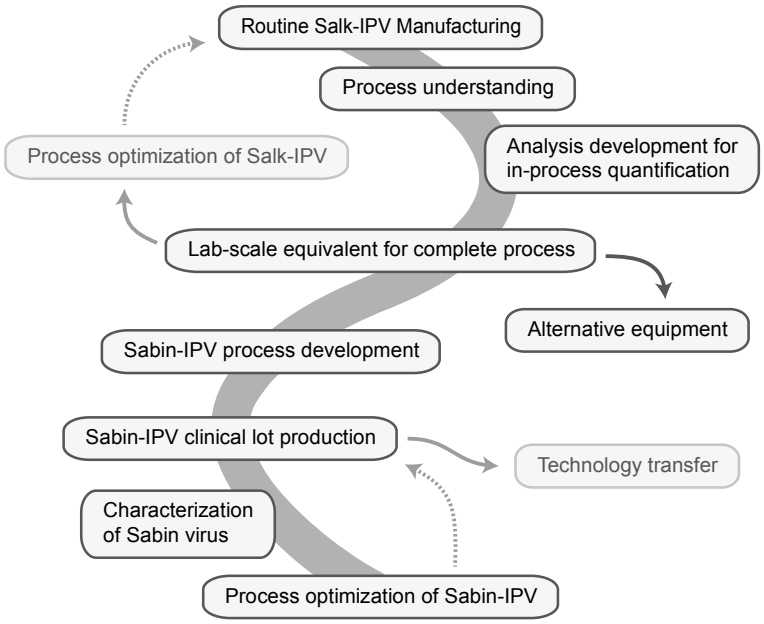

Figure 3. Thesis outline. Starting from analyzing the routine Salk-IPV manufacturing a representative model at lab-scale was developed. This model was further used to quickly implement preparation of a next generation IPV based on Sabin strains with minor process development. Ongoing steps, not described in this thesis, are indicated in grey boxes.

In the 1970s, the widely used production process for IPV, one of the first large scale cell culture based biological production processes, has been developed in Bilthoven (the Netherlands). IPV manufacturing has been part of the regular vaccine manufacturing program ever since. The history and past process developments in IPV manufacturing are described in Chapter 2. Although IPV manufacturing has been ongoing for decades, the development knowledge had faded with time. To overcome the existing gap in process knowledge and increase process understanding the current manufacturing process was

analyzed using multivariate data analysis (Chapter 3). This statistical method allows presentation and subsequent interpretation of large datasets with many variables. Both the analysis and the data acquisition provided important knowledge for the present process developers.

One of the gaps in the data was located in product quantification during processing. The available assay for D-antigen concentrations had high variability. A so-called fast D-antigen ELISA was established which could be used to measure the D-antigen concentrations in the different matrixes present during the production process (Chapter 4). Based on the refreshed knowledge, a scale-down model of the IPV production line was setup (Chapter 5). This lab-scale equivalent allows studying effects of process changes which might be related to for instance process optimization. The unit operations from the established scale-down model can be used separately, as well as sequentially, to study variations and critical product attributes in the production process. The benefit of a good scale-down model is the possibility of direct implementation of changes, which for instance result in process optimization, at large scale without intermediate pilot scale studies. The further studies on process optimization for the Salk-IPV based on this model are not described in this thesis. Alternatively, for practical reasons, the work continued aiming at Sabin-IPV development.

The upcoming of disposables in GMP manufacturing triggered the study on alternatives for the first filtration unit (clarification) (Chapter 5) and alternative, Wave-type, bioreactors (Chapter 6). This type of bioreactors makes use of sterilized disposable bags, which could be beneficial in a GMP environment.

In view of WHOs pursuit towards an IPV manufacturing process with increased biosafety the development of Sabin-IPV, an IPV based on the attenuated Sabin strains, was taken up. Prior to the production of Sabin-IPV clinical lots a proof of principle study was done (Chapter 2). Subsequently and using the available IPV scale-down model, Sabin strain specific adaptations like MOI and lower virus culture temperature were studied. To be able to quickly show proof-of-principle, no further process optimization and/or modernization was done and the manufacturing of Sabin-IPV was carried out (Chapter 7). An immunogenic product both in animals (Chapter 7) and in humans (Verdijk et al. 2013) was successfully prepared. However, the product yield was extremely low and further process development is needed to obtain an affordable Sabin-IPV. Especially the yield of Sabin poliovirus type 2 after ion exchange chromatography was low. To determine if this effect could be due to a difference in the isoelectric point (*pI*) of the poliovirus a method for *pI* measurement of live virus was developed (Chapter 8). In parallel, studies to increase virus yields during upstream processing were done. Methods for cultivations at increased

cell densities, using an animal component free medium, were compared for their effect on virus yields (Chapter 9).

In Chapter 10, the results described in the thesis are summarized and discussed with respect to future inactivated polio vaccine manufacturing at affordable costs.

Chapter 2

Inactivated polio vaccine development for technology transfer using attenuated Sabin poliovirus strains to shift from Salk-IPV to Sabin-IPV

Published as:
Bakker, W.A.M., Thomassen, Y.E., Van 't Oever, A.G., Westdijk, J, van Oijen M.G.C.T., Sundermann, L.C., Van 't Veld, P., Sleeman, E., van Nimwegen, F.W., Hamidi, A., Kersten, G.F.A., van den Heuvel, N., Hendriks, J.T., van der Pol, L.A. (2011) *Inactivated polio vaccine development for technology transfer using attenuated Sabin poliovirus strains to shift from Salk-IPV to Sabin-IPV*.

Vaccine 29(41):7188-7196
dx.doi.org/10.1016/j.vaccine.2011.05.079

Abstract

Industrial-scale inactivated polio vaccine (IPV) production dates back to the 1960s when at the Rijks Instituut voor de Volksgezondheid (RIV) in Bilthoven a process was developed based on micro-carrier technology and primary monkey kidney cells. This technology was freely shared with several pharmaceutical companies and institutes worldwide. In this contribution, the history of one of the first cell-culture based large-scale biological production processes is summarized. Also, recent developments and the anticipated upcoming shift from regular IPV to Sabin-IPV are presented. Responding to a call by the World Health Organization (WHO) for new polio vaccines, the development of Sabin-IPV was continued, after demonstrating proof of principle in the 1990s, at the Netherlands Vaccine Institute (NVI). Development of Sabin-IPV plays an important role in the WHO polio eradication strategy as biocontainment will be critical in the post-OPV cessation period. The use of attenuated Sabin strains instead of wild-type Salk polio strains will provide additional safety during vaccine production. Initially, the Sabin-IPV production process will be based on the scale-down model of the current, and well-established, Salk-IPV process. In parallel to clinical trial material production, process development, optimization and formulation research is being carried out to further optimize the process and reduce cost per dose. Also, results will be shown from large-scale (to prepare for future technology transfer) generation of Master- and Working virus seedlots, and clinical trial material (for phase I studies) production. Finally, the planned technology transfer to vaccine manufacturers in low and middle-income countries is discussed.

Introduction

As a result of continuous WHO-efforts polio eradication is moving forward. The first milestone, cessation of wild-type poliovirus transmission, is now anticipated by the end of 2012 (WHO 2010a). However, even after polio eradication, countries may consider to continue immunization against poliomyelitis to prevent the risk of a global outbreak due to accidental or deliberate re-introduction of the virus. Following the demonstration of a proof of principle in the 1990s (Kersten et al. 1999) and responding to WHO's call for new polio vaccines (Aylward et al. 2006; Heymann et al. 2005), the Netherlands Vaccine Institute (NVI) continued the development of a Sabin-IPV (inactivated poliovirus vaccine, based on attenuated 'Sabin' poliovirus strains, formalin-inactivated, injectable). In this contribution, a short history of one of the first cell-culture based large-scale biological production processes, and the roadmap towards Sabin-IPV is presented. Finally, the future perspectives will be addressed.

Global polio eradication initiative & rationale for Sabin-IPV development

The prevalence of poliovirus has largely been decreased by the use of Oral Polio Vaccine (OPV), based on life-attenuated Sabin polio strains. However, OPV appears less fit for the post-eradication era. Therefore, development of Sabin-IPV plays an important role in the WHO polio eradication strategy (www.polioeradication.org). The use of attenuated Sabin instead of wild-type Salk polio strains will provide additional safety during vaccine production. Moreover, to prevent the emergence of circulating vaccine-derived polioviruses (cVDPVs), the use of OPV should be discontinued following polio eradication, and replaced by IPV. These cVDPVs are transmissible and can become neurovirulent (similar to wild polioviruses) resulting in vaccine associated paralytic poliomyelitis (Agol 2006; Kew et al. 2005). Such strains can potentially re-seed the world with polioviruses and negate the eradication accomplishments (Minor 2009). Containment in appropriate facilities, reduction of reversion risks in virus passaging, and inactivation of the Sabin strains will further minimize this risk.

Most experts agree that worldwide use of IPV is preferable (Chumakov and Ehrenfeld 2008; John 2009; Minor 2009) because of its proven protective track-record and safety. However, when compared to OPV, the cost-prize for IPV is significantly higher (Heinsbroek and Ruitenberg 2010; John 2009; WHO 2010b). This is mainly due to requirements for: (i) more virus per dose; (ii) additional down-stream processing (i.e. concentration, purification and inactivation), and the related QC-testing, and (iii) containment. Until now, the financial challenge has been a major drawback for IPV innovation and implementation in low and middle-income countries. Therefore, cost-prize reduction is a primary objective in the development of a new IPV. The additional biosafety properties are in favour of using Sabin polio strains in such an endeavour.

Overview of worldwide Sabin-IPV development activities

In the past decades several attempts have been made to prepare a Sabin-IPV product (Doi et al. 2001; Kersten et al. 1999; Murph et al. 1988; Simizu et al. 2006). From these studies it appeared that, relative to using wild-type (Salk) strains for regular IPV, more Sabin virus (or D-antigen) was required to induce comparable levels of immune response. For this reason some companies stopped their Sabin-IPV development programmes in the past decade. However, activities continued elsewhere due to shifting factors in the risk–benefit–cost equation (Ehrenfeld et al. 2009), and the product has been reported in various stages of development. The Japanese Polio Research Institute (JPRI) conducted clinical studies (Doi et al. 2001; Simizu et al. 2006), and entered in collaboration with Takeda for the commercialization (Hickling 2010; Venczel et al. 2009). Recently, the Chinese Academy of Medical Sciences (Kunming Institute of Medical Biology), conducted phase II studies (Liao et al. 2010). Early 2011, in the Netherlands, the research and development and clinical departments of the NVI have rejoined the National Institute for Public Health and the Environment (RIVM). Therefore, Sabin-IPV development is now done at RIVM, and consequently RIVM is planning phase I studies in 2011. In Table 1 the chosen D-antigen amounts per dose for Sabin-IPV are given. From these data it can be concluded that in all cases the target dose for type 1 was chosen lower, for type 2 higher, and for type 3 equal or higher, when compared to that for regular Salk-IPV.

Table 1. Sabin-IPV target D-antigen dose used in clinical studies and compared to the dose of regular Salk-IPV.

	Salk-IPV (DU shd^{-1})	Sabin-IPV (DU shd^{-1})				
		Murph (1988)	Doi (2001)	Simizu (2006)	Liao (2010)	NVI plan 2011
Type 1	40	20	30	3	30	10
Type 2	8	12.5	30	100	32	16
Type 3	32	35	50	100	45	32

DU shd^{-1} = D-antigen Units per single human dose of 0.5 mL

Several differences in immune response between Salk-IPV and Sabin-IPV have been found (Table 1) and multiple efforts have been made to understand this. For example, antigenic properties and immunogenicity of Sabin-IPV are being studied using various methods and techniques at different laboratories (Dragunsky et al. 2004; Martin et al. 2003; Tano et al. 2007). This makes the interpretation and comparison between the various laboratories challenging. Therefore, standardization in analytics and quantification is being strived for and advised (Baca-Estrada and Griffiths 2006; Kersten et al. 1999; Minor 2006).

In order to achieve cost-prize reduction, both the production process and the immune response should be optimized. In addition to that, new stable and attenuated seed strains could be developed such that favourable immunogenic properties are included (Venczel et

al. 2009) and containment costs might be reduced. However, activities in this field are relatively recent (Cello et al. 2002; Macadam et al. 2006; Vignuzzi et al. 2008) and implementation of this approach in a GMP setting needs to be expedited. While polio eradication is moving forward, an alternative for OPV should become available shortly. Therefore, in the current study the readily available Sabin polio strains were used to prepare a Sabin-IPV product. Phase I clinical trial materials were prepared according to the current Salk-IPV production process. Further optimization of the production process is part of a parallel research and development effort, in which also optimization of the immune response is studied by alternative inactivation methods (Jiang et al. 1986) and the use of adjuvants (Dragunsky et al. 2004; Yang et al. 2009).

Salk-IPV technology by Anton van Wezel

IPV production at NVI (and its predecessors RIVM and RIV) dates back to the 1950s. Later, in the 1960s at the RIV in Bilthoven, a process was developed based on micro-carrier technology and primary monkey kidney cells. This technology, developed by Anton van Wezel (van Wezel 1967; van Wezel 1985; van Wezel et al. 1979; van Wezel et al. 1984) and co-workers, was freely shared with several pharmaceutical companies (GSK, Sanofi Pasteur, Novartis) and institutes worldwide. Even today, at various locations, comparable processes are in operation for the production of polio (Duchene 2006; Montagnon et al. 1983; Vidor et al. 1997) and other viral vaccines (van Wezel et al. 1984; van Wezel et al. 1978).

The IPV production process has been described earlier (Duchene et al. 1990; Montagnon et al. 1983; van Wezel 1985; van Wezel et al. 1979; van Wezel et al. 1984). Therefore, here it is outlined in short and a schematic overview is given in Figure 1. Cell culture can be divided in three scale-up stages. The process is started by batch-wise cell-growth on Cytodex 1 micro-carriers (GE Healthcare) in a 15 L pre-culture bioreactor on serum supplemented cell-culture medium. Subsequently, for scale-up, cells are detached from the micro-carriers by trypsinization. In the second stage the working volume is increased to 40 L, and extra micro-carriers are added. After an initial batch period, recirculation with fresh medium is started. In this way, up to 5×10^6 viable cells mL^{-1} are obtained. For further scale-up, cell detachment is performed externally in a trypsinization unit. Finally, the cell harvest is split into two identical (or 'twin') production vessels. In this third stage, the cells are grown up to 1.5×10^6 viable cells mL^{-1} in a batch-wise mode. On average, the total time-line for the cell culture stages is 15 days. For virus replication, cell-culture medium is drained and replaced by serum-free medium. Temperature is lowered and seed-virus is added. After three to four days (when full cytopathological effect is observed) poliovirus is harvested. Virus is purified by filtration (clarification by a series of filters, followed by 100 kD cut off ultrafiltration), size exclusion chromatography (SEC) on Sepharose CL-6B (GE Healthcare)

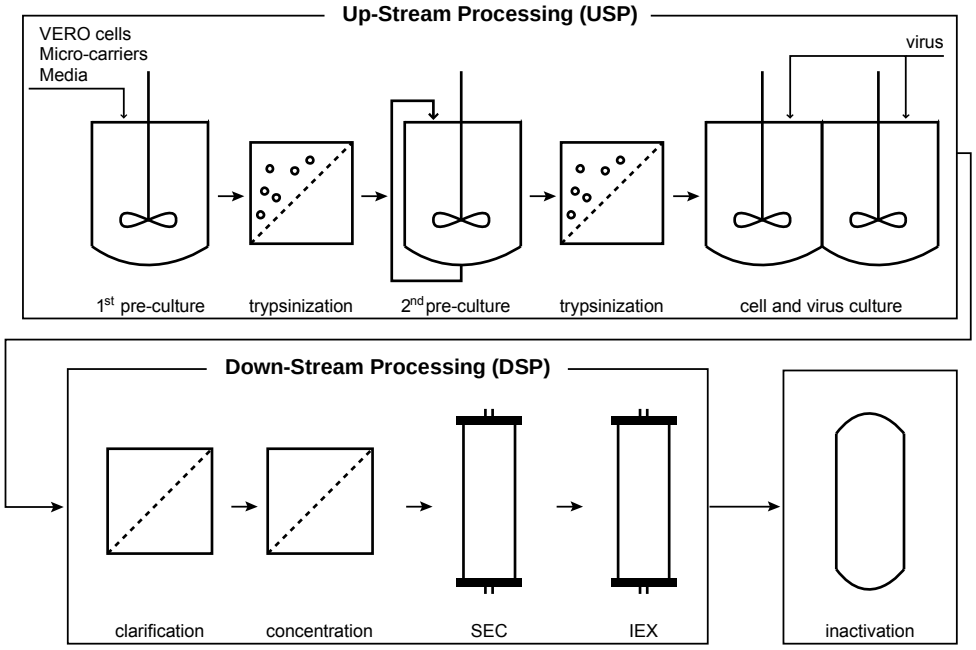

Figure 1. Schematics of the inactivated polio vaccine production process. During upstream processing cells are expanded using two pre-culture steps prior to cell culture and virus culture. The downstream processing consists of clarification, concentration, size exclusion chromatography and ion exchange chromatography followed by inactivation. To obtain trivalent polio vaccine this procedure is followed for each poliovirus type separately prior to mixing for end product formulation.

and ion exchange chromatography (IEX) on DEAE Sephadex A-50 (GE Healthcare) in a phosphate buffer. To the processed virus, M199 and glycine (final concentration 5 g L^{-1}) are added and the fluid is filtered through a 0.22 μm pore size filter (Millipak-200, Millipore) prior to inactivation. Inactivation is performed using 0.025% formalin during 13 days (with in between 0.22 μm filtration) at 37 °C according to World Health Organization (WHO) requirements. In summary, some unique characteristics of this platform production process are:

- Cell culture start-up directly from the ampoule into the pre-culture bioreactor (van Wezel 1985).
- Use of micro-carriers as surface for adherent cell culture and scale-up in bioreactors (van Wezel 1967).
- Efficient scale-up using industrial-scale production vessels in only three pre-culture expansion steps (Van Wezel and van der Velden-de Groot 1978).
- Application of engineering principles to animal cell-culture, resulting in no requirement for additional oxygen sparging (van Hemert et al. 1969; Van Wezel and van der Velden-de Groot 1978).

- Serum-free production stage due to washing-steps and media exchange before virus inoculation (Van Wezel and van der Velden-de Groot 1978).
- Highly purified virus, resulting in relatively low levels of host-cell proteins (below 0.3 µg protein nitrogen/dose) (van Wezel et al. 1979; van Wezel et al. 1984), and host-cell DNA (below 5 pg/dose) (Montagnon et al. 1984; van Wezel et al. 1981) in the trivalent vaccine.
- Applicable to various viral vaccines (van Wezel et al. 1979; van Wezel et al. 1978).

Scale-up in bioreactors (Bilthoven units)

The IPV production process has been updated several times. Initially, starting in the 1950s, primary monkey kidney cells growing in monolayers in culture flasks were used to replicate the poliovirus. However, seeing the growing IPV demand, soon scale-up and reduction of the required number of monkeys became major objectives (van Wezel 1981; van Wezel et al. 1980). This resulted in using the micro-carrier technology (van Wezel 1967) in combination with the so-called "Bilthoven Units" (bioreactor vessels and control units originally used for microbial cultures) (van Hemert et al. 1969) for large-scale (up to 300 L) production in the 1970s (Van Wezel and van der Velden-de Groot 1978). Further, secondary and tertiary monkey kidney cells were used from the 1980s onwards (van der Velden-de Groot 1995). Also in the mid 1980s, industrial scale (700 L) micro-carrier based cell cultures were realized in twin 350 L bioreactors. Subsequently, in 2004 the Vero cell line was introduced at NVI, followed by scale-up to twin 750 L bioreactors in 2005. Although polio eradication might be on the doorstep the innovation and optimization remains a topic of attention. An example of such a possible innovation is the development of Sabin-IPV based on attenuated polio strains. Moreover, awareness regarding the potential risk of introducing foreign agents is growing and may require the development of production processes free of animal-derived components.

Scale-down for future improvements

From the substantial history in polio vaccine production at RIV, RIVM and NVI, a valuable data set has been generated. It comprises more than 60 production runs, based on Vero cell culture, at two different (350 L and 750 L) bioreactor scales. To extract relevant information, like operating ranges, multivariate data analysis (MVDA) was applied (Bakker et al. 2010; Thomassen et al. 2010). This statistical approach is stimulated by ICH to improve the scientific understanding of production processes for trouble shooting, and to support better process control. Subsequently, based on the MVDA analysis, a scale-down model of the current twin 750 L bioreactors has been setup for both up-steam processing (USP: cell- and virus-culture) (Bakker et al. 2010) and down-stream processing (DSP: clarification, concentration, purification and inactivation) unit operations. Currently, at this lab-scale, both USP and DSP approximate the large-scale process and improvement studies are in progress. This includes the application of other culture methods at increased cell densities,

animal component free media, and optimizations by a design-of-experiments approach (e.g. for nutrients, micro-carrier concentration, multiplicity of infection (MOI)) in multiple parallel bioreactors.

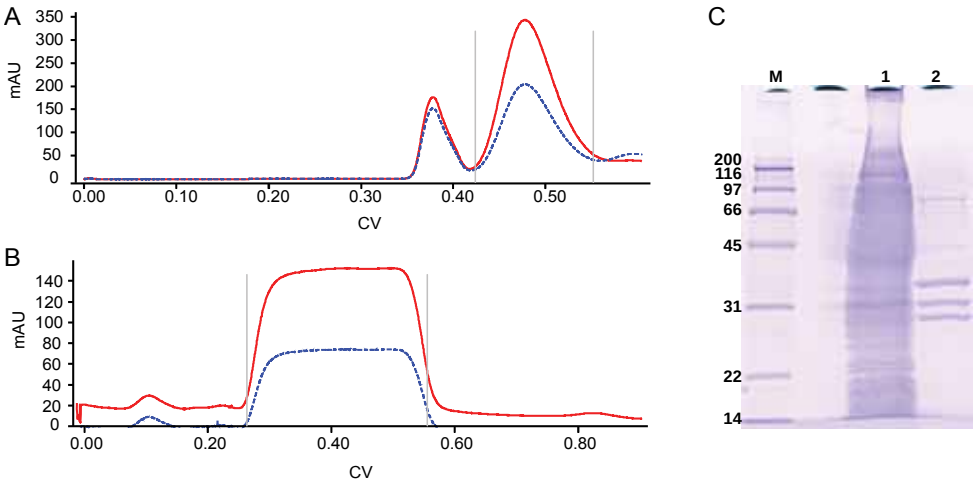

Figure 2. Purification of Sabin type 3 poliovirus. Panel A: Chromatogram of SEC, grey lines indicate product collection; Panel B: Chromatogram of IEX, grey lines indicate product collection; Panel C: SDS-Page, Lane M: Marker; Lane 1: Clarified virus harvest; Lane 2: Purified and inactivated Sabin type 3 product. Bands in lane 2 represent the viral proteins VP1 (33 kDa) VP2 (30 kDa) and VP3 (26 kDa).

Sabin-IPV development

Before moving to the preparation of clinical trial material, initial proof-of-principle studies have been done to confirm immunogenicity of Sabin-IPV. For that, monovalent OPV bulk products were provided by the largest WHO pre-qualified OPV Manufacturer (Bio Farma, Indonesia) to subsequently prepare Sabin-IPV, using the Salk-IPV scale-down model of the DSP unit operations (see Figure 1). In these lab-scale proof-of-principle studies 10–20 L OPV bulk per virus type was purified and inactivated by formalin treatment. In Figure 2, an example of results for purification of Sabin virus is given. Initial purification is done using SEC (Figure 2A) to separate virus (2nd peak) from large (intra-cellular) molecules (1st peak). During the following IEX (Figure 2B) impurities are bound to the column matrix and the product remains unbound. SDS-PAGE (Figure 2C) shows the starting material (Lane 1) compared to the purified product (Lane 2). The purified and inactivated viruses are subsequently formulated in a trivalent Sabin-IPV. The obtained trivalent product was used for characterization and formulation studies, and immunogenicity studies in rats. The results showed that the product was immunogenic in rats and indicated future human dose requirements (Table 1). Purification of OPV bulks using the scale-down model was successful. This implies that current OPV manufacturers could, in principle, switch to IPV

production by implementation of the DSP unit operations. However, for IPV production relatively large quantities of virus are required (approximately a factor 100–800 more, depending on the subtype and assumed in-process yields) when compared to that for OPV (Duchene et al. 1990; Kreeftenberg et al. 2006). Consequently, the cell- and virus-culture capacity should be scaled up accordingly. Therefore, from this point in the development no OPV was used anymore as a starting material for DSP, and a switch was made to in-house USP (cell- and virus-culture) at lab- and production-scale.

Scale-up–scale-down approach

The Sabin-IPV production process was based on the scale-down model of the current, Salk-IPV process (using wild-type poliovirus strains). After the proof-of-principle studies and using the scale-down model (Bakker et al. 2010; Thomassen et al. 2010), Sabin-strain specific adaptations like MOI and a lower virus culture temperature were initially studied at lab-scale to confirm earlier findings from large-scale OPV production (Kreeftenberg et al. 2006; van der Velden-de Groot 1995). Additionally, the clarification unit was modernized, using disposable filters (Millipore) instead of a Celite cake for depth-filtration. Subsequently, specifications were derived for the large-scale operation. The resulting Sabin-IPV process was then developed up to a production-scale (i.e. two 350 L bioreactors; working volume) using well-established equipment to produce inactivated trivalent polio vaccine (according to current GMP-guidelines) for pre-clinical studies and clinical trial purposes. The Sabin-IPV product thus obtained meets the current European release criteria for Salk-IPV and will follow, where appropriate, WHO guidelines. To be able to quickly show proof-of-principle, no further process optimization and/or modernization (e.g. application of increased cell densities or replacement of animal-derived components) was done in this stage of process development. In parallel to production of the clinical trial material, further process development, optimization and formulation research is being carried out to optimize the process and ultimately reduce cost per dose. For that, a scale-down/scale-up approach is being followed (Oosterhuis 1984; Rathore et al. 2005a; Rathore et al. 2005b; Sweere et al. 1987). In summary, the scheme in Figure 3 will be applied for shifting from large-scale routine Salk-IPV, via the lab-scale equivalent, to future Sabin-IPV production. Initially, the lab-scale process will be used for training purposes. Next, the optimized process will be used at pilot-scale. Technology transfer will allow local manufacturers to implement the production-scale version in their own facilities.

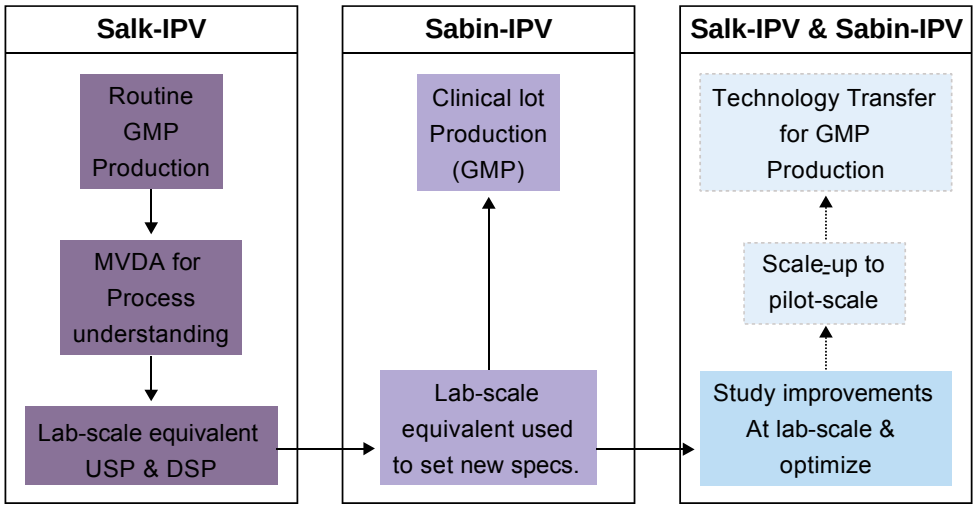

Figure 3. Schedule for shifting from routine Salk-IPV to Sabin-IPV production by using a scale-down approach. The first two panels on the left have been done. Currently, improvements and optimization are studied at lab-scale. Ultimately, the optimized process will be used at pilot-scale for Technology Transfer purposes

Virus seedlot (master & working) production

New Sabin polio master- and working-virus seeds were prepared in compliance with cGMP-guidelines and viral safety guidelines using the routinely used NVI Vero working cell bank (derived from the WHO Vero cell bank no. 87-10). The virus master- and working-seedlots were prepared at a relatively large size (10 L and 350 L bioreactor working volume, respectively) for this stage of product development. This was done to anticipate for future technology transfer purposes and the related distribution of working seedlots to collaborating partners.

Sabin poliovirus strains (starting materials) used for master seedlot production were chosen as close as possible to the Sabin original strains:

- WHO Type 1 (LSc 2ab KP_2), OPV (Sabin) Seed (SO+1 = Sabin Original + 1 passage) 1976 Behringwerke (supplied by WHO to RIVM in 1990).
- WHO Type 2 (P712 Ch2ab-KP_2): OPV (Sabin) Seed (SO+1) 1976 Behringwerke (supplied by WHO to RIVM in 1990).
- Type 3 (Lot 457-III-Pfizer) RSO1 (RNA-derived virus from Sabin strain Leon 12a$_1$b), 1963 Pfizer (supplied by Institut Mérieux to RIVM in 1991).

From the produced master seedlots working seedlots were prepared. Production of both master and working virus seedlots was done using the following conditions. Vero cell cultivation setpoints were: T = 37 °C; DO = 50%; pH = 7.2. Virus cultivations setpoints were: T

= 32.5 °C; DO = 25%; pH = 7.4. For master seedlots the used MOI for types 1, 2, and 3 was 0.04, 0.008, and 0.1, respectively (based on using one complete ampule and nominal titers). The MOI used for working seedlots was 0.01 independent of the virus type. Master seedlots were filled in 1, 10 and 20 mL vials, working seedlots were filled in 20, 25, 50, 100 and 125 mL vials. The obtained virus titers in the master- and working-seedlots (Table 2) meet general production requirements.

Table 2. Sabin poliovirus Master- and working seedlots virus titers (determined on Vero cells).

Sabin poliovirus	Master seedlot virus titer (Log_{10} $CCID_{50}$ mL^{-1})	Working seedlot virus titer (Log_{10} $CCID_{50}$ mL^{-1})
Type 1	8.85	8.90
Type 2	7.52	7.55
Type 3	8.23	8.45

(Pre)clinical trial material production of Sabin-IPV

Using the newly generated working seedlots, Sabin-IPV was produced at production-scale (2 × 350-L bioreactor working volume) under cGMP according to the slightly modified (regarding MOI, virus culture temperature, and clarification unit) Salk-IPV production process. In this way, for each Sabin polio type two monovalent pools were produced (6 monovalent pools in total). Awaiting Quality Control testing for release for human use, the pre-clinical tests are being performed. The clinical phase I study is anticipated in 2011.

Table 3. Sabin poliovirus and D-antigen yields per cell (this study) compared to that for Salk poliovirus (Montagnon et al. 1981).

	Vero cells[1)] ($\times 10^6$ cells mL^{-1})	Virus titer[1)] (Log_{10} $CCID_{50}$ mL^{-1})	D-antigen[1)] (DU mL^{-1})	DU / cell ($\times 10^{-5}$ DU $cell^{-1}$)	Virus / cell ($CCID_{50}$ $cell^{-1}$)	DU / virus [$\times 10^{-7}$ DU $CCID_{50}^{-1}$]
Type 1 Sabin	1.10 ± 0.22	8.65 ± 0.18	120 ± 9.42	11	402	2.7
Type 1 Salk	1.52 ± 0.69	8.25 ± 0.14	84.8 ± 8.68	5.6	117	4.8
Type 2 Sabin	0.97 ± 0.22	7.77 ± 0.26	24.5 ± 1.29	2.5	60	4.2
Type 2 Salk	1.06 ± 0.15	8.18 ± 0.46	20.3 ± 4.72	1.9	144	1.3
Type 3 Sabin	0.97 ± 0.14	8.28 ± 0.27	55.7 ± 11.0	5.7	195	2.9
Type 3 Salk	0.80 ± 0.27	7.83 ± 0.60	54.3 ± 9.96	6.7	83	8.1

[1)] average and standard deviation are given Sabin (n=4) Salk (n=6)

Despite the long-standing history, polio production yields from cell culture stages are rare in literature. To the authors knowledge no data on Sabin polio replication in Vero cells is available in literature. Therefore, an initial comparison with Salk polio production data available from Institut Mérieux (Montagnon et al. 1981) was made (Table 3). The observed D-antigen levels appear comparable for Salk and Sabin types 2 and 3, and slightly higher for Sabin type 1 when compared to Salk type 1 (Table 3). However, direct comparison of D-

antigen concentrations (DU mL^{-1}) is questionable as other Vero cell densities and experimental conditions were used. Therefore, yields per cell may give a better comparison. From this, DU per cell and virus per cell appeared to be in the same order of magnitude, where Sabin type 1 appears to be slightly higher. However, the amount of D-antigen per infectious virus particle appeared comparable (i.e. in the same order of magnitude) for all types at approximately 4×10^{-7} DU/$CCID_{50}$.

Before starting clinical studies pre-clinical trivalent products (both Al(OH)3-adjuvated and non-adjuvated) have been made for toxicity studies in New Zealand white rabbits. The product requirements were extracted from EP (Ph Eur 6.7:0214 ; Ph Eur 6.3:0153) and WHO guidelines (WHO 2002a; WHO 2004; WHO 2002b). Toxicity studies did not show vaccine related toxic effects. A target vaccine dose was derived from immunogenicity studies (described in the next paragraphs). The tested doses (chosen double compared to the target dose) were 10–16–32 DU shd^{-1} (D-antigen Units per single human dose) for adjuvated Sabin-IPV, and 20–32–64 DU shd^{-1} for plain Sabin-IPV. Also Salk-IPV was included in these studies as a reference. The monovalent pools and the final lots (filled in vials) are also used in stability studies at 2–8 °C, which will run for several years (four years for the monovalent pools and three years for the final lot).

Plans for further process improvements

Animal derived components (e.g. bovine serum and trypsin) have been used in the current Sabin-IPV manufacturing. These components should preferably be replaced by animal origin free alternatives to minimize the risk of adverse effects (e.g. the potential transfer of viruses and/or prions). Therefore, the use of defined and animal-component free cell culture media is being investigated (Rourou et al. 2009a; Rourou et al. 2009b). Moreover a better scientific understanding of the process resulting in improved process control and ability for trouble shooting can be created. Another potential improvement can be found in the currently used, relatively low, cell densities (at approximately 1×10^6 cells mL^{-1}). Assuming comparable virus quality and yields per cell, the use of increased cell densities can potentially result in more efficient use of bioreactor capacity, and ultimately reduce the cost per dose. The use of increased cell densities is a well-known approach that can be adapted from (heterologous) protein production processes. A drawback is the strictly adherent growth (to micro-carriers) of the Vero cells without carry-over. This limits the maximum obtainable cell-densities in suspended bioreactor cultures to a relatively lower level when compared to single cell suspension cultures. A start has been made to find alternative cell culture methods to obtain high cell densities prior to virus cultivation or for cell expansion. First experiments in animal-component free media have yielded adherent Vero cell concentrations of approx. 8×10^6 cells mL^{-1}. Another limitation at higher cell densities could be oxygen supply that may need to shift from head space aeration to (mild) sparging (without causing adverse effects on the cells on microcarriers).

Antigenicity, immunogenicity and standardization

Experimental lots (formulated both from lab-scale, and large-scale production) were characterized for their antigenic and immunogenic (rat potency test) properties. The immunogenicity of Sabin-IPV was compared with that for the Salk-IPV international reference in rats. Sabin-IPV type 1 immunogenicity per DU appeared to be higher than that for Salk-IPV. Immunogenicity of Sabin-IPV type 2 per DU vaccine was lower as compared to that of Salk-IPV. Both Sabin-IPV and the Salk-IPV type 3 have comparable immunogenicity per DU. This confirms earlier findings (Kersten et al. 1999). However, the use of Salk and Sabin strains and the absence of a clinically tested Sabin-IPV reference vaccine compromises proper quantification. Ideally, a comparison based on active concentration should be made. A detailed antigenic and immunogenic evaluation, addressing this problem will be published elsewhere (Westdijk et al. 2011).

Table 4. Proposed D-antigen content per single human dose (DU/shd) of Sabin-IPV and Aluminum hydroxide adjuvated Sabin-IPV for phase I clinical studies.

Dose	Sabin-IPV (type 1 – 2 – 3) (DU shd^{-1})	Aluminum hydroxide adjuvated Sabin-IPV (type 1 – 2 – 3) (DU shd^{-1})
High	20 – 32 – 64	10 – 16 – 32
Middle (target)	10 – 16 – 32	5 – 8 – 16
Low	5 – 8 – 16	2.5 – 4 – 8

Optimization of the immune response

From formulation research and rat potency testing, the target plain (non-adjuvated) Sabin-IPV dose was set to 10–16–32 DU shd^{-1} (for type 1, 2 and 3, respectively). For a comparison, the Salk-IPV reference is 40–8–32 DU shd^{-1}. In addition, to indicate possibilities for dose sparing purposes, the use of an adjuvant (available in the public domain) was also studied. Aluminum hydroxide increased the potency (dose 5–8–16 DU + 0.5 mg aluminum hydroxide per dose) in rats with a factor 2–3 (type 1 and 3) or with a factor 2–4 (type 2). From these results the proposed phase I clinical trial doses shown in Table 4 were derived.

Technology transfer

RIV, RIVM and NVI have a long-standing experience in large scale bioreactor-based bacterial and viral vaccine manufacturing and formulation, including combination vaccines such as DPT–IPV (*diphtheria–pertussis–tetanus*–IPV). As Dutch governmental agencies, the NVI and the RIVM strive to meet national public objectives but also contribute to international goals such as to increase access to relevant vaccine technology for Developing Country Vaccine Manufacturers (DCVM) (Jadhav et al. 2008; Milstien et al. 2007). A recent example of technology transfer by the NVI to DCVM partners is Hib

(*Haemophilus influenzae type b*) as bacterial conjugate vaccine (Hong et al. 1996; Kreeftenberg and Hamidi 2007).

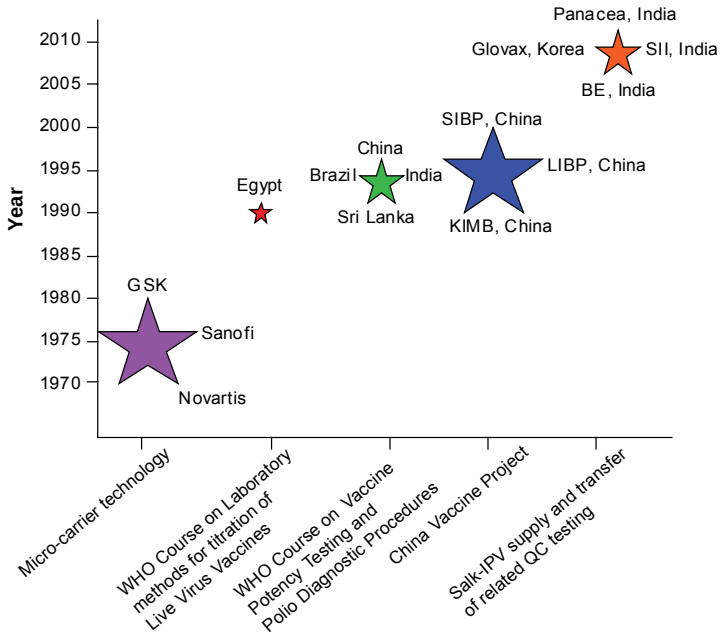

Figure 4. Overview of the transfer of know-how related to polio vaccine production. In the 1970s micro-carrier technology was transferred to different companies/institutes. After that, various courses were organized, and bulk product was supplied to local manufacturers. Sabin-IPV technology transfer will continue this tradition.

The transfer of know-how related to polio vaccine manufacturing has been a continuous activity since the 1970s and transferring the Sabin-IPV technology will be a next step in this existing tradition (Figure 4). For example, in the 1990s RIVM participated in a World Bank project to transfer large-scale production know-how on OPV, Measles Virus, and DPT to China (Kreeftenberg et al. 2006; van Noort 1992). This project not only included the process development for these vaccines at the scale needed for the Chinese market, but also the design, commissioning, realization and validation of the relevant equipment and GMP compliant buildings for vaccine facilities in Kunming, Lanzhou and Shanghai. Currently, the Kunming facilities are still in use to manufacture their Sabin-IPV product (now in phase II studies; see Table 1). Projects like the China Vaccine Project and the Hib vaccine project had a worldwide impact on both the vaccine prices and the accessibility to modern technologies.

Sabin-IPV workshop

As several DCVM have expressed interest in the Sabin-IPV technology, NVI recently organized a three-day workshop to introduce the concepts of Sabin-IPV manufacturing and quality control. During this workshop 27 representatives from DCVM discussed the feasibility of a number of crucial issues with key-persons from WHO and NVI. For example, containment regulations following GAPIII (Global Action Plan, version III, to minimize poliovirus facility associated risk) (WHO 2009) and their necessity and applicability for Sabin-IPV determine the required investment level in manufacturing facilities. Also, it was concluded that Sabin-IPV specific regulatory guidelines should be developed. Both the Sabin-IPV workshop, and a call for expression of interest by the WHO, made it possible for various parties to disclose their interest. As a result the first two potential partners were selected. The transfer of technology at the individual manufacturer site is expected to start in 2011. Future partners will receive the existing Sabin-IPV production process and related QC testing and are encouraged to participate in further optimization of the actual process in order to make the vaccine more affordable.

Sabin-IPV training course

RIVM is planning to follow approximately the same technology transfer strategy for Sabin-IPV know-how as applied earlier for Hib vaccine. At first documents and support will be provided to the partners in order to allow organization of the required infrastructure and personnel. Secondly, hands-on training will take place at the RIVM, to show the manufacturing process at lab- or pilot-scale and to transfer the related in-house QC testing. Finally, a follow-up training program will be set-up together with each partner individually. This follow-up training will most likely take place approximately 6 months later at the partners site.

The concept of technology transfer for Sabin-IPV was originally taken from WHO's hub concept applied successfully for pandemic flu (Friede et al. 2009). In essence this is designed to maximize the number of DCVM recipients, consistent with WHO's Global Plan for such pandemic vaccine supply. Consequently, the thresholds for DCVM to be admitted to courses and training activities is relatively low. In contrast, the WHO approach for Sabin-IPV technology transfer emphasizes on biocontainment criteria (GAPIII) and the historical track record of the national regulatory agency of the country where the DCVM resides. This led to a strong selection process, limiting the number of potential recipients. With the successful applicants bilateral agreements will be negotiated based on their requirements for support in bringing this new Sabin-IPV product swiftly to the local markets.

Conclusions

Recently, the NVI and the RIVM continued the development of Sabin-IPV. Such a new vaccine plays an important role in the WHO polio eradication strategy because biocontainment will be critical in the time after OPV vaccinations are stopped. The use of attenuated Sabin strains instead of wild-type Salk polio strains will significantly lower the risk of facilities related outbreaks.

Initially, the Sabin-IPV production process was based on a scale-down model of the current, and well-established, Salk-IPV process. Using this scale-down model, Sabin-strain specific adaptations like MOI, a lower virus culture temperature, modernization of the clarification, were initially studied at lab-scale. In this way, specifications were derived for the large-scale operation. The resulting Sabin-IPV process was then developed up to a production-scale to produce virus seedlots, and inactivated trivalent polio vaccine for pre-clinical studies and clinical trial purposes.

From characterization studies, it was confirmed that the immunogenicity of Sabin-IPV in rats is different as compared to Salk-IPV. Sabin-IPV type 1 is more immunogenic, type 2 is less immunogenic whereas for type 3 only small differences in immunogenicity were observed. The target dose was adapted accordingly. Further, the use of Aluminum hydroxide as an adjuvant increased the potency by at least a factor 2. In parallel, process development, optimization and formulation research is being carried out to further modernize the process and reduce cost per dose.

Finally, technology transfer to vaccine manufacturers in low and middle-income countries is being planned. To inform potential partners, recently a three-day workshop for DCVM was organized at NVI, also including WHO representatives. Crucial issues like containment (according to GAPIII), and development of Sabin-IPV specific regulatory guidelines, were addressed. Technology transfer is expected to start in 2011. Future partners will receive training courses and are encouraged to participate in further optimization of the process, and the formulation, in order to make the vaccine more affordable.

Acknowledgements

This work was supported by the World Health Organization using funds provided by a grant from the Bill and Melinda Gates Foundation. The authors are indebted to Tiny van der Velden-de Groot and Hans Kreeftenberg for their contributions to the Sabin-IPV workshop, carefully reading the manuscript, and fruitful discussions.

Chapter 3

Multivariate data analysis on historical IPV production data for better process understanding and future improvements

Published as:
Thomassen, Y.E., van Sprang, E.N.M., van der Pol, L.A., Bakker, W.A.M. (2010). *Multivariate data analysis on historical IPV production data for better process understanding and future improvements.*

Biotechnology and Bioengineering 107:96-104
dx.doi.org/10.1002/bit.22788

Abstract

Historical manufacturing data can potentially harbor a wealth of information for process optimization and enhancement of efficiency and robustness. To extract useful data multivariate data analysis (MVDA) using projection methods is often applied. In this contribution, the results obtained from applying MVDA on data from inactivated polio vaccine (IPV) production runs are described. Data from over 50 batches at two different production scales (700-L and 1,500-L) were available. The explorative analysis performed on single unit operations indicated consistent manufacturing. Known outliers (e.g., rejected batches) were identified using principal component analysis (PCA). The source of operational variation was pinpointed to variation of input such as media. Other relevant process parameters were in control and, using this manufacturing data, could not be correlated to product quality attributes. The gained knowledge of the IPV production process, not only from the MVDA, but also from digitalizing the available historical data, has proven to be useful for troubleshooting, understanding limitations of available data and seeing the opportunity for improvements.

Introduction

The discovery of an inactivated polio vaccine (IPV) dates back to 1953 (Salk 1953). Even the basis of the current Salk-IPV production process has been established over 40 years ago by van Wezel (van Wezel 1967) using microcarrier technology in the then famous Bilthoven Units. While the production processes might be called "ancient," current manufacturing is performed in modern (GMP certified) production plants equipped with systems for automated control as well as comprehensive data collection. In general, a wealth of information for process optimization or enhancement of efficiency or robustness can be found in the batch records (Charaniya et al. 2008).

Extraction of useful information from batch records requires collecting data from different sources, like paper trace and data historians (systems for data storage), to build a dataset and subsequently apply correct sophisticated statistical tools. Biopharmaceutical manufacturing data are complex, and univariate or bivariate analysis can often be inefficient and might result in misleading conclusions (Kourti 2004). Important information is found in the relationships between process parameters and this information is ignored when parameters are analyzed or tested separately. Multivariate data analysis (MVDA) by means of projection methods overcomes challenges associated with applications such as multidimensionality of the data set, missing data, and variation introduced by disturbing factors such as experimental error and noise (Martin and Morris 2002). Principal component analysis (PCA) (Ringner 2008) and partial least squares (PLS) (Wold et al. 2001) are commonly used projection methods. PCA can be used for process diagnosis in which clusters, outliers and trends evident in process data can be identified. Subsequently, PLS can be used to understand relationships between process parameters and product quantity and quality tests. These multivariate techniques have been used to investigate fermentation and cell culture processes. For example, PCA and PLS have been shown to yield useful information when applied to analyze a cell-culture unit operation (Kirdar et al. 2007). Also, Gunther et al. (Gunther et al. 2007) showed that multivariate statistical techniques allowed fault detection and diagnosis in an industrial fed-batch cell culture process using a relatively small number of batches (~20).

Analysis of manufacturing data using MVDA is stimulated by the American Food and Drug Administration (FDA 2004, guidance on "Process Analytical Technology") in order to improve process understanding of production processes. The initiative was taken up by the European EMEA and the Japanese MHLW. Changes in the production processes, made in order to improve them, bare a risk. Quantified risk assessment can only be done when the influence of the changes on the process or product quality is sufficiently well understood. Hence, central to the FDAs new approach is the knowledge about the essential details of process equipment and its dynamical operation during both upstream and downstream processing (Gnoth et al. 2007). Moreover process improvements should

be based on thorough understanding of the production process. It is therefore imperative to assess the impact of (critical) process parameter (CPP) variation on the products critical quality attributes (CQA) and understand and characterize the sources of process variability (Mitchell et al. 2008).

To improve the knowledge on the current Salk-IPV production process, data mining, using MVDA, on historical batches has been performed. By using data-driven knowledge the objective was to unveil hidden information that might provide insight on possible process improvements that lead to increased robustness and further process optimization.

Data Analysis Strategy

Seeing the rich history in Salk-IPV production at NVI, a large and unique data set has become available in the past decade. It comprised over 50 production runs of three polioviruses, Mahoney (type 1), MEF-1 (type 2), and Saukett (type 3) on the Vero cell line at two different bioreactor scales and the subsequent unit operations that deal with virus purification and inactivation. The available data are heterogeneous with respect to time and data types. It contains on-line data, which is measured continuously and recorded digitally, and off-line data, which is measured occasionally and recorded by paper trace.

The current polio vaccine production process is depicted in Figure 1. In short production of a monovalent bulk comprises the following steps: after thawing, high cell number Working Cell Bank (WCB) vials are used to directly start a 15-L fed-batch pre-culture in which the Vero cells grow on microcarriers (Cytodex 1); after trypsinization to remove cells from microcarriers a 2nd pre-culture consisting of a 40-L recirculation culture (working volume 40-L) is done. The final cell culture is, after trypsinization and reattachment to the microcarriers, carried out in twin bioreactors of either 2 × 350-L or 2 × 750-L followed by a medium change and virus culture. The end of culture for these processes is based on the time after inoculation. Downstream processing consists of clarification by means of dead end filtration followed by concentration using tangential flow filtration (TFF). The purification is done using size exclusion chromatography (SEC) and ion exchange chromatography (IEX). Finally the virus is inactivated using formaldehyde. To obtain a trivalent polio vaccine this procedure is carried out for each poliovirus type separately followed by mixing for end product formulation.

To analyze the data it is in principle preferred to have one model that captures the entire production process, from pre-culture to virus production, purification, and inactivation. However to develop such a model the individual unit operations should be explored first. Using this exploration the feasibility of an overall model can be determined. Important factors to achieve an overall model are (i) the availability of data, (ii) the quality of the

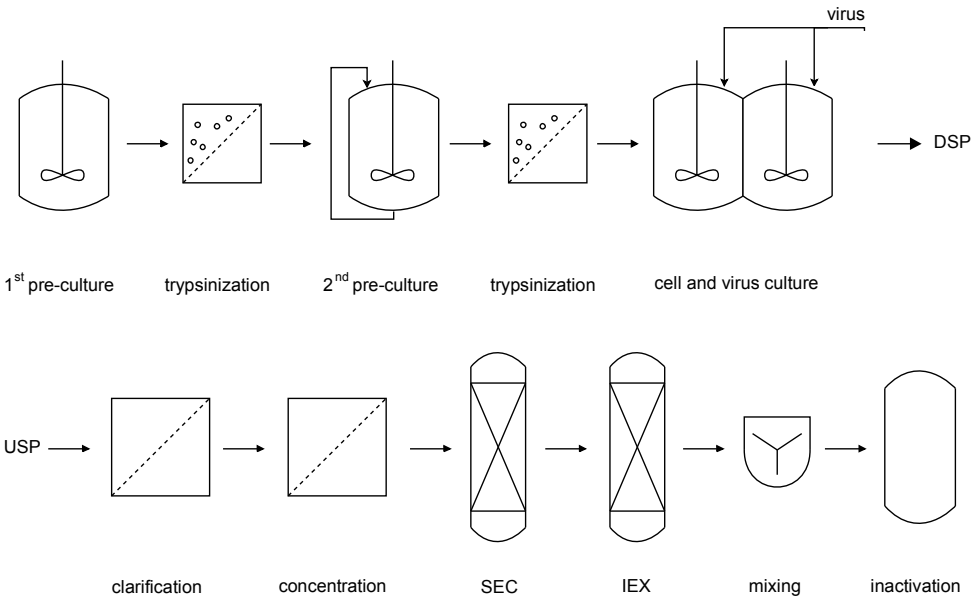

Figure 1. Schematics of the Salk-IPV production process. During upstream processing cells are expanded using two pre-culture steps prior to cell culture and virus culture. The downstream processing consists of clarification, concentration, SEC, and IEX followed by inactivation. To obtain trivalent polio vaccine this procedure is followed for each poliovirus type separately prior to mixing for end product formulation.

data, (iii) the informative power of the collected parameters, and (iv) the structure of the data. This latter factor largely determines the preferred analysis method.

The collected process data can be divided in data measured occasionally (off-line data), that is, during sampling, and continuously (on-line data). The first represents a status of the process at the time of sampling while the second reflects the physical state of the process and the controller responses that are a function of the underlying process dynamics. In an exploratory analysis it is important to keep most of the information present in the data. When combining different data types (i.e. on-line and off-line data) data reduction methods are needed and much of the information is lost. The used modeling strategy aimed at retaining as much information as possible while reducing the dimensions of the data to a degree that analysis remained practical. It was therefore chosen to analyze on-line and off-line data separately during the explorative analysis. The analysis was unbiased meaning that it was performed by a statistical expert who had no previous knowledge of the Salk-IPV production process.

Methods

Data Collection

In the past decade more than 50 production runs (including rejected and aborted batches) of the poliovirus subtypes 1, 2, or 3 on the Vero cell line were performed. Data used in this analysis comprised 38 batches produced at 700-L scale (2 × 350-L bioreactors) and 12 batches produced at 1,500-L scale (2 × 750-L bioreactors). For each unit operation both on-line data and off-line data were collected. For example for the final cell culture, data consisted of 75 off-line measured parameters and 12 or 9 (350-L or 750-L respectively) on-line parameters. Off-line parameters (like amount of media components, daily cell counts, nutrient concentrations and sterilization times) had been recorded manually and were collected from paper. On-line parameters (e.g., pH, DO, T) were in a digital format.

Data Preprocessing

Off-Line data

The data were collected for each unit operation in a matrix X (I × J), with I being the batch and J the process variables. Process variables (J) with a large amount of missing values (over 15%) and process variables with little or no variation were excluded from the analysis. Data from this matrix was used for exploration of the CPP and univariate and bivariate analysis.

Performance analysis was done using a multivariate approach as in-process variables are likely correlated. Prior to performance analysis, using PCA, data were centered (towards a mean) so that the model describes deviations from the mean, and scaled so each parameter has equal influence to the model. When applicable, volume specific data were normalized or virus type specific data were omitted to investigate operational performance.

On-Line Data

On-line data, consisting of real-time process data measured with a regular time interval, was synchronized to a reference batch to obtain equal run lengths. Synchronization was done using the dynamic time warping strategy originally developed for speech recognition (Sakoe and Chiba 1978). The synchronized batches were collected in a matrix X_{sync} (I × J) with I being the batch and J the synchronized data. Performance analysis based on on-line data were done using PCA transformation.

In general, on-line measured data could be discriminated in two groups. The first group represents dynamic variables such as pH controller output and CO_2 flow, the second group represents non-dynamic variables such as pH and temperature. Although the latter are

important and give information in the operational settings of the batch, they were run at setpoint and are not varied in this production process. For performance monitoring they are less informative (the derivative is equal to zero).

Software

Commercially available technical computing software, MATLAB (MathWorks, Inc., Natick, MA) was used to perform data analysis. Prior to analysis, process data were assembled in Excel (Microsoft, Redmond, WA).

Expert Analyses for Interpretation

As the data analysis was performed unbiased by a statistical expert, interpretation of the data for process understanding needed to be done by process development specialists (Charaniya et al. 2008).

Results

First the type of outputs that were obtained from MVDA will be introduced. Subsequently the results from the analysis of the different unit operations will be given.

Projection of the matrix X(I × J) with I observations or batches and J variables or process parameters by means of PCA is done by building a PCA model given by the mathematical expression:

$$X = TP' + E \qquad \text{(Eq.1)}$$

where T is the score vector matrix, P, the loading matrix, and E is the contains the residuals. The score vector matrix T (one vector for each component) consists of the projected values for I objects in the hyperplane. The t-values (also referred to as scores) can be used to relate objects to another in a PCA score plot. The distance to the hyper plane is determined by the residual matrix E. How the original variables J are weighted together in a principal component (PC) is expressed by the loadings P (Gabrielsson et al. 2002).

A summary of the performance or the process behavior over time can be seen in a PCA score plot (e.g., Figure 2). Here the vectors for the first two PCs are plotted, t1 and t2, against each other (Cunha et al. 2002; Martin and Morris 2002). It is important to note the percentage variability explained by the PCA model and the percentage explained by these first two PCs when interpreting the significance of the plot. It is common to also plot an ellipse on this set of axes to represent the Hotelling T^2 95% confidence interval; here also the 99% confidence intervals are depicted. Observations outside the 95% confidence interval are considered outliers and these batches can be considered out of control (Kirdar et al. 2007). Other outputs generated using PCA are the squared model residuals (E in Eq.

1) and the scores (T in Eq. 1). These PCA score plots can be used for more detailed outlier detection and root cause finding.

Pre-Cultures

While the production line has been scaled-up from 2 × 350-L to 2 × 750-L production bioreactors, the 1st and 2nd pre-culture stages have remained the same in scale. Since the pre-cultures are likely independent of the production scale, simultaneous PCA analysis of all 50 batches, with 104 (1st pre-culture) and 117 (2nd pre-culture) off-line variables, was done for both unit operations. The PCA score plots of the 1st pre-culture (Figure 2A) and 2nd pre-culture (Figure 2B) can explain 45% and 30% of the variation, respectively. The observed outliers were checked and appeared to have known and reported deviations.

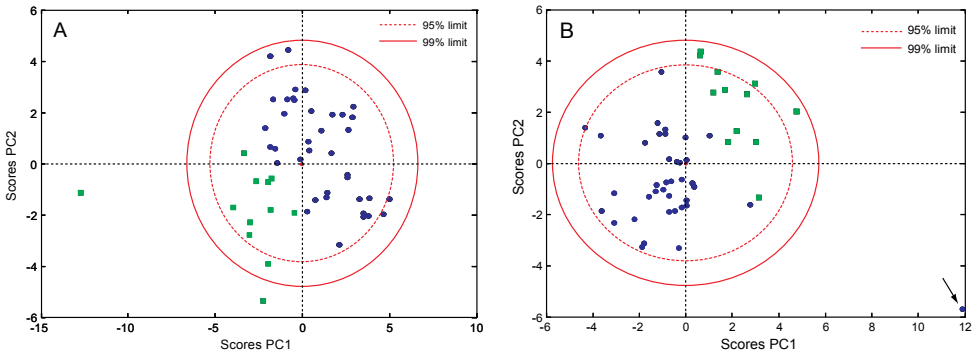

Figure 2. PCA score plot of the (A) 1st pre-culture stage and (B) 2nd pre-culture stage. Clustering between control unit 1 (blue circles) and control unit 2 (green squares) was found both indicating a structural difference introduced with the new bioreactor control unit. Outlier is indicated with an arrow.

Unexpectedly, clustering was observed when batches were marked based on production line (i.e., final production vessel 2 × 350-L or 2 × 750-L) (Figure 2). The observed clustering indicates the presence of structural operational differences. More detailed data analysis revealed that the glucose concentration at the start of cultivation (being 7.9 ± 0.6 and 8.7 ± 0.7 mmol L^{-1}, respectively) was an important factor for the variation between the production lines observed in the 1st pre-culture. This difference in glucose concentrations was caused by a minor adaptation in the media preparation. Detailed analysis for the 2nd pre-culture however did not result in a clear, or one parameter, distinction between the production lines. A possible explanation for the difference might be found in the control units that were used. Parallel to the scale-up of the production bioreactors from 2 × 350-L to 2 × 750-L the pre-culture bioreactor control units were replaced. A new control unit, same type and manufacturer, was installed. After close comparison of these units it was concluded that different mass flow controllers, different software package and automated instead of manual agitation strategy were introduced with the new unit. These

adjustments could have led to the observed differences. Likely this also is a factor during the 1st pre-culture in addition to the difference in glucose concentration at the start of cultivation.

Cell Culture

The final cell culture was done in production scale twin bioreactors at two different scales, 2 × 350-L and 2 × 750-L. Due to the volumetric differences PCA analysis should be performed for both bioreactors scales separately. When the data are analyzed simultaneously, a PCA score plot depicting two groups representing the different production scales is obtained as was shown previously (Bakker et al. 2010). Separate multivariate analysis of the 2 × 750-L bioreactors was not performed from this unit operation due to the low number of productions at this scale. The performance of the batch to batch consistency produced at 350-L scale in two different production vessels was studied by developing a subspace model. This five component PCA model (61.1% explained variance) was based on 38 runs carried out in twin vessels resulting in 76 batch runs with 48 process variables. The scatter plot of the first two PCs is given in Figure 3. The individual bioreactors are marked with either open or closed circles. In Figure 3 it can be seen that the open and closed circles are randomly distributed and that both bioreactors were operated in a similar way.

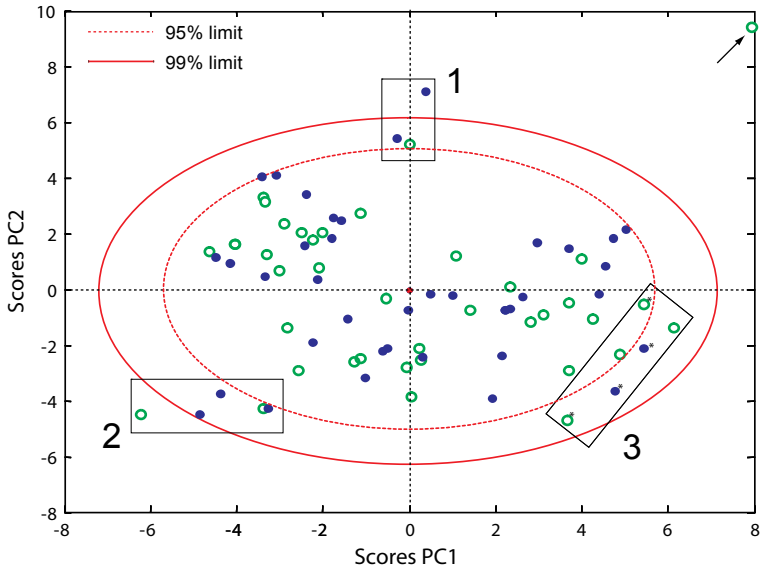

Figure 3. PCA score plot of the cell culture at 2 × 350-L scale. Individual bioreactors, marked as open green and closed blue circles, can be considered identical. Clusters indicated by boxes 1 and 2 represent batches with deviating conditions. In cluster 3 the experimental batches are indicated by an asterisk.

Following the comparison between the two vessels the batches that are far from the center of the score plot were examined. For example the open circle in the upper right corner (Figure 3) corresponds to a batch with a reported operational error. Next the interesting areas in the data were observed. These are the areas where the data seems to be clustered in the outer rim. These clusters are defined as cluster one, two, and three and are marked by a box in Figure 3. The common features for the first cluster are: DO, glucose and osmolarity. Relative low glucose concentration was observed at inoculation. The second cluster has the following features in common: relative high cell density and relative low DO. The common features for the third cluster are the microcarrier concentration, the glucose consumption, the glucose concentration and the pH. While clusters were observed in which DO or pH, both within controlled range, contributed to differentiation of these clusters from the center, no extreme values were found. The data in cluster three, four dots of the boxed data in the figure, corresponds with experimental batches in which a different medium was used. Within the inner rim a cluster may be observed in the upper left quadrant. Batches in this cluster have a lower microcarrier concentration in common.

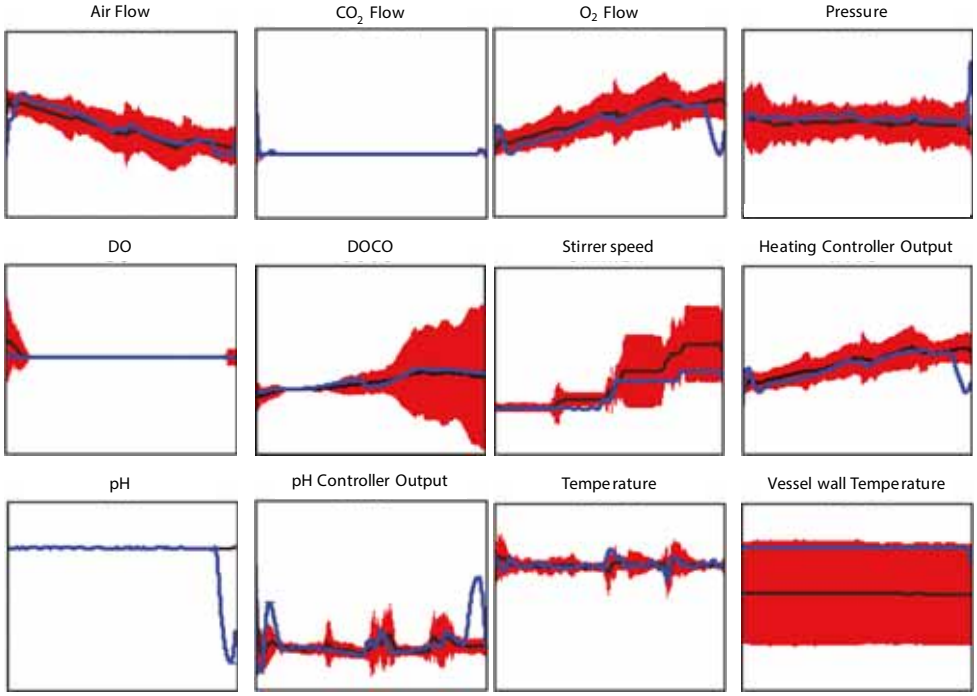

Figure 4. Example of inspection at process variables level, like controller outputs. The blue line represents the suspicious batch. The red area represents the range of operation of the synchronized profiles. The observed different behavior is caused by an event that took place at the end of the culture and is evident from multiple variables.

Time series analysis of the synchronized on-line data showed that specified ranges around setpoints were maintained and a common characteristic profile for the controller outputs was found. This confirms the conclusion based on the off-line data that there is consistency in de operational execution of the process. Moreover this synchronized data can be used for performance monitoring. Using PCA, batches with divergent profile could be discriminated (PCA score plot not shown). These batches were inspected at variables level. In Figure 4 an example of such an inspection is given. The observed different behavior is caused by an event that took place at the end of the culture and is evident from multiple variables being the O_2 flow, pH, pH controller output, temperature control, and pressure. This example illustrates the possibilities of these analysis methods for process control and their use in root cause finding for troubleshooting.

Using PLS the CQA (cell concentration at the end of culture and cell divisions) were related to process parameters. The identified process parameters were the input variables, in particular but not surprisingly the start cell concentration (data not shown). Unfortunately it was not possible to statistical significantly relate other process variables to the yield leaving a large part of the observed variation unexplained. Due to the relatively low amount of batches for this type of statistical analysis it was not possible to prove that weak relations between variables were statistical significant. Another difficulty that was encountered using regression analysis for this kind of production data are that the measurement variation (e.g., cell counts using a manually operated counting chamber) is relatively large while important process variables like temperature and pH are strictly controlled. Since the main variation during cell culture is caused by the input parameters detection of possible deviating batches can be done using relative simple monitoring tools like statistical process control charts as shown in Figure 5.

Virus Culture

On the level of process operation the poliovirus cultivation procedure is independent of the virus strain which is produced. PCA analysis on the entire data set was done. Type specific data like D-antigen concentrations or virus titers was omitted from the matrix. The analysis showed operation indeed was independent of poliovirus type (data not shown).

Using PLS, relations between process parameters that correlate with product yield were studied. However, the process variation was small while the variation of the yield measurements, an ELISA and virus titer assay (TCID50 test), was large. Therefore no process parameters could be linked to product yield.

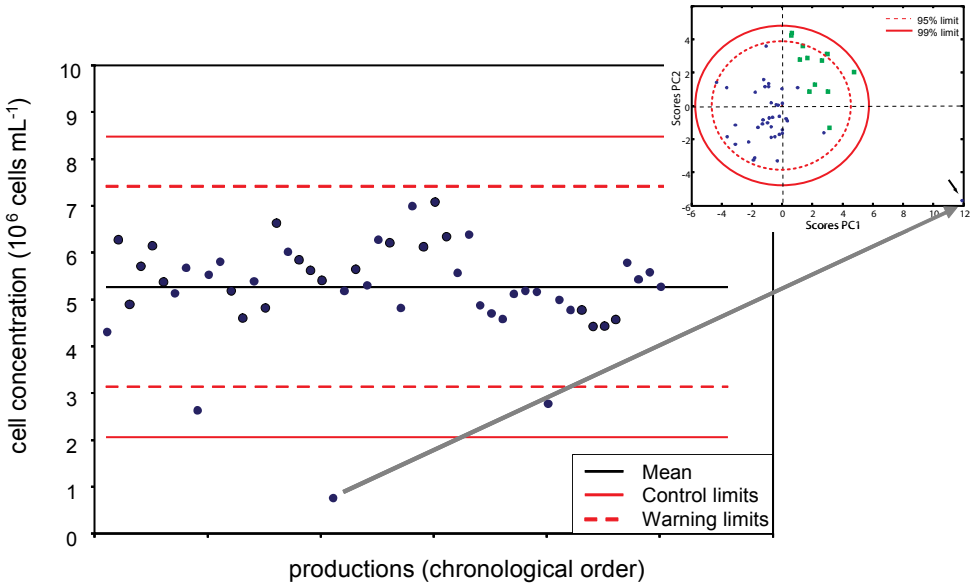

Figure 5. Statistical control chart (Shewhart) depicting the cell concentration at the end of the 2nd pre-culture stage. Outliers detected using this simple control chart correspond, indicated with arrow, with the outliers detected during PCA of the 2nd pre-culture (Small PCA score plot equals Figure 2B).

Downstream Processing

The off-line data from the unit operations in downstream processing, that is, from clarification to inactivation, from both production lines and all three virus types were analyzed simultaneously using PCA. Available data consisted of 176 variables for 38 batches at 700-L and 12 batches at 1,500-L scale. First analysis resulted in a PCA score plot which could explain 52% of the data (figure not shown). The two groups that could be distinguished represent the different production scales. This pattern was similar as was previously found for cell culture (Bakker et al. 2010). Since downstream processing is a physical operation it is expected that correction for volumes will result in a similar operational behavior. To explore the differences in operational behavior the data set was normalized for volume and the product quantities (D-antigen) were excluded as the data would have been dominated by the product quantities for individual unit operations. A new PCA model is constructed explaining 57% of the total variation (Figure 6). Although it was observed that batches from the 1,500-L production runs appear to be located in the lower part of the figure, they cannot be distinguished from the 700-L production runs. It was therefore concluded that the data are randomly distributed which implies that the operational behavior between both production scales is similar. Moreover several clusters (boxed) could be observed. Common features for the first cluster are input variables pH and water at the start of inactivation. Cluster 2 is marked by low volumes prior to

concentration and low volumes after SEC. The common feature of cluster 3 is the high volume after IEX. This indicates that these batches have a high product yield. Upon analysis of the D-antigen data of the latter cluster it was found that indeed these batches, three type 1 and one type 3 batch were the batches with the highest yield in terms of absolute amount of D-antigen per batch. It was unfortunately not possible to find a common cause for this higher yield in these batches using PCA and PLS.

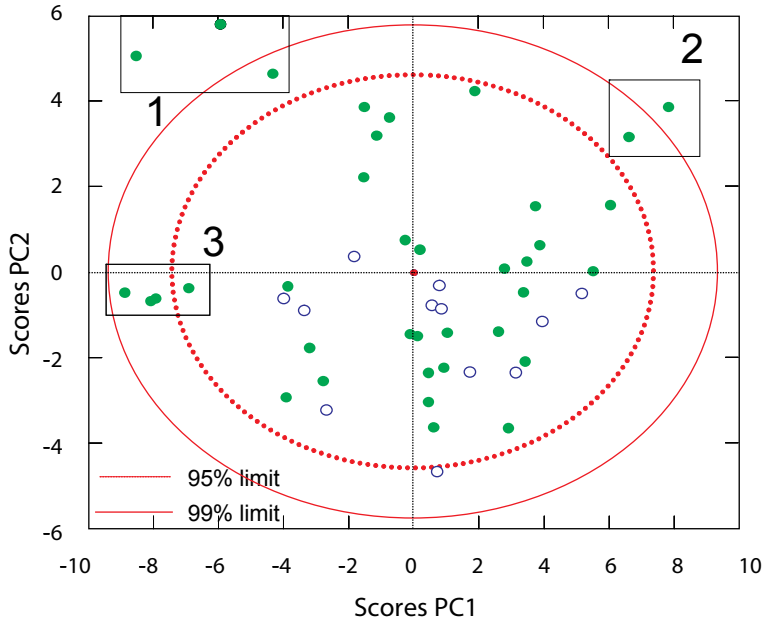

Figure 6. PCA score plot of the downstream processing phase at both 700-L and 1,500-L production scale. Green closed and blue open circles correspond with the 700-L and 1,500-L production scale respectively. The data were volume normalized. Clusters 1, 2, and 3 are boxed and show deviating process conditions.

One of the CQA during DSP is the specific activity which is determined after IEX. The specific activity is defined as the ratio D-antigen and protein nitrogen content. For prediction of the specific activity at 700-L production scale a five-factor PLS model was developed. The number of components was determined using a full cross-validation. The results are depicted in Figure 7. The model characteristics show a R^2 of 93% and a model error (RMSECV) of approximately 0.6. These results show that the specific activity can be reasonably well predicted from the process data. The highest correlation was found with the D-antigen concentration after the unit operation concentration. This result was anticipated because the D-antigen concentration is one of the determinants of the specific activity.

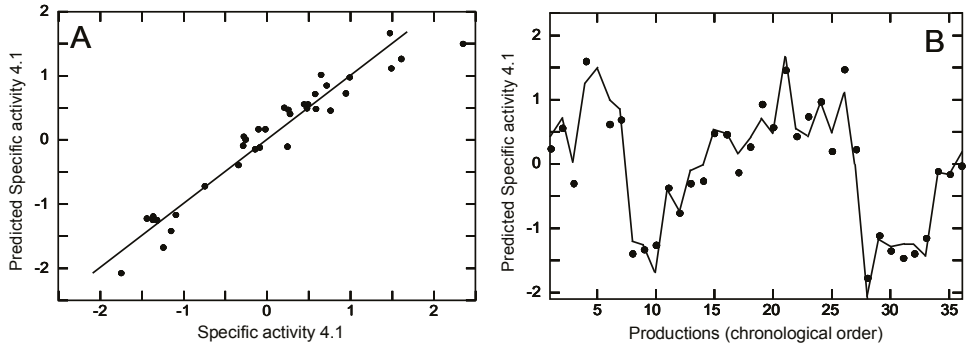

Figure 7. Prediction of specific activity. A five-component PLS model was developed (R2 = 0.931; RMSECV = 0.618). Points represent actual figures, Lines represent model prediction. A: Predicted specific activity versus actual values. B: Time series of predicted and actual values for specific activity.

Discussion

The exploratory analysis of polio vaccine manufacturing data described in this work shows that MVDA is a powerful tool to extract information from large datasets. This is illustrated by the ability to detect deviating and experimental production runs. Moreover MVDA allowed the detection of differences that were not obvious, for example, the possible influence of the control unit as was observed for the 1st and 2nd pre-culture. Also the observed differences in glucose concentration at the start of the 1st pre-culture had not been known prior to this MVDA. This observation has led to an optimization in media preparation, resulting in a more robust media composition. Throughout the different unit operations the large part of the variation was caused by a differences of input variables, for example differences in glucose concentration or osmolarity during cell cultures. The differences in input variables were incidental and thus not structural and mostly they caused variation within specified ranged not leading to batch rejections.

Outliers detected using MVDA had known deviations (noted in the GMP paper trace) moreover these outliers could also have been detected using simple statistical control charts. These univariate control (or Shewhart) charts are traditionally used for routine monitoring production performance and could be used in this case to monitor the relevant process parameters. In general, using only univariate data analysis certain valuable information will be missed (Kirdar et al. 2008; Kourti 2004). Here it is illustrated that PCA analysis can be used to determine the similarity of twin bioreactors (Figure 3) or new bioreactors (Figure 2). Moreover, based on the PCA and detailed analysis of the outliers it was concluded that manufacturing had been consistent during the analyzed production runs.

Regression analysis using PLS did not result in defining correlations between relevant process parameters and product quantity and quality attributes. The main difficulty in finding relations between process parameters and product quantity and/or quality is first of all that manufacturing is strict meaning the CPP are run at setpoint within well controlled ranges. Secondly it was observed that the used product quantification and characterization measurement methods had high standard variation which did not allow determining significant correlations. During the manufacturing process poliovirus is quantified and qualified using the tissue culture infective dose assay (TCID50) and the D-antigen ELISA, respectively. The TCID50 assay is valid within ± 0.5 log and the D-antigen ELISA is valid within a coefficient of variation (CV) of 10%. These assay variations are common for these type of analysis (Wood et al. 1995) but large compared to the variation in well controlled CPP.

The power of MVDA for yield improvement strategies in biotech processes has been shown previously (Coleman et al. 2003; Kirdar et al. 2007). Coleman et al. (Coleman et al. 2003) have shown that analysis of historical data could result in novel suggestions for increasing the product concentration. Their database consisted of experimental fermentations in which variations in CPP was included. When manufacturing of complex macromolecules is strictly controlled MVDA of production data might not result in new knowledge on statistically significant correlations between CPP and CQA. This information should be obtained using a correct scale-down model of the production line where CPP can be varied and linked to product quantity and quality by preferably using the design of experiments approach together with MVDA methods.

While the MVDA could be used for root cause finding and thereby gaining knowledge on process robustness, process optimization in terms of increased yield was not possible using results obtained in this analysis. To accommodate future process optimization, research was initiated on test development to enhance product characterization during manufacturing and process development studies. The gained knowledge on performance of the individual unit operations, in terms of ranges and their operating variation, is being used to setup experiments in which tested ranges can be related to the anticipated performance at the manufacturing site.

The gained knowledge of the IPV production process, not only from the MVDA, but also from digitalizing the available historical data, has proven to be useful for troubleshooting, understanding limitations of the available data and indicating the opportunity for future improvements. Moreover the information is applied in present process development studies in which a scale-down model of the production line is being established for research on further process improvements. Using the scale-down model, the process the knowledge and design space can be further explored. The data obtained at lab-scale will

be used for further model development. Although polio eradication is on the doorstep, improvements on IPV manufacturing remain actual as IPV plays an important role in the WHO polio eradication strategy (Aylward et al. 2006). At this moment the two main process improvements concern firstly the potential risk of introducing foreign agents by the use of bovine serum and porcine trypsin for which an animal-component free media could be used as an alternative. Secondly, NVIs current IPV manufacturing process is the basis for the development of a new IPV variant based on the attenuated Sabin strains (Kersten et al. 1999; Kreeftenberg et al. 2006).

Acknowledgements

The authors like to thank Rob Kortink, Marvin Philippi and Ronald Lijffijt for their help on data acquisition.

Chapter 4

Development of a fast ELISA for quantifying polio D-antigen in in-process samples

Published as:
Ten Have, R., Thomassen, Y.E., Hamzink, M.R.J., Bakker, W.A.M., Nijst, O.E.M., Kersten, G., Zomer, G. (2012) *Development of a fast ELISA for quantifying polio D-antigen in in-process samples.*

Biologicals 40:84-87
dx.doi.org/10.1016/j.biologicals.2011.11.004

Abstract

A fast ELISA was developed and qualified for analysis of polio D-antigen. The original 20 h-protocol was optimized by minimizing the total incubation time to 1 h, and by replacing the signal reagent 3,3′,5,5′-tetramethylbenzidine by a chemiluminogenic signal reagent with a theoretical low intrinsic background and high dynamic range.

Introduction

A sandwich enzyme-linked immunosorbent assay (ELISA) may be used to quantify D-antigen units of poliovirus (PV) serotype 1, 2 and 3 in appropriate samples (Wood et al. 1995). This ELISA is set-up to detect so-called D-antigen, an arbitrarily defined unit of which the intact D-form is immunorelevant. For detection of both PV, and vaccine (IPV, formalin inactivated PV) a serotype and D-antigen specific monoclonal or polyclonal antiserum may be used (Sawyer et al. 1997; Wood et al. 1995).

For efficient process development and proper process control, in-process samples taken from the polio vaccine production process need to be analyzed prior to the next process step is initiated. This requires a fast ELISA which will be used to measure the D-antigen concentration in for example samples with host cell debris that are taken during virus cultivation, or in samples that contain purified and concentrated PV (Thomassen et al. 2010). It was considered that analysis of this variety of in-process samples requires detection of emitted light rather than absorbed light as a theoretical low background and a high dynamic range appear to be required. Therefore, this research focuses on: A. replacing the HRP substrate 3,3′,5,5′-tetramethylbenzidine (TMB) by a chemiluminogenic signal reagent, and B. reducing the incubation times in the original 20 h ELISA protocol (Kersten et al. 1999).

A reduction in sample analysis time may be obtained by optimizing consecutive incubation steps or by combining incubation steps. In the original ELISA protocol antigen detection requires two consecutive incubation steps, the first is incubation with the detection monoclonal antibody (IgG) which is followed by incubation with the HRP-conjugate. In the literature there is at least one example on combining these two incubation steps (Lewis and Elder 2000). Co-incubation appears advantageous, but also implies that both the detection IgG, and HRP-conjugate concentration need optimization in order to achieve a proper signal to blank (S/B) ratio.

Materials and methods

ELISA

Micro titerplates (Greiner, white, high-binding) were coated with type-specific caprylated bovine antiserum diluted 1:1600 in PBS (100 µL), overnight at 4 °C. Coated plates were stored dry at a temperature of −80 °C. The plates were washed with wash buffer containing: PBS, and 0.1 v/v % Tween20.

Trivalent inactivated polio vaccine (IPV, 10-fold concentrated bulk product) was used for test optimization (type 1, 411 DU mL^{-1}; type 2, 89 DU mL^{-1}; type 3, 314 DU mL^{-1}). This vaccine

was diluted using assay buffer containing: PBS, 0.1 v/v % Tween20, and 0.5% Protifar (Nutricia, Zoetermeer, The Netherlands) and 100 µL was added to the wells. Test optimization experiments were performed once.

The sealed plate was incubated at 37 °C on a shaking incubator during 30 min and washed two times using wash buffer.

Incubation with 100 µL of a mixture of type-specific suitably diluted monoclonal (detection antibody) and HRP-labeled goat anti-mouse (HRP-conjugate) was performed at 37 °C on a shaking incubator during 30 min. The detection monoclonal antibodies were, coded 3-4E4 (type 1), 3-14-4 (type 2), and 1-12-9 (type 3), from in-house mice ascites (Sawyer et al. 1997).

After washing four times using wash buffer, the signal reagent was added.

For detection with the signal reagent HighLite (Zomerbloemen B.V., Zeist, The Netherlands), previously called GZ11 (Zomer and Hamzink 2009), buffer A, and B were mixed and 100 µL was added to each well. Buffer A contains: PBS, 0.05 v/v % Tween20, 1 mM EDTA, 0.14 µg mL^{-1} HighLite, 0.1 µg mL^{-1} 4-phenylphenol. Buffer B contains: NaOAc pH 6.0, 0.015% (w/w) H_2O_2. The emitted light was detected using a luminometer (Centro LB960, Berthold Technologies, Vilvoorde, Belgium).

The protocol for detection with TMB is described elsewhere (Kersten et al. 1999). Detection with Supersignal Pico (Pierce, Rockford, USA) and Supersignal Femto (Pierce, Rockford, USA) was performed according to the protocol of the supplier.

To increase the accuracy of the assay at least three sample dilutions are used to calculate the antigen concentration.

Processing of the raw data and test criterions

A four parameter fit was used to generate a calibration curve which is described by:

$$light\ units = \frac{(a-d)}{(1+(Conc/c)^b)} + d \qquad \text{Eq.1}$$

where a = lower asymptote, b = slope at inflexion point, c = concentration at inflexion point, and d = upper asymptote (Findlay and Dillard 2007). An in-house Excel sheet was used for data processing.

The following test criteria were used for acceptance of raw ELISA data: 1. The back calculated response of the standards differs by no more than 10% from the expected value, 2. The calibration curve contains at least five out of eight standards, and 3. The calculated

concentrations of at least three sample dilutions ran in triplicate result in a standard error of the mean of less than 15%.

Biosafety

To meet biosafety requirements the procedure for washing the 96-wells plate was performed in a biohazard cabinet. In this case removal of liquid containing biologically active virus requires careful handling, excluding the procedure of inverting the 96-wells plate and tapping it to dryness. An autoclavable Immuno-washer (Nunc, Rochester, USA) was used here and waste was collected for destruction. Removal of liquid from the wells was less efficient compared to tapping the plate to dryness. For that reason the number of wash cycles was increased to 8 for active samples using the Immuno-washer.

Results and discussion

Fast analysis of PV containing samples requires an ELISA that can be performed on the same day of sample collection. This required modification of the original 20 h ELISA protocol (Kersten et al. 1999). Table 1 shows that besides minimizing the incubation time to 1 h, also a reduction in the number of wash steps was realized. This is considered beneficial from a biosafety perspective. Also the signal reagent was changed from TMB to HighLite as this lowered the background signal and increased the theoretical dynamic range.

Table 1. Protocol of the original ELISA, and the fast D-antigen ELISA along with incubation times (t_{inc}, hours) and wash steps.

Step	ELISA layout			
	Original protocol	t_{inc} (h)	Fast protocol	t_{inc} (h)
1	Incubation with antigen	16	Incubation with antigen	0.5
	Wash step		Wash step	
2	Incubation with detecting antibody	2.5	Combined incubation of detecting antibody and HRP-labeled conjugate	0.5
	Wash step		Wash step	
3	Incubation with HRP-labeled conjugate	1.5		
	Wash step		-	
	Addition of TMB		Addition of HighLite	
	Measurement		Measurement	
Total incubation time		20		1
Total wash steps		3		2

Development and optimization of a fast D-antigen ELISA

Coating plates with a serotype specific antiserum

The effect of using different concentrations of coating antibody was studied in the range from 1:200 to 1:1600 and appeared negligible (Lewis and Elder 2000). Therefore, a dilution of 1:1600 was used throughout the experiments.

Overcoming non-specific binding to the plate by blocking

Blocking by using 0.5% BSA or 0.5% milk proteins (Protifar) was equally effective in reducing the background (not shown). Protifar was selected and was included in the assay buffer.

Optimized binding of the antigen to the coat

Figure 1A shows that static incubation (original protocol, T = room temperature, rT) resulted in an antigen concentration dependent binding rate, binding occurred faster at 20 DU mL^{-1} than at 2.5 DU mL^{-1} (5 and 10 DU mL^{-1} were in between, result not shown). This concentration dependency was not found upon shaking the microtiter plate during incubation. Moreover, binding occurred faster compared to the static incubation. Binding of antigen was anticipated to occur somewhat faster at a controlled temperature of 37 °C compared to room temperature. For that reason the former was selected for further experiments.

Upon applying these optimal conditions, a reduction in incubation time from overnight (~16 h) to 30 min was established (see Table 1).

Combined incubation of detection antibody and HRP-labeled conjugate

In the original protocol two successive incubation steps are used (see Table 1) to allow consecutive binding of the detection IgG, and the HRP-conjugate. In that case, both reagents may be used in excess to ensure complete saturation of the antigen.
It is anticipated that two successive incubation steps will render a signal that increases to a maximum level upon increasing the detection IgG concentration (by decreasing the dilution factor). Under these incubation conditions, comparable standard curves were obtained at an IgG dilution factor of 10^2 and 10^3 showing that a maximum level of saturation is obtained (see Figure 1B).

Unlike successive incubation, co-incubation of detection IgG and the HRP-conjugate results in a signal that increases upon further diluting the detection IgG reagent in the dilution factor range from 10^2 to 10^4 (see Figure 1B).

The fact that co-incubation at a low detection IgG dilution factor of 10^2 renders a very low signal compared to successive incubation may be explained by the hypothesis that the excess of detection IgG will result in considerable binding to the antigen. This excludes binding of the complex between detection IgG and the HRP-conjugate to those occupied antigenic targets which results in a reduced signal.

The ratio between detecting antibody and HRP-labeled conjugate was optimized further by using a checkerboard titration. In the case of IPV type 3 an apparent optimum in the signal to background (S/B) ratio of 15 was obtained at a detection IgG dilution of 3×10^4

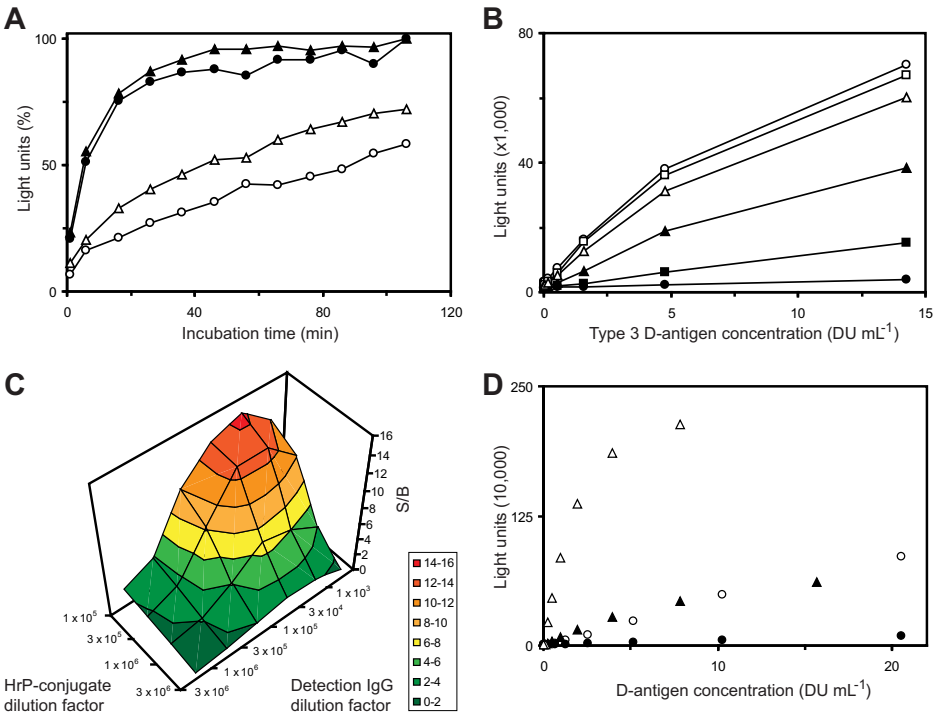

Figure 1. Test parameters involved in optimizing the fast D-antigen ELISA. Panel A shows the effect of shaking as a function of the type 1 D-antigen concentration (shaking: ▲, 20 DU mL^{-1}; ●, 2.5 DU mL^{-1}, and static: △, 20 DU mL^{-1}; ○, 2.5 DU mL^{-1}) at T = rT (n = 1). In Panel B separate incubation and co-incubation of detection IgG, and HRP-conjugate are compared and studied at several PV type 3 D-antigen concentrations (DU mL^{-1}) as a function of the detection IgG dilution factor (separate incubation: ○, 10^2; □, 10^3; △, 10^4, and co-incubation: ●, 10^2; ■, 10^3; ▲, 10^4). The HRP-conjugate dilution factor was held constant at 5×10^5 (n = 2). Panel C shows the effect of varying dilution factors of both the HRP-conjugate and detection IgG on the signal to blank (S/B) ratio of type 3 (n = 2). The S/B ratio was optimized in a similar way for type 1 and 2 (not shown). Panel D shows that besides the signal reagent HighLite also the signal reagent Supersignal Pico may be used (n = 2). The latter was studied as a function of the D-antigen concentration (Supersignal Pico: △ , type 3; ○, type 1, HighLite: ▲, type 3; ●, type 1). The standard curve of type 2 (not shown) was comparable to that of type 1.

and HRP-conjugate dilution of 1×10^5 (see Figure 1C). Similar experiments were performed for IPV type 1 and 2 (not shown). From these experiments the following dilution factors were selected for the respective polio serotypes: type 1, IgG 5×10^3, HRP-conjugate 1×10^4, and type 2 and 3, IgG 5×10^4, HRP-conjugate 1×10^5. This resulted in S/B values of 8, and 5 for type 1, and 2, respectively.

The fact that the optimized S/B ratio of type 3 is higher than that of type 1 and 2 may be related to steric hindrance lowering the amount of IgG-HRP-conjugate per antigen particle. It is hypothesized that that is supposedly more important in the case of type 1 and 2 than it is for IPV type 3. Such an S/B difference was not observed upon using the original protocol (result not shown).

This combined incubation method (step 2 in Table 1) has been used before for a protein and small organic compounds (Thomassen et al. 2010). The work described here extends the scope of that successful application by using a multi-epitope analyte; each PV particle contains 60 identical units, i.e. there are, at least in theory, 60 possible binding sites per particle.

Antigen detection

Other signal reagents besides HighLite could also be used in the fast D-antigen ELISA, examples are: TMB, Supersignal Pico, and Supersignal Femto. However, not all signal reagents perform equally.

Supersignal Femto was found to result in a disadvantageously high background of 10% of the total detector scale and a dynamic range for type 3 of just 0-1 DU mL^{-1}. Figure 1D shows that Supersignal pico increases the signal of type 1 and 3 compared to HighLite. Like Supersignal Femto the dynamic range for detection of type 3 D-antigen was reduced which is not preferred for the fast D-antigen ELISA in which a trivalent mixture is used as a reference. Therefore, use of the chemiluminescent signal reagent HighLite was preferred as the background is <0.3% of the total detector scale and the dynamic range is at least between 0 and 20 DU mL^{-1} for each polio serotype.

Qualification of the fast D-antigen ELISA

For qualification of the fast D-antigen ELISA the average relative standard deviation (RSD), reproducibility, specificity, and the estimated limit of detection (LOD) were studied (see Table 2). The average RSD of a sample was obtained by calculating the average RSD of 40 samples.The obtained values are all below 10%. The reproducibility was estimated by using data from independent D-antigen concentration measurements of a single sample. All values were below 20% which is considered acceptable.

The sample matrix is dependent on the process step. In short, the IPV production process consists of cell culture followed by virus culture, clarification, concentration, size exclusion chromatography (SEC), ion exchange chromatography (IEX), and formalin inactivation (Thomassen et al. 2010). The occurrence of several sample matrices stresses the importance of an accurate ELISA analysis result that solely depends on the antigen (and is independent of the matrix) which in its turn is required for process development purposes. The effect of the sample matrix on the assay result of IPV type 1 was studied by enriching in-process samples (that contained PV type 2) with trivalent reference vaccine. No effect of the matrix was found. It is anticipated this also applies to measurement of type 2 and 3.

Upon using the first D-antigen concentration of the calibration curve, an LOD of 0.3 DU mL^{-1} was found for all serotypes. The lowest observed D-antigen concentration in actual samples, also requiring that the raw data meets all the preset criteria, were 6, 1, and 2 DU

Table 2. Overview of test qualification results. The *average RSD* (n = 40): was assessed by determining the relative standard deviation (RSD, %) for samples analysed in triplicate on one 96-wells plate. Analysis results from samples taken throughout various stages in the production process were used. *Reproducibility* (n = 20) was assessed by determining the D-antigen concentration of a single sample on different days by two technicians. *Specificity* was determined by spiking trivalent vaccine to in-process samples containing polio type 2. The type 1 concentration was assayed and is presented as a percentage of the spike concentration of 41.1 DU mL^{-1}. The *limit of detection* (LOD) reflects the lowest D-antigen concentration of the standard curve.

Qualification item	Description	Studied parameter
		RSD (%)
Average RSD	PV type 1	7.1
	PV type 2	7.8
	PV type 3	6.2
Reproducibility	PV type 1	11.1
	PV type 2	15.1
	PV type 3	10.6
Specificity		Spike recovery (%)
Viral harvest [1]	80% v/v matrix[2]	107 ± 13
After SEC	90% v/v matrix	97 ± 5
	10% v/v matrix	111 ± 9
After IEX	90% v/v matrix	103 ± 6
	10% v/v matrix	111 ± 11
		D-antigen concentration (DU mL^{-1})
LOD	IPV type 1	0.3
	IPV type 2	0.3
	IPV type 3	0.3

1 The harvest was also spiked with 82.2 DU mL^{-1} and in that case 85.9 ± 9.1 DU mL^{-1} was recovered.

2 The effect of the matrix on the binding of the antigen to the plate (see step 1 in Table 1) is studied by adding a mixture of matrix and assay buffer (total volume= 100 µL).

mL^{-1} for PV type 1-3, respectively. This method is suitable for in-process analysis. However, for release of final product more extensive validation is required.

Conclusions

Here, a successful ELISA optimization strategy was outlined rendering a fast assay requiring only 2 wash steps, and resulting in a minimal analysis time. The described development strategy may be of use for optimizing other ELISA protocols as well.

Chapter 5

Scale-down of the inactivated polio vaccine production process

Published as:
Thomassen, Y.E., van 't Oever, A.G., Vinke, M., Spiekstra, A., Wijffels, R.H., van der Pol, L.A., Bakker, W.A.M. (2013) *Scale-down of the inactivated polio vaccine production process.*
Biotechnology and Bioengineering 110(5):1354-1365
dx.doi.org/10.1002/bit.24798

Abstract

The anticipated increase in the demand for inactivated polio vaccines resulting from the success in the polio eradication program requires an increase in production capacity and cost price reduction of the current inactivated polio vaccine production processes. Improvement of existing production processes is necessary as the initial process development has been done decades ago. An up-to-date lab-scale version encompassing the legacy inactivated polio vaccine production process was set-up. This lab-scale version should be representative of the large scale, meaning a scale-down model, to allow experiments for process optimization that can be readily applied. Initially the separate unit operations were scaled-down at setpoint. Subsequently, the unit operations were applied successively in a comparative manner to large-scale manufacturing. This allows the assessment of the effects of changes in one unit operation to the consecutive units at small-scale. Challenges in translating large-scale operations to lab-scale are discussed, and the concessions that needed to be made are described. The current scale-down model for cell and virus culture (2.3-L) presents a feasible model with its production scale counterpart (750-L) when operated at setpoint. Also, the current scale-down models for the DSP unit operations clarification, concentration, size exclusion chromatography, ion exchange chromatography, and inactivation are in agreement with the manufacturing scale. The small-scale units can be used separately, as well as sequentially, to study variations and critical product quality attributes in the production process. Finally, it is shown that the scale-down unit operations can be used consecutively to prepare trivalent vaccine at lab-scale with comparable characteristics to the product produced at manufacturing scale.

Introduction

Inactivated polio vaccine (IPV) was developed in the 1950s (Salk 1953). Soon after that, the basis for a legacy large-scale IPV production process, using microcarrier technology and primary monkey kidney cells, was developed in our laboratories (van Wezel 1967) and adopted worldwide (van Wezel et al. 1984).

The existing IPV production process has been described elsewhere (van Wezel 1985; van Wezel et al. 1984), and a summary is given here (Figure 1). Monovalent inactivated bulks of each poliovirus (PV) type (type 1 Mahoney, type 2 MEF-1, and type 3 Saukett) are manufactured separately, after which a trivalent vaccine can be formulated. To obtain a monovalent bulk, Working Cell Bank (WCB) vials are thawed and used to directly start a 15-L fed-batch bioreactor pre-culture in which Vero cells (an African green monkey kidney cell line) grow attached to microcarriers (Cytodex 1). After expansion growth and subsequent trypsinization to remove cells from microcarriers, a second pre-culture consisting of a 40-L recirculation culture is done. The final cell culture is, after a second trypsinization and reattachment to the microcarriers, carried out in twin bioreactors at 2 × 750-L scale, followed by a culture medium change and subsequent virus culture. Downstream processing consists of clarification by means of normal flow filtration (NFF) followed by concentration using tangential flow filtration (TFF). The purification is done using size exclusion chromatography (SEC) and ion exchange chromatography (IEX). The monovalent bulks are finished after inactivation of the poliovirus using formaldehyde.

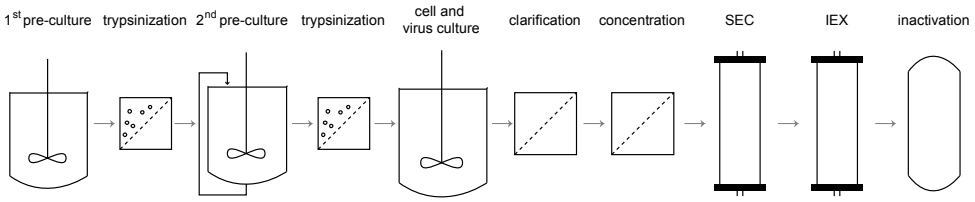

Figure 1. Schematics of the large scale IPV production process. Cells are expanded using two pre-culture steps prior to cell and subsequent virus culture. The downstream processing consists of clarification, concentration, SEC, and IEX followed by inactivation with formaldehyde. To obtain trivalent polio vaccine this procedure is followed for each poliovirus type separately prior to mixing for the formulation of the trivalent polio vaccine.

Improvements on the existing IPV manufacturing process are regularly under consideration. For instance in the 1980s, a major improvement was made when the primary monkey kidney cells were replaced by the Vero cell line (Montagnon et al. 1984; van der Velden-de Groot 1995). Other examples may be found in challenges like necessary equipment replacement due to equipment ageing, or the growing awareness for biosafety and quality issues that have led to the development of animal component free cell culture

media. Some of these changes may require new registration at the regulatory authorities. It should always be proven that anticipated changes will not affect the product quality and safety.
Current ICH guidelines (ICH Q8(R2) 2009; ICH Q9 2005; ICH Q10 2008) stimulate the increase of scientific understanding on new and existing production processes. Using this knowledge, future improvements on registered production processes may be done within an established process design space or using representative and validated scale-down models. This approach would require less runs to validate the changes at manufacturing scale.

The need for increased process knowledge, not only on new biopharmaceutical processes but also on existing processes, promotes the application of scale-down models for rapid acquisition of relevant data. Scale-down models, used in combination with a design of experiments approach, allow the development of cause and effect models on input and process parameters, their interactions and influence on product attributes, either as single unit operations or as consecutive units using for instance partition designs (Perry et al. 2007; Pieracci et al. 2010).

To gain more knowledge on the IPV manufacturing process we have analyzed the available data using multivariate data analysis (Thomassen et al. 2010). From this analysis, criteria, for example, cell growth characteristics, for a scale-down model could be derived. Here, we describe the development of a model at lab-scale, which not only allows the study of single unit operations but also the effects of changes in one unit operation to the consecutive units. The complete production process was scaled-down in such a way that lab-scale unit operations can be used to produce representative trivalent vaccine.

Materials and Methods

Cell Line, Viruses, and Medium

Vero cells obtained from WHO (10–87) originally derived from ATCC (CCL-81) were used as host for PV production. PV type 1 Mahoney, type 2 MEF-1, and type 3 Saukett were used. For scale-down experiments manufacturers working cell banks were subcultured in T-flasks (in the experiments passage no. up to 150 were used) and manufacturers virus seeds were used. Vero cells were grown adherent to Cytodex 1 microcarriers (GE Healthcare, Uppsala, Sweden; 3 g L^{-1}). Culture media, EMEM supplemented with bovine serum for cell culture, M199 for virus culture and other materials, prepared in-house for manufacturing of IPV, were used for scale-down experiments.

Cell and Virus Culture

Cell culture consisted of a fed-batch process with a daily glucose bolus feed given when the glucose concentration was below 5 mM. Prior to virus culture the media was exchanged.

Lab-scale cell and virus cultures were carried out in 5-L glass bioreactors equipped with pitched three-blade (angle 45°) impellers (axial flow impeller). Power consumption at different rotational speeds was measured using a torque transducer (ETH-Messtechnik, Gschwend, Germany; DRDL-l-1-0,1) mounted between the motor and the impeller shaft. Power consumption was measured in water and corrected for power consumption in air.

Cultivations were controlled using Sartorius DCU-3 control units and MFCS-win software (Sartorius AG, Melsungen, Germany). At manufacturing scale, twin 1,000-L stainless steel bioreactors (Applikon, Schiedam, The Netherlands) were used with axial blade impellers. Starting working volumes were 2.3 and 750-L for small and large-scale, respectively resulting in similar H/D ratios. Data from 116 cell and virus cultures (PV type 1: n = 40; PV type 2: n = 22; and PV type 3: n = 52) were available for defining manufacturing cell and virus culture characteristics.

Clarification

At manufacturing scale, the broth, after harvest through a 75 µm stainless steel sieve, was clarified using continuously added Celite (577) filteraid on stainless steel mesh filters (pore size 75 µm) followed by 0.45 and 0.22 µm filters. At lab-scale, after pre-clarification through a 75 µm stainless steel sieve, an alternative clarification method using disposable clarification units (Millipore, Billerica, MA; C0HC or Sartorius PB2) followed by a 0.45/0.22 µm combination filter was applied.

Concentration

At manufacturing scale the product was concentrated (approx. 1,000-fold) using tangential flow filtration via two consecutive UF filter steps (PTHK UF filters 100 kDa cut-off). At small-scale, first, a Millipore Pellicon 2 system with a PLCK filter (UF filter cutoff 100 kDa; filter load 166 L m^{-2}) combined with a Quattroflow-150 s (Quattroflow Fluid Systems, Kamp-Lintfort, Germany) low shear pump was used. Second, a Millipore lab-scale TFF with Biomax UF filters (PES filter cutoff 100 kDa; filter load 8 L m^{-2}) was used. The transmembrane pressure (TMP) and the pressure difference (dP) were set to a maximum of 0.6 and 0.5 bar for the TMP and dP, respectively.

Purification

SEC was done using a column (height: 80 ± 2 cm) containing separately sterilized (by autoclave) CL-6B matrix (GE Healthcare) at both scales. For IEX, a column (height:

22 ± 2 cm) containing the positively charged DEAE Sepharose Fast Flow matrix (GE Healthcare; separately sterilized by autoclave) was used at both scales. The virus was eluted using an Äkta explorer system (GE Healthcare) with a 40 mM phosphate buffer (pH 7.0) on both occasions.

Stabilization and Inactivation

Because of the limited stability of the poliovirus in the phosphate buffer used during chromatography, immediate stabilization using M199 (10×) was done after IEX fraction collection. This was followed by dilution to obtain a correct D-antigen concentration prior to inactivation. During dilution, glycine was added which is needed for inactivation with formaldehyde (Lycke et al. 1957). Prior to inactivation the pH of the product was set (7.0 ± 0.2) and filtered (0.22 µm). Inactivation was done at 37°C for 13 days in an incubator. Halfway the inactivation (after 6–8 days) an intermediate filtration (0.22 µm) was performed to remove possible incompletely inactivated poliovirus aggregates (Nathanson and Langmuir 1963) and so allow complete inactivation. Complete inactivation was, in general, observed after 72–96 h. After inactivation the monovalent bulk product was stored at 4°C. This procedure was similar at both scales.

Analytical Methods

Cell culture samples were taken daily for cell counts using a Nucleocounter NC-100 (Chemometec, Allerød, Denmark) to determine total nuclei. Alternatively, total nuclei colored with crystal violet were counted using a Fuchs-Rosenthal hemocytometer. Both methods were compared to exclude differences (data not shown). Cell culture metabolites such as glucose, lactate, glutamine, glutamate, and ammonia were monitored using a Bioprofile 100 Plus (Nova Biomedical, Waltham, MA).

Amino acid concentrations were determined using an Agilent HPLC method (Agilent, Santa Clara, CA). Primary amino acids were derivatized with o-phthalaldehyde 3-mercaptopropionic acid (OPA) detected by fluorescence at an excitation wavelength of 340 nm with an emission wavelength of 450 nm. Secondary amino acids were derivatized with 9-fluorenylmethyl chloroformate (FMOC) and were detected with an UV-detector at 262 nm and by fluorescence at an excitation wavelength of 266 nm and an emission wavelength of 305 nm. Chromatographic separation was achieved by mobile two-phase gradient elution on a reverse phase Agilent Zorbax Eclipse Plus C18 column AAA (2.1 mm × 150 mm). Mobile phase A contains 10 mM Na_2HPO_4: 10 mM $Na_2B_4O_7$, 1.25 mM NaN_3 (pH 8.2). Mobile phase B contains a mixture of Acetonitrile: Methanol: water (45:45:10 v/v/v).

Poliovirus was quantified with a virus titer assay as decribed previously (Thomassen et al. 2012) and the quality was assessed using a D-antigen ELISA (ten Have et al. 2012).

Immunogenicity of monovalent product was determined in the in vivo potency assay in rats (van Steenis et al. 1981). Immunogenicity was expressed as the relative potency compared to the reference vaccine (PU91-01) using the parallel-line method.

Vero host cell proteins were determined using the Vero Cell HCP ELISA kit F500 according to the manufacturer's instructions (Cygnus Technologies, Southport, NC).

Equivalence Testing (TOST)

To determine equivalence between the manufacturing and lab-scale unit operations the key performance parameters were tested for equivalence using a two-one-sided test (TOST) rather than a Student's *t*-test, which is used to show differences. TOST has been described in detail elsewhere (Schuirmann 1987) and is commonly used in technology transfer or to demonstrate bioequivalence (2001). Briefly, equivalence testing is done to test if the difference between two populations means (Δμ) is within a previously defined tolerance interval [ϑ_l, ϑ_u]. This tolerance interval is chosen based on practical standpoints, accounting for intrinsic process and assay variability and thus provides scientific meaning to the test outcome rather than just statistical meaning.

The null hypothesis H_o is defined as $H_{01}: \Delta\mu \leq \theta_l \; or \; H_{02}: \Delta\mu \geq \theta_u$. Equivalence is concluded when both H_{o1} and H_{o2} are rejected. The above hypothesis H_{o1} and H_{o2} can be tested separately using two one-sided *t*-tests. Thus equivalence is concluded at significance level α when

$$\frac{\Delta\overline{\overline{X-\theta_l}}}{s\sqrt{1/n_1+1/n_2}} > t_{1-\alpha(v)} \qquad \text{and} \qquad \frac{\Delta\overline{\overline{X-\theta_u}}}{s\sqrt{1/n_1+1/n_2}} < t_{1-\alpha(v)}$$

where ΔX is the difference in means between two groups, s is the pooled standard deviation, n_1 and n_2 are the respective sample size of group 1 and 2, $t_{1-\alpha(v)}$ is the upper probability α percentile of a t-distribution with v degrees of freedom.

As two separate one-sided *t*-tests are used the confidence interval should be described as (1–2α) × 100%. With a chosen significance level (α) of 0.05 the confidence interval is 90%. The P-value for equivalence is calculated as the maximum P-value (P_{max}) of either one of the two one-sided *t*-tests. Like in traditional tests when the P-value is below α, the null hypothesis is rejected and the research hypothesis (here equivalence) is established.

Results and Discussion

Scale-Down of Upstream Processing

For scaling down upstream processing (USP) or bioreactors, several generally accepted guidelines exist [see for instance (Li et al. 2006; Rathore et al. 2005b; van 't Riet and Tramper 1991)]. These can be distinguished in hardware and operational guidelines. Included in the hardware guidelines are: (i) similar vessel geometry, meaning that the H/D ratio (height/diameter) and the impeller design and placement for both vessels is nearly identical; (ii) similar (the same or scaled-down) inoculum preparation; and (iii) similar performance analysis systems (for example the cell counter system). Scale-down (for an overview see Table 1) was based on similar vessel geometry, that is, the working volume for the scale-down model was chosen such that the H/D ratio was similar. The aeration method was kept similar, at both scales head-space aeration was used. Other hardware options, like impeller design and placement were limited to availability, however, chosen such that they approximated the large-scale.

Guidelines for scaling down operational settings are: (i) the use of the same media, buffers, and microcarrier concentrations; (ii) similar sterilization procedures; (iii) similar setpoints for volume independent parameters like pH, temperature, and schedule of additions; (iv) linear adjustments of volume dependent parameters like inoculum volumes and airflow rates; (v) adjustment of the agitation to obtain either (a) equivalent oxygen transfer ($k_L a$), (b) constant Reynolds number (N_{Re}), (c) constant tip speed (v_T), or (d) constant power input per unit volume (P/V). The latter is also directly related to the shear stress, which is an important factor regarding the shear sensitivity of the cultivation methods using microcarriers (Nienow 2006). The operational variables were kept similar except for the airflow rate over the head-space which was not scaled linearly due to technical limitations of low gas flows. Application of a higher gas flow at small scale was considered acceptable since in surface aerated systems the effect of the gas flow rate on the gas-liquid oxygen transfer can be negated when the gas flow rate is above a minimum (Moreira et al. 1995). To determine the agitation speed, theapproach for comparable power input per unit volume (P/V) was chosen. This approach will also result in comparable shear forces. Based on the power number (N_p) of the large-scale impeller the applied P/V during cell culture (at 750-L scale) was calculated using $P = N_p \times \rho \times N^3 \times D^5$ (van 't Riet and Tramper 1991) and estimated to be ~5 W m^{-3}. The relation between impeller speed and power input was determined for the 5-L Univessels by measuring the torque, or rotational energy (Figure 2A). Concluding from Figure 2A, the agitation speed at small-scale should be around 65–95 rpm. This is well above the off-bottom agitation speed (Zwietering 1958) which is 40 rpm at small scale.

Table 1 Overview of scale-down strategy for each unit operation

		Parameter	Scale-down strategy
Cell and virus culture			
Hardware	Geometry	H/D	Similar
		Impeller design, placement	Approximate[1]
	Inoculum	Preparation Vero cells	Different[2]
		Preparation virus seed	Similar
	Assay systems	Cell count, metabolite analysis, virus analysis, and HCP	Similar
Operational	Volume dependent	Inoculum volume, feed volume, and working volume	Volumetric scale-down 326 times
	Volume independent	pH, DO, T, feed regime	Similar setpoints, same materials as large-scale
		media, buffers, and microcarriers (type, concentration, preparation)	
	Non-linear parameter	Impeller agitation and aeration	*P/V* equivalence scale-down 5 times[1]
Clarification			
Hardware	Equipment	First clarification	Different[2]
		Final filters	Comparable
Operational		Filter load[3] and feed material	Similar
		Harvest method	Similar
Concentration			
Hardware	Equipment	Pump	Comparable, low shear[1]
		Filters	Comparable materials[1]
Operational		dP_{max}, TMP_{max}, concentration factor, filter load, and feed material	Similar
		Filter flush	Different[2]
SEC			
	Column	Matrix, height, HETP & asymmetry, and column load	Similar
Operational		Buffers, elution rate, T, pH, conductivity, and feed material	Similar
IEX			
	Column	Matrix, height, packing procedure, and equilibration procedure	Similar
Operational		Buffers, elution rate, T, pH, conductivity, and feed material	Similar
Inactivation			
		Formaldehyde concentration, pH, T, and procedure	Similar

[1] Limited possibilities due to lab-scale limitations (like availability)

[2] See results & discussion for description

[3] For final filters only; the filter area of the 1st clarification at manufacturing was not quantifiable.

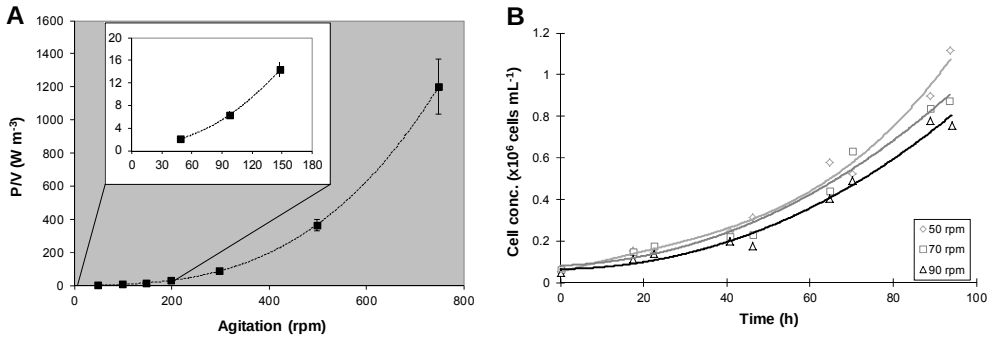

Figure 2. Determination of agitation for scale-down model. Panel A: Effect of impeller speed on the *P/V* in 5-L Univessels. Panel B: Effect of impeller speed on the growth curve of Vero cells (*n* = 1).

The effects of the agitation speed (at 50, 70, and 90 rpm) on the Vero cell growth were studied. In Figure 2B the results are depicted. Despite the small differences in viable cell density a trend was observed where increased agitation speeds resulted in lower viable cell densities and lower growth rates. Possibly this effect is due to the increased shear stress resulting from higher agitation speeds. Shear stress is directly related to the *P/V* (van 't Riet and Tramper 1991). While the difference in power input at these agitation speeds is relatively low, an effect was anticipated since adherent growing cells are more sensitive to shear than cells growing as single cell suspension (Croughan et al. 2006).

This scale-down model for cell- and virus culture was subsequently qualified at setpoint using cell growth characteristics, that is, cell concentrations, specific growth rate, specific metabolite consumption rates, virus concentrations, and specific virus productivity (virus/cell).

Qualification of Cell Culture

To qualify the scale-down model usually all operating parameters are run at setpoint of the manufacturing process. Subsequently the output parameters and sensitivity are compared. For cell culture, cell growth characteristics, like growth rates and metabolite production and consumption rates, are the main relevant performance parameters to qualify the scale-down. Moreover the product quality attributes, here virus quantity and quality, should be used to qualify the model (Rathore et al. 2005b).

The growth curve at 2.3-L lab-scale resembles the growth curve at production scale (Figure 3A). Start- and end-cell concentrations, the maximum specific growth rates, and the growth rate at the time of virus infection (TOI ~90 h) were comparable (Figures 3A & B). However, minor differences between lab-scale and production scale growth curves were

found for the lag-time. This difference was related to a difference in inoculum preparation. At lab-scale the use of a trypsinization apparatus for sub-cultivation was not feasible and therefore this procedure was carried out in a bottle. Moreover, a culture grown in regular fed-batch mode was used as pre-culture method in contrast to the recirculation methods applied at large-scale. These differences were accepted based on applicability at small-scale yet it should be noted that both the pre-culture type and the apparatus and time needed for trypsinization at production scale have a negative impact on the cell fitness, which is visible in the longer adaptation (or lag) time needed. The use of recirculation pre-cultures at lab-scale resulted in a lag time that was approximately 20 h longer while the growth curves (Figure 3A, open circles) and virus yields were similar (*t*-test results P = 0.36; $\alpha = 0.05$).

Table 2. TOST (two-one-side-test) Analysis of key performance parameters for scale comparison of cell and virus culture. Comparisons were made during exponential growth (i.e. 40-70 h cultivation time) unless indicated otherwise. $q_{Nitrogen\ a.a.}$ is calculated based on amino acid consumption without Ala and NH_3 production. $q_{Carbon\ a.a}$ is calculated based total amino acid consumption. Data from PV type 1 cultures are given.

Unit operation	Parameter	Mean	S	Θ	p_{max}	Result
Cell culture	Cell density TOI (10^6 cells mL^{-1})	0.78	0.11	0.20	0.0110	Equivalent
	Average μ (h^{-1})	0.024	0.003	0.007	0.0435	Equivalent
	μmax	0.035	0.005	0.010	0.0006	Equivalent
	μ at TOI (h^{-1})	0.031	0.003	0.010	0.0020	Equivalent
	q_{Gluc}	0.346	0.051	0.100	0.0126	Equivalent
	q_{Lac}	0.802	0.168	0.200	0.0230	Equivalent
	q_{Gln}	0.060	0.018	0.020	0.0030	Equivalent
	q_{Glu}	-0.013	0.006	0.007	0.0438	Equivalent
	q_{NH3}	0.036	0.008	0.010	0.2130	Not Equivalent*
	$q_{Nitrogen\ a.a.}$	0.172	0.046	0.050	0.0478	Equivalent
	$q_{Carbon\ a.a.}$	0.420	0.132	0.150	0.0293	Equivalent
	$Y_{Lac/Gluc}$	2.2	0.34	0.6	0.0356	Equivalent
	$Y_{Gln/Gluc}$	0.151	0.026	0.040	0.0021	Equivalent
	$Y_{NH3/Gln}$	0.744	0.098	0.2	0.4376	Not Equivalent*
Virus culture	Virus titer (10 log $TCID_{50}$ mL^{-1})	8.74	0.2	0.5	6 E-05	Equivalent
	D-antigen (DU mL^{-1})	90.0	8.9	30	0.0481	Equivalent
	Yield titer (10 TCID50 10^6 $cells^{-1}$)	2.9	0.3	0.3	0.0244	Equivalent
	Yield D-antigen (DU 10^6 $cells^{-1}$)	131.2	40.7	50	0.0286	Equivalent

***** Results at manufacturing were lower due to delayed sample analysis.

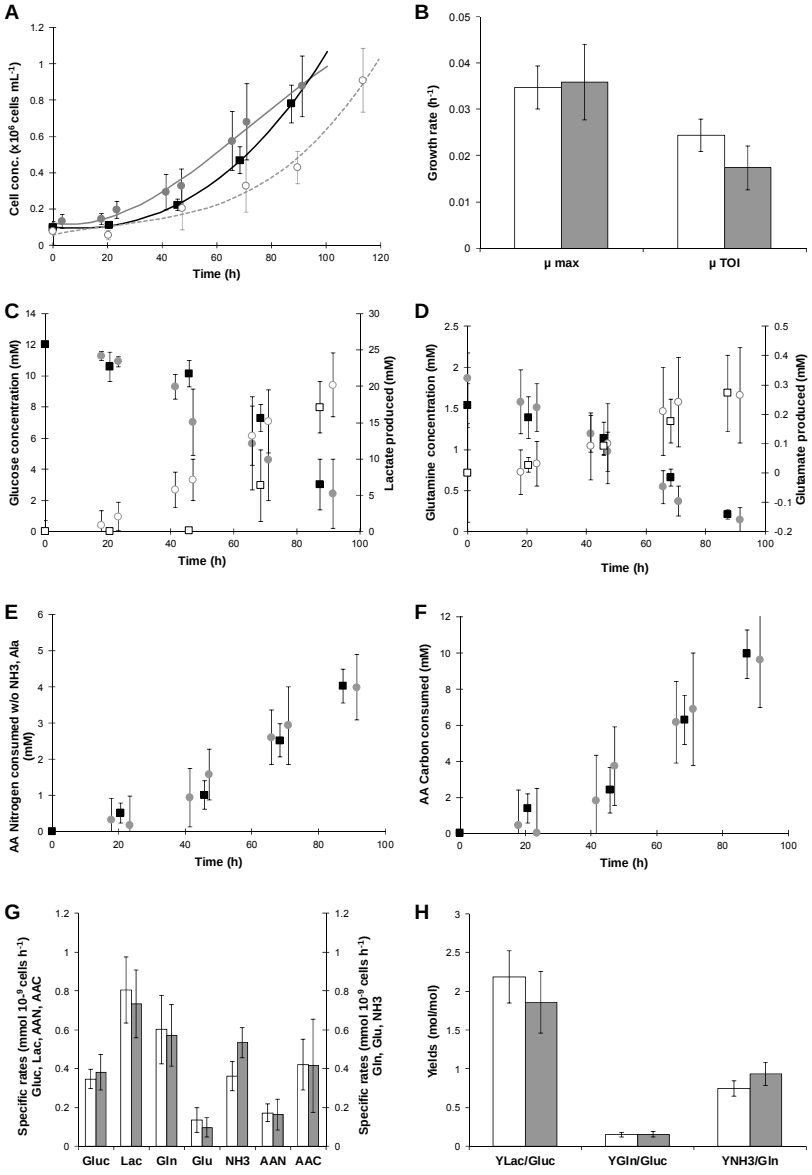

Figure 3. Comparison of cell cultures at 2.3-L (gray circles) and 750-L (black squares). Panel A: Growth curves, open circles represent cell cultures at lab-scale where inoculum was used from a recirculation pre-culture; Panel B: specific growth rates, maximum and at the time of infection; Panel C: Glucose consumption (closed symbols; corrected for feeding and cumulative) and lactate production (open symbols); Panel D: Glutamine concentration (closed symbols) and glutamate production (open symbols); Panel E and F: Amino acid consumption based on respectively nitrogen and carbon; Panel G: Specific production and consumption rates determined during exponential growth (40–70 h); Panel H: Molar yields. Production scale in white and scale-down in gray, error bars give SD.

Next to the cell growth, nutrient consumption and waste metabolite production rates were analyzed. In Figure 3C–F the cumulative consumption for glucose, glutamine, amino acids and the production of lactate, and glutamate are given. While amino acid consumption and more specifically glutamine and glutamate are similar, lactate production starts sooner in the scaled-down model. This corresponds with lower glucose uptake observed at manufacturing scale. At the end of the cultivation period however similar amounts of lactate are present and comparable amounts of glucose are consumed. Moreover, during exponential growth (40–70 h) the specific consumption and production rates for the main metabolites of Vero cell growth at lab-scale are comparable with those at manufacturing scale (Figure 3G). Also the molar yields of lactate on glucose are comparable between scales (Figure 3H). The specific ammonium production rate was lower at production scale (Figure 3G). In parallel, the yield of ammonia over glutamine was also lower at manufacturing scale compared to lab-scale. Both were related to delayed sample measurements of manufacturing scale samples, which leads to a decrease in ammonia concentrations likely caused by evaporation. Equivalence between scales for all cell culture parameters, except for the NH_3 related parameters, was shown (Table 2) using the statistical test for equivalence (TOST). Together these findings illustrate that the small-scale cell culture is comparable to the manufacturing scale cell culture.

Qualification of Virus Culture

Virus culture is started after media exchange where the serum containing cell culture medium is replaced with serum free medium. After 3 days virus culture is finished which is characterized by total cell lysis or 100% CPE (cytopathic effect). The virus yields, measured as infective particles (virus titer) and immunogenic particles (D-antigen), for all three subtypes are equal between scales (Figures 4A & B). Also the virus titer and D-antigen yields per cell were comparable (Figures 4C & D).

Previously, it was described that higher D-antigen yields per cell were observed when at manufacturing a scale-up from 350 to 750-L bioreactors was realized (Bakker et al., 2010). This phenomenon could possibly be related to the growth rate at the moment of virus infection (Bakker et al., 2010). Using the presented scale-down model, research to elucidate this relation is underway.

Scale-Down of Downstream Processing

Scaling-down of downstream processing (DSP) units can be considered straight forward as the processes are based on physics (Godavarti et al. 2005; Rathore et al. 2005a). The most important factor is the use of representative feed streams, that is, intermediate products, resins and buffers from the full scale manufacturing when scaling down. The DSP unit operations used in the IPV production process can be divided in two categories: filtration units and chromatography units.

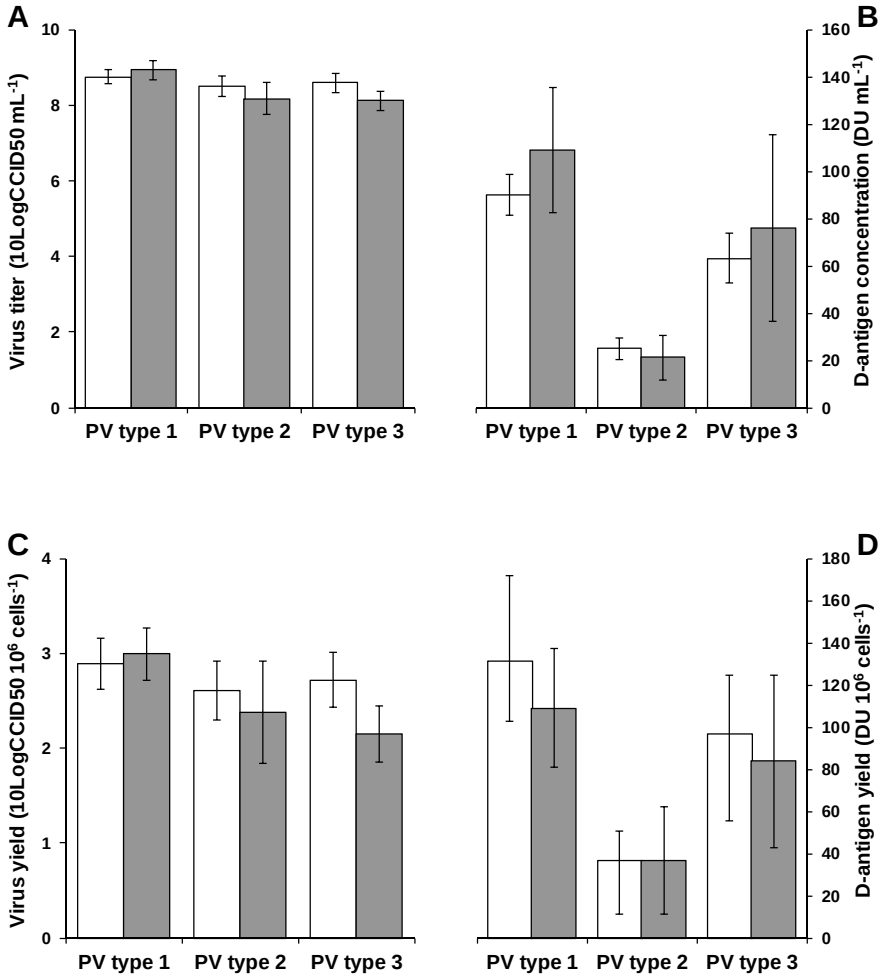

Figure 4. Comparison of virus cultures of PV type 1, 2, and 3 between scales. Panels A and B: Virus titer and D-antigen concentrations; Panels C and D: Product yield based on the production of infective particles (titer) and immunogenicity (D-antigen). Production scale in white and scale-down in gray, error bars give SD.

Filtration Units

Hardware guidelines for scale-down of filtration units concern the retentate path length and the shear stress caused by for instance the pump or system layout. In general, the units are run at setpoints for retentate cross flow rate, transmembrane pressure (TMP), inlet and outlet pressure, temperature, concentration factor, and filter load. The scale-down model can be qualified based on TMP versus flux curves and yields although the latter may be lower at small-scale due to higher system dead volumes.

Two filtration units, clarification and concentration, are used during IPV manufacturing. Lab-scale equivalent filtration units of the large-scale clarification were not available. It was chosen to select a suitable (disposable) alternative. During this selection one of the criteria was the flexibility in filter size which allows clarification of different volumes while retaining a scale-down model based on equivalent filter load.

Pre-clarification was done using a 75 µm stainless steel sieve at both scales and resulted in comparable feed material with respect to turbidity. The clarification unit was qualified based on equivalence of turbidities and recoveries after filtration with similar flows. Clarification of virus harvest at lab-scale can be done using the Millipore C0HC filter. A consecutive combination filter sized 0.45 and 0.22 µm was used. The selected scalable disposable unit was successfully implemented for the preparation of Sabin IPV clinical trial material (Bakker et al. 2011).
A lab-scale version for concentration was setup (Table 1) with which comparable recoveries, with a similar concentration factor, were observed. A drawback of this scale-down model is the inability to back-flush the filters, which is done at large-scale to retrieve more product. To mimic the back-flush of the filter, a 5 min recirculation step has been introduced for both filtersteps followed by a flush step with 3–4 mL of fresh medium (M199) to simulate the back-flush of the second filter. Many factors may influence the observed recoveries observed at manufacturing scale (73 ± 16%) among which are the filter age, system feed flow and hold times, the quality of the start material but also assay variation.

Chromatography Units

Important for scale-down of chromatography units is the chosen chromatography equipment, which should be able to accurately control flow. Concerning the column size, a minimal diameter that can be applied is 10 mm due to the ratio of system dead volume to column volume and wall effects. When this ratio is high it may result in pool concentrations significantly lower than those seen at large-scale (Rathore et al. 2005a). Column packaging performance (HETP and asymmetry) should be the same. Critical parameters for chromatography are (i) bed height and linear flow rates; (ii) column loading (mL product/L resin); (iii) temperature; pH and conductivity; (iv) pooling criteria or when applicable (v) gradient lengths. The setup of the lab-scale units SEC and IEX were essential the same as their large-scale counterparts (Table 1).

To qualify a chromatography scale-down model, the achieved separation should be at the same level as at manufacturing scale. Yields (or recoveries) and the quality attributes should be comparable to full-scale. Regarding peak shape, retention times, or pool volume some difference may be observed due to unavoidable scale differences like tubing or

detectors. When these differences are understood the scale down model can be accepted (Godavarti et al. 2005).

When applying the scale-down model for SEC at setpoint, similar results were obtained compared to large-scale. In Figure 5, examples of SEC chromatograms of PV type 3 at manufacturing and lab-scale are given. The same concentrated virus was used to load the columns. From these chromatograms it can be concluded that a similar purification is obtained, that is, the peak shape and separation are in good agreement. It was observed that retention times (expressed in %CV) at lab-scale are longer. This dissimilarity could be explained by the discrepancy in tubing path lengths and the UV detectors. The differences in retention times were therefore negated. Besides chromatograms, the purity and yields were considered important parameters to qualify the scale-down model. The yields found for the scaled-down model were comparable to those at manufacturing scale for PV type 1 (63 ± 7% and 64 ± 1%), PV type 2 (77 ± 6% and 71 ± 14%), and PV type 3 (74 ± 10% and 84 ± 7%). Purity of the intermediate fraction was assessed by SDS-Pages (data not shown), spectrophotometrically (ratio A260/A280; (Koch and Koch 1985)) and by determination of the concentration of host cell proteins (HCP). Both the ratio A260/A280, for the scale-down 1.15 ± 0.02 and for the large-scale 1.12 ± 0.03, and the HCP concentration, 11.9 ± 5.9 and 13.3 ± 4.8 µg mL^{-1} for respectively small-scale and large-scale, were in good agreement.

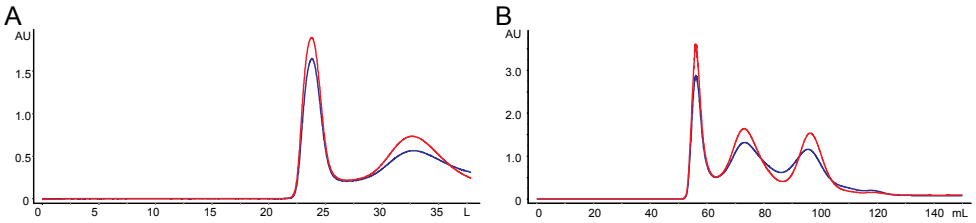

Figure 5. SEC chromatograms of PV type 3. Absorbance at 280 (blue line) and 254 nm (red line) are used to determine fractioning. The second peak corresponds to the virus peak. Panel A: at manufacturing scale; Panel B: at lab-scale. At lab-scale the SEC running time was longer to show all (impurity) fractions.

Qualification of the scale-down model for the IEX was a challenge due to observed interactions of the virus with the column matrix. Although similar chromatograms, in terms of peak shape, could be obtained also different peaks shapes were observed. Since this variation also occurs at manufacturing scale the observed peak shapes were considered to be within the existing variation at manufacturing scale and thus less critical for qualification of the scale-down model (Figure 6). IEX applied in this purification process functions to capture impurities. The performance of this function can be described by

purity analysis of the product. Another important factor is the product recovery. This is especially relevant since some interaction with the matrix was observed which may lead to product loss or undesired product dilution.

The recoveries observed for the scaled-down IEX (66% [$n = 2$], 78% [$n = 2$], and 74 ± 8% for PV type 1, 2, and 3, respectively) were compared with those observed at the manufacturing scale IEX (87% [$n = 2$], 68 [$n = 2$], and 74 ± 2% for PV type 1, 2, and 3, respectively). Additionally the purity profiles were compared. The ratio *A*260/*A*280 was 1.55 ± 0.01 and 1.54 ± 0.03 for virus purified using respectively the small-scale and the large-scale IEX. The HCP content was comparable at 0.05 ± 0.03 µg mL^{-1} (scale-down model) and 0.07 ± 0.05 µg mL^{-1} (manufacturing). It was concluded that the developed scale-down model can represent the large-scale for process optimization and troubleshooting purposes.

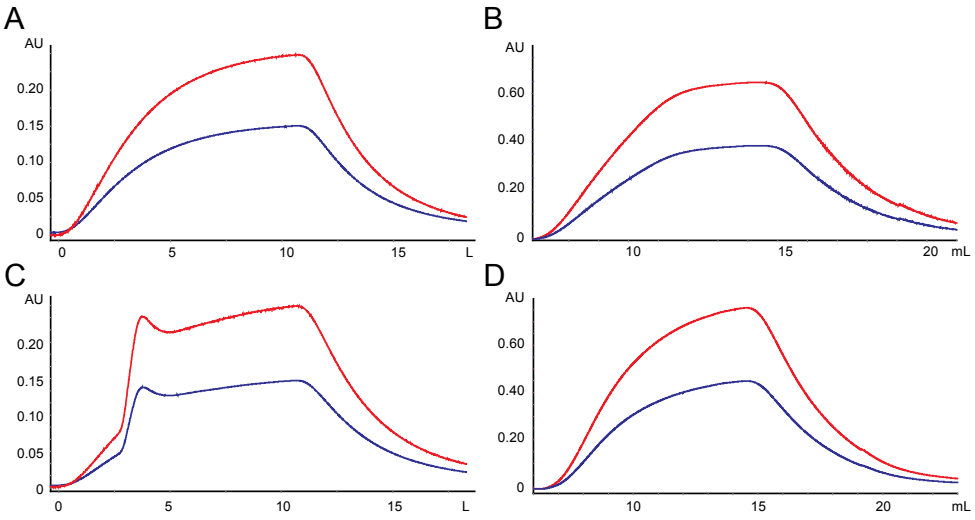

Figure 6. IEX chromatogram of two batches of PV type 2 purified at manufacturing scale (A and C) and using the scale-down model (B and D). One batch is presented in the upper panels (A and B), the second batch in the lower panels (C and D). Absorbance at 280 (blue line) and 254 nm (red line) are used to determine fractioning.

Inactivation

Inactivation of poliovirus is done for at least 13 days using formaldehyde. The time to fully inactivate the poliovirus usually ranges from 72 to 96 h. The product is filtered halfway the inactivation period to remove possible incompletely inactivated poliovirus aggregates and ensure full inactivation. Inactivation kinetics at lab-scale were comparable to those at

manufacturing scale as can be concluded from Figure 7. The product loss during inactivation was neglectable at both scales.

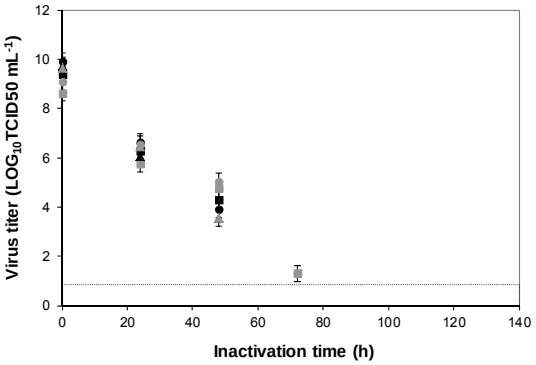

Figure 7. Time curves of inactivation of poliovirus with formaldehyde. Typical inactivation curves are depicted for PV type 1 (squares), PV type 2 (circles) and PV type 3 (triangles). Inactivation of poliovirus at manufacturing scale is given in black, the scaled down inactivation is given in gray. Error bars give the standard assay variation. Dotted line shows lower detection limit for the assay.

Overall Process

So far the described results concern the performance of the independent unit operations, meaning that when using intermediate products obtained from manufacturing the scaled down models act similarly to their large-scale counterparts. Optimization studies at lab-scale, however, need to, besides the effects on the unit of interest, also describe the effects on subsequent unit operations. It is therefore necessary to assess the performance of the scaled-down units consecutively. Three batches of monovalent PV type 1 were produced at lab-scale. To obtain sufficient harvest volumes cell and virus culture were carried out in 5 and 10 L bioreactors and virus harvest was subsequently pooled. Virus infection was done when the cell concentration was approximately 0.8×10^6 cells mL^{-1}. At this time of infection the growth rate was ~0.020 h^{-1}. Virus cultures contained on average 93 DU mL^{-1} at the harvest time. The virus harvest was subsequently clarified, concentrated and purified prior to inactivation at small-scale. Product purity profile after IEX was assessed. The A260/A280 ratio, here 1.62 ± 0.05, and HCP concentrations ranged from 0.01–0.3 µg mL^{-1} (on average 0.15 µg mL^{-1}) indicate slightly higher impurities when compared to the use of individual unit operations and to the values observed at large-scale. The difference in impurity profiles was largely due to peak collection after SEC and IEX. This process is not automated but performed manually, both at manufacturing as at lab-scale, and therefore operator dependent. Current studies focus on the possibility to automate product peak collection to decrease variation in the product profile. In Figure 8, a comparison of the yields during the DSP process is given. For all unit operations comparable product recoveries were observed. It can thus be concluded that a comparable efficiency was observed throughout the downstream processing. Assessment of the monovalent product immunogenicity was done using the batch-release rat potency test. The product prepared at lab-scale induced sufficient neutralizing antibodies and met

release criteria. From these results it was concluded that the obtained scale-down model can be used for lab-scale experiments to explore the influence and effects of the different parameters and possible changes to the production process.

A perfect scale-down model should not only operate similar on setpoint, but also react in a similar manner when operated beyond the setpoints. It is, however, not feasible to generate the data at manufacturing scale which is necessary for this comparison. Therefore, regarding process changes, confirmation runs at manufacturing scale are still required. These confirmation runs will also provide information on the performance of the scale-down model. Additionally, by mimicking the deviations occurring at manufacturing scale in the scale-down model further model development can be pursued.

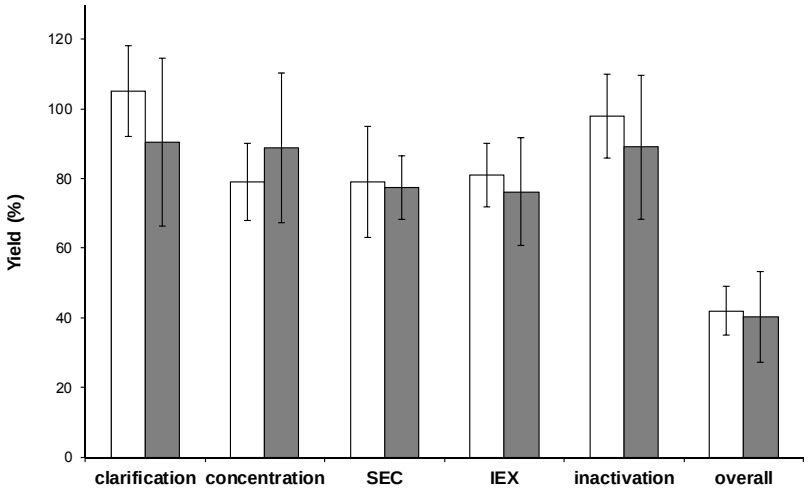

Figure 8. D-antigen recoveries for purification of PV type 1. Large-scale 1,500-L (white; n = 16) and scaled-down process 20-L (gray; n = 3). The data presented for the scale-down model represent consecutive processing, that is, the USP and DSP were done at lab-scale. No statistically significant difference was found for the yields (i.e., t-test results $\alpha = 0.05$; $P > 0.05$).

Conclusions

The current scale-down models for cell and virus culture (2.3-L) and the subsequent filtration, purification, and inactivation are in agreement with its production scale counterpart (750-L bioreactor and 1,500-L virus harvest) when operated at setpoint. With this model relatively large changes in the production process (like process optimization, the use of different culture media, and other virus types) can be studied and used to predict the large-scale outcome.

Acknowledgements

The authors would like to thank G. van Eikenhorst for characterization of the lab-scale cell culture equipment, M. de Vries for assistance during DSP and HCP analysis, A. de Haan for amino acid analysis, S. Haddad for virus titer analysis and D-antigen ELISA and J. Ferreira for help on statistical equivalence testing.

Nomenclature

A260/A280	ratio between the absorbance at 260 and 280 nm
D	bioreactor diameter (m)
DU	D-antigen Units
H	height of fluid in bioreactor (m)
HCP	Host cell proteins
$k_L a$	mass transfer coefficient (s^{-1})
MOI	multiplicity of infection
N	Agitation speed (s^{-1})
N_p	impeller power number
N_{RE}	Reynolds number
P	power input (W)
PV	poliovirus
q	specific consumption or production rates (mmol 10^9 $cells^{-1}$ h^{-1})
TOI	time of infection
V	volume of fluid (m^3)
v_T	impeller tip speed (m s^{-1})

Greek Symbols

μ	specific growth rate (h^{-1})
ρ	density of fluid (kg m^{-3})

Chapter 6

Transfer of an adherent Vero cell culture method between two different rocking motion type bioreactors with respect to cell growth and metabolic rates

Published as:
Thomassen, Y.E., van der Welle, J.E., van Eikenhorst, G., van der Pol, L.A., Bakker, W.A.M. (2012) *Transfer of an adherent Vero cell culture method between two different rocking motion type bioreactors with respect to cell growth and metabolic rates.*
Process Biochemistry 47(2): 288-296
dx.doi.org/10.1016/j.procbio.2011.11.006

Abstract

Rapid and simple cell and virus cultivation can currently be carried out using disposable bioreactors. The CELL-tainer® (CELLution Biotech BV) disposable bioreactor is a rocking-type bioreactor which not only has vertical movement but horizontal displacement as well. Due to this two-directional movement relatively high mass-transfer capacities can be reached when compared with conventional rocking motion-type bioreactors.

Using the design of experiments (DoE) approach we have developed models for the mixing times in both the CELL-tainer® and the BIOSTAT® CultiBag RM (Sartorius Stedim Biotech) bioreactor (standard rocking motion-type). The conditions for cultivation of Vero cells in the CELL-tainer® bioreactor were chosen based on comparable mixing times.

Vero cells growing adherent to Cytodex 1 microcarriers were cultivated in the CELL-tainer® and in the BIOSTAT® CultiBag RM. Both bioreactors were controlled with regard to temperature, pH and % dissolved oxygen. Vero cell growth in both bioreactors was comparable with respect to the growth characteristics and main metabolite production and consumption rates. Additionally, poliovirus production in both bioreactors was shown to be similar.

Introduction

Vero (African green monkey kidney) cells can be regarded as a platform for vaccine production (Barrett et al. 2009). They have been widely used for over 30 years for the production of inactivated polio and rabies vaccines (Montagnon et al. 1981; van Wezel et al. 1978). Recent work regarding vaccine developments using Vero cells range from a pandemic H5N1 influenza (Crowe et al. 2010) to flaviviruses like Dengue (Petiot et al. 2010b) or pediatric vaccines like respiratory syncytial virus (RSV) vaccine (Widjojoatmodjo et al. 2010). Some of these anticipated vaccines, for instance a vaccine against a pandemic influenza virus, would benefit from a fast-track concept for development and manufacture. In this respect, multi-purpose bioprocess equipment and the use of standard blue-prints for protocols are essential.

Over the past few years disposable bioreactors have been increasingly used in biopharmaceutical industry. The main advantages of disposable bioreactors are their flexibility, ease of handling, reduced incidence of cross-contamination and savings in time and costs, mainly due to the pre-sterility of the cultivation container which is guaranteed by the vendor (Eibl et al. 2010). New systems for disposable bioreactors are continuously under development. Fast application of these new systems using existing protocols on essential operating parameters and cultivation conditions are indispensable for their implementation.

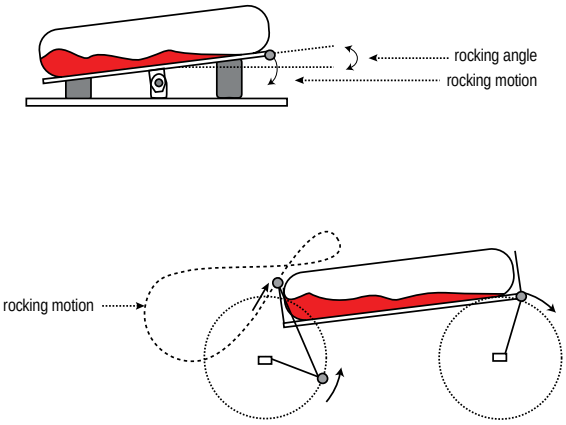

Figure 1. Schematics of the motions of rocking motion type bioreactors. In panel a the conventional rocking motion type bioreactor (RM) (figure adapted from (Singh 1999)) is shown. Both the rocking speed and the angle can be adjusted. In panel b the CELL-tainer® bioreactor (CT) (figure adapted from (van der Heiden et al. 2008)) is depicted, here the rocking speed, the horizontal and the vertical displacement and the phase between the horizontal and the vertical movement can be adjusted

Recently, a novel rocking motion type bioreactor, the CELL-Tainer® (CT), was developed (van der Heiden et al. 2008). The CT has a different type of rocking motion compared with the conventional rocking motion or wave bioreactor (RM) described by Singh (Singh 1999) (Figure 1). In rocking motion type bioreactors agitation and mixing are induced by a

vertical displacement, which generates a wave in the cell culture. The RM tilts at a central pivot point to generate the wave motion. The CT has such a movement that the pivot axis follows a cyclical closed loop motion which causes the bioreactor to swivel both in vertical as well as in horizontal direction. This two-dimensional motion results in more gentle waves and superior oxygen transfer capabilities.

Oxygen transfer coefficients (k_La) ranging from 200 h^{-1} to 700 h^{-1} are reported for the CT (Chaudet et al. 2011; Oosterhuis and van den Berg 2011; Oosterhuis and van der Heiden 2010) compared to 2–4 h^{-1} for conventional RM bioreactors (Hanson et al. 2009; Singh 1999) or 0.7–1.5 h^{-1} (surface aerated cell culture) for standard stirred tank bioreactor (Lavery and Nienow 1987).

Process transfer or scale-up for stirred tank bioreactors is done based on different criteria (Rathore et al. 2005b; Schmidt 2005; van 't Riet and Tramper 1991). Common criteria next to geometric similarity are: (a) constant tip speed (v_T), (b) constant Reynolds number (N_{RE}), (c) equivalent oxygen transfer (k_La), or (d) constant power input per unit volume (P/V). The latter two are the preferred methods and result in similar mixing across scales (Rathore et al. 2005b).

Consequently, mixing is one of the most significant factors affecting performance and is often used in scale-up and process transfer. One of the methods used to characterize mixing is determination of the mixing time (Θ_m), which is defined as the time needed to obtain a specific degree of homogeneity after a pulse signal of tracer. Although scaling using a constant Θ_m is not always feasible due to increasing power needs at higher volumes (Schmidt 2005; van 't Riet and Tramper 1991), it can be applied for process transfer at comparable scales.

Protocols and cultivation conditions for growth of Vero cells adherent to microcarriers in RM are available (Blüml 2007; Genzel et al. 2010; Schouwenberg et al. 2010). In this work, we have determined the Θ_m in relation to operational settings using a design of experiments approach for both the RM and the CT. Process transfer from the RM to the CT was successfully done at comparable scale based on comparable Θ_m considering Vero cell growth characteristics and poliovirus production.

Materials and methods

Cell lines and culture media

Adherent growing Vero cells obtained from WHO (10-87) originally derived from ATCC (CCL-81) were adapted to grow in VP-SFM (Invitrogen, #12559-019) supplemented with L-

glutamine (2 mM final concentration, Invitrogen, #25030-123) at 37 °C. This medium is further referred to as SFM.

Virus type and assays

The poliovirus strain used was Sabin type 1 (LS-c 2ab KP_2).

Virus titers were determined by 50% tissue culture infective dose ($TCID_{50}$). Serial dilutions (10-fold) of the culture supernatants were prepared in culture medium. Vero cells in culture medium (1×10^4 cells/well) were added to a 96-wells plate. Virus suspension (50 µL/well) was added. $TCID_{50}$ assays were visually inspected for cytopathic effect (CPE) after 7 days incubation at 37 °C.

D-antigen concentrations were determined via sandwich ELISA using monoclonal antibodies (Kersten et al. 1999). In short, samples (when necessary diluted in PBS, 0.1 v/v% Tween-20, and 0.5% Protifar (Nutricia, Zoetermeer, The Netherlands) were added to microtiter plates (Greiner, white, high-binding) coated with caprylated bovine-anti-poliovirus type 1. After washing with wash buffer (PBS, 0.1% v/v Tween-20) poliovirus was detected using an in-house monoclonal antibody (3–4E4) and HRP-labeled goat anti-mouse. For detection the luminescence signal reagent HighLite (Zomerbloemen B.V., Zeist, The Netherlands) was used. The emitted light was detected using a luminometer (Fluostar OPTIMA, BMG Labtech, Ortenberg, Germany).

Pre-cultures

T-flasks or HYPERflasks (Corning) were inoculated with approximately 3×10^4 cells cm^{-2} and grown for 4 days in SFM. When fully confluent ($\sim 2.5 \times 10^5$ cells cm^{-2}) cells were washed using PBS without Ca^{2+}/Mg^{2+} (Invitrogen, #20012019) and detached using 1× TrypLE Select (Invitrogen, #12563-029). The TrypLE Select activity was not stopped. The cell suspension was used to inoculate the bioreactors.

Microcarrier preparation

Microcarriers (Cytodex 1, GE healthcare #17-0448-03) were swollen in Ca^{2+}/Mg^{2+} free PBS for at least 3 h at room temperature and subsequently washed using fresh Ca^{2+}/Mg^{2+} free PBS before sterilization. Prior to use the microcarriers were washed twice using SFM.

Vero cell culture in standard rocking motion type bioreactor

For Vero cell cultivation in a 2 L BIOSTAT® Cultibag RM bioreactor (Sartorius Stedim Biotech) 1 L SFM, 0.1% Pluronic F-68 (Sigma-Aldrich, #P5556), 3 g L^{-1} Cytodex 1 (GE Healthcare, #17-0448-03), 4 mM Ca^{2+} and cells (start cell concentration 0.2×10^6 cells mL^{-1}; corresponding with 10 cells/MC) were transferred to the Cultibag RM (Sartorius Stedim Biotech, #DBO002L). The cultivation conditions were T: 37 °C; pH: 7.2 (controlled using CO_2

and $NaHCO_3$); DO: 50% air saturation; rock speed: 16 rocks per minute (rpm); angle: 8°. The DO was controlled using air, O_2 and N_2 via headspace aeration. Due to the large surface area no sparging is required in rocking motion type bioreactors. A bolus feed of L-glutamine was given when the concentration was <0.5 mM. Cultures were performed at least in triplicate.

Virus cultures (cultivation conditions: T 32.5 °C; pH 7.4; DO 25%) were performed without media exchange. The used multiplicity of infection (MOI) was 0.01. Virus cultures were complete (100% CPE) after 3 days.

Vero cell culture in CELL-tainer® bioreactor

For cell and virus cultivations (3 L working volume) in a 20 L CELL-tainer® Bioreactor Bag (Cellution Biotech, #CB00010220) culture conditions were comparable to that in the RM. CT (Figure 1) settings were phase: 25%; rock speed: 15 rpm; horizontal displacement: 40%; vertical displacement: 30%.

Mixing time measurement

Mixing times (Θ_m) were determined using an acid (HCl) pulse in PBS. Homogeneity was set at 85% of the final equilibrium. For determination of Θ_m optical pH sensors do not qualify due to their relatively high response time (τ_p). As a rule of thumb the τ_p should be much smaller than Θ_m (van 't Riet and Tramper 1991). Therefore, a glass pH sensor (VWR, 662-1788) with a response time (95% homogeneity) of <1 s was mounted in the center of the disposable cell culture bags.

Microcarrier homogeneity

Determination mixing efficiency of Cytodex 1 microcarriers, or MC homogeneity, was done visually. Microcarriers were stained using Trypan Blue, suspended in water and added to the culture bag. The homogeneity of MC distribution throughout the fluid was quantified using four categories. A: not mixed, microcarriers remain at bottom of bag; B: part of the microcarriers is at the bottom of the bag, the other part is moving in the fluid; C: all microcarriers are moving but some clouds are visible; D: microcarriers are evenly distributed throughout the fluid. The categories were given values of 1, 3, 7 and 10, respectively, for data analysis purposes.

Culture samples and analysis

Samples (5–10 mL) from the Cultibag and CELL-tainer® were taken using a syringe through a Luer-Lock-septum. Cell counts were measured using a Nucleocounter (Chemometec) to determine total nuclei. Using a Bioprofile 100 Plus (Nova Biomedical) glucose, lactate, glutamine, glutamate and ammonium were determined directly after sampling.

Cells were stained with hematoxylin and observed with inverted light microscopy (20× magnification).

Calculation of specific rates and yields

Cell concentrations (cells mL^{-1}) were corrected for the volume of the microcarriers. Specific rates for growth rate (μ), glucose or glutamine consumption (q_{Glc}, q_{Gln}) and lactate, glutamate and ammonia production (q_{Lact}, q_{Glu}, and q_{NH_3}) were calculated according to the following equations:

$$\mu = \left(\frac{1}{X}\right) \times \left(\frac{dX}{dt}\right) \quad \text{(eq.1)}$$

$$q = -\left(\frac{1}{X_v}\right) \times \left(\frac{dS}{dt}\right) \quad \text{or} \quad \left(\frac{1}{X_v}\right) \times \left(\frac{dP}{dt}\right) \quad \text{(eq.2)}$$

where X is the viable cell concentration, S and P, respectively, are the concentrations of substrate and products. Smoothing of experimental points and generation of intermediate points was achieved by fitting a polynomial curve, either 3^{rd} of 4^{th} order, to the experimental data.

Design of experiments (DoE)

Response surface modeling using MODDE 9.0 software for design of experiments and optimization (Umetrics) was applied to characterize the influence of the rocking settings on the mixing times and MC homogeneity.

The fractional factorial design for mixing times and MC homogeneity in the CT consisted of five factors namely, rocking speed, horizontal displacement, vertical displacement, phase and volume at two levels comprising all the possible combinations. All mixing times were measured in triplicate. Moreover a center point was measured in triplicate (phase excluded this was only set at 25 or 50). A first analysis indicated a squared term in the model therefore the factorial design was complemented to a response surface model design namely a composite face centered design (CCF). All factors, that were significant after the first screening have five levels in the CCF design.

For the RM a full factorial design for two factors, angle and rocking speed, was created on 2 levels. Also a center point was included. All measurements were performed in triplicate. The design was complemented to a CCF with 2 factors and 5 levels due to the indication that a squared term should be included in the model.
Experimental design and measured responses are given in supplementary data.

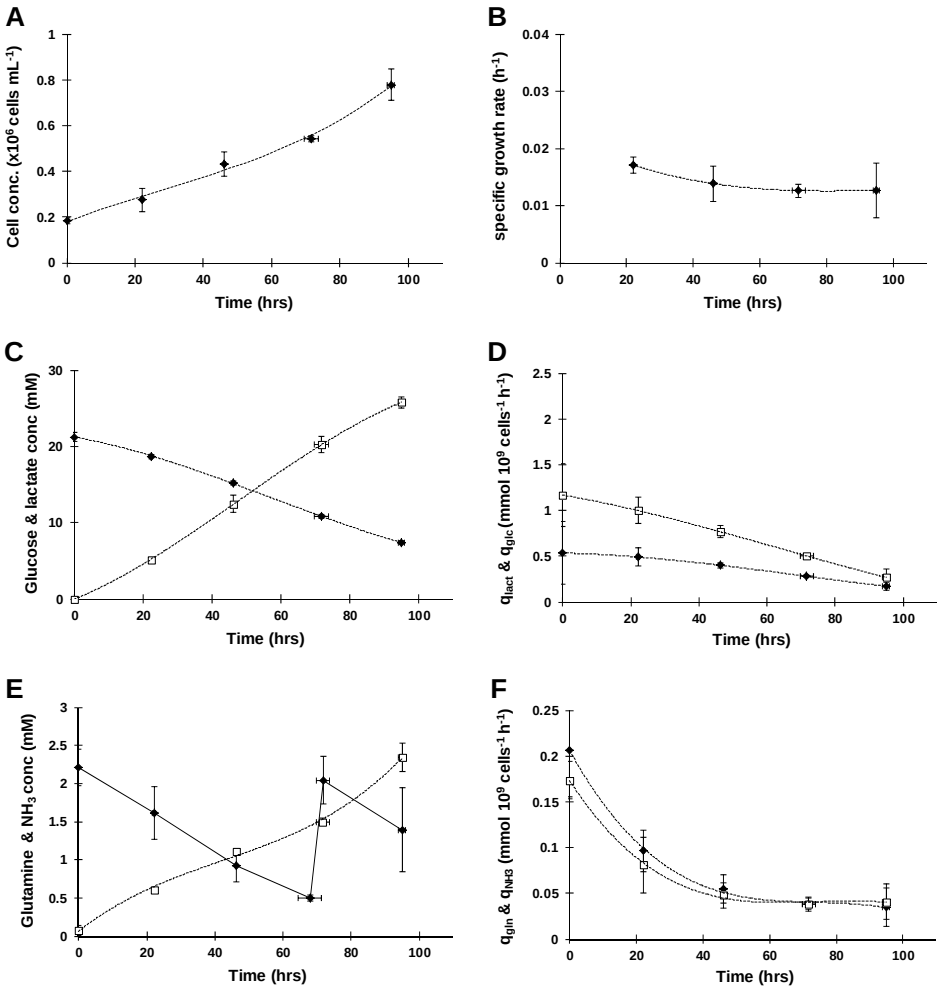

Figure 2. Growth kinetics of Vero cells grown adherent to Cytodex 1 microcarriers in a 2 L RM in SFM. Graphs show the average curves with standard deviation (n = 3). Concentration of attached cells and specific growth rate are shown in panel a and b, respectively; panel c shows glucose (closed diamonds) and lactate (open squares) concentrations, their specific consumption or production rates are shown in panel d; panels e and f, respectively, show concentrations and specific rates for glutamine (closed diamonds) and ammonium (open squares). At 70–80 h glutamine was fed to the bioreactor. Lines are for guidance.

Results

Cultivation of Vero cells in BIOSTAT® Cultibag RM bioreactor (RM)

In the following section, results obtained by cultivation of Vero cells grown adherent to microcarriers in SFM medium in a conventional rocking motion type bioreactor are described (Figure 2).

Previously a protocol for cultivation of Vero cells attached to Cytodex 1 microcarriers has been reported (Blüml 2007). In this protocol it is described that during the first hours of cultivation the angle and rock speed is adjusted repeatedly to allow cells to attach to the microcarriers. For practical reasons the protocol was adapted to a single angle and rock speed throughout the culture. The chosen angle and rock speed (8°; 16 rpm) were based on MC homogeneity at the lowest possible rock speed.

Initial experiments were done to determine cultivation conditions with respect to microcarrier concentration (2–4 g L^{-1}), seeding cell concentration (5–20 × 10^4 cells mL^{-1}) and Ca^{2+} content (3–5 mM). Based on these initial experiments (results not shown) the optimal conditions for cultivation of Vero cells in the RM bioreactor were chosen (see Section 2). Using these culture conditions, Vero cells seeded at a cell concentration of 0.2 × 10^6 cells mL^{-1} reached a cell concentration of 0.8 × 10^6 cells mL^{-1} after 95 h of cultivation (Figure 2; Table 1). Cells were equally distributed on the microcarriers both at the start (day 1) of the cell culture as at the end (day 4; Figure 3). The observed growth rate was reasonably constant during the culture time. Consumption of glucose and glutamine resulted in accumulation of by-products lactate and NH_4^+. Steady lactate on glucose yield ($Y_{Lact/glc}$) of 1.9 was obtained indicating that nearly all of the glucose consumed was converted to lactate. After 70 h of cultivation glutamine was added (to a concentration of 2 mM) to prevent limitation of glutamine for growth (Figure 2E). Vero cell growth in the RM was reproducible with respect to cell and metabolite concentrations as well specific rates for growth and metabolite consumption (Figure 2).

Mixing times

To be able to transfer the cultivation protocols from the RM to the CT, mixing times (Θ_m) in both systems were determined. Besides an appropriate Θ_m, conditions in which microcarriers remained suspended were chosen as prerequisite for cultivation. To assess both Θ_m and MC homogeneity a design of experiments (DoE) approach was used. A first screening was based on (fractional) factorial design which was later complemented to a response surface model design namely a central composite face centered design (CCF). In Figure 4A & B the prediction results of the models (Table 2) for the 2-L RM are given. An increase in angle or rocking speed correlates similarly with increased MC homogeneity as decreased Θ_m. The applied conditions for cultivation of Vero cells as shown in Figure 2

Table 1. Growth characteristics and metabolic rates for adherent Vero cell growth in RM and CT bioreactors

	CultiBag RM	CELL-tainer®	Literature (RM)	Literature (STR)[a]	References RM	STR
start cell concentration (10^6 cells mL^{-1})	0.2	0.2	0.2	0.1-0.4	(Genzel et al. 2010; Schouwenberg et al. 2010)	(Merten et al. 1999; Petiot et al. 2010a; Quesney et al. 2003; Rourou et al. 2007)
cell concentration at 95h (10^6 cells mL^{-1})	0.8	0.9	0.7-1.2	0.9-2.6	(Genzel et al. 2010; Schouwenberg et al. 2010)	(Merten et al. 1999; Petiot et al. 2010b; Rourou et al. 2007; Toriniwa and Komiya 2007)
µmax (h^{-1})	0.017	0.027	-	0.017-0.033		(Merten et al. 1999; Petiot et al. 2010a; Quesney et al. 2003; Rourou et al. 2007)
accumulation of lactate (mM)	26	27	~17	9-32	(Genzel et al. 2010)	(Petiot et al. 2010b; Quesney et al. 2003; Rourou et al. 2007)
accumulation of ammonia (mM)	2.3	2.0	~2.3	0.8-1.5	(Genzel et al. 2010)	(Petiot et al. 2010b; Quesney et al. 2003; Rourou et al. 2007)
q_{Glc} (mmol 10^9 $cells^{-1}$ h^{-1})[b]	0.5	0.5	-	0.3-0.5		(Petiot et al. 2010b; Quesney et al. 2003)
q_{Gln} (mmol 10^9 $cells^{-1}$ h^{-1})[b]	0.1	0.1	-	0.09-0.11		(Petiot et al. 2010b)
q_{Lact} (mmol 10^9 $cells^{-1}$ h^{-1})[b]	1.0	1.3	-	0.7		(Petiot et al. 2010b)
q_{NH3} (mmol 10^9 $cells^{-1}$ h^{-1})[b]	0.1	0.1	-	0.05		(Petiot et al. 2010b)
$Y_{Lact/Glc}$	1.9	2.0	1.6	1.14-1.7	(Genzel et al. 2010)	(Petiot et al. 2010b; Quesney et al. 2003)
$Y_{NH3/Gln}$	1.0	1.0	-	0.5		(Petiot et al. 2010b)

[a] Literature values for STR or spinner flasks are given when similar cultivation conditions ((fed-) batch cultivation with 2–3 g L^{-1} Cytodex 1 and SFM) are used.

[b] Given specific rates are those ~20 h after inoculation

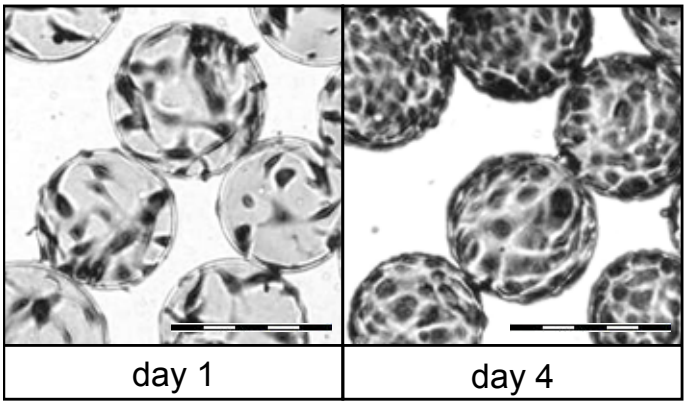

Figure 3. Distribution of Vero cells growing adherent to microcarriers in the RM at day 1 and 4 of the cell culture. Cells were stained using hematoxylin and observed with inverted light microscopy (size bar = 200 µm).

Table 2. RSM models for mixing time and MC homogeneity in the RM and CT

	Factor	Coefficient (scaled & centered)	Standard error	P-value
RM	Mixing time			
	Rocking speed	-125.815	8.662	< 0.000
	Angle	-42.891	7.945	< 0.000
	(Rocking speed)^2	135.652	15.283	< 0.000
	(Rocking speed)×(Angle)	42.084	8.987	< 0.000
RM	MC homogeneity			
	Rocking speed	5.432	0.921	< 0.000
	Angle	2.766	0.685	0.001
CT	Mixing time			
	Rocking speed	-0.308	0.053	< 0.000
	Vertical displacement	-0.345	0.053	< 0.000
	Volume	0.179	0.053	0.002
	(Vertical displacement)^2	0.219	0.104	0.042
	(Rocking speed)×(Vertical displacement)	-0.112	0.054	0.046
CT	MC homogeneity			
	Horizontal displacement	1.188	0.288	< 0.000
	Vertical displacement	2.313	0.288	< 0.000
	Rocking speed	1.813	0.288	< 0.000
	(Vertical displacement)^2	-3.806	1.003	0.001
	(Horizontal displacement)×(Vertical displacement)	-0.938	0.288	0.003
	(Rocking speed)×(Vertical displacement)	1.063	0.288	0.001

RM models for mixing time (s) (R^2 0.961; Q^2 0.930) and MC homogeneity (R^2 0.762; Q^2 0.626) are described by rocking speed (rpm) and angle (°). The CT model for mixing time (s) (R^2 0.721; Q^2 0.631) is described by rocking speed (rpm), vertical displacement (%) and volume (mL). The CT model for MC homogeneity (R^2 0.853; Q^2 0.777) is described by horizontal and vertical displacement (%) and rocking speed (rpm).

obtained in the RM were angle 8° and rocking speed 16 rpm. Under these conditions the microcarriers were in suspension and mixed, the corresponding Θ_m was 89 s (95% confidence interval 69.6–108.5 s).

The settings for the CT can be adjusted with regard to rocking speed, movement in horizontal and vertical direction and phase between the horizontal and vertical movement. Additionally, the effects of different volumes in the 20 L disposable bag were taken into account. Therefore, a five factor CCF design was used to assess the effects of all factors. Phase was eliminated from both models as the effects of the high and low settings of this factor could not be modeled with statistical significance. The predictions based on the resulting models (Table 2) for Θ_m and MC homogeneity are depicted in Figure 5. In both models the vertical displacement is squared, which results in a similar characteristic pattern for mixing. Additionally, it can be seen that higher rocking speed and higher vertical and horizontal displacements results in lower Θ_m. Further, it is shown that higher Θ_m were observed when the reactor volume is increased (Figures 5A–C). From the model for Θ_m in the CT the settings (vertical movement 30%, rocks 15 rpm) were derived for cultivation of Vero cells at a desired working volume of 3.0 L. These conditions have a predicted Θ_m of 88 s (95% confidence interval 53.8–142.6 s), which is similar to the Θ_m estimated for the applied cultivation conditions in the RM. The setting for horizontal movement (40%) was obtained from the MC homogeneity model using the outcome from the Θ_m model and the prerequisite of homogeneity for MC.

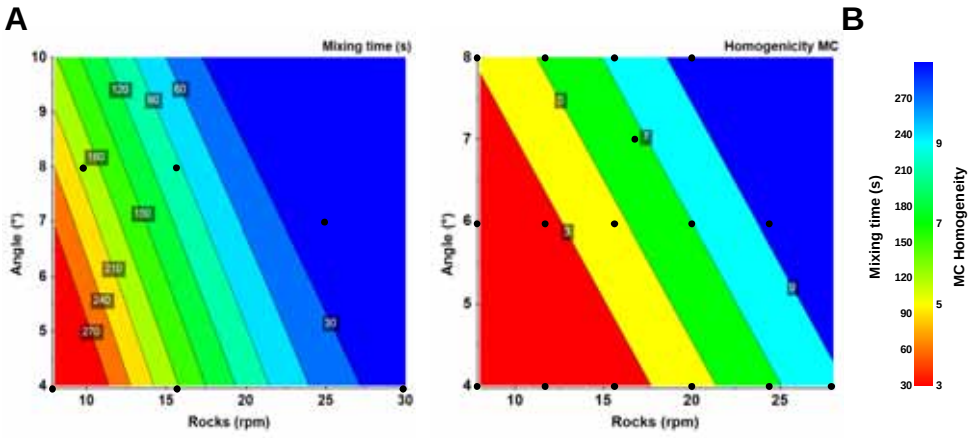

Figure 4. Model predictions for (A) mixing times and (B) degree of MC homogeneity for the RM. RSM model for mixing time in seconds (R^2 0.961; Q^2 0.930) and the RSM model for MC homogeneity (R^2 0.762; Q^2 0.626) are described by rocking speed and angle (Table 2). MC homogeneity is acceptable when the value is above 7. Measurements are indicated with dots.

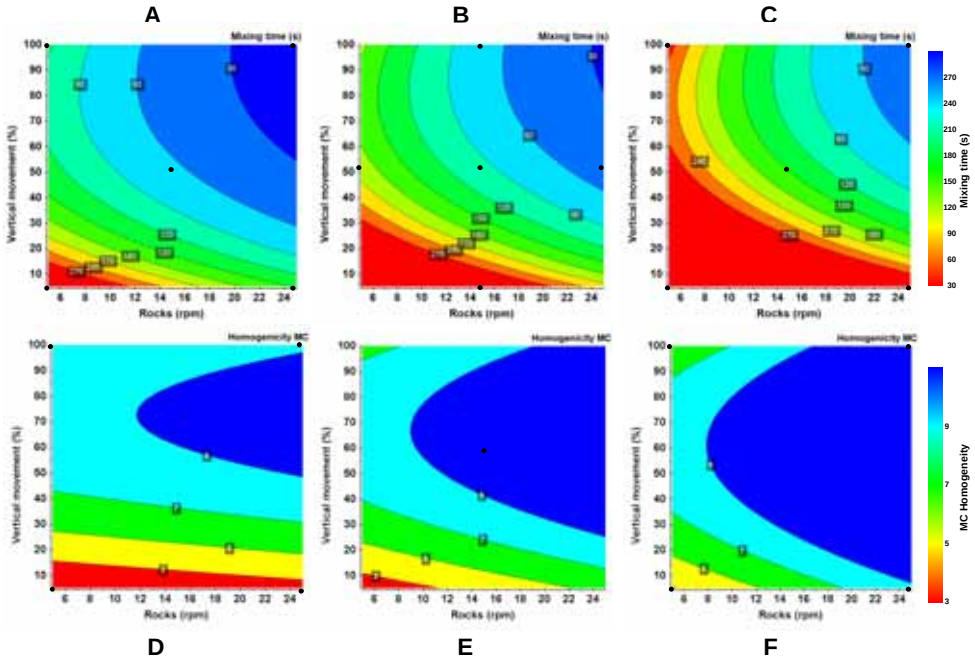

Figure 5. Model predictions for mixing times in the CT at different volumes: (a) 5-L, (b) 10-L and (c) 15-L and the MC homogeneity at different horizontal displacement (d) 5%, (e) 53% and (f) 100%. RSM model for mixing time in seconds (R^2 0.721; Q^2 0.631) is described by rocking speed, vertical displacement and volume (Table 2). The RSM model for MC homogeneity (R^2 0.853; Q^2 0.777) is described by horizontal and vertical displacement and rocking speed (Table 2). MC homogeneity is acceptable when the value is above 7. Measurements are indicated with dots.

Cultivation of Vero cells in CELL-tainer® bioreactor (CT)

The settings used for cultivation of Vero cells in the CT were obtained from the mixing models described above. Other settings like temperature, cell concentration and medium composition were kept constant when transferring the process from the RM to the CT.

Growth kinetics and metabolite concentration time courses for Vero cell culture in the CT are presented in Figure 6 and Table 1. The specific growth rate of Vero cells in the CT peaked to 0.027 h^{-1} at ~30 h. Distribution of the cells on the microcarriers was comparable with the photos shown in Figure 3. Specific glucose consumption rate was fairly constant and decreased near the end of the culture. Glutamine consumption rate declined with culture time. Glutamine was added to the bioreactor when the concentration was below 0.5 mM to prevent glutamine depletion (around 70–80 h). Accumulation of by-products was observed, lactate was produced to a maximum concentration of 27 mM with a yield of

$Y_{lact/gluc}$ 2.0 which suggests that all glucose was converted to lactate. Reproducibility of the cell culture in the CT was reasonable with respect to cell and metabolite concentrations. Larger variations were observed for specific rates mainly at the beginning of the culture.

Comparison of Vero cell growth and metabolic rates in RM and CT

Process transfer from the RM to the CT was considered satisfactory when both systems performed equivalent with respect to Vero cell growth characteristics. Cells were equally distributed over the carriers in both bioreactor systems. After 95 h cultivation a similar cell density was obtained (Figures 2 & 6; Table 1). The maximum specific growth rate seemed to differ between both systems. At a culture time of 20–40 h the growth rate in the CT was significantly higher compared with the growth rates in the RM (Figures 2 & 6). This might be due to the slightly longer lag phase observed in the CT. However, at the end of the exponential phase the cells had the same growth rates. Glucose and glutamine concentrations as well as the concentrations of the by-products lactate and ammonium were comparable throughout the culture (Figures 2 & 6). Moreover, the specific consumption and production rates were similar (Figures 2 & 6; Table 1). Overall the growth characteristics between both systems were considered equivalent showing that process transfer at comparable scales based on mixing characteristics is applicable for rocking motion bioreactors.

Table 3. Poliovirus production

	Cell concentration at infection (10^6 cells mL^{-1})	Virus culture time (h)	Virus titer (10log $TCID_{50}$ mL^{-1})	D-antigen (DU mL^{-1})	DU per cell (10^{-5} DU $cell^{-1}$)
RM	0.8	76	8.3	75	9.3
CT	0.8	72	8.3	77	9.6

Virus culture in the RM and CT

Vero cells grown in the RM or CT were infected with poliovirus (Sabin type 1) to assess virus production capabilities of cells grown in these rocking motion type bioreactors. Cells were infected at the end of the exponential phase when the cell concentration was 0.8 × 10^6 cells mL^{-1} with a multiplicity of infection (MOI) of 0.01. Virus culture was complete when 100% cytopathic effect (CPE) was observed; this occurred after approximately 75 h both in the RM as in the CT. Virus yields based on virus titer were 8.3 log 10 $TCID_{50}$ mL^{-1} for both the RM as the CT. The D-antigen content, a measure for the amount of immunorelevant poliovirus, was similar at 75 and 77 DU mL^{-1} in the RM and CT, respectively (Table 3). Therefore, it was concluded that the process transfer from the RM to the CT based on mixing characteristics was suitable not only for the cell culture but also for the virus culture.

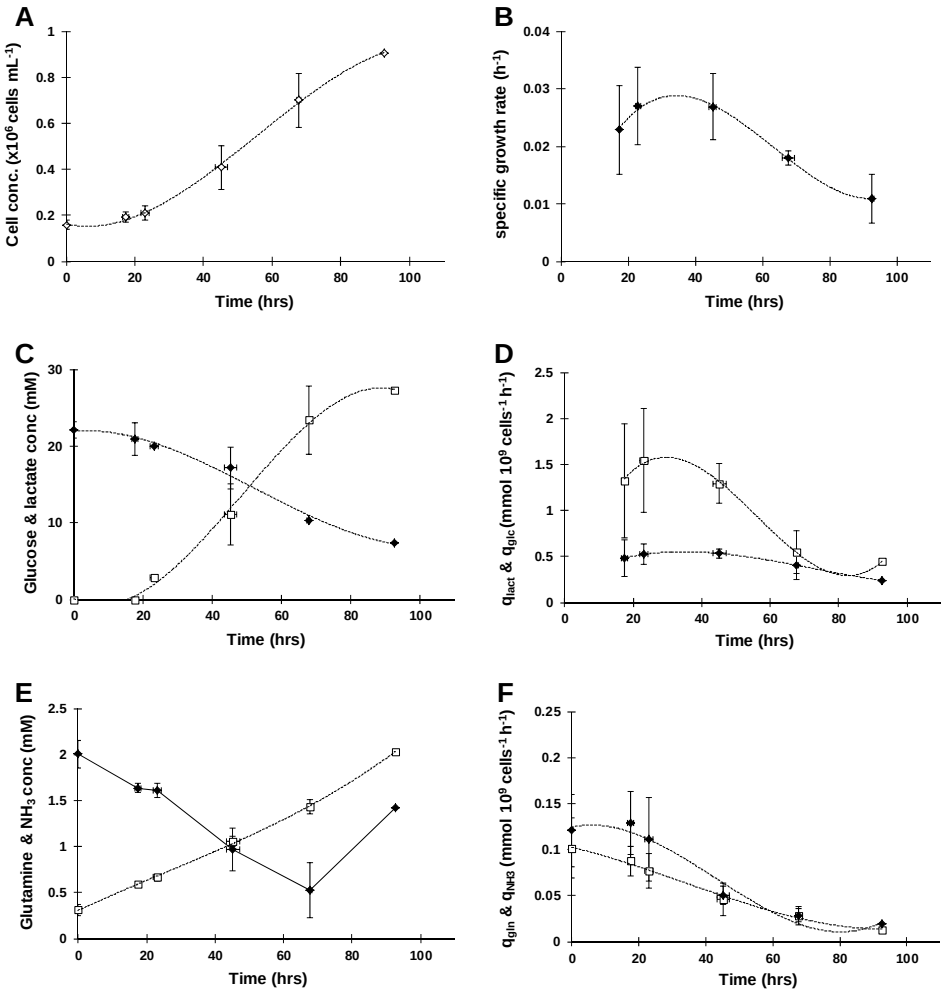

Figure 6. Growth kinetics of Vero cells grown adherent to Cytodex 1 microcarriers in a 3 L CT in SFM. Graphs show the average curves with standard deviation (n = 3). Concentration of attached cells and specific growth rate are shown in panel a and b, respectively; panel c shows glucose (closed diamonds) and lactate (open squares) concentrations, their specific consumption or production rates are shown in panel d; panels e and f, respectively, show concentrations and specific rates for glutamine (closed diamonds) and ammonium (open squares). At 70–80 h glutamine was fed to the bioreactor. Lines are for guidance.

Discussion

Vero growth characteristics

Vero cells are widely used and several reports are available on Vero cell growth characteristics in serum containing (SC) and serum free media (Genzel et al. 2010; Mendonça and Pereira 1998; Merten et al. 1999; Petiot et al. 2010a; Quesney et al. 2003; Rourou et al. 2007). The majority of these reports concerns data obtained in stirred tank bioreactors. The first report on Vero cell growth in rocking motion type bioreactors described yields of 1.4×10^6 cells mL^{-1} after 96 h of growth using an inoculation density of 0.2×10^6 cells mL^{-1} and 3 g L^{-1} Cytodex 1 microcarriers (Schouwenberg et al. 2010). In this study the labor intensive protocol described by Pörtner (Pörtner 2007) was used. The second article on Vero cell growth using a similar inoculation procedure as used here, yielded 1.0×10^6 cells mL^{-1} after 119 h of growth (Genzel et al. 2010). Using batch cultivation in spinners with serum free medium, Vero cell yields may vary from 0.96 to 1.8×10^6 cells mL^{-1} (Table 1). In stirred tank bioreactors, cultivations in serum free media have resulted in higher cell densities up to 2.6×10^6 cells mL^{-1} (Rourou et al. 2007) using higher inoculation densities and longer cultivation times. Application of different microcarrier concentrations or different culture procedures as recirculation or perfusion may further increase cell yields (Mendonça and Pereira 1998; Trabelsi et al. 2006).

Comparison of Vero cell growth between different systems and conditions is more accurate when considering specific growth rates. In RM maximum specific growth rates have not been reported previously. The maximum specific growth rates found here are comparable to previously reported growth rates observed for Vero cells grown in stirred tank bioreactors (Table 1). The growth rates found for the RM and the CT are in the same range. Vero cell growth and cell yields can therefore be considered comparable between the different rocking motion type bioreactors and between rocking motion type and stirred tank bioreactors.

Specific rates for glucose and glutamine consumption for Vero cell growth were 0.5 and 0.1 mmol 10^9 $cells^{-1}$ h^{-1} for glucose and glutamine consumption rates, respectively, in the RM as well as in the CT. These specific consumption rates are in the same range observed of other cultivation conditions for Vero cells and other kidney cell lines such as HEK293 cells (Garnier et al. 1994; Nadeau et al. 2000), BHK cells (Cruz et al. 2000) or MDCK cells (Cruz et al. 2000; Glacken et al. 1986). High levels of lactate and ammonium were accumulated during cultivation in rocking motion type bioreactors (Table 1). Ammonium levels up to 2.5 mM were found not to be limiting Vero cell yields (Hassell et al. 1991). In another study the ammonium concentration causing 50% reduction in cell yield (IC_{50}) for Vero cells was determined to be 5 mM (Huang et al. 2006). Based on these data we assume that the ammonium concentration was not limiting cell growth. Lactate

concentrations around 20 mM at the end of batch cultivation have been found previously (Petiot et al. 2010b; Trabelsi et al. 2005; Trabelsi et al. 2006). These currently observed concentrations may be inhibitory (Quesney et al. 2003), yet also have been reported to have negligible effects (Hassell et al. 1991). When both lactate and ammonium levels are high a synergistic inhibitory effect may be observed (Hassell et al. 1991). $Y_{lact/glc}$ is relatively high (1.9–2.0) compared to literature data. This high lactate over glucose yield indicates that nearly all glucose is converted to lactate. This may occur when oxygen is limiting, however, no oxygen depletion was observed during the culture (DO was successfully controlled at 50%). This overflow metabolism is commonly observed in cultures of stable cell lines like Vero (Quesney et al. 2003) or MDCK (Wahl et al. 2008). Medium optimization, for instance the use of fructose as carbon source instead of glucose (Petiot et al. 2010b) may be beneficial to lower the $Y_{lact/glc}$.

The observed Vero cell growth and metabolite kinetics in the RM and CT are within usual observed ranges. In particular growth resembles observations described for Vero cell growth in the RM (Genzel et al. 2010), or in media containing similar amounts of glucose (Petiot et al. 2010b).

Vero cell concentrations in rocking motion type bioreactors may be further increased using different cultivation conditions like perfusion or recirculation strategies as shown for STR cultivations (Mendonça and Pereira 1998; Trabelsi et al. 2006), alternative carbon sources or feed strategies.

Virus production

Vero cells were infected with poliovirus at the end of the exponential phase. Virus yields, both in the RM as in the CT, were 8.3 log 10 $TCID_{50}$ mL^{-1}. The obtained virus titers and yields (in DU $cell^{-1}$) are in good agreement with data obtained in stirred tank bioreactors (Merten et al. 1999) and at industrial scale (Bakker et al. 2011; Kreeftenberg et al. 2006). In the experiments described here virus culture was started without refreshing the medium. Although the remaining glucose and glutamine levels were considered sufficient the relatively high amounts of by-products may have had a negative impact on virus production. It has been reported that the presence of ammonia may be inhibitory for virus production (Schneider et al. 1996). Further improvements to optimize virus yields may therefore be possible.

Mixing characteristics

The first report on mixing times for rocking motion type bioreactors mentions Θ_m to range from 5 to 10 s for 10-L Wave bioreactors (Singh 1999). These figures were determined using fluorescent dye and therefore may be an underestimation of the actual Θ_m. Later Eibl et al. have reported that Θ_m in the RM range between 9 and 264 s in 2-L bioreactors, and up to

65–874 s in 200-L bioreactors. Mixing times currently observed in the RM correspond with those observed by Eibl et al. Settling of microcarriers has been reported to occur when rocking speed is below 6 rpm (Singh 1999). In our study it was observed that rocking speed should be as high as 15 rpm to avoid settling of microcarriers.
Mixing times in the CT are notably lower than in the RM, especially at lower rocking speed (Figures 4 & 5). Also the MC homogeneity is better, at the lowest rocking speed sufficient MC homogeneity can be obtained by applying a higher vertical displacement. However, for the CT lower mixing times may be expected considering the difference in k_La values reported for the CT (200–700 h^{-1} (Chaudet et al. 2011; Oosterhuis and van den Berg 2011; Oosterhuis and van der Heiden 2010)) and the RM (2–60 h^{-1} (Glazyrina et al. 2010; Hanson et al. 2009; Singh 1999)). This difference may be ascribed to the extremely large surface area that can be generated in the CT which is due to its two-dimensional motion.

Process transfer based on mixing characteristics

Mixing times for the RM and CT were determined using the pH response technique (van 't Riet and Tramper 1991). In this method a tracer (here acid) is used and its concentration is followed in time at a fixed point. This method is preferred above dye methods which are often used for first indications on mixing configuration (Brown et al. 2004). Concerning disposable bag bioreactors where the plastics are slightly opaque, pulse methods which are detected using pH or conductometry are preferred. Although the use of conductivity measurements is straightforward and allows detection of very low Θ_m a conductivity electrode is not always available. All bioreactors are equipped with pH probes and determining Θ_m using this method is therefore relatively simple. Critical is the response time needed for the pH electrode to detect a change in H^+ concentration. Since optical probes usually used in disposable bioreactors have a long response time, a separate glass pH electrode was applied to the bioreactor bags.

Process transfer from the RM to the CT was based on mixing times. Multiple rules can be applied for process transfer or scale-up (see for example (Rathore et al. 2005b; Schmidt 2005)). Mostly, constant volumetric oxygen transfer coefficients (k_La), Reynolds number or ungassed power input per unit volume (P/V) are used in process transfer. In general, it is not preferred to use constant mixing times as for scale-up extremely high power consumption may be needed to obtain a similar Θ_m compared to small scales (van 't Riet and Tramper 1991). However, this rule could be applied since cultivation volumes were in the same order of magnitude.
Using constant Θ_m for process transfer and determination of Θ_m with the pH method is feasible in many laboratories and here it was shown that it can be applied to transfer processes between different types of rocking motion bioreactors.

Acknowledgements

The authors would like to thank CELLution Biotech BV for providing the CELL-tainer® bioreactor systems. The work was partially supported by NL Agency (no. IVG091769).

Supplemental data

Table S1. Experimental design and measured responses for modeling mixing times in the BIOSTAT CultiBag RM.

Run no.	Rocking speed (rpm)	Angle (°)	Mixing time (s)
1	8	4	414.1
2	8	10	151.5
3	8	4	343.2
4	8	10	227.8
5	8	4	327.2
6	8	10	183.6
7	16	8	78.9
8	16	8	61.9
9	16	8	65
10	16	4	156.3
11	16	4	184.7
12	16	4	146.7
13	25	7	28.2
14	25	7	24.6
15	25	7	30
16	30	4	21.1
17	30	4	10.8
18	42	10	14.3
19	42	4	8.9
20	42	10	8.5
21	42	10	16.1

Table S2. Experimental design and measured responses for modeling microcarrier homogeneity in the BIOSTAT CultiBag RM.

Run no.	Rocking speed (rpm)	Angle (°)	MC Homogeneity
1	8	4	1
2	12	4	1
3	16	4	1
4	20	4	1
5	24	4	7
6	28	4	10
7	8	6	1
8	12	6	1
9	16	6	1
10	20	6	7
11	24	6	10
12	17	7	7
13	8	8	1
14	12	8	7
15	16	8	10
16	20	8	10

Table S3. Experimental design and measured responses for modeling mixing times in the CELL-tainer®.

Run no.	Rocking speed (rpm)	Horizontal displacement (%)	Vertical displacement (%)	Phase (%)	Volume (mL)	Mixing time (s)
1	5	100	100	50	5000	170.5
2	25	100	5	25	5000	33.75
3	25	100	100	50	5000	27.6667
4	5	5	100	50	5000	83.25
5	5	100	5	50	5000	282.75
6	5	5	5	25	5000	314
7	5	100	100	25	5000	154.5
8	25	100	5	50	5000	53
9	5	5	100	25	5000	95
10	5	5	5	50	5000	196
11	25	5	100	50	5000	35.5
12	25	5	5	50	5000	398.5
13	5	100	5	25	5000	324
14	25	5	100	25	5000	52.75
15	25	5	5	25	5000	390
16	25	100	100	25	5000	21.75
17	15	53	53	25	10000	40.5
18	15	53	53	25	10000	31.5
19	15	53	53	25	10000	30.5
20	25	100	5	50	15000	378.25
21	25	100	5	25	15000	228.75
22	5	100	5	25	15000	968.5
23	25	5	5	25	15000	663
24	25	5	100	50	15000	19.25
25	5	5	5	25	15000	1497
26	5	100	100	25	15000	255.75
27	5	5	100	50	15000	288.25
28	25	5	5	50	15000	414
29	5	5	100	25	15000	302.25
30	25	100	100	50	15000	27
31	25	100	100	25	15000	25
32	5	5	5	50	15000	647
33	25	5	100	25	15000	34.25
34	15	52.5	52.5	25	5000	34.1333
35	15	52.5	52.5	25	10000	196.933
36	5	52.5	52.5	25	10000	478.6
37	25	52.5	52.5	25	10000	28.8
38	15	5	52.5	25	10000	182.067
39	15	100	52.5	25	10000	197.267
40	15	52.5	5	25	10000	612.8
41	15	52.5	100	25	10000	51.0667
42	15	52.5	52.5	50	10000	156.067
43	15	52.5	52.5	25	15000	294.467

Table S4. Experimental design and measured responses for modeling microcarrier homogeneity in the CELL-tainer®.

Run no.	Rocking speed (rpm)	Horizontal displacement (%)	Vertical displacement (%)	Phase (%)	Volume (mL)	MC homogeneity (-)
1	5	100	100	25	4500	7
2	5	5	100	50	4500	7
3	5	100	5	25	4500	3
4	25	5	100	25	4500	10
5	25	100	100	25	4500	10
6	5	5	5	50	4500	3
7	5	5	5	25	4500	3
8	25	5	5	25	4500	1
9	25	100	100	50	4500	10
10	5	100	5	50	4500	1
11	25	100	5	50	4500	10
12	25	100	5	25	4500	10
13	25	5	100	50	4500	10
14	5	100	100	50	4500	7
15	25	5	5	50	4500	1
16	5	5	100	25	4500	7
17	15	53	59	25	10000	10
18	15	53	59	25	10000	10
19	15	53	59	25	10000	10
20	25	100	5	25	15000	10
21	5	5	100	25	15000	7
22	25	5	100	50	15000	10
23	25	5	100	25	15000	10
24	25	5	5	50	15000	1
25	5	5	5	25	15000	1
26	25	100	100	50	15000	10
27	25	5	5	25	15000	1
28	5	5	100	50	15000	3
29	5	100	5	25	15000	1
30	5	5	5	50	15000	1
31	5	100	100	25	15000	7
32	5	100	100	50	15000	7
33	25	100	5	50	15000	10
34	5	100	5	50	15000	1
35	25	100	100	25	15000	10

Chapter 7

Next generation inactivated polio vaccine manufacturing to support post polio-eradication biosafety goals

Published as:
Thomassen, Y.E., van 't Oever, A.G., van Oijen M.G.C.T., Wijffels, R.H., van der Pol, L.A., Bakker, W.A.M. (2013) *Next generation inactivated polio vaccine manufacturing to support post polio-eradication biosafety goals.*

PLoS ONE 8(12):e83374
dx.doi.org/10.1371/journal.pone.0083374

Abstract

Worldwide efforts to eradicate polio caused a tipping point in polio vaccination strategies. A switch from the oral polio vaccine, which can cause circulating and virulent vaccine derived polioviruses, to inactivated polio vaccines (IPV) is scheduled. Moreover, a manufacturing process, using attenuated virus strains instead of wild-type polioviruses, is demanded to enhance worldwide production of IPV, especially in low- and middle income countries. Therefore, development of an IPV from attenuated (Sabin) poliovirus strains (sIPV) was pursued.

Starting from the current IPV production process based on wild type Salk strains, adaptations, such as lower virus cultivation temperature, were implemented. sIPV was produced at industrial scale followed by formulation of both plain and aluminium adjuvanted sIPV. The final products met the quality criteria, were immunogenic in rats, showed no toxicity in rabbits and could be released for testing in the clinic.

Concluding, sIPV was developed to manufacturing scale. The technology can be transferred worldwide to support post polio-eradication biosafety goals.

Introduction

Vaccines that provide protection against poliomyelitis have been available for decades (Salk and Salk 1984). Yet large efforts are undertaken in WHO's global polio eradication initiative (GPEI) to obtain the next generation vaccines that are safe and available at low costs (Aylward and Tangermann 2011). These vaccines are needed both for the 'endgame' in polio eradication and after eradication to prevent the risk of a global outbreak due to accidental or deliberate re-introduction of the virus. One of the anticipated next generation vaccines is an inactivated polio vaccine (IPV) based on the attenuated Sabin poliovirus strains resulting in a so-called Sabin-IPV (sIPV) (Bakker et al. 2011). The Sabin polioviruses (PV) are currently used in live oral polio vaccines (OPV) (Sabin and Boulger 1973) and will provide additional bio-safety, over the wild-type viruses, during the manufacturing process (WHO 2002a). Bio-safety requirements are becoming more stringent as new containment guidelines are drafted by the WHO's Global Action Plan for Wild Poliovirus Laboratory Containment III (GAPIII) (WHO 2009). Future production and quality control of IPV using wild-type strains will require at least biosafety level 3 facilities (WHO 2004). This will not only increase manufacturing costs but will also limit the possibility of IPV manufacturing in low- and middle income countries for instance due to requirements on immunization coverage. The use of alternative strains like Sabin PV would require less stringent biocontainment, is encouraged by the WHO (WHO 2002a) and allows manufacturing in low- and middle income countries, which potentially lowers manufacturing costs (Venczel et al. 2009). Moreover, the use of an IPV instead of OPV will prevent the emergence of circulating vaccine-derived PV (cVDPVs), which may potentially re-seed the world with PV and negate the GPEI accomplishments (Kew et al. 2005).

The development of the currently used IPV production process (for a process overview see Figure 1) dates back to the 1960s when at the RIV in Bilthoven a process was developed based on micro-carrier technology and primary monkey kidney cells (van Wezel 1967; van Wezel et al. 1979). This process was scaled-up to 350-L and later 750-L bioreactors. Additionally, the Vero cell line was introduced to replace the then used tertiary monkey kidney cells. To support manufacturing and increase the knowledge on IPV manufacturing, efforts like multivariate data analysis and the development of scale-down models, i.e. lab-scale equivalents of the manufacturing-scale processes, have been undertaken (Thomassen et al. 2013b; Thomassen et al. 2010). The availability of scale-down models, unique in the vaccine world, allows rapid assessment of process changes.

Based on our vast history in IPV development and production (van Wezel et al. 1979), our previous experience with sIPV (Kersten et al. 1999) and technology transfer (Kreeftenberg and Hamidi 2007; Kreeftenberg et al. 2006; van Noort 1992) a project for the development and technology transfer of sIPV manufacturing under supervision of the WHO was initiated. Initially a proof-of-principle study was performed. In this study, sIPV was

prepared from OPV as virus source. The three PV sub-types, obtained separately (Bio Farma, Indonesia), were concentrated, purified and inactivated and shown to yield a sIPV that was immunogenic in an animal model (Bakker et al. 2011). In principle, OPV manufacturers could, by acquiring correct downstream processing (DSP) equipment, produce sIPV. However, larger quantities of virus harvest (100-800 fold of current production quantities) are needed and upstream processing (USP) should be scaled-up (Duchene et al. 1990).

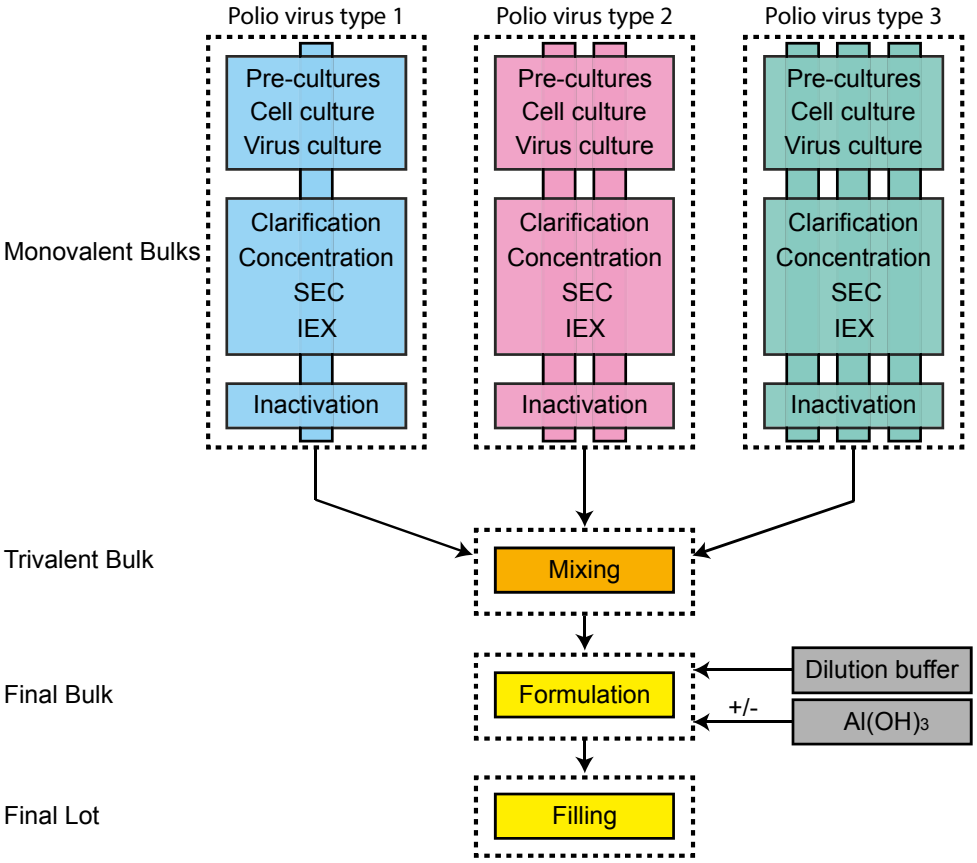

Figure 1. Process overview for preparation of trivalent IPV. Monovalent bulks are prepared for each PV (type 1, 2 and 3) separately. During monovalent bulk preparation Vero cells are expanded using two pre-culture steps and a cell culture followed by virus culture. Virus is purified using normal flow filtration for clarification, tangential flow filtration for concentration and two chromatography units, size exclusion and ion exchange chromatography. Purified virus is subsequently inactivated using formaldehyde. Subsequently these are mixed to obtain trivalent bulk prior to formulation and filling.

Here we report the results of limited (to be able to quickly show proof of concept) process development for sIPV based on the established IPV production process, the subsequent manufacturing of clinical lots, their stability and pre-clinical studies. This work resulted in a vaccine that has recently been tested in the clinic (phase I/IIa) (Verdijk 2012; Verdijk et al. 2013).

Methods

Ethics statements regarding animal studies

The abnormal toxicity study in suckling mice and guinea pigs and immunogenicity tests in rats used in this study were agreed upon by the Committee on Animal Experimentation of the Netherlands Vaccine Institute (Bilthoven, the Netherlands) (Study Permit numbers AAP 201000262, 201000302, 201000303, 2010000304, 2010000305, 2010000306, 2010000307, 201000310, 201100030, 201100054, 201100056, 201100101, 201100151, 201100170, 201100195, 201100214, 201100289, 201100345, 201200137, 201200154, 201200227 and 201200262). Animal handling in this study was carried out in accordance with relevant Dutch national legislation, including the 1997 Dutch Act on Animal Experimentation.

The protocol for the toxicity study in rabbits was reviewed and approved by the Animal Welfare Officer and Ethical Committee of WIL Research Europe B.V. (former name: NOTOX B.V.) as required by the Dutch Act on Animal Experimentation (Study Permit Numbers: DEC 08-48 and 10-18). The OECD guidance document on humane endpoints (ENV/JM/MONO/ 2000/7) is applicable for all animal studies carried out at WIL Research Europe B.V.. No distress or discomfort was noted during this study.

Lab scale experiments

Upstream processing

Vero cells obtained from WHO (10-87) originally derived from ATCC (CCL-81) were used as host for PV production. Sabin PV type 1 (LSc 2ab KP_2), Sabin PV type 2 (P712 Ch2ab-KP_2) and Sabin PV type 3 (Lot 457-III-Pfizer) were used.

Studies on virus culture conditions were carried out in 5-L glass bioreactors (Sartorius Stedim Biotech). Cell cultures were done in EMEM supplemented with bovine serum (BS) and 3 g L^{-1} micro-carriers (Cytodex 1; GE Healthcare) with the following settings: T of 37°C, pH of 7.2 and DO (dissolved oxygen) of 50% by headspace aeration. Glucose was added daily when the concentration was below 5 mM. Prior to virus culture the media was exchanged to M199. Virus cultures conditions were: T of 32.5 or 33.5°C, pH of 7.4, DO of 25% by headspace aeration.

Downstream processing

Virus was harvested, clarified, concentrated, purified, first on size using size exclusion chromatography (SEC) and second by ion exchange chromatography (IEX), and finally inactivated as described previously (Thomassen et al. 2013b).

Analytics

Cell counts were determined using a Nucleocounter (Chemometec). Glucose concentration was determined using a Bioprofile 100 plus (Nova Biomedical, MA). Cytopathic effects (CPE) were monitored microscopically. Virus was quantified by titer measurements ($CCID_{50}$) (Thomassen et al. 2012) and by a modified D-antigen ELISA (ten Have et al. 2012) for in-process samples.

Clinical lots manufacturing

Cell and virus culture

Vero cells from a manufacturers working cell bank were used. Master and working seedlots were prepared from Sabin type 1 LSc 2ab KP_2 (WHO/Beringwerke SO+1, 1976), type 2 P712 Ch2ab-KP_2 (WHO/Behringwerke SO+1, 1976) and type 3 (Pfizer RSO1, SO+5, lot 457-III, 1963; supplied by Institute Mérieux to RIVM in 1991) (Bakker et al. 2012). Working seedlots were additionally tested for neurovirulence in monkeys (Bio Farma, Indonesia) (WHO 2002b) and analyzed with MAPREC (mutant analysis by PCR and restriction enzyme cleavage; NIBSC/HPA, UK) (WHO 2012a) and RCT40 (replicating properties 36°C- 40°C; AFSSAPS, France) (WHO 2002b) to assess genetic stability with respect to biosafety (Table 1).

Table 1. Biosafety and viral safety testing of Sabin PV master (MS) and working (WS) seedlots.

Seedlot	Virus titer (Log_{10} $CCID_{50}$ mL^{-1})	Monkey Neurovirulence[1]	MAPREC[2]	RCT40[1]	Extraneous agents/Viral safety[3]
MS PV type 1	8.85	Not determined	Conform	Conform	Conform
MS PV type 2	7.52	Not determined	Conform	Conform	Conform
MS PV type 3	8.23	Not determined	Conform	Conform	Conform
WS PV type 1	8.90	Conform	Conform	Conform	Conform
WS PV type 2	7.55	Conform	Conform	Conform	Conform
WS PV type 3	8.45	Conform	Conform	Conform	Conform

[1] Reproductive Capacity at 40°C Temperature (RCT40) and Monkey Neurovirulence: Tests and requirements according to WHO recommendations for OPV (WHO 2002b). [2] Mutant Analysis by PCR and Restriction Enzyme Cleavage (MAPREC): Test and requirements according to new WHO recommendations for OPV (WHO 2012a). [3] Test and requirements according to the European Pharmacopoeia (Ph Eur 7.0:0214 ; Ph Eur 7.0:20616).

Cell and virus culture was carried out in two 350-L (working volume) bioreactors. In short, thawed Vero cells were used to directly inoculate a 15-L fed-batch pre-culture (EMEM supplemented with BS and Cytodex 1 microcarriers) (van Wezel 1985). After trypsinization (van Wezel 1985); a 2nd pre-culture using the recirculation culture method (van Hemert et al. 1969) was done to have sufficient cell to inoculate two 350-L bioreactors at 0.1 × 10^{6} cells mL^{-1}. After medium exchange (van Wezel 1973), virus culture was started (M199; Multiplicity of infection (MOI)=0.01; T=32.5°C).

Purification

Virus from the two 350-L (working volume) bioreactors was harvested via a sieve (mesh 75 µm) to obtain a virus harvest free of micro-carriers (Thomassen et al. 2013b). Clarification was done using normal flow filtration with a Millipore POD-holder containing C0HC depth filters followed by an Express SHC 0.45/0.22 µm combination filter (Millipore) (Bakker et al. 2011; Thomassen et al. 2013b) . Concentration was done by tangential flow filtration using 100 kDa filters (Thomassen et al. 2013b). Purification was done by size exclusion chromatography (Sepharose CL-6B (GE Healthcare) (van Wezel et al. 1979; van Wezel et al. 1978); elution buffer 20mM phosphate buffer pH 7.0) and ion exchange chromatography (DEAE-Sephadex A50 (GE Healthcare) (van Wezel 1972; van Wezel et al. 1979); elution buffer 20mM phosphate buffer pH7.0).

Inactivation

Purified virus was stabilized with concentrated M199 containing glycine (final conc. 5g L^{-1}). Inactivation was done following the standard method: 0.025% formaldehyde incubation for 13 days at 37°C. An intermediate filtration (0.22 µm) was performed at day 6-8 (WHO 2002a). The resulting monovalent bulk was stored at 2-8°C.

Preparation of trivalent vaccine

Monovalent bulks of PV type 1, 2 and 3 were mixed to a ratio of 60:96:192 D-antigen prior to sterile filtration. The sIPV final bulk was subsequently prepared by addition (via 0.22 µm filter) of the mixed trivalent bulk and dilution buffer containing phosphate, phenoxyethanol and formaldehyde. Aluminium hydroxide adjuvanted sIPV final bulk was prepared as described above with the inclusion of the addition of sterile Alhydrogel (Brenntag) (directly) to the final bulk. Final bulks were mixed for 10 minutes prior to setting the pH. The final lots were prepared by filling the final bulk in aliquots of 0.6-0.7g in 3 mL sterile siliconized vials using a Bausch & Ströbel ksf 1027 machine.

Analytics

During the process, sampling was done, as required for release of sIPV final lots. In Table 2 a list of the most relevant assays for release is given. A qualified QC department carried out these assays.

Cell counts were performed using a hemocytometer. Cythopathic effects (CPE) were monitored microscopically. Virus was quantified by titer measurements ($CCID_{50}$) and D-antigen ELISA (Kersten et al. 1999) for release. SDS-PAGE was done using precast 4-20% gradient gel (Pierce) with Tris-HEPES buffer (Pierce). Vero host cell protein concentrations were determined using a Vero Cell HCP ELISA kit F500 according to the manufacturer's instructions (Cygnus Technologies, NC). MAPREC and RCT40 were performed as described in WHO guidelines (WHO 2012a; WHO 2002b).

Preclinical studies - Rat immunogenicity

The rat immunogenicity was determined essentially as described previously (Ph Eur 7.0:0214 ; van Steenis et al. 1981). In short, TOX rats (weighing 175-250 g) that were screened for the absence of PV antibodies were injected intramuscularly with 0.5 mL of prepared vaccine dilutions (group size 10 per dilution). Blood samples were taken 21 days after injection. Collected sera (stored at -20°C until use) were analyzed for neutralizing antibodies. Serial dilutions (with M199) of heat inactivated sera (30 min 56°C) were prepared in a 96-wells plate and incubated with 50 µl (2×10^3 $CCID_{50}$ mL^{-1}) PV type 1 Mahoney, PV type 2 MEF-1, or PV type 3 Saukett for 3h at 35-37°C in a CO_2 incubator and subsequently stored overnight at 2-8°C. After addition of Vero cells (50 µL at 2×10^5 cells mL^{-1}) the 96-wells plates were incubated for 7 days at 35-37°C. Supernatants were discarded and cells were stained with a crystal violet solution containing 5% formaldehyde. Presence of full monolayers of Vero cells indicated a complete neutralization of the virus. The neutralization antibody score represents the highest dilution (log_2; with a test maximum of 12) where complete neutralization was observed. For comparison of sIPV with conventional IPV, the international standard PU91-01 was diluted towards the conventional IPV dose (40/8/32 DU shd^{-1}).

Preclinical studies - Toxicity study in rabbits

A repeated dose and local tolerance toxicity study followed by a two week recovery period was carried out in rabbits (NOTOX, the Netherlands) according to EMA guidelines ((EMEA/CPMP) 1998). In short, New Zealand white rabbits (group size of 16, equally distributed among sexes) were treated by intramuscular injection with 0.5 mL vaccine or placebo (vaccine without D-antigen) at day 1, 15, 29, 43 and 57). Animals were necropsied at day 60 (n=10) or day 71 (n=6). The following observations and examinations were evaluated: clinical signs (daily), skin irritation (24 and 48 hours after each administration), body weight (weekly), food consumption (twice weekly), ophthalmoscopic examination (during pretest, end of treatment and end of recovery), rectal body temperature (during pretest, prior to each dosing and approximately 2 hours after dosing), clinical pathology (Pretest, Days 4, 57, 60 and 71), macroscopy at termination and organ weights and histopathology on a selection of tissues.

Statistical analysis

Two sided Student t-tests were performed with α=0.05. Numbers are given as means with standard deviations.

To determine the regression line slopes, no weighted regression was used. This was chosen based on the use of medians when concerning animal tests in contrast to the use of the means. In addition, the observed standard deviation from the median did not increase with increasing values. The significance (95% confidence) of the slopes was tested using an extra sum of squares F-test with the null hypothesis being a horizontal line (i.e. slope=0) (Graphad Prism 6 for Windows).

Results

Drafting product and process specifications

The specifications (Table 2) for the release and control of sIPV and aluminium hydroxide adjuvanted sIPV were drafted based on WHO (WHO 2002a) and EP monograph (Ph Eur 7.0:0214) for IPV manufacturing. Some product requirements, like formaldehyde content and pH, were based on the available IPV experience. Requirements related to the adjuvation with aluminium hydroxide were set after initial research (Westdijk et al. 2013). The WHO OPV guidelines (WHO 2002b) were taken into account to assess the Sabin PV genetic stability with respect to biosafety, i.e. temperature sensitivity and revertants.

Process development prior to manufacturing of clinical lots

In view of the relatively short timelines in the polio eradication program it was chosen to prepare a sIPV with limited process development time prior to production of clinical lots. Process development therefore focused on Sabin strain specific adaptations like MOI and virus cultivation temperature and chromatography (discussed below). In addition, a disposable clarification unit was introduced to replace the Celite cake for depth-filtration. On all other aspects the production process was similar to conventional IPV manufacturing.

Selection of MOI and virus cultivation temperature

In OPV manufacturing, the virus cultivation temperature for Sabin PV is lower (at a maximum of 35°C (WHO 2002b)) than the temperature used for wild-type PV in conventional IPV manufacturing (36-37°C) (Bakker et al. 2010; Duchene et al. 1990). This lower temperature is required to ensure the temperature sensitivity of the Sabin PV and minimize revertants to ensure a safe OPV. Although here an inactivated product has been developed, manufacturing itself should be biosafe and one of the prerequisites was to ensure the safety of the prepared virus harvest with respect to revertants of Sabin PV.

Table 2. Release requirements[1)] of plain and adjuvanted sIPV

Cell culture		
Identity	Vero cells	
Mycoplasma	Absent	
Extraneous viruses	Absent	
Virus harvest		
Sterility	Absence of growth (Tryptic Soy Broth & Thioglycollate broth)	
Mycoplasma	Absent	
Extraneous viruses	Absent	
Purified virus		
Purity (ratio total protein and D-antigen)	≤0.1 µg DU^{-1}	
Sterility	As above	
Identity	PV type 1, 2 OR 3	
Residual host cell proteins	Consistent clearance	
Monovalent Bulk		
Inactivation kinetics	PV titer below detection limit after 120h	
Formaldehyde	>2 mM	
Sterility	As above	
PV identity	Contains PV type 1, 2 OR 3	
Inactivation	Full absence of active PV after 10 and 13 days	
D-antigen content	Information for calculation	
Trivalent bulk		
Inactivation	Full absence of active PV in 1,500 calculated human doses	
Sterility	As above	
D-antigen content	Information for calculation	
Final bulk	**Plain**	**Adjuvanted**
pH	6.8-7.4	6.8-7.4
Phenoxyethanol	31-42 mM	31-42 mM
Formaldehyde [2)]	0.7-2.4 mM	0.7-1.3 mM
Sterility	As above	As above
D-antigen content	≥75% nominal value	≥75% nominal value
Final lot	**Plain**	**Adjuvanted**
Appearance	Bright red-orange fluid	Turbid red-orange fluid
PV identity	Contains type PV 1, 2 and 3	Contains type PV 1, 2 and 3
D-antigen content	≥75% nominal value	≥75% nominal value
Residual host cell DNA [3)]	≤100 pg shd^{-1}	≤100 pg shd^{-1}
Bovin Serum Albumin [3)]	≤50 ng shd^{-1}	≤50 ng shd^{-1}
Total protein	≤20 µg mL^{-1}	≤20 µg mL^{-1}
Endotoxin	≤10 IU mL^{-1}	≤10 IU mL^{-1}
Extractable volume	≥0.5 mL	≥0.5 mL
pH	6.8-7.4	6.8-7.4
Sterility	As above	As above
Free D-antigen	Not applicable	< 1%
Aluminium	Not applicable	0.26-0.36 mg mL^{-1}
Abnormal toxicity (in mice and guinea pigs)	No illness	No illness

[1] Most important release tests drafted for the production of the phase I clinical lots are given. It should be noted that the release criteria could change due to further product development. [2] Formaldehyde requirement is dependent on the amount of monovalent bulk used to prepare the final bulk. [3] Test is performed at an earlier stage in view of the lower detection limit.

The effects of virus culture temperature and multiplicity of infection (MOI) on the virus culture yields and culture time were assessed using PV type 2. No differences in virus yields were observed when the MOI was decreased from 0.1 to 0.01. Decreasing the temperature from 33.5°C to 32.5°C, had a negative effect on virus yields. Virus titers were 7.7 ± 0.1 (*n*=3) and 7.2 ± 0.1 (*n*=3) Log_{10} $CCID_{50}$ mL^{-1} for cultures at respectively 33.5°C and 32.5°C. D-antigen (a measure for immunogenic virus) concentrations were 25 ± 3 (at 33.5°C) and 11 ± 5 DU mL^{-1} (at 32.5°C). Under all tested conditions virus culture was complete within 4 days, i.e. cytopathic effect (CPE) >90% and both virus titers and D-antigen (a measure for immunogenic virus) concentrations remained constant. Despite the lower yields at 32.5°C, this cultivation temperature was selected for preparing the virus seeds and clinical trial material. This choice was made to minimize the risk of PV revertants. Since no difference was observed when using a lower MOI, an MOI of 0.01 was used as it is preferred since smaller amounts of virus working seedlots will be needed.

Chromatography resin selection and buffer strength

Initial process development was done to confirm the use of resins and procedures available for wild-type PV. The present SEC resin and procedure were applicable for use with Sabin PV (data not shown). For IEX a choice between two validated resins needed to be made. Both DEAE Sephadex A-50 (van Wezel 1972) and DEAE Sepharose Fast Flow (Thomassen et al. 2013b) have been used for purification of PV. In both cases impurities are captured while Salk PV flows through. Initial studies using Sabin PV Type 1 showed some non-specific binding of the PV to DEAE Sepharose Fast Flow; this was confirmed for Sabin PV Type 2. The alternative resin DEAE Sephadex A50 allowed efficient separation of Sabin PV type 1, 2 and 3.

During the proof of principle study (Bakker et al. 2012) in which OPV bulks were obtained to generate IPV, a precipitate was noticed during inactivation. Analysis showed that this precipitate was a phosphate based precipitate without product. The main source of the phosphate was traced back to the purification process where a 40mM phosphate buffer was used during chromatography (both SEC and IEX). Application of a weaker phosphate buffer (20mM) and the impact on product elution and inactivation was assessed. Product elution profiles in SEC and IEX using a 20mM phosphate buffer were comparable with those obtained after eluting with a 40mM phosphate buffer. Inactivation of virus eluted with 20mM phosphate was comparable while precipitates were absent.

Manufacturing of clinical lots

Preparation of virus seed

Sabin PV strains closest to the Sabin original strains (PV T1: SO+1 Behringwerke 1976; PV T2: SO+1 Behringwerke 1976; and PV T3: RSO+1 Pfizer 1963) were used to produce new virus

master seedlots at 10-L scale. The virus working seedlots were produced at 350-L scale (Bakker et al. 2011). These seeds were tested for neurovirulence using the monkey neurovirulence test (WHO 2002b). However, due to limited global test capacity and to minimize costs it was chosen to only test the working seedlots. It was argued that the working seeds represent, on a worst case base, the quality of the master seed with respect to neurovirulence. Next to passing the neurovirulence test, the master and working seedlots also passed the tests for extraneous agents, RCT40 (reproductive capacity at 40°C temperature) and MAPREC (Mutant Analysis by PCR and Restriction Enzyme Cleavage) (Table 1).

Upstream processing

The preparation of sIPV was done in a physically separated production area in the established cGMP facilities for conventional IPV manufacturing. For each virus type two monovalent bulks were prepared. Vero cell culture was carried out in twin 350-L bioreactors (Thomassen et al. 2010). In Figure 2A, the average growth curve of the 12 cultures (6 bulks in twin bioreactors) at 350-L scale is given. Cell culture was started at an inoculation density of 0.1×10^6 cells mL^{-1}. Cells grew adherent to micro-carriers (average growth rate 0.025 h^{-1}) to reach 1.1×10^6 cells mL^{-1} after 4 days when the micro-carriers were covered by a confluent layer of cells. At this point, the bovine serum containing medium was exchanged with serum free virus culture media. Subsequently, cells were infected with Sabin PV. Virus culture proceeded comparably and was independent of the virus type used for infection. Cell lysis was complete after 4-5 days as was determined based on the CPE observed microscopically (Figure 2B). Virus yields were based on virus titers (Figure 2C) and D-antigen (Figure 2D). While comparable virus titers were observed for the production of Sabin PV type 1 and 3, the yields for Sabin PV type 2 were significantly lower (2-tailed t-test; α=0.05 p=0.0043). D-antigen yields are not comparable between virus types as they are type (and antibody) specific (Westdijk et al. 2011). From Figures 2C&D it was concluded that virus cultures were reproducible. The virus harvests were negative for revertants of Sabin PV as analyzed by RCT40 and MAPREC.

Downstream processing

Virus from the twin bioreactors was harvested and pooled prior to purification. Harvested virus was first clarified using normal flow filtration (NFF), which resulted in a decrease in fluid turbidity from 54 ± 6 NTU (Nephelometric Turbidity Unit) to 0.4 ± 0.4 NTU (n=5; determined mid-processing). The clarified virus was subsequently concentrated from approx. 700L to 1L using tangential flow filtration (TFF). Product recoveries, based on D-antigen units (DU), during the filtration steps were 90% ± 3% and 68% ± 11% for respectively NFF and TFF (Table 3).

The concentrated product was purified using 2-step chromatography starting with SEC. In Figure 3A a typical SEC elution pattern for Sabin PV is given. The 1st peak contains mostly large cell components. PV is found in the 2nd peak as is illustrated by SDS-PAGE (Figure 3B) where the presence of the viral proteins is more pronounced when purification with SEC was done. An average D-antigen recovery of 68% ± 11% was found for SEC (Table 3).

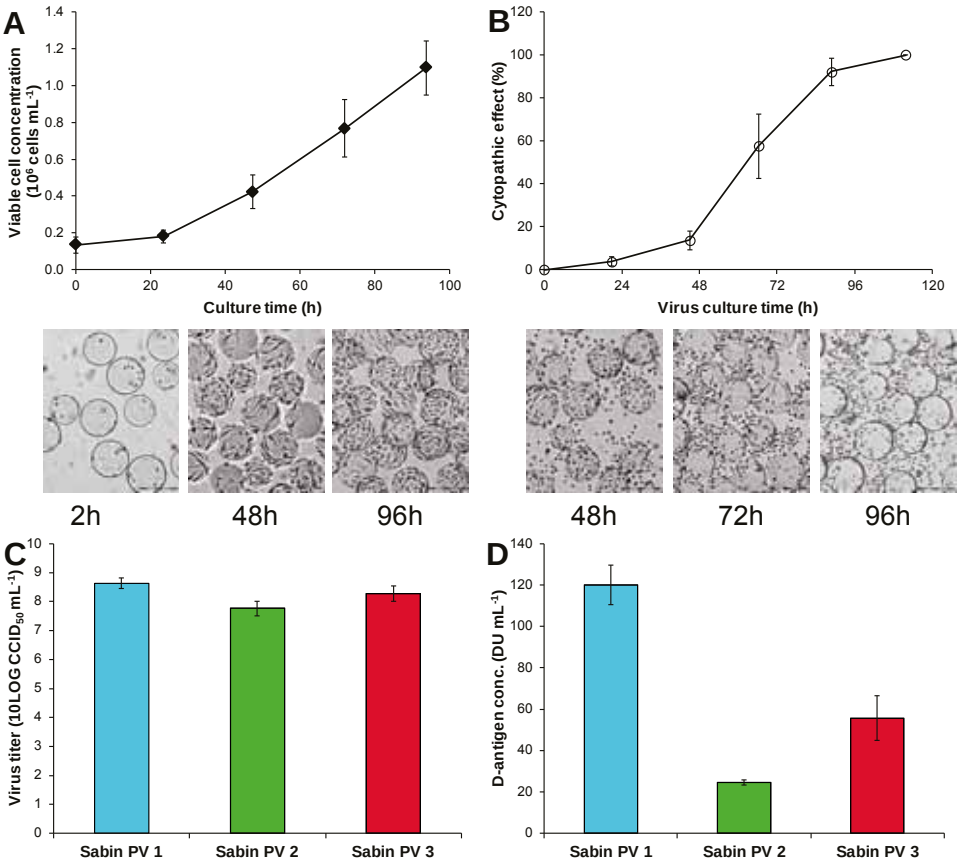

Figure 2. Cell and virus culture. Panel A shows the average Vero cell growth curve (*n*=12; error bars represent SD) in 350-L bioreactors. Photographs are light microscopy images (size bar 200 µm). Panel B shows the average (of the three subtypes) Vero cell death during virus culture determined microscopically (*n*=12; error bars represent SD). Photographs show corresponding images. Panel C shows average virus titers for Sabin PV type 1, 2 and 3 (*n*=4; error bars represent SD). Panel D shows average D-antigen concentrations after virus culture for Sabin PV type 1, 2 and 3 (*n*=4; error bars represent SD).

Table 3. Product recovery during processing of two batches for each serotype. Losses due to sampling were not considered for recovery calculations of individual unit operations. The overall product recovery includes losses due to sampling for in-process and release tests as well as sampling for research purposes.

Virus subtype	Harvest	Clarification	Concentration	SEC[2]	IEX[3]	Inactivation	Overall[1]
Sabin PV type 1	100%	86%	82%	62%	90%	84%	38%
	100%	89%	73%	67%	107%	85%	41%
Sabin PV type 2	100%	92%	77%	69%	20%	50%	<15%
	100%	96%	54%	51%	35%	64%	<15%
Sabin PV type 3	100%	91%	75%	75%	87%	36%	18%
	100%	88%	70%	83%	114%	72%	24%

[1] The overall DSP yield was calculated by dividing the amount of D-antigen units of the monovalent bulk by the amount of D-antigen units from the harvest.[2] Size Exclusion Chromatography [3] Ion Exchange Chromatography

Subsequently the negatively charged molecules, like nucleic acids and proteins, were removed using IEX chromatography. PV should not interact with the matrix as was the case for Sabin PV type 1 and 3, where a plug flow was observed (Figure 3C). However, Sabin PV type 2 showed some interaction with the matrix as is apparent from the chromatogram (Figure 3C). The presence of the plug flow type chromatogram for Sabin PV type 1 and 3 allowed collection of the PV after IEX without major losses. Sabin PV type 1 and 3 were collected with 99.5% D-antigen recovery (Table 3). Relatively high losses (72%) were observed during IEX for Sabin PV type 2 (Table 3). The efficiency of the purification is illustrated by the SDS-PAGE in Figure 3B. After IEX the viral proteins are clearly purified from the other protein present after SEC. Removal of impurities was also shown for Vero host cell proteins and host cell DNA (Figure 3D). After IEX host cell protein concentrations were below 0.3 µg mL^{-1}, corresponding to an over 1,000 times removal. Host cell DNA concentrations were below the detection limit of 78.13 pg mL^{-1} which is below the maximum level allowed in a single human dose (shd) (Table 2).

After IEX the Sabin PV was inactivated during a 13-day incubation period with formaldehyde. PV was inactivated rapidly, i.e. within 4 days, as shown in Figure 3E. After 6 to 8 days an intermediate filtration step was carried out to remove possible aggregates and ensure full inactivation. After inactivation a large variation in D-antigen recovery was observed, especially for Sabin PV type 3. Overall recoveries ranged from acceptable (in conventional IPV manufacturing on average approximately 40% for all three sub-types (Thomassen et al. 2013b; van Wezel et al. 1984)), for Sabin PV type 1 (at 40%) to very low, with respect to future cost competitive processing, for PV type 2 (Table 3). The obtained monovalent bulks met all release criteria and were stored at 4°C prior to mixing for formulation.

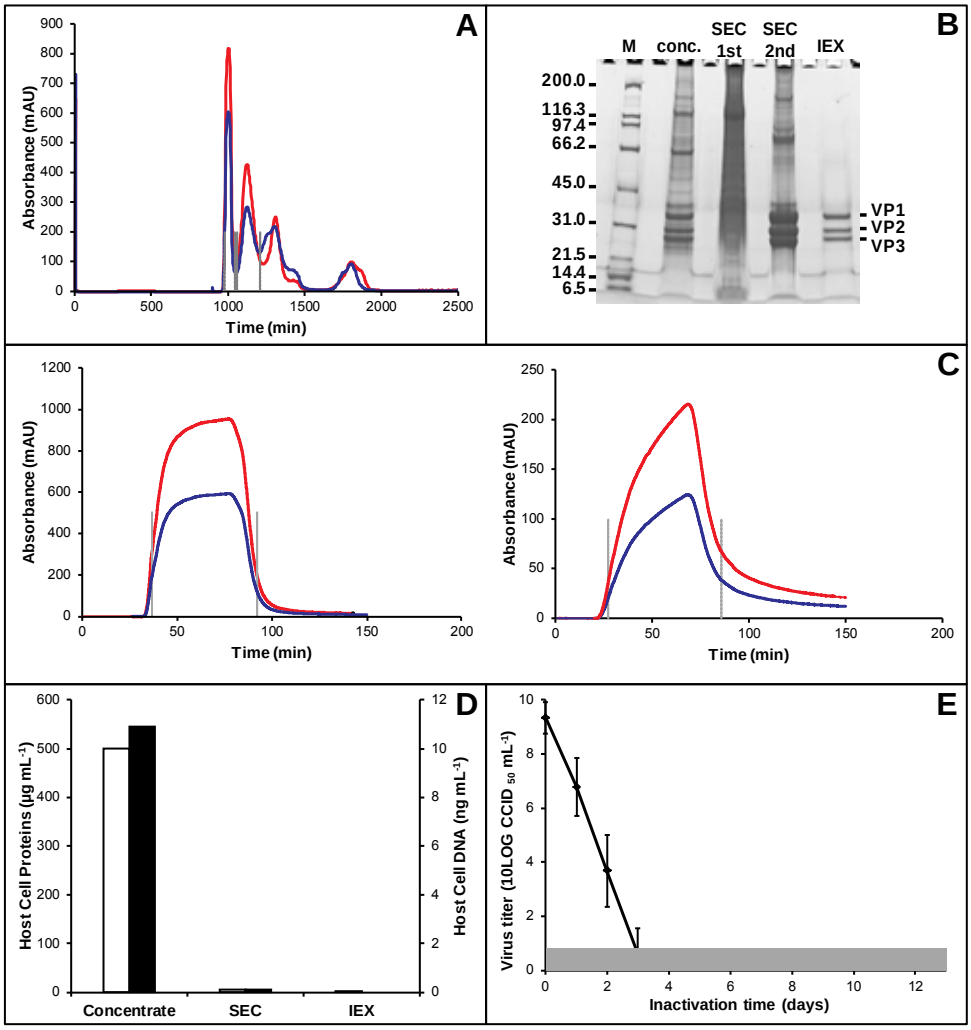

Figure 3. Purification of Sabin PV. Panel A depicts a SEC chromatogram of Sabin PV type 1. The 1st peak contained mostly large cell components; the 2nd peak contained the majority of PV, following peaks consist of smaller components. Panel B shows a SDS-PAGE (4-20% gel); lanes represent (from left to right) the marker, the concentrated product, followed by the 1st and 2nd fraction of SEC and finally the IEX purified PV. Panel C shows chromatograms of Sabin PV type 1 (left) and Sabin PV type 2 (right) IEX purification. Panel D shows host cell protein (open) and DNA (solid) impurities. Panel E depicts the inactivation of PV, the gray area indicates the lower detection limit. In chromatograms A and C, the red and blue lines represent absorbance at respectively 254nm and 280nm. Gray dotted lines indicate peak fractioning.

Formulation

Monovalent bulks were mixed to a trivalent bulk (Sabin PV type 1-2-3) in a ratio of 60-96-192 DU mL^{-1} prior to formulation to a final bulk. Different final bulks were prepared. Plain sIPV was prepared in different final concentrations of D-antigen to be able to test low (5-8-16 DU shd^{-1}) middle (10-16-32 DU shd^{-1}) and high (20-32-64 DU shd^{-1}) dosages in (non-)clinical studies. Aluminium ($Al(OH)_3$) adjuvanted vaccine was mixed at 2-fold lower D-antigen values being: low (2.5-4-8 DU shd^{-1}), middle (5-8-16 DU shd^{-1}) and high (10-16-32 DU shd^{-1}). Vaccine was filled in vials as 0.5 mL per single human dose.

Pre-clinical studies

The immunogenicities in terms of the capacity to induce virus neutralizing antibody titers (VNT) against the wild-type PVs (PV Type 1 Mahoney, PV Type 2 MEF-1 and PV Type 3 Saukett) of the six differently formulated vaccines were determined in rats (Ph Eur 7.0:0214 ; van Steenis et al. 1981). High VNT against wild-type viruses were observed for all prepared formulations (i.e. 0.5 mL of high, middle and low DU). The maximum VNT for PV type 1 was lower than for PV type 2 and 3 (Figures 4A-C). For all types, the VNT increased with the dose and the addition of aluminium as adjuvant had a positive effect. For PV type 2 this effect was larger than for PV type 1 and PV type 3. Compared to conventional IPV, immunization of rats with sIPV resulted in comparable wild-type VNTs for PV type 1 and 3. Lower VNTs were found for PV type 2 when immunized with sIPV, however the levels of antibodies raised are very high (>8 log_2) (Figures 4D-F). These data suggest that sIPV may be able to raise sufficient protective antibodies against all PV sub-types in humans, where the threshold for protection is 3 log_2 (Vidor and Plotkin 2013) and thereby would be non-inferior to conventional IPV.

Stability of the clinical lots over a period of 24 months was assessed based on immunogenicity in rats, D-antigen concentration, amount of free D-antigen (in case of adjuvanted vaccine) and more general parameters like sterility, appearance and pH. Vaccine stability with respect to immunogenicity in rats is illustrated in Figure 5A-D. Based on the regression line slopes (derived from Figure 5A) and their 95% confidence intervals (Figure 5B) it was concluded that all formulated clinical lots were stable with respect to immunogenicity in rats (null hypothesis slope=0; α=0.05; result p>0.05).

In a similar way, the stability of the D-antigen content in the formulated clinical lots was reviewed. Slopes and their 95% confidence intervals of the regression lines (as illustrated in Figure 5C) were calculated. The measurement of D-antigen in aluminium adjuvanted formulations was difficult as the D-antigen needed to be desorbed from the aluminium prior to performing the D-antigen ELISA. This hurdle is illustrated by the larger confidence intervals found for the regression lines for D-antigen stability for the adjuvanted vaccines (Figure 5D).

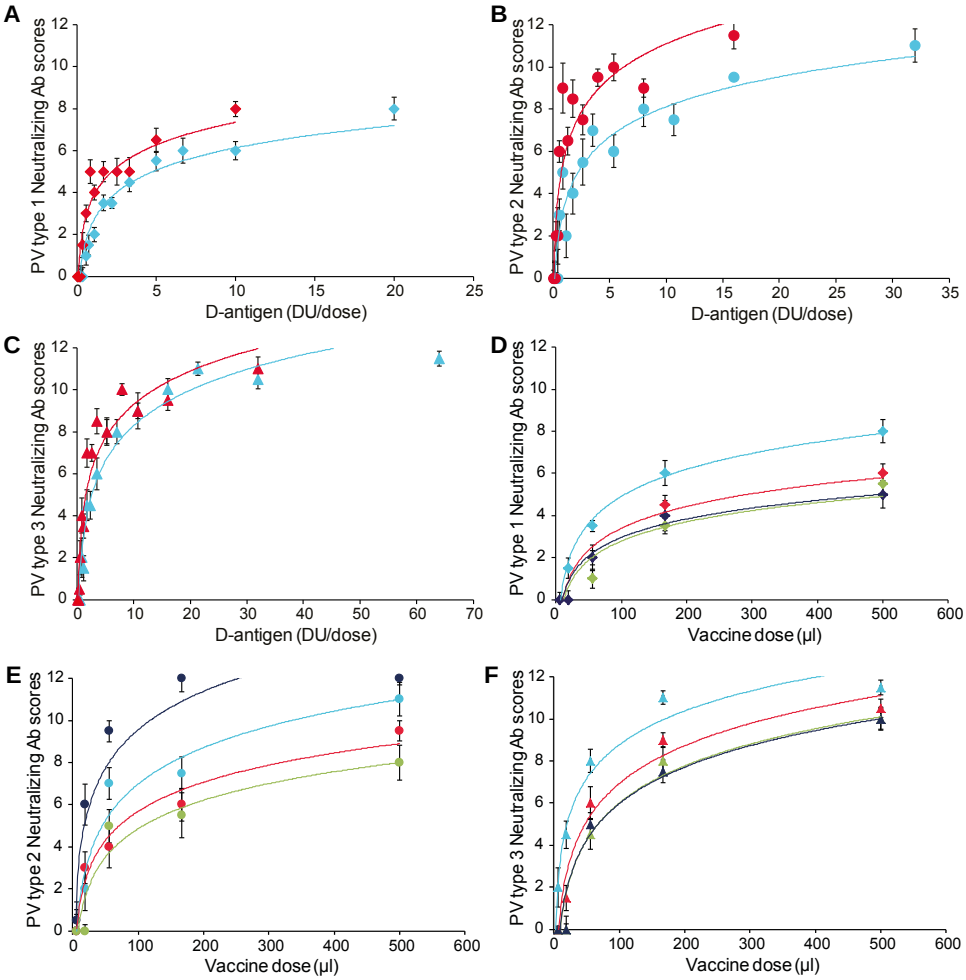

Figure 4. Rat immunogenicity (VNT against wild-type viruses). Panel A, B and C: VNT (log_2 titer) to immunization with plain sIPV (blue) and adjuvanted sIPV (red) for PV type 1, 2 and 3 respectively; Panel D, E and F: VNT of plain sIPV 20/32/64 (light blue), 10/16/32 (red), 5/8/16 (green) and plain IPV 40/8/32 (dark blue) for PV type 1, 2 and 3 respectively. Error bars in panel A-F depict standard deviation of the median (*n*=10 rats).

As a result no conclusions with respect to D-antigen stability could be drawn for the adjuvanted vaccine. Stability regarding the D-antigen content of the non-adjuvanted (plain) vaccine was good (null hypothesis slope =0; α=0.05; result p>0.05).

A repeated dose and local tolerance toxicity study in rabbits was conducted. Highest dose plain and adjuvanted sIPV were compared to a placebo and conventional licensed IPV. Some enlargement in local lymph nodes was found in all vaccine treated groups. Generally, minimal to mild inflammation was observed microscopically at the injection sites of all groups and could be attributed to the injection trauma. More intense inflammation was shown in the adjuvanted sIPV group, which was, in contrast to the other groups, not diminished after the two week recovery period. This was solely attributed to the apparent persistence of the adjuvant. A longer recovery period should have been chosen. The changes at the injection sites as well as the changes noted in the local lymph nodes are common findings in intramuscular vaccine studies meaning that the vaccines are safe to use in clinical trials.

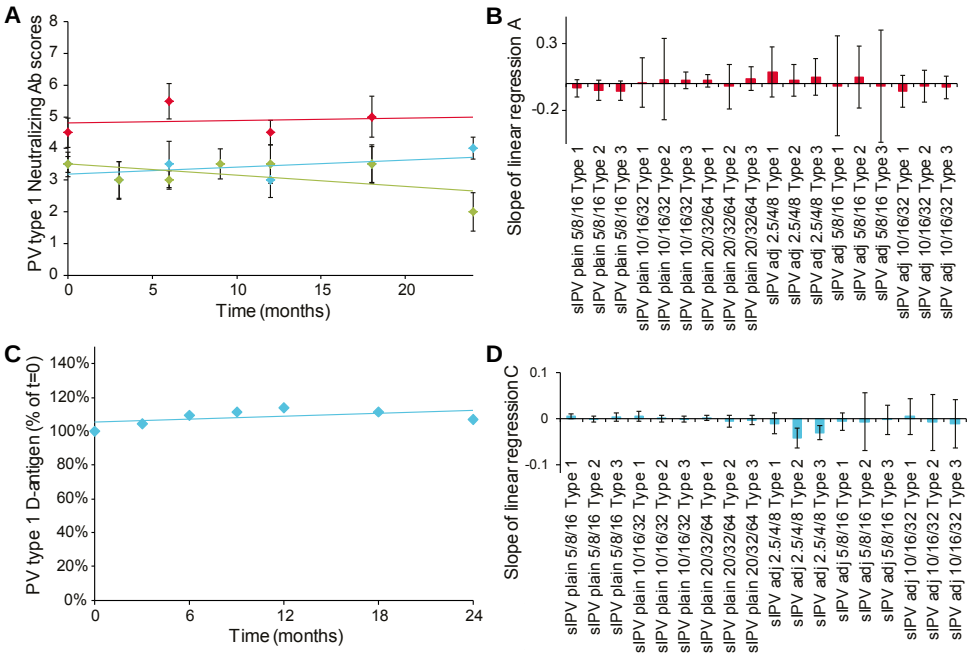

Figure 5. Stability of sIPV. Panel A: PV type 1 VNT of plain sIPV 20/32/64 (blue), 10/16/32 (red), 5/8/16 (green) in time, error bars depict standard deviation of the median (*n*=10 rats); Panel B: slopes of linear regression lines determined for stability based on rat immunogenicity as illustrated in panel A, error bars depict 95% confidence interval; Panel C: Stability of PV type 1 D-antigen of sIPV 20/32/64; Panel D: slopes of linear regression lines determined for stability based on D-antigen as illustrated in panel C, error bars depict 95% confidence interval.

Discussion

The polio eradication program strives to a switch from OPV to sIPV and currently at least one dose of IPV is recommended (WHO 2013a). In view of the relatively short timelines in the polio eradication program it was chosen to prepare a sIPV with limited process development time prior to production of clinical lots. Based on the existing large scale IPV manufacturing process development of sIPV was achieved. Main operating differences were related to the observed precipitate during inactivation, intrinsic virus properties resulting in adjustments in tests (i.e. aluminium desorption prior to D-antigen quantification) and limits required with respect to biosafety (i.e. virus culture temperature). The final product met quality criteria and could be released for testing in the clinical phase I/IIa studies in adults and infants to show safety and proof of principle.

Although a sIPV with required immunogenicity and purity could be produced, the purification yields with respect to Sabin PV type 2 were very low. These low levels will not result in a cost competitive IPV product. However, in light of the polio eradication program, and to pursue the fast implementation of worldwide sIPV manufacturing, sIPV production was continued despite the low type 2 yields. In this way it could be illustrated whether such a product would be comparable or better for polio vaccination compared to the conventional IPV.

The next step in the project is to transfer the manufacturing knowledge to current vaccine manufacturers in low- and middle income countries to replace the OPV production with sIPV production (Bakker et al. 2011). The presented manufacturing process is being optimized in parallel with technology transfer. As product registration for market authorization at local authorities will require local clinical studies, necessary process optimizations for an economically feasible product can be implemented prior to this stage.

Worldwide efforts in the development of sIPV have recently resulted in market authorization for two vaccines containing sIPV in Japan (Tanimoto et al. 2012). Further, the Institute of Medical Biology, Chinese Academy of Medical Sciences (Kunming, China) (Liao et al. 2012a) is currently performing clinical phase III studies (Liao et al. 2012b). This parallel development of sIPV allows a solid base for future IPV availability and minimization of risks with respect to biosafety during manufacturing.

Acknowledgements

The authors thank Patrick Koedam (Bilthoven Biologicals) for the virus neutralization assays performed for the rat immunogenicity studies carried out in collaboration with the Intravacc Animal Research Center (formerly part of the Netherlands Vaccine Institute).

Chapter 8

Isoelectric point determination of live polioviruses by capillary isoelectric focusing with whole column imaging detection

Published as:
Thomassen, Y.E., van Eikenhorst, G., van der Pol, L.A., Bakker, W.A.M. (2013) *Isoelectric point determination of live polioviruses by capillary isoelectric focusing with whole column imaging detection.*

Analytical Chemistry 85(12):6089-6094
dx.doi.org/10.1021/ac400968q

Abstract

Using a capillary isoelectric focusing–whole column imaging detection (CIEF-WCID) method, the isoelectric points (p*I*) of complete intact polioviruses were determined. The polioviruses that were analyzed are the commonly used viruses for the production of inactivated polio vaccines (IPV)—Mahoney (type 1), MEF-1 (type 2), and Saukett (type 3)—as well as for attenuated oral polio vaccines (OPV) and Sabin types 1, 2, and 3. A method for analyzing biological hazardous components (biological safety level 2) was set up for the CIEF-WCID analyzer used. This method is based on closed circuits. The determined p*I*'s were 6.2 for Mahoney, 6.7 for MEF-1, and 5.8 for Saukett. The p*I*'s of Sabin types 1, 2, and 3 viruses were 7.4, 7.2, and 6.3, respectively. Resolution of the virus peaks was shown to be reproducible. Using this adjusted CIEF-WCID technique, the p*I* of biologically hazardous components like toxins or viruses can be determined, which is beneficial for the development of vaccine production methods among others.

Introduction

Polioviruses are members of the *Picornaviridae*. Picornaviruses are small (30 nm in diameter), nonenveloped viruses with a capsid buildup of 60 replicas of four small viral proteins (VP1, VP2, VP3, and VP4) arranged in an icosahedral lattice. The capsids enclose a positive-stranded 7200–8500-nucleotide-long RNA (Koch and Koch 1985; Racaniello 2007). Poliovirus (PV) is the causative agent of poliomyelitis, a disease that can be prevented by vaccination. Currently, two types of polio vaccines are in use, the live oral polio vaccine (OPV) based on attenuated Sabin strains (types 1, 2, and 3) (Sabin and Boulger 1973) and an injectable inactivated polio vaccine (IPV) based on wild type strains Mahoney (type 1), MEF-1 (type 2), and Saukett (type 3) (Salk 1953). The production processes of these vaccines differ in that OPV is prepared by clarification of virus cultures (WHO 1999), while IPV is further purified after virus culture and inactivated using formaldehyde (WHO 2002a).

For process development purposes, it is important to know the isoelectric point (p*I* or IEP) of the product that is being produced. The p*I* is the pH value at which the virus, or a protein, has a net charge of zero. Purification using ion exchange chromatography (IEX) is based on the charge differences of the product and contaminants. Also, product aggregation and choice of buffers in which the product stability can be ensured is, among others, dependent on the product p*I* (Floyd and Sharp 1978a; Floyd and Sharp 1978b; Vrijsen et al. 1983) (the electrochemical surface properties of the product). During the production process of inactivated polio vaccine (IPV), IEX is used to purify the virus (Thomassen et al. 2013b; Thomassen et al. 2010); moreover poliovirus has the tendency to form aggregates (Floyd and Sharp 1979), which needs to be avoided especially during inactivation and final storage. In the polio eradication effort (Aylward et al. 2006), a new IPV based on the attenuated Sabin strains is under development (Bakker et al. 2011). In this task, work on process development is being done to achieve a feasible production process. Until now, the p*I*'s of PV Sabin type 2 and PV Sabin type 3 have not been reported.

Isoelectric focusing (IEF) is a high-resolution technique in which molecules are separated based on charge. It can be used to determine the p*I* of biomolecules or large complexes like viruses. Capillary isoelectric focusing (CIEF) combines the high resolving power of conventional gel IEF with automation and quantification of capillary electrophoresis (CE) (Hjertén and Zhu 1985). The first applications of CIEF used a long (20–60 cm) capillary to focus the molecule of interest and detect it with an on-column UV absorbance meter. Samples mixed with ampholytes are introduced on the column. After application of a high DC voltage, a relatively stable pH gradient is established by the carrier ampholytes (Hjerten et al. 1987). The molecule of interest, often a protein, moves to the pH where its net charge is zero, or where its p*I* value equals the pH. Following focusing, a mobilization process is required to move the focused protein zones through the detection point (Hjertén and Zhu 1985). Problems associated with this mobilization include distortion of

the pH gradient, risk of protein precipitation, uneven resolution due to nonuniform mobilization speed, and increased analysis time (Mao and Pawliszyn 1999).

The development of whole column imaging detection (WCID) eliminates the requirement of mobilization and allows detection during the focusing process (Wu and Pawliszyn 1994). In CIEF-WCID, the p*I* values of separated molecules are directly determined based on the position of the focused molecule and the linear pH gradient in the column. CIEF-WCID has been applied successfully for the p*I* determination of various large complexes like virus-like particles (Goodridge et al. 2004), bacteriophages (Liu and Pawliszyn 2005), and bacteria (Liu et al. 2007).

Determination of the p*I* of polioviruses poses another laboratory challenge, namely a biosafety risk. The iCE280 analyzer (Convergent Bioscience; Toronto Canada) was adapted to allow measurement of live viruses while biosafety is maintained. The here described technique, for accurate measurement of p*I* of hazardous viruses, adds to the field of vaccine production. In addition, other processes where adhesion or sorption of hazardous viruses is important, like virus removal from drinking water (Michen et al. 2013), will benefit from knowing the p*I* of these viruses.

Methods

Virus Samples

Six different PV strains were used in this study. Wild type strains, Mahoney (type 1), MEF-1 (type 2), and Saukett (type 3), and attenuated strains Sabin type 1 (LSc 2ab KP_2), type 2 (P712 Ch2ab-KP_2), and type 3 (Pfizer 457-III).

Vero cells were cultivated adherent to microcarriers (Cytodex 1, GE Healthcare) in stirred tank bioreactors, followed by PV infection (at low multiplicity of infection or MOI of 0.01–0.05) and cultivation for 3–4 days. PV was purified by clarification, concentration, size exclusion chromatography, and IEX in a phosphate buffer (pH 7) (van Wezel et al. 1979). Virus samples had virus concentrations ranging from 8 to 48 mg mL^{-1} assuming *A*260 nm = 81.6 for a 10 mg mL^{-1} solution (Charney et al. 1961).

To prepare virus samples for analysis with CIEF-WCID, 70 µL of 1% methyl cellulose solution was mixed with 8 µL of Pharmalytes (pH 3–10), 50 µL of purified virus, 2 µL of p*I* marker (pH 4.65), 2 µL of p*I* marker (pH 9.22), and 68 µL of Milli-Q to make a final volume of 200 µL. The concentration of carrier ampholytes was 4%. Samples were analyzed at least in triplicate.

Virus Purity

Virus purity was assessed by analysis with SDS-PAGE using 12% polyacrylamide gels (Precise precast protein gels; Pierce). Samples (100 µL) were precipitated using TCA, reconstituted, and loaded on the gel, which was stained after running with Coomassie Brilliant Blue.

Also, the A260/A280 ratio was used to determine virus purity. A ratio of 1.6–1.7 can be considered to represent pure virus (Simizu et al. 2006; Westdijk et al. 2011).

Apparatus

CIEF-WCID was done using the iCE280 analyzer (Convergent Bioscience; Toronto Canada). It was equipped with a 50 mm × 100 µm internal diameter × 200 µm outer diameter silica capillary column with its outside polyamide coating removed. On the inside, the capillary was coated with fluoracarbon (Restek, Bellefonte, CA). The ends of the column were connected with two pieces of 3 mm dialysis hollow fiber membrane (molecular weight cutoff 18,000 Da; Spectrum Medical Industries, Los Angeles, CA).

The used electrolytes were 80 mM H_3PO_4 (anolyte) and 100 mM NaOH (catholyte).

The inlet capillary to the IEF column was connected to a tube which at the other end was put in the sample vial (see Figure 1). The outlet capillary of the IEF column was connected to a tube which at the other end was put in a waste vial containing chloride solution (Actisan). Sample injection was done by applying a vacuum (using a 10 mL syringe) at the waste site of the vial (Figure 1). When the whole capillary was filled (determined by WCID), the sample was considered injected, and the vacuum was lifted. Subsequently the voltage was applied to allow focusing.

The detection system consisted of a UV CCD camera for whole column optical adsorption imaging detection operated at 280 nm. The used lamp was a deuterium lamp.

Reagents

Carrier ampholytes (Pharmalytes 3–10) were obtained from GE Healthcare. The pI markers and methyl cellulose solution (1%) were obtained from Convergent Bioscience (Toronto Canada).

Solutions were prepared in Milli-Q. Electrolytes were prepared by dilution of H_3PO_4 or NaOH in a 0.1% methyl cellulose solution to final concentrations of 80 and 100 mM, respectively.

Isoelectric Focusing

Virus samples were applied to the column as described above. Once the column was filled with the sample (as detected by WCID), after approximately 8 min, a 1.5 kV dc voltage prefocus was applied for 1 min followed by 3 kV dc voltage for 5 min to get IEF separation. After this period, the focusing was complete, and an electropherogram was recorded. Following focusing, the 3 kV dc voltage was turned off, and the sample solution in the IEF column was washed to the waste vial by applying a vacuum in the waste vial. Between the runs, the column was washed with 0.1% methyl cellulose for 3 min.

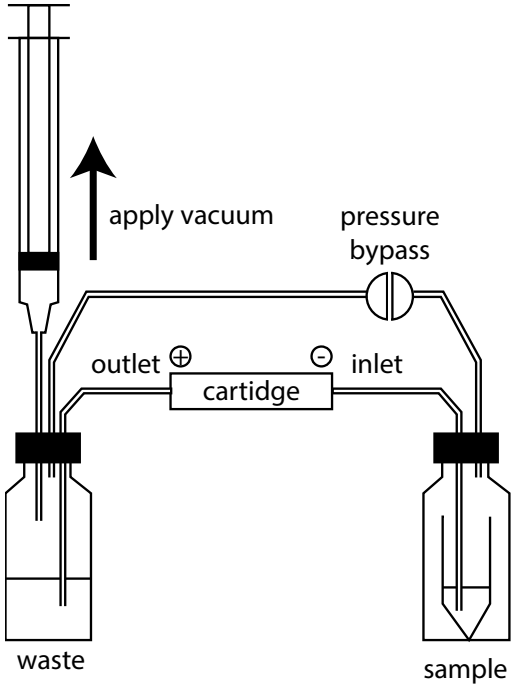

Figure 1. Schematic drawing of the method for analysis.

Results and Discussion

Equipment Setup

Analysis of infectious viruses needs to be done with care for biosafety. To minimize hazardous situations, the iCE280 analyzer was adjusted according to the schematics in Figure 1 to obtain a closed system. This closed system allowed analysis of biologically active poliovirus samples. The sample loading was done by applying a vacuum at the exit site to draw the sample into the cartridge. After full loading of the cartridge, as could be observed using the WCID camera, the vacuum was lifted and voltage was applied. Focusing of PV was complete within 6 min.

Sample Preparation

To obtain highly pure PV, purification was done using size exclusion chromatography and ion exchange chromatography. The purity of the virus was assessed by SDS-PAGE (Figure 2). As is shown in this figure, nearly all of the proteins present after ion exchange chromatography are the viral proteins. This was confirmed by the ratio A260/A280, which was on average 1.62; a value of 1.7 is expected when pure poliovirus is analyzed (Simizu et al. 2006; Westdijk et al. 2011).

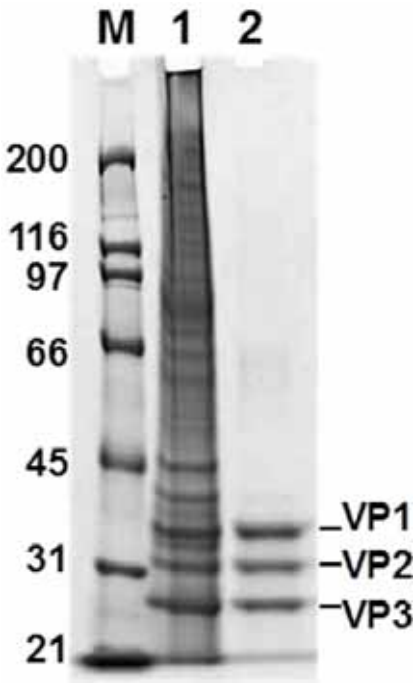

Figure 2. SDS-PAGE of purified PV type 1. Lane 1 of live virus using the iCE280 analyzer represents the product after size exclusion chromatography, lane 2 after ion exchange chromatography, and lane M is the marker.

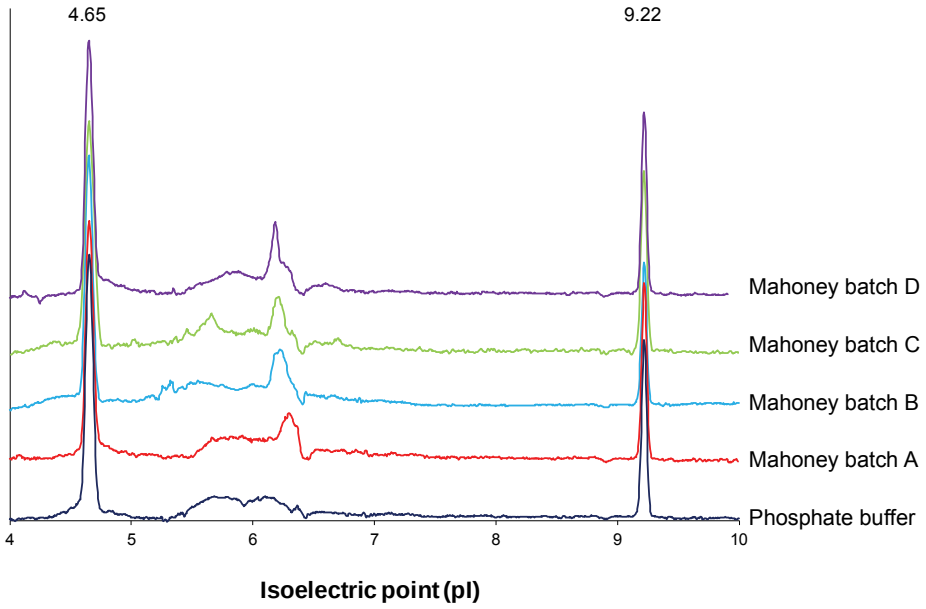

Figure 3. Electropherograms of PV type 1 Mahoney, different production batches (n = 4), and phosphate buffer. Batch A represents a fresh sample; batches B–D represent samples that have been frozen (–80 °C). PVs were mixed with Pharmalytes (pH 3–10) and p*I* markers (4.65 and 9.22), which were used to calibrate the p*I* scale. Detection at 280 nm was done after 6 min of focusing.

Poliovirus Elution Peak Shape and Reproducibility

Polioviruses are small (30 nm), rigid RNA viruses that consist of 60 replicates of four small capsid proteins (VP1–4, 33, 30, 26 and 7 kDa respectively) (Koch and Koch 1985). Such large biomolecules and microbes may be challenging in CIEF separation as not only size but also the composition (lipid, proteins, and carbohydrates) and the higher-order structure can cause changes in the net surface p*I*. It has been shown that CIEF separation of norovirus VLP (30–35 nm), consisting of a single major capsid protein, results in a main peak with few side peaks. The peak shape and p*I* of these VLPs had good reproducibility (Goodridge et al. 2004). Yeast cells, which are much larger (4 µm), were found to have the tendency to interact with the capillary inner wall. This was resolved by using a larger inner diameter and low concentrations (1 cell μL^{-1}) (Shen et al. 2000).

In Figure 3, the electropherograms of purified PV type 1 Mahoney are given. The IEF profiles show a broad peak. Aspects which could result in this peak shape are sample interaction with the inner capillary wall, the focusing time, or sample related aspects like impurities or virus characteristics. Prolonged focusing time did not result in a better resolution. Neither did the virus interact with the capillary wall, as was concluded by

running an electropherogram after flushing the cartridge with running buffer. In Figure 3, the electropherogram of the buffer, a phosphate buffer, is given, which explains most of the broad peak shape. Although the virus samples were very pure (Figure 2), minor impurities were present which may have attributed to the peak shape.

Table 1. Isoelectric point of polioviruses.

	strain		isoelectric point
PV type 1	Mahoney	Overall	**6.22 ± 0.05 (*n*=21)**
		Batch A	6.28 ± 0.01 (*n*=5)
		Batch B	6.23 ± 0.03 (*n*=7)
		Batch C	6.21 ± 0.01 (*n*=5)
		Batch D	6.13 ± 0.03 (*n*=4)
	Sabin	Overall	**7.42 ± 0.07 (*n*=7)**
		Batch E	7.37 ± 0.04 (*n*=4)
		Batch F	7.49 ± 0.03 (*n*=3)
PV type 2	MEF-1	Overall	**6.68 ± 0.07 (*n*=7)**
		Batch G	6.74 ± 0.03 (*n*=4)
		Batch H	6.62 ± 0.03 (*n*=3)
	Sabin	Overall	**7.18 ± 0.08 (*n*=7)**
		Batch I	7.24 ± 0.02 (*n*=4)
		Batch J	7.10 ± 0.04 (*n*=3)
PV type 3	Saukett		**5.84 ± 0.05 (*n*=4)**
	Sabin		**6.34 ± 0.03 (*n*=4)**

The main peak, for PV type 1 Mahoney around a p*I* of 6.2, was used to determine the p*I*. To assess the repeatability of the analysis of a single sample, it was analyzed at least three times. Although the peak was not very sharp, possibly due to a low virus concentration, the relative standard deviation of 0.5% was good. Additionally, four batches of PV 1 Mahoney were prepared separately, i.e. from cell and virus culture up to the purification to assess the repeatability of p*I* determination between different sample preparations (Figure 3). The peak shapes of batches A–D were comparable. In addition to that, no effect of sample freezing on the IEF profiles was seen. Batch A represents a fresh sample, while batches B–D were stored at –80 °C prior to analysis. A similar observation was found for the freezing and thawing of echovirus (Zerda and Gerba 1984). Calculations of the p*I* showed minor variation (Table 1). To determine the p*I* of PV type 1 Mahoney, the average of all analysis was taken, resulting in a p*I* of 6.22 ± 0.05 (*n* = 21).

Determining the pI of Other Polioviruses

Other PV strains used in IPV manufacturing are PV type 2 MEF-1 and type 3 Saukett. Next to that, an IPV based on using attenuated Sabin polioviruses is under development (Bakker et al. 2011). The pI's of these Sabin polioviruses were also determined (Table 1) to aid future process development. In Figure 4, the IEF profiles of the different PVs are compared. On

the basis of these profiles, a distinction between the different viruses can be made. Remarkable is the big difference in p*I* between PV type 1 Mahoney and Sabin type 1 virus. The latter was established by attenuation of the Mahoney strain (Sabin and Boulger 1973).

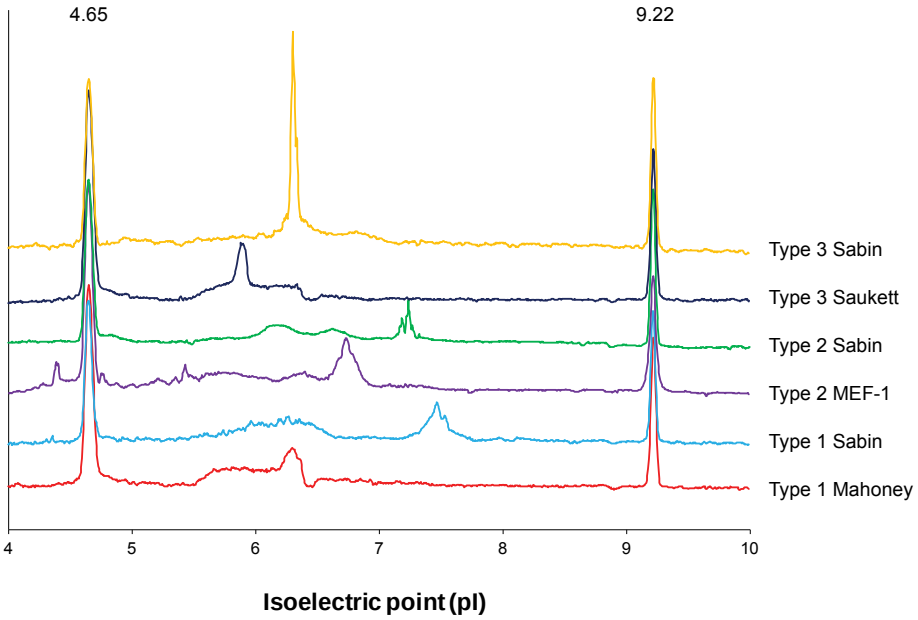

Figure 4. Electropherograms of wild type and attenuated poliovirus strains. PVs were mixed with Pharmalytes (pH 3–10) and p*I* markers (4.65 and 9.22), which were used to calibrate the p*I* scale. Detection at 280 nm was done after 6 min of focusing.

Literature Review

The p*I*'s of most of the PVs were determined earlier by others in the 1970s or early 1980s (Table 2). When regarding the reported p*I*'s for PV type 1 Mahoney, the p*I* ranges from 6.7 to 8.2; in some cases, a second p*I* was found around 4.5. It was proposed that this second p*I* represented an isoform (Mandel 1976). However, Vrijsen et al. (1983) suggested that the second peak represented aggregated PV. These extremes in reported p*I* make comparison with literature data challenging.

Recently, Michen and Graule (Michen and Graule 2010) reviewed the literature on the p*I* of viruses. They concluded that variation in the data resulted from (i) the difference in virus strains, (ii) insufficient purification, (iii) interactions of charged agents with the virus interface such as specific adsorption and/or surface complexation, and (iv) diversity in host cells. While the p*I* determination method may also be a potential source for variation, this could not be assessed.

Table 2. Literature overview on pI's of various PV strains (only the pI of the monomeric "A" form is given).

		IEP	Method[2]	Host	Purity	Reference
PV type 1	Mahoney	8.3 ± 0.1	IEF-DA	HEp-2[3]	High	(Floyd and Sharp 1978a)
		7.0	IEF-DA	HeLa	High	(Alvarez and O'Brien 1982)
		7.5	IEF-DA	HeLa	High	(O'Brien and Newman 1979)
		7.0	IEF-DA	HeLa S3	High	(Emini et al. 1983)
		7.2	IEF-A	HeLa	High	(Rombaut et al. 1989)
		7.0-7.2	IEF-A	HeLa S3	High	(Onodera and Phillips 1987)
		6.7	IEF-A	HeLa S3	High	(Putnak and Phillips 1981)
	Brunhilde	7.0	IEF-DA	HeLa	High	(Mandel 1971)
		7.0	IEF-DA	HeLa	High	(Mandel 1976)
		6.5	IEF-DA	HeLa	High	(Vrijsen et al. 1983)
		6.9	IEF-DA	HeLa	High	(Brioen et al. 1985)
		7.3	IEF-DA	HEp-2[3]	High	(Sharp and Leong, 1980)
		7.1	IEF-A	nd[1]	nd	(Zerda and Gerba 1984)
	Brunender	7.4	IEF-DA	Nd	nd	(Colla La et al. 1972)
	CHAT	7.0	IEF-DA	HeLa	High	(Ward 1980)
		7.5	IEF-DA	HeLa	High	(Ward 1978)
	E206	7.4-7.6	TLE	KB cells	High	(Bengtsson et al. 1964)
	nd	7.4	IEF-DA	Nd	nd	(Nasser et al. 1992)
	Sabin	7.4	IEF-DA	HeLa	High	(Mandel 1976)
		7.0	IEF-DA	HeLa S3	High	(Emini et al. 1983)
		6.75	IEF-DA	Vero	Low	(Butler et al. 1985)
		6.6	IEF-A	Nd	nd	(Zerda and Gerba 1984)
		7.4-7.6	TLE	KB cells	High	(Bengtsson et al. 1964)
		6.6	Calc.[4]	HeLa	High	(Murray and Parks 1980)
PV type 2	MEF-1	6.8	IEF-DA	HeLa	High	(Mandel 1976)
	Sabin	7.5 ± 0.2	IEF-DA	HeLa	High	(Taylor et al. 1981)
		6.5	IEF-DA	HeLa-O	High	(Butler et al. 1985)[5], (Korant and Lonberg-Holm 1974)
		6.85	IEF-DA	GMK cells	High	(Eggers and Rosenwirth 1988)
PV type 3	Saukett	6.6	IEF-DA	HeLa	High	(Mandel 1976)

[1] nd = not described

[2] Various methods of IEF are available: i) IEF in dense aqueous solutions, e.g. sucrose, ampholine (IEF-DA); ii) IEF in agarose gel (IEF-A); iii) IEF in polyacrylamide gels (IEF-PA); iv) capillary IEF (CIEF); v) thin layer electrophoresis (TLE).

[3] HEp-2 cells are contaminated with HeLA (Chen 1988)

[4] calculated based on zeta potential

[5] reference to Korant personal communication (Taylor et al. 1981)

In Table 2, reported values for the p*I* of PV are given in addition to the analysis method, the host cell used, and the sample purity. In general, the sample purity was high; mostly either sedimentation (using sucrose) or isopycnographic (using CsCl) centrifugation was done. Mostly HeLa cells were used to produce the virus, and the common method for analysis was iso-electrofocusing in dense aqueous solution (IEF-DA). PV type 1 Mahoney is the most analyzed poliovirus strain (n = 7). On average, a p*I* of 7.3 was measured with a wide range, 6.7–8.3. Other PV type 1 viruses have an average p*I* of 7.0, for both PV type 1 Brunhilde (range 6.5–7.3) and PV type 1 Sabin (range 6.6–7.5).

In our studies, the p*I* of PV type 1 Mahoney and PV type 3 Saukett were lower (1.0 and 0.8 pH units, respectively) than reported in the literature. The observed p*I*'s of the other strains are within 0.5 pH units of the mean of their respective strains. Comparing the observed p*I*'s with the literature data appeared to be challenging, as in this study the Vero cell line (a cell line most often used in the production of PV for vaccines) and different purification methods have been applied. Concluding from these observed differences, it can be stated that the p*I* of viruses needs to be determined at the conditions which are relevant, meaning the conditions for the specific process development.
Although for some strains a large difference with reported literature data was found, the CIEF-WCID method was robust when analyzing different batches of PV. Additionally, the accuracy of the CIEF-WCID analysis is high. These findings back the significance of our measurements. Using the p*I* of the PV will aid us in our current process improvement efforts for a more affordable (Sabin-)IPV.

Chapter 9

Improved poliovirus D-antigen yields by application of different Vero cell cultivation methods

In press as:
Thomassen, Y.E., Rubingh, O., Wijffels, R.H., van der Pol, L.A., Bakker, W.A.M. (2014) *Improved poliovirus D-antigen yields by application of different Vero cell cultivation methods.* Vaccine
dx.doi.org/10.1016/j.vaccine.2014.02.022

Abstract

Vero cells were grown adherent to microcarriers (Cytodex 1; 3 g L^{-1}) using animal component free media in stirred-tank type bioreactors. Different strategies for media refreshment, daily media replacement (semi-batch), continuous media replacement (perfusion) and recirculation of media, were compared with batch cultivation. Cell densities increased using a feed strategy from 1×10^6 cells mL^{-1} during batch cultivation to 1.8, 2.7 and 5.0×10^6 cells mL^{-1} during semi-batch, perfusion and recirculation, respectively.

The effects of these different cell culture strategies on subsequent poliovirus production were investigated. Increased cell densities allowed up to 3 times higher D-antigen levels when compared with that obtained from batch-wise Vero cell culture. However, the cell specific D-antigen production was lower when cells were infected at higher cell densities. This cell density effect is in good agreement with observations for different cell lines and virus types. From the evaluated alternative culture methods, application of a semi-batch mode of operations allowed the highest cell specific D-antigen production.

The increased product yields that can easily be reached using these higher cell density cultivation methods, showed the possibility for better use of bioreactor capacity for the manufacturing of polio vaccines to ultimately reduce vaccine cost per dose. Further, the use of animal-component-free cell- and virus culture media shows opportunities for modernization of human viral vaccine manufacturing.

Introduction

Recently, we have produced Sabin-IPV (inactivated polio vaccine based on attenuated Sabin strains) clinical lots under cGMP for phase I safety (and indicative immunogenicity) studies in human adults and infants (Bakker et al. 2011; Thomassen et al. 2013a). The applied production process was based on a scale-down model of the Salk-IPV manufacturing process (Thomassen et al. 2013b). The use of this scale-down model allowed fast development of a first generation Sabin-IPV, for which the specifications are closely related to that for the regular IPV product (Thomassen et al. 2013a). In parallel to this fast-track development an optimization and modernization research program for the manufacturing of Sabin-IPV was started. Examples for modernization are replacement of the used animal derived components (e.g. bovine serum and porcine trypsin) and antibiotics. These components should preferably be omitted (for the antibiotics primarily to prevent any potential allergic reaction), or respectively replaced by animal component free (ACF) alternatives to minimize the risk of adverse effects (e.g. the potential transfer of viruses and/or prions). Moreover, a better scientific understanding of the process, resulting in improved process control and ability for troubleshooting, can be created. Optimization improvements can possibly be found in the currently used, low cell densities (1×10^6 cells mL^{-1}). Assuming comparable virus quality and yields per cell, the use of increased cell densities can potentially result in more efficient use of bioreactor capacity, and ultimately reduce the cost per dose. The demand for IPV is increasing as in 2012 the WHO SAGE group advised all countries to introduce at least one dose IPV in their routine immunization schedules (WHO 2013a). With the increased IPV demands, which will further increase after oral polio vaccine (OPV) cessation, the production capacity will have to increase by scale-up and optimization causing the current IPV price of $ 3.00 per dose to decrease to $ 0.52 - $ 1.95 (Venczel et al. 2009). This is still four to fifteen times the current price of OPV (cost per dose $ 0.14), the vaccine used in most countries. Process optimization for IPV manufacturing will be needed to be able to further reduce manufacturing costs below $ 0.50 to keep polio vaccination economically feasible when switching from OPV to IPV (Sangrujee et al. 2004).

Here we report initial studies where four different adherent Vero cell cultivation methods were applied using ACF cell culture media: i) batch, the currently used method for Sabin-IPV preparation; ii) semi-batch, where daily media refreshments were applied; iii) perfusion where continuous media refreshment was applied; and iv) recirculation where media was circulated through the bioreactor and re-used. With these commonly known cell culture methods (Pirt 1975) higher cell densities were obtained and the subsequent virus culture, also using ACF virus culture media, produced higher quantities of infectious and immunogenic poliovirus.

Materials and methods

Cells, virus

Vero cells obtained from WHO (10-87) originally derived from ATCC (CCL-81) were used as host for poliovirus production. Poliovirus seeds (Bakker et al. 2011) Sabin type 1 (LSc 2ab KP_2; SO+3), Sabin type 2 ((P712 Ch2ab-KP_2; SO+3) and Sabin type 3 (Lot 457-III-Pfizer; RSO3) were used.

Cultivation methods

Pre-cultures

Vero cells were cultured in T-flasks and Hyperflasks (Corning) in VP-SFM (Invitrogen) to expand the cell number. After trypisinization (TrypLE Select; Invitrogen) cells were resuspended in VP-SFM and added to the bioreactor.

Bioreactor Vero cell cultures

Different cultivation methods have been applied where Vero cells were grown adherent to microcarriers (3 g L^{-1} Cytodex 1; GE Healthcare). The cultures were maintained at pH 7.2, 37°C, 50% dissolved oxygen (DO) by headspace aeration only (1 L min^{-1}) and sampled at least once a day.

Cell cultures were carried out in standard glass stirred-tank type bioreactors, optionally equipped with a spin filter (70 µm) to retain cells on microcarriers in the bioreactor when needed (perfusion and recirculation culture mode). Alternatively, a harvest pipe with a 75µm sieve was used to remove media while retaining microcarriers. Cultivations were controlled using Sartorius DCU-3 control units and MFCS-win software (Sartorius AG, Melsungen, Germany).

Batch cultivations were carried out at 4L working volume with inoculation densities of 0.1 × 10^6 cells mL^{-1}. During cultivation, glucose and glutamine were added by bolus feeding to 10 mM glucose and 2 mM glutamine when concentrations were below 5 mM and 0.5 mM respectively.

Semi-batch cultivations were essentially performed as described by Mendonça (1998) (Mendonça and Pereira 1998) at 3L working volume with an inoculation density of 0.1 × 10^6 cells mL^{-1}. From day two onwards, daily 1L culture medium (1/3 culture volume) was replaced with fresh medium. Media replacement was done after sedimentation of the microcarriers without agitation. In addition, bolus feeding of glucose and glutamine was done once 4 days after the start of cultivation to obtain concentrations of 20 mM glucose and 2 mM glutamine.

Perfusion cultivations were carried out using 1.5L working volume. Cells were inoculated at 0.1×10^6 cells mL^{-1} and retained in the bioreactor. After 2 days of batch cultivation, continuous media feed was started at 1.5 L day^{-1} (1 culture volume per day). Media feed rate was kept constant for the remainder of the perfusion cultures.

Recirculation cultures, where cells are retained in the bioreactor (3L working volume) while medium (15L total volume= culture volume + circulated volume) is circulated, were carried out essentially as described previously (van Wezel 1985). Cells were inoculated at a cell density of 0.6×10^6 cells mL^{-1}. After 1 day, a continuous recirculation flow was started with 15 L day^{-1} (5 culture volumes per day), followed by daily increments to 22 L day^{-1} and 30 L day^{-1} (respectively 7.3 and 10 culture volume per day) at days 3 and 4.

Virus culture

Prior to virus infection, using the same bioreactor vessel used for Vero cell culture, the media feed was stopped and pH, DO and temperature settings were adjusted to 7.4, 25% and 32.5°C, respectively. Media was not refreshed but glucose and glutamine were fed when concentrations were below 5 mM and 0.5 mM, respectively. Cells were infected with poliovirus with an MOI (multiplicity of infection) of 0.01. Virus cultivation was considered finished when 100% CPE (cytopathic effect) was observed microscopically.

Analytics

Cells were counted daily using a Nucleocounter NC-100 (Chemometec).

Cell culture metabolites such as glucose, lactate, glutamine, glutamate and ammonia were monitored using a Bioprofile 100 Plus (Nova Biomedical Waltham, MA).

Poliovirus was quantified with a virus titer assay as decribed previously (Thomassen et al. 2012). The amount of D-antigen was assessed using a D-antigen ELISA (ten Have et al. 2012).

Results

Vero cell growth

Vero cell cultures were performed in four different cultivation modes, batch, semi-batch, perfusion and recirculation. Batch cultivations were performed to obtain a reference growth curve for later comparison with the more sophisticated culture methods where either media is refreshed (semi-batch and perfusion) or circulated (recirculation). After 3-4 days of cultivation, a cell density at 1.0×10^6 cells mL^{-1} was reached in batch cultivation with an average growth rate of 0.036 h^{-1} during exponential growth and a growth rate of 0.022

h^{-1} at the moment of virus infection on day 4 (Figure 1; Table 1). At this point cells are present as a monolayer on the microcarriers (Figure 2). Applying a daily partial medium renewal in a semi-batch mode allowed cell growth to continue and after 2 additional days of culture (6 days in total) a cell density of 1.8×10^6 cells mL^{-1} was obtained. Here comparable growth rates to batch cultivation were observed. The growth rate declined during the feed phase from 0.034 h^{-1} at day 3 to 0.006 h^{-1} at day 6. Using a perfusion mode, where medium renewal is continuous, cell growth could be prolonged to yield a cell density of 2.7×10^6 cells mL^{-1} in 7 days. The growth rates of the Vero cells were lower during the feed phase compared to the growth rates observed in semi-batch cultivations and decreased from 0.018 h^{-1} at day 3 to 0.005 h^{-1} at day 7.

Table 1 Cell culture characteristics of different Vero cell cultivation methods

Cultivation method	Inoculation cell density ($\times 10^6$ cells mL^{-1})	Cell density at time of infection ($\times 10^6$ cells mL^{-1})	Culture time (days)	Growth rate at virus infection (h^{-1})
batch (n=5)	0.10 ± 0.04	1.02 ± 0.07	4	0.022
semi-batch (n=3)	0.14 ± 0.01	1.75 ± 0.32	6	0.006
perfusion (n=3)	0.08 ± 0.01	2.72 ± 0.10	7	0.005
recirculation (n=3)	0.64‡ ± 0.11	5.01 ± 0.40	4‡	0.0004

Cells were present in a multilayer on the microcarriers at these cell concentrations (Figure 2). In the so-called recirculation method (van Wezel 1985) cells were retained in the bioreactor while medium from an external container was circulated. When starting with an inoculation density of 0.6×10^6 cells mL^{-1} a monolayer was already formed after one day of cultivation, and cells started to grow in a multilayer rapidly. Cell concentrations of 5.0×10^6 cells mL^{-1} were found after a culture time of 4 days, while growth rates decreased linearly during the feed phase from 0.025 h^{-1} at day 2 to 0.0004 h^{-1} at day 4. It should be noted, that the latter cultivation method was applied using higher inoculation densities, which implies that a more extensive (or longer) pre-culture was needed.

Glucose and glutamine concentrations during cell culture

The concentrations of glucose and glutamine were analyzed during the Vero cell growth in different cultivation modes. Glucose and glutamine concentrations decreased rapidly when the culture was in batch mode (Figure 3). When media was refreshed daily (semi-batch) or continuously (perfusion) or when media was circulated (recirculation), sufficient glucose and glutamine were present during the complete cultivation time. During perfusion and recirculation cultivations it is clear that from the moment the feed was started the glucose and glutamine levels remained reasonably constant, whereas during semi-batch cultivations glucose and glutamine concentrations varied more. This was directly correlated to the feeding times. It should be noted that during semi-batch

cultivations, an additional bolus feed of glucose and glutamine was given at day 4 (Figure 3).

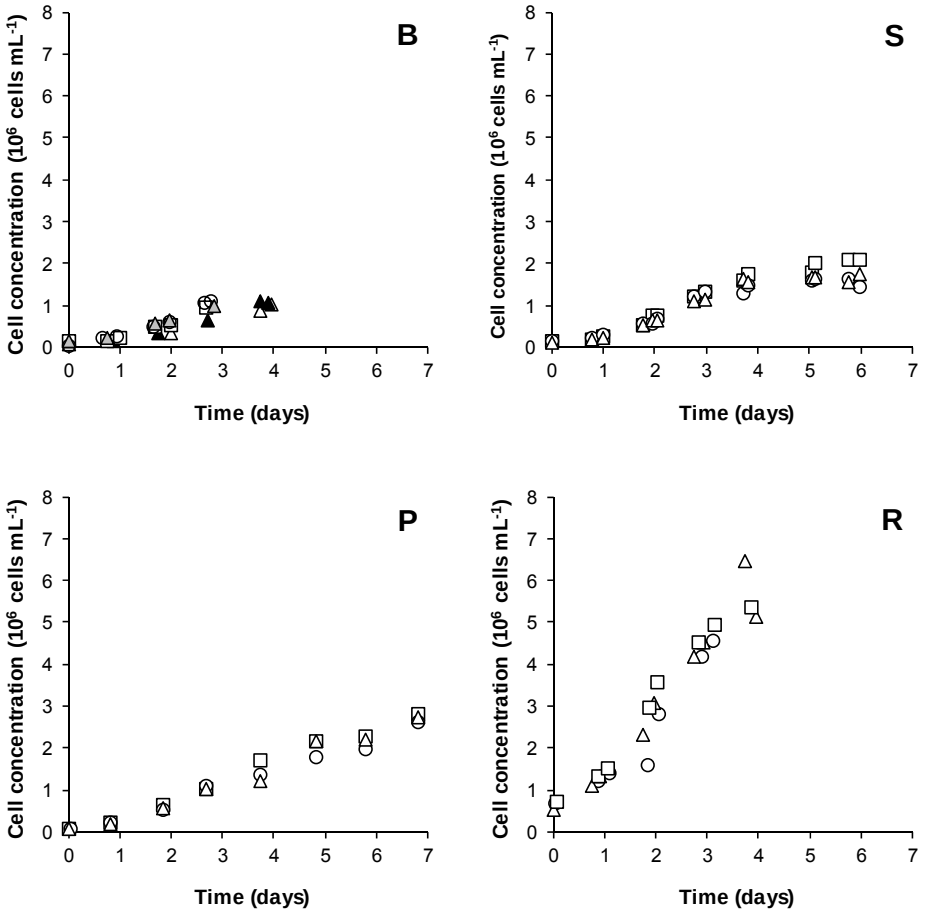

Figure 1. Growth curves of Vero cells using different cultivation modes batch (B), semi -batch (S), perfusion (P) and recirculation (R). Different batches are indicated with different colours and symbols, where squares, circles and triangles represent cultures that were infected with poliovirus type 1, 2 and 3 respectively. Infection of cultures was done at the end of the shown growth curve.

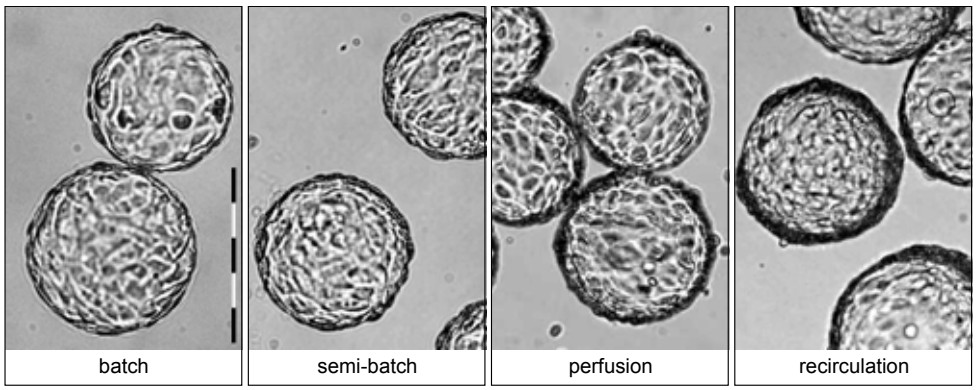

Figure 2. Photographs of Vero cells on microcarriers at the time of virus inoculation. Presence of multilayers at higher cell concentrations (1.0, 1.8, 2.7 and 5.0 × 10^6 cells mL^{-1} for respectively batch, semi-batch, perfusion and recirculation) is clearly visible.

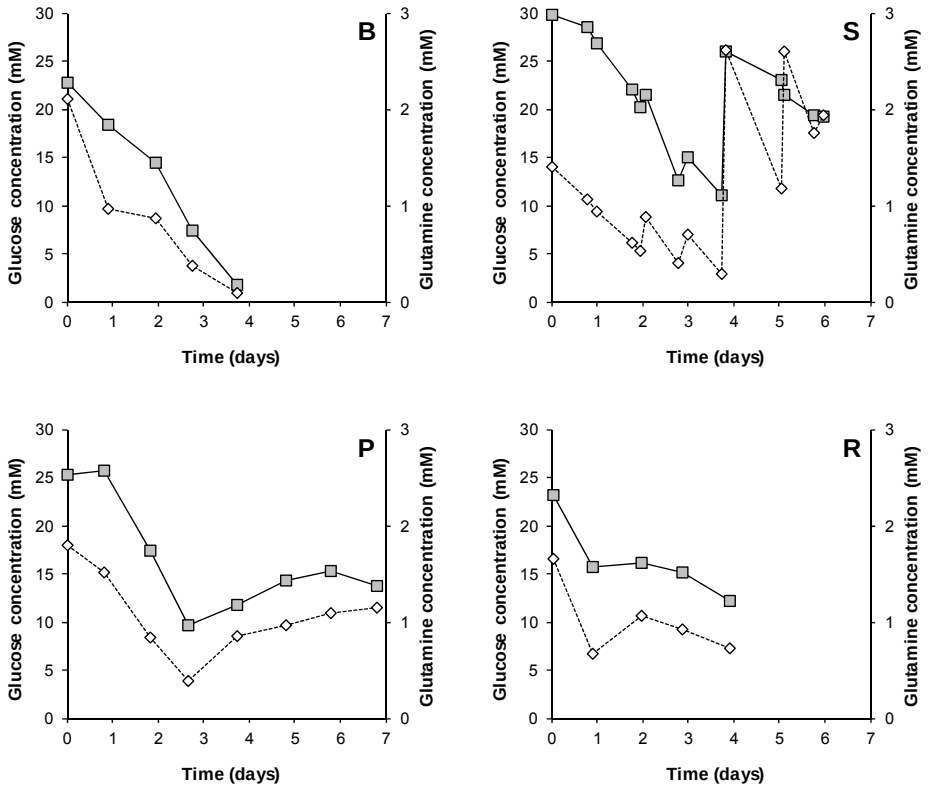

Figure 3. Glucose (squares) and glutamine (diamonds) concentrations present in Vero cell cultivations using batch (B), semi-batch (S), perfusion (P) or recirculation (R). Figures are averaged numbers. Daily media exchange was started at day 2 (S), media feed at day 3 (P) and circulation at day 1 (R).

Lactate and ammonia concentrations

During the batch cultivation lactate and ammonia concentrations increased and within 3 days concentrations up to 30 mM lactate were reached. Daily media replacements allowed to keep lactate concentration below 30 mM whereas continuous media replacement lowered the lactate concentration. Recirculation of media caused a relative constant lactate and ammonia concentration during the cultivation time. Although lactate levels reach high concentrations (above 20 mM), the Vero cell growth continued and therefore it was concluded that this did not inhibit cell growth severely. Ammonia concentrations were below 2 mM under all growth conditions.

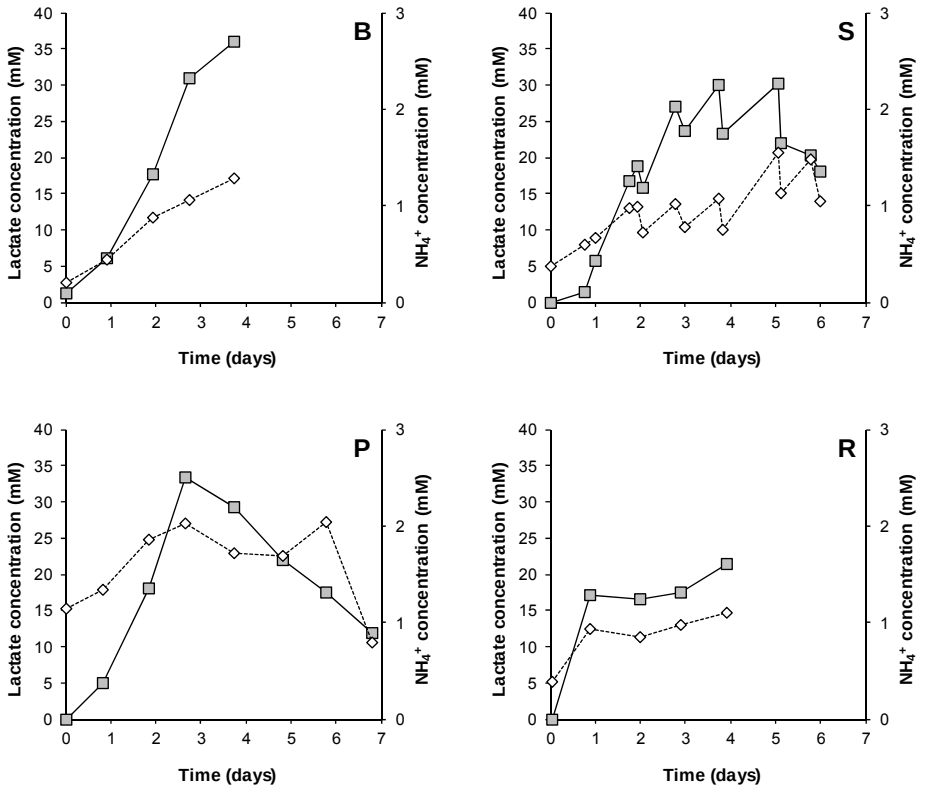

Figure 4. Lactate (squares) and NH_4^+ (diamonds) concentrations present in Vero cell cultivations using batch (B), semi-batch (S), perfusion (P) or recirculation (R). Figures are averaged numbers. Daily media exchange was started at day 2 (S), media feed at day 3 (P) and circulation at day 1 (R).

Virus culture

To determine the variability in poliovirus yields, three cell cultures (in batch mode) were infected with poliovirus type 3. When virus culture was complete, virus titers were measured to determine the amount of infectious poliovirus and D-antigen was measured to quantify the amount of immunogenic poliovirus. The RSD (relative standard deviations) were 9% for the virus titer and 8% for the D-antigen concentration. Both are within 10%, which can be considered comparable. This means that cultures were very comparable as the virus titer assay is valid within 0.5 log (=6%) and the RSD for test reproducibility for the D-antigen ELISA is 10.6% (ten Have et al. 2012). Based on good virus culture reproducibility, it was chosen to compare the effects of different cell culture strategies on the virus yield with *n*=1 for all three virus types.

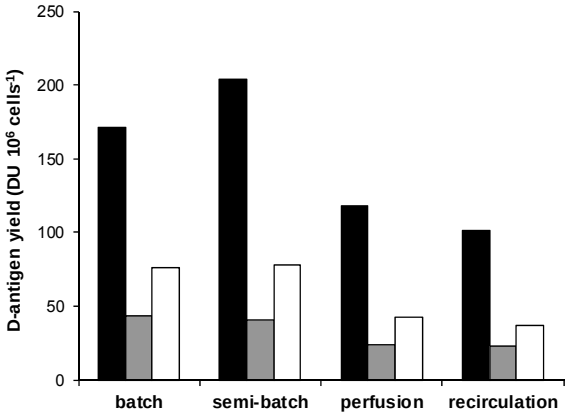

Figure 5. Cell specific D-antigen yields (poliovirus type 1, black; type 2, grey; type 3, white) after different cell culture methods. Similar virus culture conditions were applied.

Comparable virus titers were found independent of the cell culture method that was applied (Table 2). On the other hand, for all three poliovirus types differences in D-antigen concentrations were more pronounced. In all cases where media refreshments were used during cell cultures an increase of the D-antigen yield was observed, when compared with batch-wise cell culture. These increases ranged from approx. 1.5- to 2-fold when cell cultures were carried out in semi-batch and perfusion mode to approx. 2.4- to 2.9-fold when cell cultures were executed in recirculation mode. Since cell concentrations at the start of virus culture were different in the different settings (Table 1), the cell specific D-antigen yields were calculated and compared (Figure 5). Cell specific D-antigen yields were the highest when virus culture was carried out based on semi-batch cell cultures for poliovirus type 1 and batch or semi-batch cell cultures for type 2 and 3. When perfusion or recirculation cultures were used prior to virus culture, the cell specific D-antigen yields were a factor 2 lower.

Table 2 Virus titers and D-antigen concentrations observed using different Vero cell culture methods before virus replication.

Cultivation method during cell culture	poliovirus type 1		poliovirus type 2		poliovirus type 3	
	Virus titer (10 LOG $TCID_{50}$ mL^{-1})	D-antigen (DU mL^{-1})	Virus titer (10 LOG $TCID_{50}$ mL^{-1})	D-antigen (DU mL^{-1})	Virus titer (10 LOG $TCID_{50}$ mL^{-1})	D-antigen (DU mL^{-1})
batch	8.7	175	8.8	44	8.8 ± 0.8 (*n*=3)	78 ± 6 (*n*=3)
semi-batch	8.8	356	8.7	72	7.9	137
perfusion	9.3	320	8.3	65	8.6	115
recirculation	9.5	508	8.8	115	8.9	185

Discussion

The Vero cell line is one of the commonly used cell lines to produce viral vaccines (Barrett et al. 2009). Classic cell culture processes used in vaccine manufacturing are often based on batch-wise cell and virus cultivations followed by extensive downstream processing, concentration, purification and inactivation to yield a product (Montagnon et al. 1984; van Wezel et al. 1984). While downstream processing is important, the virus of interest is generated during upstream processing, i.e. cell and virus culture. It is also at this stage where the intrinsic product quality is determined. Whereas product yields may be related to both the cell concentration and the metabolic state of the cells, product quality is likely largely influenced by the cells metabolic condition and the virus culture conditions. In other words, the cell culture method may impact product quality. The cell cultures are discussed first, followed by the observed D-antigen levels as indicator of product quality.

The application of different cell culture strategies resulted in higher cell densities, up to 5×10^6 cells mL^{-1} during recirculation cultures. These cell concentrations were at comparable levels to those previously reported for recirculation cultures (Trabelsi et al. 2005). In addition, the cell densities reached using perfusion, semi-batch and batch cultures were comparable to those reported by others (Mendonça and Pereira 1998; Petiot et al. 2010b; Rourou et al. 2007).

At the higher cell densities, cells were growing in multilayers on the microcarriers. Recently it has been reported that the tumorgenicity of Vero cells is dependent not only on the passage level as reported previously (Levenbook et al. 1984), but also on the culture conditions (Manohar et al. 2008). The growth in dense cultures as well as the adaptation to serum free media may result in the acquisition of a tumorgenic phenotype. Moreover differences in cell morphology, i.e. the compactness of the monolayer, have been reported for Vero cell growth in different serum free media (Chen et al. 2011). As such, tumorgenicity of the Vero cells growing in multilayers in a specific ACF medium should be investigated before these cells are used to produce clinical materials.

During all cell cultures, sufficient concentrations of glucose and glutamine were present. At the end of cell culture lactate concentrations were high, up to 36 mM during batch, approx. 20 mM during semi-batch and recirculation and 12 mM during perfusion cultures. Reports of high lactate concentrations during Vero cell growth are abundant when the carbon source is glucose, see for example Petiot (2010b), and are caused by the overflow metabolism. High lactate concentrations may be prevented by using other carbon sources like fructose or galactose (Mendonça and Pereira 1998; Petiot et al. 2010b). The ammonia concentration was around 1 mM at the end of the cultivations, which is at an acceptable level that does not inhibit cell growth (Hassell et al. 1991). Since media was not changed

prior to virus culture, these lactate and ammonia concentrations were present at virus infection.

The use of VP-SFM during cell and virus culture appeared beneficial for virus yields when compared to cultivation using serum containing medium during cell culture and M199 during virus culture. In earlier studies (Bakker et al. 2011), using the latter media, D-antigen levels reported for production at 350-L scale were 120, 25 and 56 DU mL^{-1} for respectively Sabin poliovirus type 1, 2 and 3. The use of VP-SFM resulted in a 1.5 times higher level of antigenic product concentration using batch cultivations and 4 fold when using a recirculation culture prior to virus infection. It should be noted that here virus cultures were carried out using spent media. Regarding the nutrient and waste metabolite concentrations it might be even more beneficial to change the media prior to virus culture or to feed possible depleted nutrients during virus culture. This type of optimization may result in a favourable host cell metabolic condition with respect to virus production.

Differences in D-antigen yield per cell between batch or semi-batch and perfusion or recirculation were observed (Figure 5). At higher cell densities the virus yield per cell decreased. This might be an example of the so-called "cell density effect" first described by Wood (Wood et al. 1982) and observed for different virus cultivation systems (Bock et al. 2011; Chen et al. 2011; Kamen and Henry 2004; Rourou et al. 2007). In several cases nutrient limitation or the presence of inhibitory factors may have caused this effect (Bock et al. 2011; Kamen and Henry 2004; Rourou et al. 2007). In others, the cause remains to be found (Chen et al. 2011; Le Ru et al. 2010). Here, the concentrations of the main nutrients, glucose and glutamine, and waste products, lactate and ammonia, were at less favourable levels during batch or semi-batch, while the highest specific product yields were observed under these conditions. We thus concluded that these concentrations are less relevant when compared with other phenomena that influence the cells ability to produce virus. These other aspects could be the growth rate at virus infection, the presence of multilayers, or the capacity (surface space) to continue growth after virus infection. Cell growth rates at time of virus infection were lower under all high cell density strategies compared to the growth rates observed in batch cultivations and thus do not explain for the difference in cell specific D-antigen yield observed between semi-batch and perfusion or recirculation cultures. Possibly, the presence of a multilayer has a more important negative effect. It could be that in a multilayer not all cells present on the microcarrier support virus replication in the same way. Moreover, the capacity to continue cell growth at the moment of virus infection may be important as the applied MOI was 0.01 which means 99% of the cells will not be infected during the first virus replication cycle and can potentially grow further. These topics are currently under investigation to be able to further optimize the virus culture at increased cell densities.

The highest virus yields, based on D-antigen concentrations, were observed using the recirculation mode for cell culture. At a first glance, to maximize bioreactor capacity, this seems to be the best choice. However, it should be mentioned that a larger pre-culture needs to be prepared as here the cell culture is started at 0.6×10^6 instead of 0.1×10^6 cells mL^{-1} used for the other cell culture strategies. Hence, extending the overall process throughput time. Further, considering the cell specific D-antigen productivity, the semi-batch cell culture strategy appeared to be a good alternative. In addition, this method can be applied in existing manufacturing equipment without large investments. At present, we are optimizing this method with respect to microcarrier concentration, feed frequency and feed/bioreactor volume ratio. In addition, adaptation of downstream processing to concentrate and purify the poliovirus obtained from increased cell density cultures is studied. Focus points are the filter load with cell debris during clarification and concentration and the removal of the increased concentrations of host cell proteins and host cell DNA during column chromatography. Also, product quality and immunogenicity after purification remains to be assessed. In that way, discrimination between intact virus particles and virus progeny, which may have attributed to the observed increased D-antigen levels, can be made.

Conclusions

This study shows that adherent Vero cell culture using different methods of medium refreshment allows higher cell densities. Increased cell densities allowed up to 3 times higher D-antigen levels when compared with that obtained from batch-wise Vero cell culture. The cell specific D-antigen production was lower when cells were infected at higher cell densities. Application of a semi-batch mode of operations allowed the highest cell specific D-antigen production, while 2 fold lower cell specific D-antigen yields were found using perfusion or recirculation cultures. This reduction may be related to the presence of multilayers of cells on the microcarriers, which were observed at higher cell densities that were reached using perfusion or recirculation mode. In our view, the most promising concept for polio D-antigen yield optimization would be semi-batch cultivations. This strategy has potential to be further improved and can be implemented in current manufacturing facilities. Using the here presented method for semi-batch cell culture and subsequent virus culture, D-antigen yields per run can be doubled.

Concluding, the use of increased cell densities can result in more efficient use of bioreactor capacity, and may so reduce the vaccine cost per dose.

Acknowledgements

This work was supported by the World Health Organization using funds provided by a grant from the Bill and Melinda Gates Foundation.

Chapter 10

General discussion

IPV v2.0 – Upgrading the established inactivated polio vaccine production process

Introduction

The current available polio vaccines, introduced in the middle of the 20th century, are among the most successful and widely used vaccines ever produced (Ehrenfeld et al. 2009). For the 1st inactivated polio vaccine (IPV) preparation, virus production was done in roller bottles: poliovirus (PV) was propagated on primary monkey testis or kidney tissue in Medium 199 (Morgan et al. 1950) followed by clarification through centrifugation and storage at -20°C. After thawing, purification was done by centrifugation "until crystal clear". The purified PV was pooled and inactivated with formaldehyde resulting in an IPV (Salk 1953). Later, in the 1960s in Bilthoven, a process was developed based on microcarrier technology and primary monkey kidney cells (van Wezel 1967). Also, the purification methods for PV were improved by applying both filtration (for concentration) and chromatography, to obtain concentrated highly pure PV to be used for the vaccine formulation (van Wezel et al. 1979). The developed technologies were freely shared with several pharmaceutical companies (GSK, Sanofi Pasteur, Novartis) and institutes worldwide (Duchene 2006; Montagnon et al. 1981). From the 1980s onwards, the Vero cell line was introduced to replace the primary and tertiary monkey kidney cells (Montagnon and Vincent-Falquet 1998). Today, at various locations, comparable processes are in operation for the production of polio (Duchene 2006; Montagnon et al. 1983; Thomassen et al. 2013b; Vidor et al. 1997) and other viral vaccines (van Wezel et al. 1984; van Wezel et al. 1978) (Chapter 2).

With the soon anticipated polio eradication, process development studies regarding this legacy process have been given a boost. Studies on yield optimization aiming at cost price reduction as well as the use of alternative, more biosafe (for manufacturing), PV are actual. Here it is discussed how a new IPV production process using attenuated Sabin PV strains can be setup based on the existing, legacy, IPV production process (Figure 1) with its roots in the 1960s. Moreover aspects on cost price reduction and the impact of process optimization on IPV costs are reviewed.

Reviving knowledge on existing manufacturing processes

Historical manufacturing data can potentially harbour a wealth of information for process optimization and enhancement of efficiency and robustness. In Chapter 3, the historical data from conventional IPV (cIPV) manufacturing using the Vero cell line and wild type polioviruses has been analysed by multivariate data analysis (MVDA). This approach is stimulated by the ICH (International Conference on Harmonization) to improve the scientific understanding of production processes for troubleshooting, and to support better process control (ICH Q8(R2) 2009; ICH Q9 2005; ICH Q10 2008; ICH Q11 2012). As the process development for IPV was done decades ago, application of MDVA on the historical data was also applied to bring manufacturing knowledge up-to-date for the current

process developers. Moreover, it was anticipated that leads for yield optimization would be unravelled. The results of the analysis were disappointing on the latter which could be attributed to two factors. First, manufacturing followed strict operating procedures, according to cGMP guidelines. Therefore, too few critical process parameters were varied,

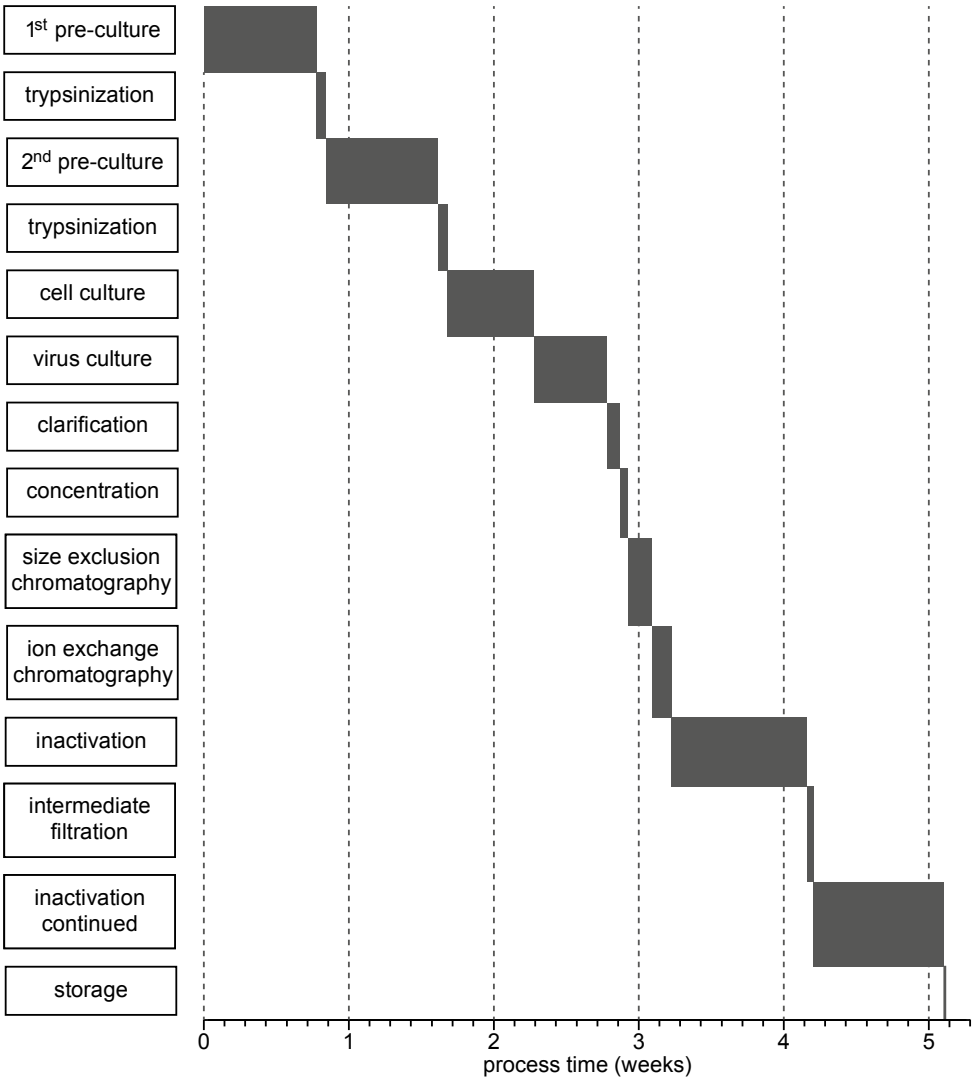

Figure 1 Process overview currently used for the preparation of a monovalent bulk. Cells are expanded using two pre-culture steps prior to cell and virus culture. Purification is done by clarification, concentration, size exclusion chromatography and ion exchange chromatography followed by inactivation. To obtain trivalent polio vaccine this procedure is followed for each poliovirus type separately prior to mixing for end product formulation.

mostly as a result of (planned) process deviations, to indicate directions for yield optimization. Second, the used product analytical methods, virus titers by tissue culture infective dose and D-antigen ELISA, had a relative high variation compared to the yield variations (Chapter 3). Operating conditions of batches with high product yields could thus not be identified. The MVDA did however allow robustness analysis, assessment of the impact of equipment change and identification of batches deviating from the normal.

Knowledge on the existing production process for the current process developers was, however, revived. Not only the analysis but also the data acquisition itself gave an impulse on the process knowledge. Within the exercise, many aspects of manufacturing were disclosed; from the type of measurements done at each processing step to the variation in them; and the process changes and deviations that have occurred to the choices that were made in the past. Follow ups on the MVDA include improvement of analytics (Chapter 4) and introduction of Shewhart control charts, at manufacturing, to closely follow the identified critical production parameters.

Scale-down models for new process developments

Based on the data acquired during the MVDA a lab-scale model representing the manufacturing process was setup. Following the guidelines for scale-down, selections on equipment and operational setting were made resulting in a full set of unit operations required to make monovalent bulks for IPV (Chapter 5). A perfect scale-down model is one that not only operates comparably to manufacturing at setpoint but one where the response of changes of key operating parameters is similar (Rathore et al. 2005b). This means that when new operating conditions are selected at lab-scale they can be directly translated to production scale resulting is a similar process. Due to the unavailability of data at large scale, the scale-down model could only be made at setpoints. This is a common problem in industrial settings as performing the necessary experiments at large-scale is too expensive. The development of a full scale-down model should be an iterative process where deviations occurring at manufacturing scale are mimicked at lab-scale (Li et al. 2006). The scale-down model can subsequently be tweaked based on the newly available data. With the scale-down model set, process development is up to current standards and can accommodate IPV related manufacturing questions and changes to support the drug master file.

In parallel, the scale-down model also can be used as a platform to develop similar vaccine production processes with a higher success rate as scale-up is more straightforward because the large scale counterparts already exists. Both the upstream processing (USP) unit operations, which are in place for adherent Vero cell culture, as the downstream processing (DSP) unit operations representing normal and tangential flow filtrations as

well as chromatography units are valuable for new development projects. One can think of the process development of alternative IPV, either based on the attenuated Sabin strains (Chapter 7) or newly designed attenuated PV (Macadam et al. 2006; Mueller et al. 2006; Vignuzzi et al. 2008). As Vero cells are susceptible to a whole range of viruses, other vaccine production processes based on Vero cells may also be developed using the available scale-down model. Among the viruses Vero cells are susceptible to are *Flaviviridae* (Dengue, Yellow Fever, West Nile or Japanese Encephalitis) *Rhabdoviridae* (Rabies), *Reoviridae* (Rotavirus), *Rubiviridae* (Rubella) or *Paramyxoviridae* (Measles or Respiratory Syncytial virus). The production process for rabies vaccine for instance closely resembles the IPV production process. To prepare rabies vaccine, the virus is propagated on Vero cells, concentrated, inactivated and purified by chromatography using the DEAE-sepharose CL-6B resin (Prem Kumar et al. 2005).

Viruses can be very diverse; they come in all shapes and sizes (up to 1 µm (Philippe et al. 2013)), can have different types of genetic material and can be enveloped or non-enveloped. Resulting, the chosen DSP methods for virus purification in production processes are very different. Often, for the initial purification of viruses, the preferred unit operation is gradient centrifugation, mostly using sucrose gradients. This method is chosen as it is reasonably straightforward with a high success rate. Using gradient centrifugation offers the availability of purified virus which is necessary for characterization, aiding in selection of other possible purification methods, and assay development, required both for the studies on process development as defining release criteria and development of QC tests. While gradient centrifugation can be done batch wise, the use of continuous gradient centrifugation is favoured at large scale. To further be able to quickly design an initial (proof-of–concept) vaccine production process the available scale-down unit operations should be expanded with a continuous centrifugal unit operation for gradient centrifugation that is readily scalable to manufacturing. This addition would provide a full platform to accommodate the development of new vaccine production processes within a limited time frame.

IPV v2.0 – Yield

A new IPV (v2.0), from attenuated Sabin strains (referred to as sIPV), was produced at manufacturing scale based on the existing cIPV process (Chapter 7). The chosen timelines were such that only limited process development, after an initial proof of principle study, could be done prior to the production of clinical lots. Studies focused on i) virus cultivation conditions: the multiplicity of infection and the temperature; and ii) the selection of the ion exchange chromatography (IEX) resin combined with a lower molarity of the elution buffer. Although research prior to manufacturing was limited we were surprised with the low yields that were observed for Sabin PV type 2. These low yields were mainly attributed

to low recoveries during purification. The lowest recovery was found during IEX. While for Sabin PV type 1 and 3 high recoveries were observed (99.5%), for Sabin PV type 2 only 28% of the product was retrieved (Chapter 7).

To explain the differences in the observed recoveries follow-up studies were based on product characterization. A method to determine the isoelectric point (p*I*), the pH value at which the net charge on the molecule is zero, for polioviruses was setup (Chapter 8) since IEX is a process based on the charge of the molecules passing through a charged matrix. The difference in the products p*I* and the pH conditions during processing is pivotal. When the pH is similar to the p*I* the product will aggregate. Moreover the IEX column is chosen to bind negatively charged molecules while the PV flows through. The p*I* of Sabin PV type 2 was determined to be 7.2. During chromatography a pH of 7.0 is used both to equilibrate the column as for the elution buffer. The small difference in the p*I* of Sabin PV type 2 with the buffer pH could have resulted in aggregation of the PV. This aggregation will result in product losses during the chromatography. In addition, unwanted product binding was observed for Sabin PV type 2. This is related to the aggregation; self-aggregated PV is strongly negatively charged (Vrijsen et al. 1983) and thus binds to the positively charged IEX resin. While PV-resin binding may be expected for Sabin PV type 3, with a p*I* of 6.3 thus resulting in a PV with a weak negative charge as pH> p*I* it was only observed for Sabin PV type 2. Remarkably all wild type PV also are weakly negatively charged during IEX (p*I*s were 6.2, 6.7 and 5.8 for type 1, 2 and 3 respectively) and no product-matrix interactions have been observed in the past. It therefore seems that the main cause for the low recoveries of Sabin PV type 2 is self-aggregation. Optimization of the purification should be focused on preventing the aggregation. In addition, the downstream processing for the three serotypes of sIPV may need to be optimized for the serotypes individually resulting in virus specific production settings.

When the new viruses had been better characterized prior to process development and full scale manufacturing the low yields for Sabin PV type 2 probably would have been predicted. Product characterization especially related to physical features like size, p*I*, hydrophobicity or density, but also quality (or potency) aspects, is essential for process development and should go hand in hand with process development.

IPV v2.0 – Biosafety and Immunogenicity goals

The prepared clinical lots met all release criteria and despite the low yields discussed in the previous paragraph sufficient material was prepared for phase I clinical studies. Pre-clinical studies with sIPV were done to assess vaccine safety and vaccine immunogenicity. These studies using animal models are required prior to studies in human. The repeated dose and local tolerance toxicity in rabbits showed vaccine safety was comparable to cIPV.

Furthermore, the studies on immunogenicity illustrated that sIPV can elicit an immune response comparable to cIPV (Chapter 7). Recently, the corresponding phase I study in healthy male adults (first in human) has been reported (Verdijk et al. 2013). The study was done to assess vaccine safety and tolerability (local and systemic reactions) upon intramuscular injection with sIPV or adjuvanted sIPV. Reported side effects were mild or moderate and transient. This is comparable to the side effects observed when vaccinated with cIPV. Moreover, in all subjects, an increase in antibody titer for all types of poliovirus (both Sabin and wild type strains) was observed 28 days after vaccination. sIPV as a booster dose was equally immunogenic as cIPV (Verdijk et al. 2013). The follow up studies, phase II/III, which are required prior to market introduction will be done after technology transfer to partners in low- and middle income countries. The essential process optimizations to obtain an economically feasible process (see below) can be implemented prior to these studies.

While vaccine safety is pivotal, the development of an sIPV was done to increase biosafety during the production process. Although Sabin PV are attenuated viruses, they are genetically unstable and may revert to infectious PV which possess the same neurovirulence and transmission properties as wild-type PV. Regarding the production process, this might occur during virus culture where new PV are produced (Taffs et al. 1995). To minimize the mutations in the Sabin PV during virus cultures, virus seed lots closest possible to the Sabin original were prepared (Chapter 2). In addition, a low virus culture temperature has been applied (Chapter 2 & 7). Genetic stability of the virus seed lots has been assessed by the monkey neurovirulence test, the so-called golden standard, as well as by RCT40 (reproductive capacity at. 40˚C) and MAPREC (mutant analysis by PCR and restriction enzyme cleavage). The genetic stability of the PV obtained after virus culture during the production of monovalent bulk has been assessed by RCT40 and MAPREC. All tests results were within specification concluding that the production process was biosafe. These results show that the upgrade form cIPV to sIPV was successful in terms of biosafety and product quality.

How affordable is IPV v2.0?

The reason to develop an IPV v2.0 was not only to have a more biosafe production process but to have an IPV which would be affordable for low- and middle income countries. Current cIPV cost prices range from $2.25 to $4.14 per dose (Unicef 2012). A cost analysis using the BioSolve software (v3.0) (Biopharm Services Ltd., Chesham, UK) for the sIPV was performed.

BioSolve is an Excel-based tool with which the cost of good based on the overheads of the facility and the operating costs of the process can be calculated. The facility overhead

consists of capital charges, taxes, and insurance. The operating costs of the process are the direct costs and include materials, labour, and waste management. The cost model is defined by describing a process definition including for example USP and DSP unit operations, process scale (equipment sizing), product titer, resource allocation. A cost database, which is built with data consisting of benchmarking information of among others equipment and materials, is coupled to calculate costs for the process. Together with the required utilities the manufacturing cost of goods can be determined.

The complete sIPV manufacturing process (Figure 1) was described to calculate the manufacturing costs per dose, assess the costs drivers, and identify targets for cost price reduction. Prior to analysis of the calculated manufacturing costs for sIPV the cost model was justified using data on cIPV manufacturing at 2×1,000-L bioreactor scale (based on data from chapter 5). The calculated cost of goods were in good agreement with those reported recently (Lopes et al. 2013). It was subsequently concluded that the model was correct and suitable to analyse the manufacturing costs for sIPV produced at 700-L scale (2×350-L bioreactors). As expected, based on the relatively low recoveries for Sabin PV type 2, the calculated costs of goods of sIPV indicate the requirement for process optimizations to reduce the costs of goods for a more cost competitive sIPV product.

To assess the main cost drivers for this process a cost breakdown was worked out. The cost breakdown was done using the following categories: i) capital; ii) materials; iii) labour; and iv) other. Capital costs were estimated based on the installed process, both unit operations as required containers, and general equipment that was used. In addition the costs for a new to build cGMP facility, its installations and validation were taken along. Material costs include for example media costs based on in house media preparation and listings for the primary raw materials in addition to costs for filters and reusable chromatography resins. A labour headcount was estimated based on the allocated time for batch productions. Also labour costs for logistics and QC, QA were included. Other costs reflect costs for waste management, maintenance and utilities. The cost breakdown for Sabin PV type 2 monovalent bulk production is depicted in Figure 2. Calculations for the production of type 1 and 3 monovalent bulks resulted in a similar cost breakdown.

A major part of the manufacturing costs could be attributed to capital. The relative contribution of capital investment can be lowered by increasing the production scale (here 2×350-L bioreactors). This will also lower relative contribution of the costs for labour. The most important target for manufacturing cost reduction however, is the low recovery for Sabin PV type 2. In addition, optimization of the USP, i.e. cell and virus culture, to increase product titers also will lower the cost price.

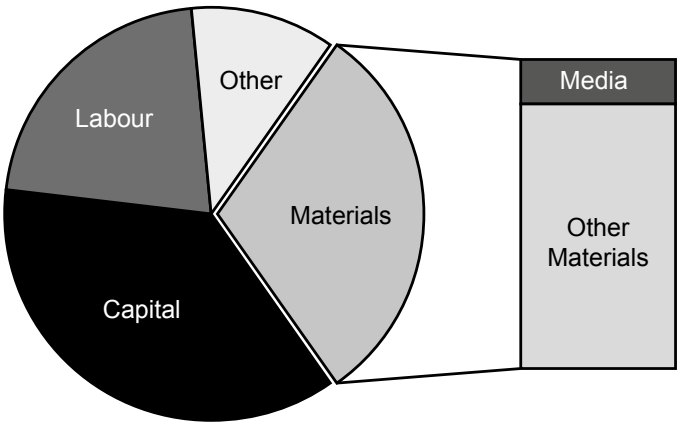

Figure 2. Cost breakdown of manufacturing costs for the production of Sabin PV type 2 monovalent bulk. Largest costs are represented by capital. Media costs (here serum containing cell culture media) attribute approximately 5% of total costs.

IPV v2.x: Cost price reduction

On several aspects of the production process improvements can be envisaged. To increase the yield of the total production process both an increase in PV, or D-antigen units, per bioreactor volume as well as reduction of the losses during purification can be tackled. In chapter 9, optimization of the cell and virus culture is described. Several cell culture methods, batch, semi-batch, perfusion and recirculation, have been tested for their capacity on increased cell numbers and the impact on the virus yields have been assessed. In addition, these studies have been carried out using an animal component free (ACF) medium for both the cell and the virus culture. The use of an animal component free medium in the standard batch cultivation could increase the PV yield approximately 1.5 times (Chapter 9). Alternative cell culture methods to obtain high cell density cultures resulted in an even higher product yields up to 3 times (Chapter 9). While the highest PV yield was obtained with a cell culture in recirculation mode, it was considered not the most practical method at large scale. The semi-batch cell culture using ACF media was selected as the most appropriate method to apply during cell culture to increase PV yields.

Using the developed cost model, the implication of the introduction of ACF media and/or semi-batch cultivations on the sIPV manufacturing costs (at 2×350-L scale) was calculated. In Figure 3, the cost reduction compared to the base case described in the previous paragraph is illustrated. The manufacturing costs can be reduced at least by a factor 2 by

changing the cell culture process to a semi-batch culture and using ACF media for cell and virus culture. Other process optimizations should focus on reducing the losses during DSP. Assuming these process optimizations would result in DSP recoveries comparable to cIPV figures the costs of sIPV can be further lowered. With these manufacturing costs, sIPV would be more than cost-competitive. In view of the costs breakdown (Figure 2) reduction of the relative contribution of capital and labour by process scale-up should be considered. A feasible scale for cell – and virus culture would be 1,000-L bioreactors (Montagnon et al. 1983). Increasing the scale to 2×1,000-L bioreactors nearly halves the manufacturing costs for the USP and DSP optimized process. Even the use of bioreactors up to 6,000-L has been described for Vero cell culture (Barrett et al. 2009) meaning further scale-up can be considered. In Figure 4, the cost breakdown for this 2×1000-L optimized process is given. As can be seen the contribution of both capital and labour is greatly reduced. Main costs for the preparation of monovalent bulks can now be found in the materials, in which 22% are medium costs.

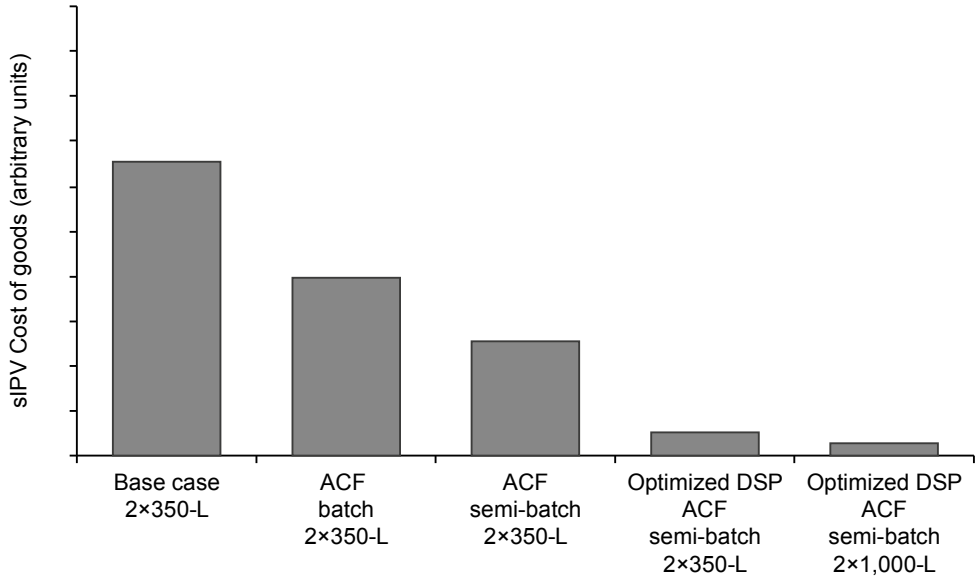

Figure 3. Relative cost of goods for sIPV (at a formulation of plain 10/16/32 DU shd^{-1} for PV type 1, 2 and 3 respectively), corresponding with different production scenarios.

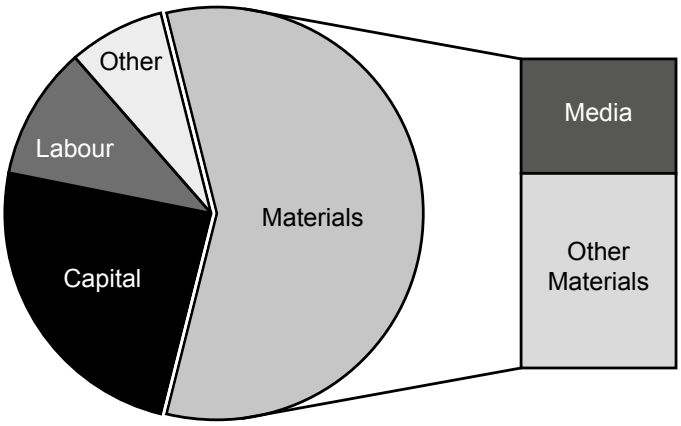

Figure 4. Cost breakdown of manufacturing costs for the production of Sabin PV type 2 monovalent bulk (at 2×1,000-L scale) using the optimized USP (ACF and semi-batch) and DSP process. Largest costs are represented by materials. Media costs contribute 22% of total costs.

Manufacturing costs of sIPV may be further reduced when manufacturing is located in low- and middle income countries. In addition, facility debottlenecking may increase amount of batches that can be produced in a year and so reduce costs. Unit operations that currently have the longest operation time are inactivation and cell and virus culture (Figure 1). Inactivation can easily be done in parallel with other processes. Acquisition of an additional production line for cell and virus culture would optimize the use of the downstream unit operations and so increase the annual facility output. More drastically would be a change in the cell line used for virus production. The use of single cell suspension cell lines may allow for the use of technologies (e.g. perfusion systems) that support increased cell densities. Recently, virus (wild-type) yields obtained on Per.C6 cells have been published to be on average 30-fold higher compared to the yields on Vero cells (Sanders et al. 2013). While these data seem promising, the impact of introducing another cell line than the established Vero cell line will bring about technical, cost- and time-consuming challenges as the Per.C6 cell line is not used in an approved vaccine production process.

Other ways of cost reduction for IPV immunization can be found formulation and delivery. The current sIPV is dosed at 10/16/32 DU shd^{-1}. Vaccine formulations with a lower D-antigen content may results in comparable protective immune response. Whether this is feasible needs to be tested in clinical studies. Alternatively this lower D-antigen content may be adjuvated with for instance aluminium ($Al(OH)_3$) (Chapter 7, (Verdijk et al. 2013)),

monophosphoryl lipid A (MPLA) or oil in water emulsions (e.g. EM030 or SWE02) (Westdijk et al. 2013) to induce a protective immune response.

Instead of a standalone IPV, IPV could also be combined in vaccine formulations. For instance when in a hexavalent vaccine (DTP-HepB-Hib-IPV; diphtheria, tetanus, pertussis, hepatitis B, *Haemophilus influenzae* b, and IPV) together with the other necessary childhood vaccines, costs for administration due to fewer injections (reduce in cold chain costs, syringes, waste management) will go down (Venczel et al. 2009). Moreover, often these combination vaccines make use of adjuvants which in turn might allow the IPV antigen content to be reduced.

A last cost reduction with respect to formulation is the use of multi-dose (for instance 5 or 10 doses) instead of the single-dose vials. Multi-dose vaccine formats can lower production, medical waste disposal, and storage costs per vaccinated individual but may cause clinic-level vaccine wastage or safety issues. In high patient demands, as is realistic with childhood vaccinations, a greater dose is favored with respect to costs (Lee et al. 2010).

Recently studies on intradermal delivery of fractional or reduced doses, i.e. administering a smaller volume of the existing formulation, of cIPV were done (Resik et al. 2010; Resik et al. 2013). The feasibility of fractional doses ($1/5^{th}$) of cIPV given intradermally as an antigen-sparing strategy could be demonstrated (Resik et al. 2010). Moreover, it was shown that intradermal administration of a single fractional ($1/5^{th}$) dose cIPV might be used for priming (Resik et al. 2013). Altogether, it can be said that many different approaches can be followed next to process optimizations to reduce the costs of cIPV and the new, biosafer sIPV.

Currently the technology of the base case sIPV manufacturing is transferred to manufacturers in low- and middle income countries. Depending on their preferred time to market as well as the economic risks they may be willing to take, a selection of the most appropriate method for cost price reduction to have a cost competitive sIPV product needs to be made.

Acknowledgements

I thank Ramona Ursache for the cost calculations.

References

A

Agol VI. 2006. Vaccine-derived polioviruses. Biologicals 34(2):103-108.

Alvarez ME, O'Brien RT. 1982. Mechanisms of inactivation of poliovirus by chlorine dioxide and iodine. Appl. Environ. Microbiol. 44(5):1064-1071.

Aylward B, Tangermann R. 2011. The global polio eradication initiative: Lessons learned and prospects for success. Vaccine 29, Supplement 4:D80-D85.

Aylward BR, Sutter RW, Cochi SL, Thompson KM, Jafari H, Heymann D. 2006. Risk Management in a Polio-Free World. Risk Anal. 26(6):1441-1448.

B

Baca-Estrada M, Griffiths E. 2006. Regulation and standardization of IPV and IPV combination vaccines. Biologicals 34(2):159-61.

Bakker WAM, Thomassen YE, van der Pol LA. 2010. Scale-down approach for animal-free polio vaccine production. In: Noll T, editor. Cells and Culture; Proceedings of the 20th ESACT Meeting, Dresden, Germany, June 17-20, 2007: Springer Netherlands. p 541-550.

Bakker WAM, Thomassen YE, van 't Oever AG, Westdijk J, van Oijen MGCT, Sundermann LC, van 't Veld P, Sleeman E, van Nimwegen FW, Hamidi A and others. 2011. Inactivated Polio Vaccine development for technology transfer using attenuated Sabin poliovirus strains to shift from Salk-IPV to Sabin-IPV. Vaccine 29(41):7188-7196.

Bakker WAM, Thomassen YE, 't Oever AG, Westdijk J, Oijen MGCT, Kersten GFA, Pol LA, Hertroys R, Heuvel N, Hendriks J. 2012. Development of Inactivated Polio Vaccine (IPV) Derived from Attenuated Sabin Strains. Proceedings of the 21st Annual Meeting of the European Society for Animal Cell Technology (ESACT), Dublin, Ireland, June 7-10, 2009. In: Jenkins N, Barron N, Alves P, editors: Springer Netherlands. p 667-670.

Barrett PN, Mundt W, Kistner O, Howard MK. 2009. Vero cell platform in vaccine production: moving towards cell culture-based viral vaccines. Expert Rev. Vaccines 8(5):607-618.

Beale AJ, Ungar J. 1962. Potency and stability of combined pertussis, diphtheria, tetanus, and poliomyelitis (quadruple) vaccine. The Lancet 280(7260):805-808.

Bengtsson S, Philipson L, Persson H, Laurent TC. 1964. The basis for the interaction between attenuated poliovirus and polyions. Virology 24:617-625.

Blüml G. 2007. Microcarrier Cell Culture Technology. In: Pörtner R, editor. Animal Cell Biotechnology: Humana Press. p 149-178.

Bock A, Schulze-Horsel J, Schwarzer J, Rapp E, Genzel Y, Reichl U. 2011. High-density microcarrier cell cultures for influenza virus production. Biotechnol. Prog. 27(1):241-250.

Bodian D. 1951. Immunologic classification of poliomyelitis viruses. I. A cooperative program for the typing of one hundred strains. Am. J. Hyg. 54(2):191-204.

Brioen P, Rombaut B, Boeye A. 1985. Hit-and-run neutralization of poliovirus. J. Gen. Virol. 66 (Pt 11):2495-2499.

Brown DAR, Jones PN, Middleton JC, Papadopoulos G, Arik EB. 2004. Experimental methods. In: Paul EL, Atiemo-Obeng VA, Kresta SM, editors. Handbook of industrial mixing:science and practice. Hoboken: John Wiley & Sons. p 145-201.

Butler M, Medlen AR, Taylor GR. 1985. Electrofocussing of viruses and sensitivity to disinfection. Water Sci. Technol. 17:201-210.

C

Cello J, Paul AV, Wimmer E. 2002. Chemical synthesis of poliovirus cDNA: generation of infectious virus in the absence of natural template. Science 297(5583):1016-1018.

Charaniya S, Hu WS, Karypis G. 2008. Mining bioprocess data: opportunities and challenges. Trends Biotechnol. 26(12):690-699.

Charney J, Machlowitz R, Tytell AA, Sagin JF, Spicer DS. 1961. The concentration and purification of poliomyelitis virus by the use of nucleic acid purification. Virology 15:269-280.

Chaudet N, Roze D, Guillaume JM, Jourdat C. Single-use bioreactor for high density bacterial fermentation: evaluation of the CELL-tainer bioreactor; 2011 in: RPP-6 Conference 16-19 February 2011; Vienna, Austria.

Chen A, Poh SL, Dietzsch C, Roethl E, Yan ML, Ng SK. 2011. Serum-free microcarrier based production of replication deficient influenza vaccine candidate virus lacking NS1 using Vero cells. BMC Biotechnol 11:81.

Chen TR. 1988. Re-evaluation of HeLa, HeLa S3, and HEp-2 karyotypes. Cytogenet. Cell Genet. 48(1):19-24.

Chumakov K, Ehrenfeld E. 2008. New generation of inactivated poliovirus vaccines for universal immunization after eradication of poliomyelitis. Clin. Infect. Dis. 47(12):1587-1592.

Coleman MC, Buck KK, Block DE. 2003. An integrated approach to optimization of Escherichia coli fermentations using historical data. Biotechnol. Bioeng. 84(3):274-285.

Colla La P, Marcialis MA, Mereu GP, Loddo B. 1972. Behaviour of a guanidine-dependent strain of poliovirus 1 in sucrose density and pH gradients. Experientia 28(9):1115-1117.

Croughan MS, Hamel JF, Wang DI. 2006. Hydrodynamic effects on animal cells grown in microcarrier cultures. 1987. Biotechnol. Bioeng. 95(2):295-305.

Crowe BA, Brühl P, Gerencer M, Schwendinger MG, Pilz A, Kistner O, Koelling-Schlebusch K, Aichinger G, Singer J, Zeitlinger M and others. 2010. Evaluation of the cellular

immune responses induced by a non-adjuvanted inactivated whole virus A/H5N1/VN/1203 pandemic influenza vaccine in humans. Vaccine 29(2):166-173.

Cruz HJ, Moreira JL, Carrondo MJT. 2000. Metabolically optimised BHK cell fed-batch cultures. J. Biotechnol. 80(2):109-118.

Cunha CC, Glassey J, Montague GA, Albert S, Mohan P. 2002. An assessment of seed quality and its influence on productivity estimation in an industrial antibiotic fermentation. Biotechnol. Bioeng. 78(6):658-669.

D

De Jesus NH. 2007. Epidemics to eradication: the modern history of poliomyelitis. Virol. J. 4:70.

Doi Y, Abe S, Yamamoto H, Horie H, Ohyama H, Satoh K, Tano Y, Ota Y, Miyazawa M, Wakabayashi K and others. 2001. Progress with inactivated poliovirus vaccines derived from the Sabin strains. Dev. Biol. (Basel) 105:163-169.

Dragunsky EM, Ivanov AP, Wells VR, Ivshina AV, Rezapkin GV, Abe S, Potapova SG, Enterline JC, Hashizume S, Chumakov KM. 2004. Evaluation of immunogenicity and protective properties of inactivated poliovirus vaccines: a new surrogate method for predicting vaccine efficacy. J. Infect. Dis. 190(8):1404-1412.

Duchene M, Peetermans J, D'Hondt E, Harford N, Fabry L, Stephenne J. 1990. Production of poliovirus vaccines: past, present, and future. Viral Immunol. 3(4):243-72.

Duchene M. 2006. Production, testing and perspectives of IPV and IPV combination vaccines: GSK biologicals' view. Biologicals 34(2):163-166.

E

Eggers HJ, Rosenwirth B. 1988. Isolation and characterization of an arildone-resistant poliovirus 2 mutant with an altered capsid protein VP1. Antiviral Res. 9(1-2):23-35.

Ehrenfeld E, Modlin J, Chumakov K. 2009. Future of polio vaccines. Expert Rev. Vaccines. 8(7):899-905.

Eibl R, Kaiser S, Lombriser R, Eibl D. 2010. Disposable bioreactors: the current state-of-the-art and recommended applications in biotechnology. Appl. Microbiol. Biotechnol. 86(1):41-49.

Emini EA, Kao SY, Lewis AJ, Crainic R, Wimmer E. 1983. Functional basis of poliovirus neutralization determined with monospecific neutralizing antibodies. J. Virol. 46(2):466-474.

European agency for the evaluation of Medicinal products/Committee for Proprietary Medicinal Products (EMA/CPMP). 1998. Note for guidance on preclinical pharmacological and toxicological testing of vaccines (CPMP/SWP/465/95, June 1998).

European Pharmacopoeia 6.7 2009 Monograph 0214. Poliomeylitis Vaccine (Inactivated). Strasbourg, France

European Pharmacopoeia 6.3 2009 Monograph 0153. Vaccines for human use. Strasbourg, France.

European Pharmacopoeia 7.0 2010 Monograph 0214. Poliomeylitis Vaccine (Inactivated). Strasbourg, France.

European Pharmacopoeia 7.0. 2011 Monograph 20616. Tests for extraneous agents in viral vaccines for human use. Strasbourg, France.

F

Findlay JW, Dillard RF. 2007. Appropriate calibration curve fitting in ligand binding assays. AAPS J 9(2):E260-267.

Floyd R, Sharp DG. 1978a. Viral aggregation: effects of salts on the aggregation of poliovirus and reovirus at low pH. Appl. Environ. Microbiol. 35(6):1084-1094.

Floyd R, Sharp DG. 1978b. Viral aggregation: quantitation and kinetics of the aggregation of poliovirus and reovirus. Appl. Environ. Microbiol. 35(6):1079-1083.

Floyd R, Sharp DG. 1979. Viral aggregation: buffer effects in the aggregation of poliovirus and reovirus at low and high pH. Appl. Environ. Microbiol. 38(3):395-401.

Food and Drug Administration. 2001. Guidance for industry. Statistical approaches to establishing bioequivalence. Rockville, MD.

Food and Drug Administration. 2004. Guidance for Industry PAT—A framework for innovative pharmaceutical development, manufacturing, and quality assurance. Available from: http://www.fda.gov/downloads/Drugs/GuidanceComplianceRegulatoryInformation/Guidances/UCM070305.pdf [accessed 01.10.2009].

Friede M, Serdobova I, Palkonyay L, Kieny MP. 2009. Technology transfer hub for pandemic influenza vaccine. Vaccine 27(5):631-632.

G

Gabrielsson J, Lindberg N-O, Lundstedt T. 2002. Multivariate methods in pharmaceutical applications. J. Chemometrics 16(3):141-160.

Garnier A, Cote J, Nadeau I, Kamen A, Massie B. 1994. Scale-up of the adenovirus expression system for the production of recombinant protein in human 293S cells. Cytotechnology 15(1-3):145-155.

Genzel Y, Dietzsch C, Rapp E, Schwarzer J, Reichl U. 2010. MDCK and Vero cells for influenza virus vaccine production: a one-to-one comparison up to lab-scale bioreactor cultivation. Appl. Microbiol. Biotechnol. 88(2):461-475.

Glacken MW, Fleischaker RJ, Sinskey AJ. 1986. Reduction of waste product excretion via nutrient control: Possible strategies for maximizing product and cell yields on serum in cultures of mammalian cells. Biotechnol. Bioeng. 28(9):1376-1389.

Glazyrina J, Materne EM, Dreher T, Storm D, Junne S, Adams T, Greller G, Neubauer P. 2010. High cell density cultivation and recombinant protein production with Escherichia coli in a rocking-motion-type bioreactor. Microb. Cell Fact. 9:42-53.

Gnoth S, Jenzsch M, Simutis R, Lubbert A. 2007. Process Analytical Technology (PAT): batch-to-batch reproducibility of fermentation processes by robust process operational design and control. J. Biotechnol. 132(2):180-186.

Godavarti R, Petrone J, Robinson J, Wright R, Kelly BD. 2005. Scale-down models for purification processes: approaches and applications. In: Rathore AS, Sofer G, editors. Process validation in manufacturing of biopharmaceuticals: guidelines, current practices, and industrial case studies: CRC Press.

Goodridge L, Goodridge C, Wu J, Griffiths M, Pawliszyn J. 2004. Isoelectric point determination of norovirus virus-like particles by capillary isoelectric focusing with whole column imaging detection. Anal. Chem. 76(1):48-52.

Gunther JC, Conner JS, Seborg DE. 2007. Fault detection and diagnosis in an industrial fed-batch cell culture process. Biotechnol. Prog. 23(4):851-857.

Hadler SC, Dietz V, Okwe-Bele JM, Cutts FT. 2008. Immunization in developing countries. In: Plotkin SA, Orenstein WA, Offit PA, editors. Vaccines. 5 ed. Philidelphia: WB Saunders. p 1541-1572.

Hanson MA, Brorson KA, Moreira AR, Rao G. 2009. Comparisons of optically monitored small-scale stirred tank vessels to optically controlled disposable bag bioreactors. Microb. Cell Fact. 8:8-44.

Hassell T, Gleave S, Butler M. 1991. Growth inhibition in animal cell culture. The effect of lactate and ammonia. Appl. Biochem. Biotechnol. 30(1):29-41.

Heinsbroek E, Ruitenberg EJ. 2010. The global introduction of inactivated polio vaccine can circumvent the oral polio vaccine paradox. Vaccine 28(22):3778-3783.

Heymann DL, Sutter RW, Aylward RB. 2005. A global call for new polio vaccines. Nature 434(7034):699-700.

Hickling J JR, Nundy N. 2010. Improving the affordability of inactivated poliovirus vaccines (IPV) for use in low- and middle-income countries—an economic analysis of strategies to reduce the cost of routine IPV immunization. PATH and Working in Tandem report. Available from: www.polioeradication.org/content/publications/TS_IPV_econ_analysis.pdf [accessed: 04.10.2010]

Hjertén S, Zhu M-d. 1985. Adaptation of the equipment for high-performance electrophoresis to isoelectric focusing. J. Chromatogr. A 346:265-270.

Hjertén S, Liao JL, Yao KQ. 1987. Theoretical and experimental study of high-performance electrophoretic mobilization of isoelectrically focused protein zones. J. Chromatogr. 387:127-138.

Hogle JM, Chow M, Filman DJ. 1985. Three-dimensional structure of poliovirus at 2.9 A resolution. Science 229(4720):1358-1365.

Hong HA, Ke NT, Nhon TN, Thinh ND, van der Gun JW, Hendriks JT, Kreeftenberg JG. 1996. Validation of the combined toxin-binding inhibition test for determination of neutralizing antibodies against tetanus and diphtheria toxins in a vaccine field study in Viet Nam. Bull. World Health Organ. 74(3):275-282.

Huang H, Yi X, Zhang Y. 2006. Improvement of Vero cell growth in glutamate-based culture by supplementing ammoniagenic compounds. Process Biochem. 41(12):2386-2392.

I

ICH Q8(R2). 2009. Harmonized tripartite guideline on pharmaceutical development. Available from: http://www.ich.org/fileadmin/Public_Web_Site/ICH_Products/Guidelines/Quality/Q8_R1/Step4/Q8_R2_Guideline.pdf [accessed 04.10.2010]

ICH Q9. 2005. Harmonized tripartite guideline on quality risk management. Available from: http://www.ich.org/fileadmin/Public_Web_Site/ICH_Products/Guidelines/Quality/Q9/Step4/Q9_Guideline.pdf [accessed 04.10.2010]

ICH Q10. 2008. Harmonized tripartite guideline on pharmaceutical quality system. Available from: http://www.ich.org/fileadmin/Public_Web_Site/ICH_Products/Guidelines/Quality/Q10/Step4/Q10_Guideline.pdf [accessed 04.10.2010]

ICH Q11. 2012. Harmonized tripartite guideline on development and manufacture of drug substances (chemical entities and biotechnological/biological entities). Available from: http://www.ich.org/products/guidelines/quality/article/quality-guidelines.html [accessed 04.10.2013]

J

Jadhav S, Datla M, Kreeftenberg H, Hendriks J. 2008. The Developing Countries Vaccine Manufacturers' Network (DCVMN) is a critical constituency to ensure access to vaccines in developing countries. Vaccine 26(13):1611-1615.

Jiang SD, Pye D, Cox JC. 1986. Inactivation of poliovirus with beta-propiolactone. J. Biol. Stand. 14(2):103-109.

John J. 2009. Role of injectable and oral polio vaccines in polio eradication. Expert Rev Vaccines 8(1):5-8.

K

Kamen A, Henry O. 2004. Development and optimization of an adenovirus production process. J. Gene Med. 6(S1):S184-S192.

Kersten G, Hazendonk T, Beuvery C. 1999. Antigenic and immunogenic properties of inactivated polio vaccine made from Sabin strains. Vaccine 17(15-16):2059-2066.

Kew OM, Sutter RW, de Gourville EM, Dowdle WR, Pallansch MA. 2005. Vaccine-derived polioviruses and the endgame strategy for global polio eradication. Ann. Rev. Microbiol. 59(1):587-635.

Kirdar AO, Conner JS, Baclaski J, Rathore AS. 2007. Application of Multivariate Analysis toward Biotech Processes: Case Study of a Cell-Culture Unit Operation. Biotechnol. Prog. 23(1):61-67.

Kirdar AO, Green KD, Rathore AS. 2008. Application of Multivariate Data Analysis for Identification and Successful Resolution of a Root Cause for a Bioprocessing Application. Biotechnol. Prog. 24(3):720-726.

Koch F, Koch G. 1985. The molecular biology of poliovirus. Wien: Springer-Verlag.

Korant BD, Lonberg-Holm K. 1974. Zonal electrophoresis and isoelectric focusing of proteins and virus particles in density gradients of small volume. Anal. Biochem. 59(1):75-82.

Kourti T. 2004. Process analytical technology and multivariate statistical process control. Part 1. Process Anal. Technol. 1:13-19.

Kreeftenberg H, van der Velden T, Kersten G, van der Heuvel N, de Bruijn M. 2006. Technology transfer of Sabin-IPV to new developing country markets. Biologicals 34(2):155-158.

Kreeftenberg H, Hamidi A. 2007. Annex 5. Lessons learned in the transfer of Hib conjugate vaccine technology and the consequences for access to this vaccine in developing countries. WHO Meeting Report. Intellectual Property Rights and Vaccines in Developing Countries, April 19–20, 2004. WHO Document WHO/IVB/04.21.

L

Lavery M, Nienow AW. 1987. Oxygen transfer in animal cell culture medium. Biotechnol. Bioeng. 30(3):368-373.

Le Ru A, Jacob D, Transfiguracion J, Ansorge S, Henry O, Kamen AA. 2010. Scalable production of influenza virus in HEK-293 cells for efficient vaccine manufacturing. Vaccine 28(21):3661-3671.

Lee BY, Norman BA, Assi TM, Chen SI, Bailey RR, Rajgopal J, Brown ST, Wiringa AE, Burke DS. 2010. Single versus multi-dose vaccine vials: an economic computational model. Vaccine 28(32):5292-5300.

Levenbook IS, Petricciani JC, Elisberg BL. 1984. Tumorigenicity of Vero cells. J. Biol. Stand. 12(4):391-398.

Lewis JG, Elder PA. 2000. Abbreviated direct and indirect ELISAs: a new and simple format. Clin. Chem. 46(1):137-139.

Li F, Hashimura Y, Pendleton R, Harms J, Collins E, Lee B. 2006. A systematic approach for scale-down model development and characterization of commercial cell culture processes. Biotechnol. Prog. 22(3):696-703.

Liao G, Li R, Li C, Sun M, Li Y, Chu J, Jiang S, Li Q. 2012a. Safety and Immunogenicity of Inactivated Poliovirus Vaccine Made From Sabin Strains: A Phase II, Randomized, Positive-Controlled Trial. J. Infect. Dis. 205(2):237-243.

Liao G, Li Y, Li C. 2012b. The Clinical Trial Protocol for the Inactivated Poliomyelitis Vaccine Made From Sabin Strains (Sabin IPV). Clinicaltrials.gov [internet]: Bethesda (MD): National Library of Medicine (US) 2000-[cited 2013 May 30], Available from http://clinicaltrials.gov/show/NCT01510366 NLM Identifier NCT01510366.

Liao GY, Li R, Li C. 2010. The Clinical Trial Protocol for the Inactivated Poliomyelitis Vaccine Made From Sabin Strains (IPV) (Sabin IPV). Clinicaltrials.gov [internet]: Bethesda (MD): National Library of Medicine (US) 2000-[cited 2010 Oct 04], Available from http://clinicaltrials.gov/show/NCT01056705 NLM Identifier NCT01056705.

Liu Z, Pawliszyn J. 2005. Behaviors of the MS2 virus and related antibodies in capillary isoelectric focusing with whole-column imaging detection. Electrophoresis 26(3):556-562.

Liu Z, Wu SS, Pawliszyn J. 2007. Characterization of plant growth-promoting rhizobacteria using capillary isoelectric focusing with whole column imaging detection. J. Chromatogr. A 1140(1-2):213-218.

Lopes AG, Sinclair A, Titchener-Hooker N. 2013. Inactivated poliovirus vaccine made in modular facilities with single-use technology. BioProcess Int. 11(S9):12-19.

Lycke E, Melen B, Wrange G. 1957. Studies of the inactivation of poliomyelitis virus by formaldehyde. Arch. Gesamte Virusforsch. 7(4):378-383.

Macadam AJ, Ferguson G, Stone DM, Meredith J, Knowlson S, Auda G, Almond JW, Minor PD. 2006. Rational design of genetically stable, live-attenuated poliovirus vaccines of all three serotypes: relevance to poliomyelitis eradication. J. Virol. 80(17):8653-8663.

Mandel B. 1971. Characterization of type 1 poliovirus by electrophoretic analysis. Virology 44(3):554-568.

Mandel B. 1976. Neutralization of poliovirus: a hypothesis to explain the mechanism and the one-hit character of the neutralization reaction. Virology 69(2):500-510.

Manohar M, Orrison B, Peden K, Lewis AM, Jr. 2008. Assessing the tumorigenic phenotype of VERO cells in adult and newborn nude mice. Biologicals 36(1):65-72.

Mao Q, Pawliszyn J. 1999. Capillary isoelectric focusing with whole column imaging detection for analysis of proteins and peptides. J. Biochem. Biophys. Methods 39(1-2):93-110.

Martin EB, Morris AJ. 2002. Enhanced bio-manufacturing through advanced multivariate statistical technologies. J. Biotechnol. 99(3):223-235.

Martin J, Crossland G, Wood DJ, Minor PD. 2003. Characterization of formaldehyde-inactivated poliovirus preparations made from live-attenuated strains. J. Gen. Virol. 84(Pt 7):1781-1788.

Mayer MM, Rapp HJ, Roizman B, Klein SW, Cowan KM, Lukens D, Schwerdt CE, Schaffer FL, Charney J. 1957. The Purification of Poliomyelitis Virus as Studied by Complement Fixation. J. Immunol. 78(6):435-455.

Mendonça RZ, Pereira CA. 1998. Cell metabolism and medium perfusion in VERO cell cultures on microcarriers in a bioreactor. Bioproc. Biosyst. Eng. 18(3):213-218.

Merten OW, Kallel H, Manuguerra JC, Tardy-Panit M, Crainic R, Delpeyroux F, Van der WS, Perrin P. 1999. The new medium MDSS2N, free of any animal protein supports cell growth and production of various viruses. Cytotechnology 30(1-3):191-201.

Michen B, Graule T. 2010. Isoelectric points of viruses. J. Appl. Microbiol. 109(2):388-397.

Michen B, Fritsch J, Aneziris C, Graule T. 2013. Improved virus removal in ceramic depth filters modified with MgO. Environ. Sci. Technol. 47(3):1526-1533.

Milstien JB, Gaule P, Kaddar M. 2007. Access to vaccine technologies in developing countries: Brazil and India. Vaccine 25(44):7610-7619.

Minor PD. 1990. Antigenic structure of picornaviruses. Curr. Top. Microbiol. Immunol. 161:121-154.

Minor P. 2006. Gaps in scientific knowledge for the post eradication world. Biologicals 34(2):167-70.

Minor P. 2009. Vaccine-derived poliovirus (VDPV): Impact on poliomyelitis eradication. Vaccine 27(20):2649-2652.

Mitchell JD, Abhinava K, Griffiths KL, McGarvey B, Seibert KD, Sethuraman S. 2008. Unit Operations Characterization Using Historical Manufacturing Performance. Ind. Eng. Chem. Res. 47(17):6612-6621.

Montagnon BJ, Fanget B, Nicolas AJ. 1981. The large-scale cultivation of VERO cells in micro-carrier culture for virus vaccine production. Preliminary results for killed poliovirus vaccine. Dev. Biol. Stand. 47:55-64.

Montagnon B, Vincent-Falquet JC, Fanget B. 1983. Thousand litre scale microcarrier culture of Vero cells for killed polio virus vaccine. Promising results. Dev. Biol. Stand. 55:37-42.

Montagnon BJ, Fanget B, Vincent-Falquet JC. 1984. Industrial-scale production of inactivated poliovirus vaccine prepared by culture of Vero cells on microcarrier. Rev. Infect. Dis. 6 Suppl 2:S341-S344.

Montagnon BJ, Vincent-Falquet JC. 1998. Experience with the Vero cell line. Dev. Biol. Stand. 93:119-123.

Moreira JL, Cruz PE, Santana PC, Feliciano AS, Lehmann J, Carrondo MJT. 1995. Influence of power input and aeration method on mass transfer in a laboratory animal cell culture vessel. J. Chem. Technol. Biotechnol. 62(2):118-131.

Morgan JF, Morton HJ, Parker RC. 1950. Nutrition of animal cells in tissue culture; initial studies on a synthetic medium. Proc. Soc. Exp. Biol. Med. 73(1):1-8.

Mueller S, Papamichail D, Coleman JR, Skiena S, Wimmer E. 2006. Reduction of the rate of poliovirus protein synthesis through large-scale codon deoptimization causes attenuation of viral virulence by lowering specific infectivity. J. Virol. 80(19):9687-9696.

Murph JR, Grose C, McAndrew P, Mickiewicz C, Mento S, Cano F, Radick L, Ritchey M, Stout MG. 1988. Sabin inactivated trivalent poliovirus vaccine: first clinical trial and seroimmunity survey. Pediatr. Infect. Dis. J. 7(11):760-765.

Murray JP, Parks GA. 1980. Polio Virus Adsorption on Oxide Surfaces. Particulates in water. Washington, DC: American Chemical Society. p 97-133.

N

Nadeau I, Jacob D, Perrier M, Kamen A. 2000. 293SF Metabolic Flux Analysis during Cell Growth and Infection with an Adenoviral Vector. Biotechnol. Prog. 16(5):872-884.

Nasser AM, Battagelli D, Sobsey MD. 1992. Isoelectric focusing of hepatitis A virus in sucrose gradients. Isr. J. Med. Sci. 28(1):73.

Nathanson N, Langmuir AD. 1963. The Cutter Incident. Poliomyelitis Following Formaldehyde- Inactivated Poliovirus Vaccination in the United States during the Spring of 1955. Ii. Relationship of Poliomyelitis to Cutter Vaccine. Am. J. Hyg. 78:29-60.

Nienow AW. 2006. Reactor engineering in large scale animal cell culture. Cytotechnology 50(1-3):9-33.

Nkowane BM, Wassilak SG, Orenstein WA, Bart KJ, Schonberger LB, Hinman AR, Kew OM. 1987. Vaccine-associated paralytic poliomyelitis. United States: 1973 through 1984. JAMA 257(10):1335-1340.

O'Brien RT, Newman J. 1979. Structural and compositional changes associated with chlorine inactivation of polioviruses. Appl. Environ. Microbiol. 38(6):1034-1039.

Ogra PL, Okayasu H, Czerkinsky C, Sutter RW. 2011. Mucosal immunity to poliovirus. Exp. Rev. Vaccines 10(10):1389-1392.

Okayasu H, Sutter RW, Czerkinsky C, Ogra PL. 2011. Mucosal immunity and poliovirus vaccines: impact on wild poliovirus infection and transmission. Vaccine 29(46):8205-8214.

Onodera S, Phillips BA. 1987. A novel method for obtaining poliovirus 14 S pentamers from procapsids and their self-assembly into virus-like shells. Virology 159(2):278-287.

Oosterhuis NMG. 1984. Scale-up of bioreactors: a scale-down approach. Delft, the Netherlands: Delft University of Technology. Available from: http://repository.tudelft.nl/view/ir/uuid:03a887b7-8c20-4052-8d6b-7fe76918d7ec/ [accessed 04.10.2010]

Oosterhuis NMG, van den Berg HJ. 2011. How Multipurpose is a Disposable Bioreactor? BioPharm int. 24(3):51-56.

Oosterhuis NMG, van der Heiden P. 2010. Mass Transfer in the CELL-tainer Disposable Bioreactor. In: Noll T, editor. vol;. 4 Cells and Culture: Springer Netherlands. p 371-373.

Perry LA, Montgomery DC, Fowler JW. 2007. A partition experimental design for a sequential process with a large number of variables. Qual. Reliab. Eng. Int. 23(5):555-564.

Petiot E, Fournier F, Geny C, Pinton H, Marc A. 2010a. Rapid screening of serum-free media for the growth of adherent Vero cells by using a small-scale and non-invasive tool. Appl. Biochem. Biotechnol. 160(6):1600-1615.

Petiot E, Guedon E, Blanchard F, Geny C, Pinton H, Marc A. 2010b. Kinetic characterization of vero cell metabolism in a serum-free batch culture process. Biotechnol. Bioeng. 107(1):143-153.

Philippe N, Legendre M, Doutre G, Coute Y, Poirot O, Lescot M, Arslan D, Seltzer V, Bertaux L, Bruley C and others. 2013. Pandoraviruses: amoeba viruses with genomes up to 2.5 Mb reaching that of parasitic eukaryotes. Science 341(6143):281-286.

Pieracci J, Perry L, Conley L. 2010. Using partition designs to enhance purification process understanding. Biotechnol. Bioeng. 107(5):814-824.

Pirt SJ. 1975. Principles of microbe and cell cultivation. Oxford, United Kingdom: Blackwell scientific publication.

Pörtner R, editor. 2007. Animal Cell Biotechnology: Methods and Protocols. 2nd ed. Totowa, New Jersey: Humana Press Inc. 529 p.

Prem Kumar AA, Mani KR, Palaniappan C, Bhau LNR, Swaminathan K. 2005. Purification, potency and immunogenicity analysis of Vero cell culture-derived rabies vaccine: a comparative study of single-step column chromatography and zonal centrifuge purification. Microbes Infect. 7(9–10):1110-1116.

Putnak JR, Phillips BA. 1981. Differences between poliovirus empty capsids formed in vivo and those formed in vitro: a role for the morphopoietic factor. J. Virol. 40(1):173-183.

Quesney S, Marc A, Gerdil C, Giminez C, Marvel J, Richard Y, Meignier B. 2003. Kinetics and metabolic specificities of Vero cells in bioreactor cultures with serum-free medium. Cytotechnology 42(1):1-11.

Racaniello VR. 2007. Field's Virology. 5th ed. Knipe DM, Howley PM, editors. Philidelphia: Lippincott Williams & Wilkins. 3177 p.

Rathore A, Krishnan R, Tozer S, Smiley D, Rausch S, Seely J. 2005a. Scaling down of biopharmaceutical unit operations - Part 2: Chromatography and filtration. BioPharm Int. 18(4):58-64.

Rathore A, Krishnan R, Tozer S, Smiley D, Rausch S, Seely J. 2005b. Scaling down of biopharmaceutical unit operations - Part I: Fermentation. BioPharm Int. 18(3):60-68.

Resik S, Tejeda A, Lago PM, Diaz M, Carmenates A, Sarmiento L, Alemani N, Galindo B, Burton A, Friede M and others. 2010. Randomized controlled clinical trial of fractional doses of inactivated poliovirus vaccine administered intradermally by needle-free device in Cuba. J. Infect. Dis. 201(9):1344-52.

Resik S, Tejeda A, Sutter RW, Diaz M, Sarmiento L, Alemani N, Garcia G, Fonseca M, Hung LH, Kahn AL and others. 2013. Priming after a fractional dose of inactivated poliovirus vaccine. N. Engl. J. Med. 368(5):416-24.

Ringner M. 2008. What is principal component analysis? Nat. Biotechnol. 26(3):303-304.

Rombaut B, Vrijsen R, Boeye A. 1989. Denaturation of poliovirus procapsids. Arch. Virol. 106(3-4):213-220.

Rourou S, van der Ark A, van der Velden T, Kallel H. 2007. A microcarrier cell culture process for propagating rabies virus in Vero cells grown in a stirred bioreactor under fully animal component free conditions. Vaccine 25(19):3879-3889.

Rourou S, van der Ark A, van der Velden, Kallel H. 2009a. Development of an animal-component free medium for vero cells culture. Biotechnol. Prog. 25(6):1752-1761.

Rourou S, van der Ark A, Majoul S, Trabelsi K, van der Velden T, Kallel H. 2009b. A novel animal-component-free medium for rabies virus production in Vero cells grown on Cytodex 1 microcarriers in a stirred bioreactor. Appl. Microbiol. Biotechnol. 85(1):53-63.

Sabin AB, Boulger LR. 1973. History of Sabin attenuated poliovirus oral live vaccine strains. J. Biol. Stand. 1(2):115-118.

Sabin AB. 1985. Oral poliovirus vaccine: history of its development and use and current challenge to eliminate poliomyelitis from the world. J. Infect. Dis. 151(3):420-436.

Sakoe H, Chiba S. 1978. Dynamic programming algorithm optimization for spoken word recognition. IEEE Trans. Acoust., Speech, Signal Process. 26(1):43-49.

Salk D, Salk J. 1984. Vaccinology of poliomyelitis. Vaccine 2(1):59-74.

Salk JE. 1953. Studies in human subjects on active immunization against poliomyelitis. I. A preliminary report of experiments in progress. J. Am. Med. Assoc. 151(13):1081-1098.

Salk JE, Bazeley PL, Bennett BL, Krech U, Lewis LJ, Ward EN, Youngner JS. 1954. Studies in human subjects on active immunization against poliomyelitis. II. A Practical Means for Inducing and Maintaining Antibody Formation. Am. J. Public Health Nations Health 44(8):994-1009.

Sanders BP, Edo-Matas D, Custers JHHV, Koldijk MH, Klaren V, Turk M, Luitjens A, Bakker WAM, Uytdehaag F, Goudsmit J and others. 2013. PER.C6® cells as a serum-free suspension cell platform for the production of high titer poliovirus: A potential low cost of goods option for world supply of inactivated poliovirus vaccine. Vaccine 31(5):850-856.

Sangrujee N, Caceres VM, Cochi SL. 2004. Cost analysis of post-polio certification immunization policies. Bull. World Health Organ. 82(1):9-15.

Sawyer LA, Wood D, Ferguson M, Crainic R, Beuvery EC, McInnis J, Albrecht P. 1997. Potency of wild-type or sabin trivalent inactivated poliovirus vaccine, by enzyme-linked immunosorbent assay using monoclonal antibiotics specific for each antigenic site. Biologicals 25(3):299-306.

Schmidt FR. 2005. Optimization and scale up of industrial fermentation processes. Appl. Microbiol. Biotechnol. 68(4):425-35.

Schneider M, Marison IW, von Stockar U. 1996. The importance of ammonia in mammalian cell culture. J. Biotechnol. 46(3):161-185.

Schouwenberg JE, Velden-de Groot T, Blueml G. 2010. Vaccine Production Utilizing the Potential of Microcarriers in Disposable Bioreactor. In: Noll T, editor. Cells and Culture vol 4: Springer Netherlands. p 795-801.

Schuirmann DJ. 1987. A comparison of the two one-sided tests procedure and the power approach for assessing the equivalence of average bioavailability. J. Pharmacokinet. Biopharm. 15(6):657-680.

Sharp DG, Leong J. 1980. Inactivation of poliovirus I (Brunhilde) single particles by chlorine in water. Appl. Environ. Microbiol. 40(2): 381-385.

Shen Y, Berger SJ, Smith RD. 2000. Capillary isoelectric focusing of yeast cells. Anal. Chem. 72(19):4603-4607.

Simizu B, Abe S, Yamamoto H, Tano Y, Ota Y, Miyazawa M, Horie H, Satoh K, Wakabayashi K. 2006. Development of inactivated poliovirus vaccine derived from Sabin strains. Biologicals 34(2):151-154.

Singh V. 1999. Disposable bioreactor for cell culture using wave-induced agitation. Cytotechnology 30(1-3):149-158.

Sutter RW, John TJ, Jain H, Agarkhedkar S, Ramanan PV, Verma H, Deshpande J, Singh AP, Sreevatsava M, Malankar P and others. 2010. Immunogenicity of bivalent types 1 and 3 oral poliovirus vaccine: a randomised, double-blind, controlled trial. Lancet 376(9753):1682-1688.

Sweere APJ, Luyben KC, Kossen NWF. 1987. Regime analysis and scale-down: Tools to investigate the performance of bioreactors. Enz. Microb. Technol. 9(7):386-398.

T

Taffs RE, Chumakov KM, Rezapkin GV, Lu Z, Douthitt M, Dragunsky EM, Levenbook IS. 1995. Genetic Stability and Mutant Selection in Sabin 2 Strain of Oral Poliovirus Vaccine Grown under Different Cell Culture Conditions. Virology 209(2):366-373.

Tanimoto T, Murashige N, Hosoda M, Kusumi E, Ono S, Kami M, Shibuya K. 2012. Vaccination for whom? Time to reinvigorate Japanese vaccine policy. Lancet 380(9854):1647.

Tano Y, Shimizu H, Martin J, Nishimura Y, Simizu B, Miyamura T. 2007. Antigenic characterization of a formalin-inactivated poliovirus vaccine derived from live-attenuated Sabin strains. Vaccine 25(41):7041-7046.

Taylor DH, Moore RS, Sturman LS. 1981. Influence of pH and electrolyte composition on adsorption of poliovirus by soils and minerals. Appl. Environ. Microbiol. 42(6):976-984.

ten Have R, Thomassen YE, Hamzink MRJ, Bakker WAM, Nijst OEM, Kersten G, Zomer G. 2012. Development of a fast ELISA for quantifying polio D-antigen in in-process samples. Biologicals 40(1):84-87.

Thomassen YE, van Sprang ENM, van der Pol LA, Bakker WAM. 2010. Multivariate data analysis on historical IPV production data for better process understanding and future improvements. Biotechnol. Bioeng. 107(1):96-104.

Thomassen YE, van der Welle JE, van Eikenhorst G, van der Pol LA, Bakker WAM. 2012. Transfer of an adherent Vero cell culture method between two different rocking motion type bioreactors with respect to cell growth and metabolic rates. Process Biochem. 47(2):288-296.

Thomassen YE, van 't Oever AG, Van Oijen MGCT, Wijffels RH, Van der Pol LA, Bakker WAM. 2013a. Next generation inactivated polio vaccine manufacturing to support post polio-eradication biosafety goals. PLoS ONE 8(12):e83374

Thomassen YE, van 't Oever AG, Vinke M, Spiekstra A, Wijffels RH, van der Pol LA, Bakker WAM. 2013b. Scale-down of the inactivated polio vaccine production process. Biotechnol. Bioeng. 110(5):1354-1365.

Toriniwa H, Komiya T. 2007. Japanese encephalitis virus production in Vero cells with serum-free medium using a novel oscillating bioreactor. Biologicals 35(4):221-226.

Trabelsi K, Rourou S, Loukil H, Majoul S, Kallel H. 2005. Comparison of various culture modes for the production of rabies virus by Vero cells grown on microcarriers in a 2-l bioreactor. Enz. Microb. Technol. 36(4):514-519.

Trabelsi K, Rourou S, Loukil H, Majoul S, Kallel H. 2006. Optimization of virus yield as a strategy to improve rabies vaccine production by Vero cells in a bioreactor. J. Biotechnol. 121(2):261-271.

Unicef. 2012. Current IPV supply and recent tender results & outlook for the future. Available from: http://www.unicef.org/supply/index_66260.html [accessed 04.10.2013]

van 't Riet K, Tramper J. 1991. Basic bioreactor design. New York: Marcel Dekker, Inc.

van der Heiden P, Buevink M, Oosterhuis NMG; CELLUTION BIOTECH B.V. (Veendam, NL), assignee. 2008. Method and apparatus for cultivating cells utilizing wave motion. US Patent US20080160597.

van der Velden-de Groot CAM. 1995. Microcarrier technology, present status and perspective. Cytotechnology 18(1-2):51-56.

van Hemert P, Kilburn DG, van Wezel AL. 1969. Homogeneous cultivation of animal cells for the production of virus and virus products. Biotechnol. Bioeng. 11(5):875-85.

van Noort RB. 1992. The Children's Vaccine Initiative and vaccine supply: the role of the public sector. Vaccine 10(13):909-910.

van Steenis G, van Wezel AL, Sekhuis VM. 1981. Potency testing of killed polio vaccine in rats. Dev. Biol. Stand. 47:119-128.

van Wezel AL. 1967. Growth of cell-strains and primary cells on micro-carriers in homogeneous culture. Nature 216(5110):64-65.

van Wezel AL. 1972. New trends in the preparation of cell substrates for the production of virus vaccines. Prog. Immunobiol. Stand. 5:187-192.

van Wezel AL. 1973. Microcarrier cultures of animal cells. Tissue culture, methods and applications VII Cell propagations on culture supports. New York and London: Academic press. p 372-376.

van Wezel AL, van Steenis G, Hannik CA, Cohen H. 1978. New approach to the production of concentrated and purified inactivated polio and rabies tissue culture vaccines. Dev. Biol. Stand. 41:159-168.

Van Wezel AL, van der Velden-de Groot CAM. 1978. Large scale cultivation of animal cells in microcarrier culture. Process Biochem. 13(3):6-8.

van Wezel AL, van Herwaarden JA, van de Heuvel-de Rijk EW. 1979. Large-scale concentration and purification of virus suspension from microcarrier culture for the preparation of inactivated virus vaccines. Dev. Biol. Stand. 42:65-69.

van Wezel AL, van der Velden-de Groot CA, van Herwaarden JA. 1980. The production of inactivated poliovaccine on serially cultivated kidney cells from captive-bred monkeys. Dev. Biol. Stand. 46:151-158.

van Wezel AL. 1981. Present state and developments in the production of inactivated poliomyelitis vaccine. Dev. Biol. Stand. 47:7-13.

van Wezel AL, van der Marel P, van Beveren CP, Verma I, Salk PL, Salk J. 1981. Detection and elimination of cellular nucleic acids in biologicals produced on continuous cell lines. Dev. Biol. Stand. 50:59-69.

van Wezel AL, van Steenis G, van der Marel P, Osterhaus AD. 1984. Inactivated poliovirus vaccine: current production methods and new developments. Rev. Infect. Dis. 6 Suppl 2:S335-S340.

van Wezel AL. 1985. Monolayer growth systems: homogeneous unit processes. In: Spier RE, Griffith JB, editors. Animal Cell Biotechnology. London: Academic Press. p 265-282.

Venczel L, Landry S, Aylward B, Sutter R, Sabow A, Smith G. 2009. Global post-eradication IPV supply and demand assessment: integrated findings commissioned by the Bill & Melinda Gates Foundation and prepared by Oliver Wyman Inc. Available from www.polioeradication.org/content/publications/SupplyLandscapeEconomics.09.06.2010.pdf [accessed 04.10.2010].

Verdijk P. 2012. Safety and Immunogenicity of a New Inactivated Polio Vaccine in Healthy Adults. In: Clinicaltrials.gov [internet]: Bethesda (MD): National Library of Medicine (US) 2000-[cited 2013 may 30], Available from http://clinicaltrials.gov/show/NCT01708720 NLM Identifier: NCT01708720.

Verdijk P, Rots NY, Van Oijen MGCT, Oberste MS, Boog CJ, Okayasu H, Sutter RW, Bakker WA. 2013. Safety and Immunogenicity of inactivated poliovirus vaccine based on Sabin strains with and without aluminum hydroxide: a phase I trial in healthy adults. Vaccine 31(47):5531-5536.

Vidor E, Meschievitz C, Plotkin S. 1997. Fifteen years of experience with Vero-produced enhanced potency inactivated poliovirus vaccine. Pediatr. Infect. Dis. J. 16(3):312-322.

Vidor E, Plotkin SA. 2013. Poliovirus vaccine-inactivated. In: Plotkin SA, Orenstein WA, Offit PA, editors. Vaccines. 6th ed: Elsevier.

Vignuzzi M, Wendt E, Andino R. 2008. Engineering attenuated virus vaccines by controlling replication fidelity. Nat. Med. 14(2):154-161.

Vrijsen R, Rombaut B, Boeye A. 1983. pH-dependent aggregation and electrofocusing of poliovirus. J. Gen. Virol. 64 (Pt 10):2339-2342.

W

Wahl A, Sidorenko Y, Dauner M, Genzel Y, Reichl U. 2008. Metabolic flux model for an anchorage-dependent MDCK cell line: characteristic growth phases and minimum substrate consumption flux distribution. Biotechnol. Bioeng. 101(1):135-152.

Ward RL. 1978. Mechanism of poliovirus inactivation by ammonia. J. Virol. 26(2):299-305.

Ward RL. 1980. Mechanisms of poliovirus inactivation by the direct and indirect effects of ionizing radiation. Radiat. Res. 83(2):330-344.

Westdijk J, Brugmans D, Martin J, Oever AV, Bakker WA, Levels L, Kersten G. 2011. Characterization and standardization of Sabin based inactivated polio vaccine: Proposal for a new antigen unit for inactivated polio vaccines. Vaccine 29(18):3390-3397.

Westdijk J, Koedam P, Barro M, Steil BP, Collin N, Vedvick TS, Bakker WAM, van der Ley P, Kersten G. 2013. Antigen sparing with adjuvanted inactivated polio vaccine based on Sabin strains. Vaccine 31(9):1298-1304.

WHO. 1999. Recommendations for the production and control of Poliomyelitis Vaccine, Oral; Revised 1999 TRS 904, Annex 1. Geneva: World Health Organization.

WHO. 2002a. Recommendations for the production and control of poliomyelitis vaccine (inactivated). Annex 2 Technical report series No.910 Geneva: World Health Organization.

WHO Expert committee on Biological Standardization. 2002b. Recommendations for the production and control of poliomyelitis vaccine (oral). Fifthied report. Technical report series No.904 World Health Organization 31-93.

WHO. 2004. Guidelines for the safe production and quality control of inactivated poliomyelitis vaccine manufactured from wild polioviruses (Addendum, 2003, to the Recommendations for the Production and Quality Control of Poliomyelitis Vaccine (Inactivated)). Annex 2 Technical report series No.926: 65-89

WHO. 2009. WHO global action plan to minimize poliovirus facility-associated risk after eradication of wild polioviruses and cessation of routine OPV use. Available from:

http://www.polioeradication.org/content/publications/GAPIIIWORKINGDRAFT_07.pdf [accessed 16.09.2013].

WHO. 2010a Global polio eradication initiative – strategic plan 2010–2012. Available from: http://www.polioeradication.org/content/publications/GPEI.StrategicPlan.2010-2012.ENG.May.2010.pdf [accessed: 04.10.2010]

WHO. 2010b. Polio vaccines and polio immunization in the pre-eradication era: WHO position paper--recommendations. Vaccine 28(43):6943-6944.

WHO. 2012a. Recommendations to assure the quality, safety and efficacy of live attenuated poliomyelitis vaccine (oral). Replacement of TRS 904, annex 1 and addendum TRS 910, annex 1.

WHO. 2012b. Global polio eradication initiative. Poliomyelitis: intensification of the global eradication initiative. Geneva: World Helath Organization. Available from http://apps.who.int/gb/ebwha/pdf_files/WHA66/A66_18-en.pdf [accessed 01.07.2013].

WHO. 2013a. Meeting of the Strategic Advisory Group of Experts on Immunization, November 2012 - conclusions and recommendations. Wkly. Epidemiol. Rec. 88(1):1-16.

WHO. 2013b. The "Stop transmission of Polio (STOP)" programme of the Global Polio Eradication Initiative, 1999-2013. Wkly. Epidemiol. Rec. 88(25):257-260.

WHO 2013c. Global polio eradication initiative. Polio Eradication & Endgame Strategic Plan 2013-2018. Geneva: WHO. Available from http://www.polioeradication.org/Resourcelibrary/Strategyandwork.aspx [accessed 04.10.2013]

Widjojoatmodjo MN, Boes J, van Bers M, van Remmerden Y, Roholl PJ, Luytjes W. 2010. A highly attenuated recombinant human respiratory syncytial virus lacking the G protein induces long-lasting protection in cotton rats. Virol. J. 7:114-123.

Wimmer E, Hellen CU, Cao X. 1993. Genetics of poliovirus. Annu. Rev. Genet. 27:353-436.

Wold S, Sjöström M, Eriksson L. 2001. PLS-regression: a basic tool of chemometrics. Chemometr. Intell. Lab. Syst. 58(2):109-130.

Wood DJ, Heath AB, Sawyer LA. 1995. A WHO Collaborative study on assays of the antigenic content of inactivated poliovirus vaccines. Biologicals 23(1):83-94.

Wood HA, Johnston LB, Burand JP. 1982. Inhibition of Autographa californica nuclear polyhedrosis virus replication in high-density Trichoplusia ni cell cultures. Virology 119(2):245-254.

Wu J, Pawliszyn J. 1994. Application of capillary isoelectric focusing with absorption imaging detection to the analysis of proteins. J. Chromatogr. B: Biomed. Appl. 657(2):327-332.

Yang C, Shi H, Zhou J, Liang Y, Xu H. 2009. CpG oligodeoxynucleotides are a potent adjuvant for an inactivated polio vaccine produced from Sabin strains of poliovirus. Vaccine 27(47):6558-63.

Zerda KS, Gerba CP. 1984. Agarose isoelectrofocusing of intact virions. J. Virol. Methods 9(1):1-6.

Zomer G, Hamzink MRJ. 2009. Development and optimization of a fast and sensitive ELISA for polio D-antigen using a GZ11 based signal reagent. In: Shen X, Yang X-L, Zhang X-R, Cui ZJ, Kricka LJ, Stanley PE, editors. Bioluminescence and chemiluminescence. Singapore: World Scientific Publishing Co. Pte. Ltd. p 291-294.

Zwietering TN. 1958. Suspending of solid particles in liquid by agitators. Chem. Eng. Sci. 8(3-4):244-253.

Summary

The first vaccine against poliovirus (PV), the causative agent of poliomyelitis, was developed in the 1950s by Jonas Salk. The vaccine (IPV) consists of an injected dose of purified and inactivated wild-type PVs (all three serotypes). Soon after this discovery, at the Rijks Instituut voor de Volksgezondheid (RIV) in Bilthoven, an industrial-scale production process for IPV was developed based on micro-carrier technology and primary monkey kidney cells. In the 1970s, the manufacturing of IPV was scaled up to 300-L by the development of well-controlled bioreactors for cell culture, the so-called "Bilthoven Units" (originally used for bacterial fermentations). In 2004, the Vero cell line was introduced to replace the then used tertiary monkey kidney cells followed by a scale-up from 700 to 1,500-L (from two 350-L to two 750-L bioreactors). IPV manufacturing has been part of the regular vaccine manufacturing activities in Bilthoven ever since the establishment of the IPV production process.

With polio eradication on our doorstep, the World Health Organization (WHO) is pursuing a new IPV based on non-wild-type strains to increase the biosafety of vaccine manufacturing. In addition, and due to the pending cessation of oral polio vaccines (OPV), the global demand for affordable IPV is increasing. To accommodate these questions two research programs were started at the Netherlands Vaccine Institute (now Institute for Translational Vaccinology). One concerned optimization of the current conventional IPV production process, the other the manufacturing of an affordable sIPV, an IPV based on the attenuated Sabin PV strains normally used for OPV production. The technology of the sIPV production process, developed in the latter project, is also aimed to be transferred to developing countries manufacturers (Chapter 2).

From the substantial history in polio vaccine production in Bilthoven, a valuable dataset has been generated. Data from over 50 batches at two different production scales (700-L and 1,500-L) were analyzed using multivariate data analysis (MVDA). This statistical method is stimulated by the ICH (International Conference on Harmonization of Technical Requirements for Registration of Pharmaceuticals for Human Use) to improve scientific understanding of production processes for troubleshooting and improved process control. The initial explorative analysis, performed on single unit operations, indicated consistent manufacturing. Known outliers (e.g., rejected batches) were identified using principal component analysis (PCA). The source of operational variation was pinpointed to variation of input such as cell- and virus culture media. Other relevant process parameters were in control and, using this manufacturing data, could not be correlated to product quality attributes. The gained knowledge of the IPV production process, not only from the MVDA, but also from digitalizing the available historical data, has proven to be useful for troubleshooting, understanding limitations of available data and seeing the opportunity for improvements (Chapter 3).

One of the gaps in the data was located in the product quantification during processing. The available assay used for determining the D-antigen concentration in in-process samples had high variability. A so-called fast ELISA was developed and qualified for analysis of polio D-antigen. The original 20h-protocol was optimized by minimizing the total incubation time to 1h, and by replacing the signal reagent 3,3',5,5'-tetramethylbenzidine by a chemiluminogenic signal reagent with a theoretical low intrinsic background and high dynamic range. This fast D-antigen ELISA was suitable for measurement of D-antigen concentrations in the different matrixes present during the different unit-operations in the production process (Chapter 4).

To accommodate research to improve and optimize the current cIPV production process an up-to-date lab-scale version encompassing the legacy inactivated polio vaccine production process was set-up based on the knowledge obtained during the MVDA of historical data. This lab-scale version was designed to be representative of the large scale, meaning a scale-down model, to allow experiments for process optimization that can be readily applied to manufacturing scale. Initially the separate unit operations were scaled-down at setpoint. Subsequently, the unit operations were applied successively in a comparative manner to large-scale manufacturing. This allows the assessment of the effects of changes in one unit operation to the consecutive units at small-scale. The developed scale-down model for cell and virus culture (2.3-L) presents a feasible model with its production scale counterpart (750-L) when operated at setpoint. Also, the scale-down models for the DSP unit operations clarification, concentration, size exclusion chromatography, ion exchange chromatography, and inactivation are in agreement with the manufacturing scale. The small-scale units can be used separately, as well as sequentially, to study variations and critical product quality attributes in the production process. Finally, it has been shown that the scale-down unit operations can be used consecutively to prepare trivalent vaccine at lab-scale with comparable characteristics to the product produced at manufacturing scale (Chapter 5).

The upcoming of disposables in GMP manufacturing triggered the study on alternatives for the clarification unit (Chapter 5) and alternative Wave-type, bioreactors (Chapter 6). This type of bioreactors makes use of sterilized disposable bags, which could be beneficial in a GMP environment, for example to reduce the cleaning validation burden, or to facilitate change-over to another product using the same equipment. Wave-type bioreactors make use of vertical (standard rocking motion-type) or both vertical and horizontal displacement (CELL-tainer® (CELLution Biotech BV)) for mixing instead of an impeller, which is used in stirred tank reactors. Using the design of experiments (DoE) approach, models for the mixing times in both the CELL-tainer® and the BIOSTAT® CultiBag RM (Sartorius Stedim Biotech) bioreactor (standard rocking motion-type) were developed. The conditions for cultivation of Vero cells in the CELL-tainer® bioreactor were

chosen based on comparable mixing times. Vero cells growing adherent to Cytodex 1 microcarriers were cultivated in the CELL-tainer® and in the BIOSTAT® CultiBag RM. Vero cell growth in both bioreactors was comparable with respect to the growth characteristics and main metabolite production and consumption rates. Additionally, poliovirus production in both bioreactors was shown to be similar.

In view of WHOs pursuit towards an IPV manufacturing process with increased biosafety, the development of sIPV was taken up. Prior to large scale production of clinical lots, an initial proof of principle study was done (Chapter 2). Starting from the conventional IPV (cIPV) production process, minimal adaptations, such as lower virus cultivation temperature, were implemented. Also, the selected disposable filter unit (Chapter 5) was implemented. To quickly prepare sIPV clinical lots and show proof-of-principle of sIPV in human, no further process optimization and/or modernization was done. sIPV was produced at industrial scale followed by formulation of both plain and aluminium adjuvanted sIPV (Chapter 7). The final products met the quality criteria, were immunogenic in rats, showed no toxicity in rabbits and could be released for testing in the clinic. While an immunogenic product, both in animals as in humans was prepared, the product yield was extremely low and further process development will be needed to obtain an affordable sIPV.

Especially the yield of Sabin PV type 2 after ion exchange chromatography was low. To determine if this effect could be due to a difference in the isoelectric point (p*I*) of the poliovirus a method for p*I* measurement of live virus was developed (Chapter 8). A method for analyzing biological hazardous components (biological safety level 2) was set up for the capillary isoelectric focusing-whole column imaging detection (CIEF-WCID) analyzer. This method is based on closed circuits. Subsequently, the p*I*'s of complete intact polioviruses were determined. The polioviruses that were analyzed are the commonly used viruses for the production of IPV - Mahoney (type 1), MEF-1 (type 2), and Saukett (type 3) - as well as for OPV - Sabin types 1, 2, and 3. The determined p*I*'s were 6.2 for Mahoney, 6.7 for MEF-1, and 5.8 for Saukett. The p*I*'s of Sabin types 1, 2, and 3 viruses were 7.4, 7.2, and 6.3, respectively. With a p*I* of 7.2, Sabin PV type 2 is prone to self-aggregation at the pH used during chromatography (pH 7.0). Self-aggregation was thus suggested to be the main cause of low product yield and prevention of this self-aggregation was suggested to be the main focus point for process optimization.

Besides optimization of the downstream processing, optimization of the upstream processing, i.e. increased virus yields after cell and virus culture was studied (Chapter 9). Vero cells were grown adherent to microcarriers (Cytodex 1; 3 g L^{-1}) using animal component free media in stirred-tank type bioreactors. Different strategies for media refreshment, daily media replacement (semi-batch), continuous media replacement

(perfusion) and recirculation of media, were compared with batch cultivation. Cell densities increased using a feed strategy from 1×10^6 cells mL^{-1} during batch cultivation to 1.8, 2.7 and 5.0×10^6 cells mL^{-1} during semi-batch, perfusion and recirculation, respectively. The effects of these different cell culture strategies on subsequent poliovirus production were investigated. Increased cell densities allowed up to 3 times higher D-antigen levels when compared with that obtained from batch-wise Vero cell culture. However, the cell specific D-antigen production was lower when cells were infected at higher cell densities. This cell density effect is in good agreement with observations for different cell lines and virus types. From the evaluated alternative culture methods, application of a semi-batch mode of operations allowed the highest cell specific D-antigen production. The increased product yields that can easily be reached using these higher cell density cultivation methods, showed the possibility for better use of bioreactor capacity for the manufacturing of polio vaccines to ultimately reduce vaccine cost per dose. Further, the use of animal-component-free cell- and virus culture media shows opportunities for modernization of human viral vaccine manufacturing.

To assess the affordability of sIPV the manufacturing costs were determined (Chapter 10). The sIPV manufacturing costs, when produced as described in Chapter 7, indicate the requirement for process optimizations. However, the manufacturing costs can be reduced at least a factor 2 when implementing the upstream processing optimization, ACF media and a semi-batch process, as described in Chapter 9. Assuming improvements in downstream processing will result in a process with yields comparable to the cIPV process costs can be further lowered. In addition, a scale-up from two 350-L bioreactors to two 1,000-L bioreactors would nearly halve the manufacturing costs resulting in a more than cost competitive sIPV. These costs analysis showed that an affordable sIPV is feasible.

Samenvatting

Poliomyelitis, ofwel polio, is een zeer besmettelijke ziekte die veroorzaakt wordt door het poliovirus. Infecties met het poliovirus komen voornamelijk via de mond het lichaam in. Het virus vermenigvuldigt zich vervolgens in de darmen. Het merendeel van de besmettingen heeft geen of slechts een mild ziektebeeld tot gevolg, zoals keelpijn, koorts of diarree. Het bekendste ziektebeeld is echter dat van verlamming van de ledematen. In deze gevallen is het poliovirus het zenuwstelsel binnengekomen. Dit komt voor bij één op de 200 besmettingen. In zeldzame gevallen treedt er verlamming van de ademhalingsspieren op, wat de dood tot gevolg kan hebben. Er is geen geneesmiddel voor polio.

Het poliovirus is een klein RNA virus van slechts 30 nm. Er bestaan 3 serotypes, ofwel varianten, type 1, 2 en 3. Bij infectie met het poliovirus worden er door het lichaam beschermende antilichamen gemaakt. Deze beschermende antilichamen zijn specifiek voor het subtype en herkennen intacte poliovirussen, die dan dus in hun D-antigeen vorm zijn. De beschermende antilichamen zullen bij een nieuwe infectie het poliovirus snel laten opruimen door het immuunsysteem. Met behulp van vaccinatie tegen polio kunnen er beschermende antilichamen worden opgewekt (Figuur 1) die de ziekte voorkomen.

In de jaren 50 van de vorige eeuw is het eerste vaccin tegen het poliovirus ontwikkeld door Jonas Salk. Dit vaccin (geïnactiveerd polio vaccin ofwel IPV) bestaat uit gezuiverde en geïnactiveerde poliovirussen (alle drie de subtypes) en wordt toegediend door middel van een injectie. Het andere poliovaccin (oraal polio vaccin ofwel OPV), ontwikkeld door Albert Sabin in 1962, bestaat uit levende verzwakte poliovirussen (ook wel de Sabin stammen genoemd) en wordt toegediend via de mond. OPV staat ook bekend als het suikerklontjes vaccin.

OPV is door de meeste landen, met uitzondering van Nederland, Zweden en Finland, opgenomen in het vaccinatieschema vanwege het gemak van toediening en de lage prijs. OPV wordt ook door de wereld gezondheidsorganisatie (WHO) gebruikt in het "polio eradicatie programma" om polio uit te roeien. Hoewel beide vaccins bekend staan vanwege hun goede veiligheid kunnen er in uitzonderlijkere gevallen (1 op 2,7 miljoen) verlammingsverschijnselen optreden bij het gebruik van OPV. Daarnaast kunnen er vaccin gerelateerde poliovirussen ontstaan die dezelfde neurovirulente eigenschappen als de wild type virussen hebben. Dit kan niet gebeuren bij vaccinatie met IPV omdat daar geen levende poliovirussen in zitten. Om deze redenen gebruiken steeds meer landen IPV in het vaccinatieprogramma.

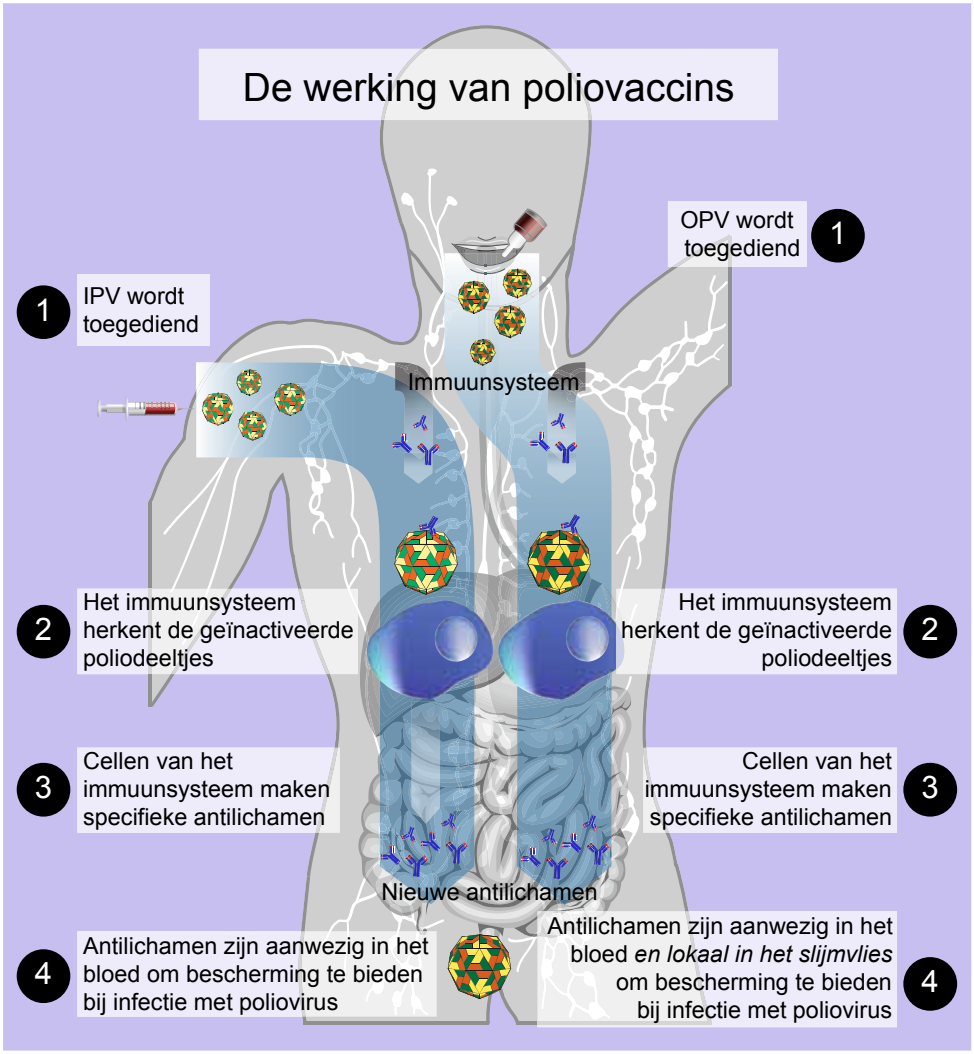

Figuur 1. De werking van poliovaccins. Er bestaan 2 vaccins tegen poliovirus. IPV, wat wordt toegediend door middel van een injectie, en OPV, toegediend via de mond. Beide vaccins zorgen voor een reactie van het immuunsysteem wat de vorming van beschermende antilichamen tot gevolg heeft. Het gebruik van OPV zorgt ook voor een lokale immuunreactie in de slijmvliezen.

Kort na de uitvinding van het eerste poliovaccin (IPV) is bij het toenmalige rijksinstituut voor volksgezondheid (RIV) in Bilthoven een productie proces opgezet op basis van primaire apennier cellen en microcarrier technologie. Deze technologie maakt het mogelijk dierlijke cellen te laten groeien op een klein bolletje (de microcarrier) (Figuur 2). De cellen op deze microcarriers kunnen in een bioreactor onder gecontroleerde omgevingsfactoren (bij onder andere constante temperatuur, zuurgraad en zuurstof concentratie) gekweekt worden. In de jaren 70 is de productie van IPV opgeschaald naar 300-L (liter) bioreactoren

voor celkweek. Later, in 2004, is de Vero cellijn in gebruik genomen om de tertiaire apennier cellen te vervangen. Ook is een verdere schaalvergroting van 700-L naar 1.500-L uitgevoerd (van twee 350-L naar twee 750-L bioreactoren). Na de productie van het virus in de bioreactoren wordt het virus gezuiverd op basis van grootte en lading. Vervolgens wordt het product geïnactiveerd met formaline voordat het gemengd voor de eindformulering (Figuur 3). De productie van IPV is sinds de ontwikkeling van het productieproces altijd onderdeel geweest van de routine vaccin productie in Bilthoven.

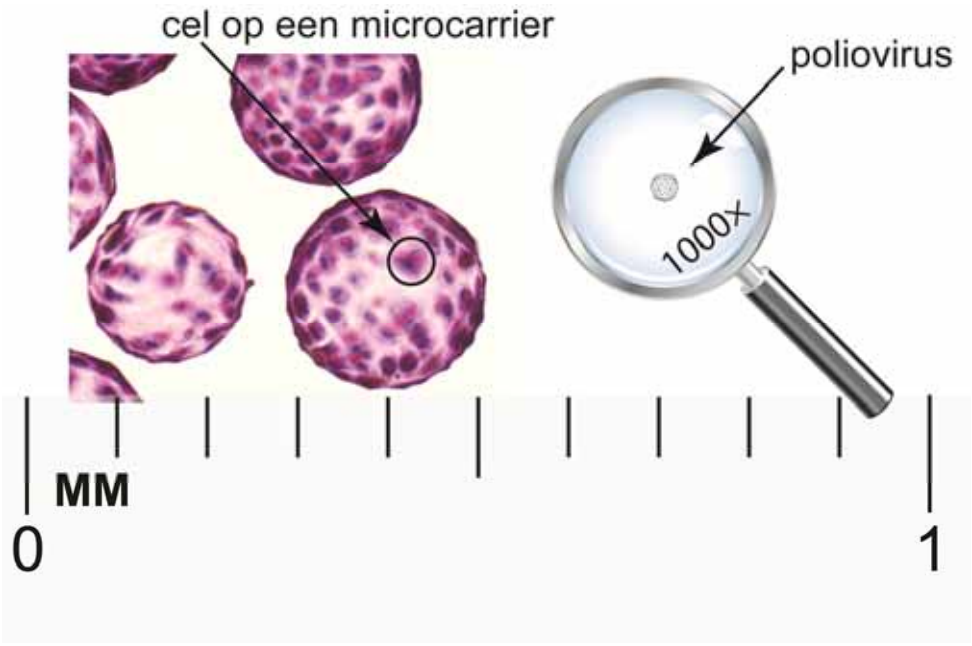

Figuur 2. Vero cellen op microcarriers (links) en poliovirus onder het vergrootglas (1.000 maal vergroting). Cellen zijn niet met het blote oog te zien. De microcarriers waar de cellen op groeien zijn ongeveer 0,2 millimeter (mm) groot, een cel diameter is maar ongeveer 0,05 mm en een poliovirus slechts 0,00003 mm ofwel 30 nm.

Met de eradicatie van polio in het vooruitzicht wordt er door de WHO gestreefd naar een nieuw IPV op basis van verzwakte poliovirussen om zo de biologische veiligheid van de vaccinproductie te vergroten. Na eradicatie zal het gebruik van OPV wereldwijd gestopt worden en zal de vraag naar betaalbare IPV toenemen. Om de IPV productie veiliger en goedkoper te maken zijn er twee onderzoeksprogramma's gestart bij het Nederlands Vaccin Instituut (nu het Instituut voor Translationele Vaccinologie). Het eerste programma betrof de optimalisatie van het huidige conventionele IPV (cIPV), het tweede de productie van een betaalbaar sIPV, een IPV op basis van de verzwakte Sabin poliovirussen die normaal gebruikt worden voor de productie van OPV. Het is daarnaast de bedoeling dat de

ontwikkelde technologie voor de productie van sIPV overgedragen wordt naar producenten in ontwikkelingslanden (Hoofdstuk 2).

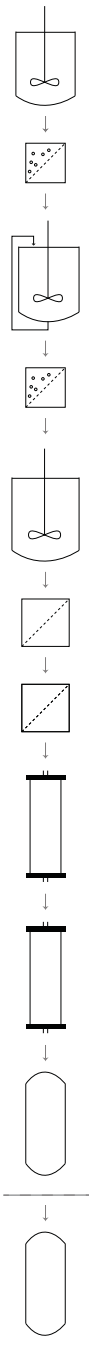

1e voorkweek
Vero cellen worden ontdooid en toegevoegd aan een bioreactor (40-L) met kweekmedium en microcarriers. In de bioreactor wordt de temperatuur, zuurgraad, en zuurstof concentratie gecontroleerd. De cellen gaan groeien en regelmatig wordt er nieuw medium toegevoegd. Na een kleine week zitten de microcarriers vol en worden de cellen geoogst.

1e trypsinisatie
Om cellen te oogsten moeten ze van de microcarriers afgehaald worden. Dit gebeurt met het enzyme trypsine. Wanneer ze los zijn van de microcarriers worden ze aan een nieuwe bioreactor toegevoegd voor verdere vermenigvuldiging.

2e voorkweek
Vero cellen worden na de oogst toegevoegd aan een bioreactor (40-L) met nieuw kweekmedium en nieuwe microcarriers. Ook hier wordt de temperatuur, zuurgraad en zuurstof concentratie gecontroleerd. De cellen gaan groeien en medium (het totale mediumvolume is 200 L) wordt gerecirculeerd. Zo is er geen gebrek aan voedingsstoffen en is de concentratie afvalstoffen niet te hoog. Na een wederom een kleine week worden de cellen geoogst.

2e trypsinisatie
Eenzelfde procedure wordt gevolgd als bij de 1e trypsinisatie in hetzelfde apparaat. In het apparaat zit een zeef waar de microcarriers niet doorheen kunnen. Op deze manier kan het oude kweekmedium verwijderd worden.

celkweek gevolgd door viruskweek
De Vero cellen uit oogst van de 2e voorkweek worden verdeeld over twee 750-L bioreactoren met nieuw kweekmedium en nieuwe microcarriers, wederom onder gecontroleerde omstandigheden. Er wordt geen medium toegevoegd, alleen glucose wanneer deze bijna op is. Na 4 dagen wordt het medium verwisseld en wordt er poliovirus toegevoegd dat de cellen infecteerd. Er wordt maar één type poliovirus per keer gekweekt. Na 4 dagen barsten de cellen en komt het virus vrij in het medium. De viruskweek is nu klaar.

clarificatie
De virusoogst wordt via een zeef uit de bioreactor gehaald zodat de microcarriers in de bioreactor achterblijven. Vervolgens wordt de eerste zuivering, de clarificatie, gestart. Hierbij wordt de virusoogst gefilterd. Grote celresten blijven achter op het filter, de (kleinere) virussen worden doorgelaten.

concentratie
Wederom een filtratiestap. Hier blijven echter de virussen achter terwijl water en kleine moleculen door het filter gaan. Op deze manier komen de virussen in een kleiner volume te zitten en zijn dus geconcentreerd.

kolomchromatografie op deeltjesgrootte
Bij kolomchromatografie is een buis gevuld met een materiaal wat voor scheiding kan zorgen. Deze scheiding is gebaseerd op een verschil in de verblijftijd in de kolom, in dit geval doordat de te scheiden deeltjes verschillen in grootte. Het materiaal in de kolom bevat poreuze korreltjes. De kleine deetjes kunnen hierin en zijn langer onderweg dan de grote deeltjes die er niet in kunnen. De overgebleven grotere celresten lopen het snelst door de kolom gevolgd door de virussen en daarna de nog kleinere deeltjes zoals bijvoorbeeld eiwitten. Door specifiek de fractie met het virus op te vangen vindt er zuivering plaats.

ionenuitwisselingschromatografie
Idem als bij kolomchromatografie is de scheiding is gebaseerd op de verblijftijd in de kolom. Bij deze methode worden deeltjes langer in de kolom gehouden door verschillen in lading. Het kolommateriaal is positief geladen waardoor negatief geladen deeltjes binden. Hoe sterker de deeltjes negatief geladen zijn hoe beter de binding en hoe langer ze op de kolom blijven. Poliovirus bindt niet aan de kolom terwijl de resterende vervuilingen zoals eiwitten en DNA wel binden. Door de eerste fractie met het virus op te vangen vindt er verdere zuivering plaats.

inactivatie
Het gezuiverde poliovirus wordt geïnactiveerd met formaline gedurende 13 dagen. De formaline gaat een chemische reactie aan met delen van het poliovirus. Hierdoor wordt het virus gefixeerd en wordt het inactief ofwel het virus gaat dood. Het virus behoudt wel zijn D-antigene vorm die nodig is voor het opwekken van beschermende antilichamen in het lichaam.

---

eindformulering
Bovenstaand proces wordt per poliovirus serotype uitgevoerd. Het moet dus driemaal (voor type 1, 2 en 3) gedaan worden voordat deze stap, de menging van een trivalent vaccin, kan plaats vinden. In deze stap worden, naast het mengen van de geïnactiveerde poliovirussen, ook eventuele hulpstoffen toegevoegd, die bijvoorbeeld de houdbaarheid vergroten of het immuunsysteem extra stimuleren.

Figuur 3. Beschrijving van het productieproces voor IPV.

Een waardevolle dataset is verzameld op basis van de historische poliovaccin-productie te Bilthoven. Gegevens van meer dan 50 partijen op twee verschillende productieschalen (700 en 1.500-L) zijn geanalyseerd met behulp van multivariate data analyse (MVDA). Deze statistische methode wordt aanbevolen door de ICH (Internationale Conferentie voor Harmonisatie van Technische Voorwaarden voor de Registratie van Farmaceutica voor Humaan Gebruik) om het wetenschappelijke begrip van productieprocessen te vergroten en zo foutopsporing en procescontrole te verbeteren. De eerste verkennende analyse, uitgevoerd op een enkele productie eenheid, gaf een consistente productie aan. Bekende uitschieters (bijv. afgekeurde partijen) werden geïdentificeerd met behulp van principale componenten analyse (PCA). Als bron van operationele variatie werd de variatie van de input, zoals cel- en virus kweekmedia, aangewezen. Andere relevante procesparameters waren onder controle en konden op basis van deze productiegegevens niet worden gecorreleerd met de productkwaliteit. De MVDA, en de daaraan voorafgaande digitalisatie van de beschikbare historische gegevens, heeft bijgedragen aan extra kennis van het IPV productieproces, heeft bewezen nuttig te zijn voor het oplossen van problemen, heeft het begrip van de beperkingen van de beschikbare gegevens vergroot en bracht mogelijkheden voor proces verbeteringen aan het licht (Hoofdstuk 3).

Eén van de beperkingen van de productiegegevens was terug te leiden naar het kwantificeren van het product tijdens de productie. De beschikbare test om de D-antigeen concentratie te bepalen in monsters, die tijdens het proces genomen worden, had een hoge variabiliteit. Een zogenaamde snelle ELISA werd ontwikkeld en gekwalificeerd voor de analyse van polio D-antigeen. Het originele 20-uur-durende protocol werd geoptimaliseerd door het minimaliseren van de totale incubatietijd tot 1uur. Verder werd het signaalreagens (3,3',5,5'-tetramethylbenzidine) vervangen door een signaalreagens dat licht uitzendt na een chemische reactie. Dit chemiluminogene signaalreagens heeft theoretisch een hoge signaal/ruis verhouding en heeft een hoog dynamisch meetbereik. De snelle D-antigeen-ELISA bleek geschikt voor het meten van D-antigen concentraties in de mengsels waar het poliovirus in zit tijdens de verschillende processtappen (Hoofdstuk 4).

Om onderzoek naar procesverbeteringen voor het huidige cIPV productie proces te kunnen doen is een up-to-date laboratorium schaal versie van het bestaande grootschalige IPV productie proces opgezet. Hiervoor is de kennis die uit de multivariate data analyse is gekomen gebruikt. Met dit zogenaamd scale-down model kunnen experimenten in het laboratorium gedaan worden die vervolgens direct, zonder schaalvergrotings-experimenten, te vertalen zijn naar de productieschaal. Als eerste zijn kleine versies van de losse productie stappen ontwikkeld. Deze kleine productie eenheden zijn vervolgens achter elkaar geschakeld zoals bij de grote productieschaal zodat de effecten van variaties

in het ene productie apparaat op de rest van het productieproces in het laboratorium bestudeerd kunnen worden.

Het ontworpen scale-down model bleek een goede weergave van de grootschalige werkelijkheid. Bij gebruik met de bestaande standaard instellingen bleek het scale-down model voor de cel en viruskweek (2,3-L) vergelijkbaar met de tegenhanger op grote schaal. Ook de afzonderlijke productie apparaten die gebruikt worden bij de zuivering: de clarificatie, concentratie, chromatografie op basis van deeltjesgrootte, ionenuitwisselingschromatografie, en inactivatie, bleken in overeenstemming met de grote schaal. Het model kan nu gebruikt worden om procesvariaties en productkwaliteit te bestuderen. Tenslotte is aangetoond dat de scale-down modellen gebruikt kunnen worden om op laboratoriumschaal een trivalent poliovaccin met vergelijkbare eigenschappen als het product geproduceerd op productieschaal te maken (Hoofdstuk 5).

De opkomst van wegwerpartikelen in GMP producties (GMP of "good manufacturing practice" is een kwaliteitsborgingssysteem voor een goede wijze van produceren van farmaceutische producten) heeft geleid tot de studie naar alternatieven voor de clarificatie (Hoofdstuk 5) en alternatieve Wave-type bioreactoren (Hoofdstuk 6). Dit type bioreactoren maakt gebruik van gesteriliseerde wegwerpzakken, die schoonmaakprotocollen en overgangsprocedures tussen productie processen voor verschillende producten kunnen vergemakkelijken. Wave-type bioreactoren maken, voor het realiseren van menging, gebruik van verticale verplaatsing die lijkt op een wipwap beweging, of van zowel verticale als horizontale verplaatsing waardoor de vloeistof minder klotsend beweegt. Met behulp van een design of experiments (DoE) aanpak, zijn modellen voor de mengtijden in beide bioreactoren ontwikkeld. Voor het eerste type bioreactoren (met alleen verticale verplaatsing) bestaat een voorschrift voor het kweken van Vero cellen. De instellingen voor het kweken van Vero-cellen in andere bioreactor zijn gekozen op basis van vergelijkbare mengtijden. Vero-cellen, die gehecht aan Cytodex 1 microcarriers groeien, vertoonden vergelijkbare groeikarakteristieken. Consumptie van voedingsstoffen en productie van afvalstoffen waren vergelijkbaar, evenals de poliovirus-productie.

Gezien het streven van de WHO naar een IPV productieproces met verhoogde biologische veiligheid is een sIPV ontwikkeld. Het cIPV proces is gebruikt als basis voor het nieuwe sIPV proces. Kleine aanpassingen zoals verlaagde viruskweek temperatuur zijn toegepast op dit proces. Ook is het geselecteerde (Hoofdstuk 5) wegwerpfilter voor de clarificatie gebruikt. Om snel sIPV partijen voor klinische studies, waarbij het product op veiligheid en werkzaamheid in mensen getest kan worden, te kunnen maken is verder geen procesoptimalisatie en/of modernisatie gedaan. sIPV is geproduceerd op industriële schaal gevolgd door eindformulering met en zonder aluminium als immuun-stimulerende stof

(Hoofdstuk 7). De eindproducten voldeden aan de kwaliteitscriteria, waren immunogeen in ratten, lieten geen toxiciteit in konijnen zien en konden vrijgegeven worden voor testen in de mens. Hoewel er een veilig en werkzaam product was bereid, was de productieopbrengst erg laag, wat hogere productiekosten tot gevolg heeft. Verdere procesontwikkeling is dus nodig om een betaalbaar sIPV te verkrijgen.

Vooral de opbrengst van Sabin poliovirus type 2 na de laatste zuiveringsstap middels ionenuitwisselingschromatografie was laag. Om te bepalen of dit resultaat komt door een verschil in het iso-elektrisch punt (p*I*; zuurgraad waarbij het molecuul geen lading heeft) van de poliovirussen is een methode opgezet voor de p*I* bepaling van levende virussen (Hoofdstuk 8).Deze methode is gebaseerd op gesloten circuits om de biologische veiligheid te waarborgen. Vervolgens zijn de p*I*s van complete intacte poliovirussen bepaald. Zowel de poliovirussen die gebruikt worden bij cIPV – Mahoney (type 1), MEF-1 (type 2), Saukett (type 3) – productie alsook de poliovirussen die gebruikt worden bij OPV en sIPV – Sabin poliovirus type 1, 2 en 3 – zijn geanalyseerd. Het bleek dat de p*I* van Sabin poliovirus type 2 dicht bij de pH ligt die gebruikt wordt tijdens de chromatografie, waardoor dit poliovirus gevoelig voor zelf-aggregatie. Deze zelf-aggregatie is waarschijnlijk de belangrijkste reden voor de lage productopbrengst (zoals gevonden in Hoofdstuk 7) en het voorkomen hiervan is het voornaamste aandachtspunt voor procesoptimalisatie.

Naast optimalisatie van de zuivering is de optimalisatie van de kweek, en met name de virusopbrengst na cel- en viruskweek, bestudeerd (Hoofdstuk 9). Vero cellen, die gehecht aan microcarriers (Cytodex 1; 3 g L^{-1}) groeien, zijn gekweekt op medium vrij van dierlijke componenten in geroerde bioreactoren. Verschillende strategieën voor media verversing: dagelijkse media vervanging (semi-batch), continue media verversing (perfusie) en recirculatie van media, werden vergeleken met batchkweek waarbij het medium niet vervangen wordt. Mediaverversing zorgde voor verhoogde cel dichtheden, variërend van 1 × 10^6 cellen mL^{-1} tijdens batchkweek tot 1,8, 2,7 en 5,0 x 10^6 cellen mL^{-1} tijdens respectievelijk de semi-batch, perfusie en recirculatie strategie. De effecten van deze verschillende celkweek strategieën op de latere poliovirus productie zijn onderzocht. Verhoogde cel dichtheden resulteerden in tot 3 keer hogere D-antigeen niveaus in vergelijking met die bij batchkweek. Echter, de specifieke D-antigeen productie per cel was lager wanneer cellen werden geïnfecteerd bij hogere cel dichtheden. Dit effect is eerder beschreven voor andere cellijnen en virussen. De semi-batch strategie leidde tot de hoogste cel specifieke D-antigeen productie. De verhoogde productopbrengsten, die gemakkelijk te bereiken zijn met deze hogere cel dichtheid kweekmethode, toonde de mogelijkheid voor een beter gebruik van bioreactorcapaciteit voor het bereiden van poliovaccins. Deze toepassing kan uiteindelijk de vaccinkosten verminderen. Verder blijkt

het gebruik van cel - en viruskweekmedium vrij van dierlijke componenten mogelijk voor de modernisering van virale vaccins voor de mens.

Om de betaalbaarheid van sIPV te beoordelen zijn de productiekosten bepaald (Hoofdstuk 10). De productiekosten voor sIPV, geproduceerd zoals beschreven in hoofdstuk 7, laten de noodzaak van procesoptimalisaties zien. Een grote stap kan plaatsvinden, wanneer de semi-batch strategie in combinatie met dierlijke componenten vrij media wordt toegepast, zoals beschreven in hoofdstuk 9. De productiekosten verminderen dan met tenminste een factor 2. Verdere verlaging van de kosten kan gerealiseerd worden door optimalisatie van de zuivering. Bij vergelijkbare productopbrengsten als die van van cIPV kunnen de proceskosten verder verlaagd worden. Door schaalvergroting van twee 350-L bioreactoren naar twee 1.000-L bioreactoren kunnen de productiekosten bijna gehalveerd worden. Deze kostenanalyse toont de haalbaarheid van een betaalbaar sIPV aan.

The research described in this thesis was financed by the Institute for Translational Vaccinology (part of the ministry of Health, Welfare and Sport, the Netherlands). Chapters 2, 7 and 9 were supported by the World Health Organization using funds provided by a grant from the Bill and Melinda Gates Foundation. Chapter 6 was partially supported by NL Agency (no. IVG091769).

Financial support from Wageningen University and the Institute for Translational Vaccinology for printing this thesis is gratefully acknowledged.

Cover design by Cees van Dorland